Defining the Contributors to Mammalian Cell Mass

by

Aaron M. Hosios

A.B. Molecular Biology
Princeton University, 2011

Submitted to the Department of Biology
in Partial Fulfillment of the Requirements for the Degree of

DOCTOR OF PHILOSOPHY

at the

MASSACHUSETTS INSTITUTE OF TECHNOLOGY

June 2017

Signature of the author _____ **Signature redacted**

Department of Biology
April 7, 2017

Signature redacted

Certified by _____

Matthew G. Vander Heiden
Associate Professor of Biology
Thesis Supervisor

Signature redacted

Accepted by _____

Amy E. Keating
Professor of Biology
Chair of the Graduate Committee

1
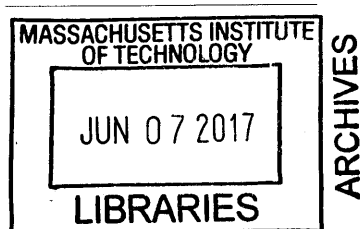
Defining the Contributors to Mammalian Cell Mass

by

Aaron M. Hosios

Submitted to the Department of Biology on May 26, 2017
in Partial Fulfillment of the Requirements for the Degree of
Doctor of Philosophy in Biology

Abstract

Proliferation can be thought of as the sum of many biosynthetic processes. To proliferate, a cell must not only physically divide but must also newly synthesize each of its components as it progresses through the cell cycle. Metabolism allows a cell to meet these demands. Metabolic alterations associated with proliferating cells have been characterized, and increasing research interest seeks to provide mechanistic and teleological insight into these metabolic alterations. The following dissertation provides a framework for understanding how proliferating mammalian cells use the nutrients available to them to synthesize macromolecule precursors that are ultimately used to synthesize new cell mass. Substantial research efforts have focussed on the abilities of glucose and glutamine to serve as sources of biosynthetic material for cell growth, especially since proliferating cells avidly consume these nutrients. Many other nutrients are consumed at much lower rates, and we have quantified how each contributes to biosynthesis, demonstrating that amino acids are the primary contributors to mammalian cell mass. Although glucose consumption does not directly relate to its contribution to cell mass, glycolytic flux is important to sustain cell growth, and activation of this pathway is thought to promote biosynthesis. To better understand regulation of this pathway, we have explored the biochemical properties of two glycolytic enzymes, pyruvate kinase and enolase. Although pyruvate kinase isoform M2 (PKM2) expression enables proliferation in some contexts, we demonstrate that this is not because of its putative activity as a protein kinase. We additionally characterize a novel modification of enolase by its substrate, phosphoenolpyruvate, which can covalently modify a catalytic residue and inhibit enzyme activity. These studies collectively contribute to an understanding of how metabolism can support rapid proliferation in mammalian cells, and lay the foundation for future studies to understand proliferative metabolism.

Thesis supervisor: Matthew G. Vander Heiden
Title: Associate Professor of Biology

Biographical Note

Education:

Ph.D. (Biology), Massachusetts Institute of Technology, Cambridge MA   2011-2017
A.B. (Molecular Biology), Princeton University, Princeton NJ   2007-2011

Research Experience:

2012-2017: Graduate Studies
Laboratory of Dr. Matthew Vander Heiden, Massachusetts Institute of Technology

2010-2011: Undergraduate Research
Laboratory of Dr. Joshua Rabinowitz, Princeton University, Princeton NJ

Summer 2009: Summer Undergraduate Research
Laboratory of Dr. Charles Boone, University of Toronto, Toronto, Ont.

Awards:

HHMI International Student Research Fellowship, Howard Hughes Medical Institute   2014-2016
Vertex Scholarship, Vertex Pharmaceuticals   2013-2014
Gene Brown-Merck Teaching Award   2013
Magna cum laude graduate in Molecular Biology, Princeton University   2011

Publications:

Hosios, A.M., and Vander Heiden, M.G. (2017). Endothelial Cells Get β-ox-ed In to Support Lymphangiogenesis. Developmental Cell *40*, 118-119.

Mayers, J.R., Torrence, M.E., Danai, L.V., Papagiannakopoulos, T., Davidson, S.M., Bauer, M.R., Lau, A.N., Ji, B.W., Dixit, P.D., Hosios, A.M., *et al.* (2016). Tissue of origin dictates branched-chain amino acid metabolism in mutant Kras-driven cancers. Science *353*, 1161-1165.

Gui, D.Y., Sullivan, L.B., Luengo, A., Hosios, A.M., Bush, L.N., Gitego, N., Davidson, S.M., Freinkman, E., Thomas, C.J., and Vander Heiden, M.G. (2016). Environment Dictates Dependence on Mitochondrial Complex I for NAD+ and Aspartate Production and Determines Cancer Cell Sensitivity to Metformin. Cell Metabolism *24*, 716-727.

Hosios, A.M., Hecht, V.C., Danai, L.V., Johnson, M.O., Rathmell, J.C., Steinhauser, M.L., Manalis, S.R., and Vander Heiden, M.G. (2016). Amino Acids Rather than Glucose Account for the Majority of Cell Mass in Proliferating Mammalian Cells. Developmental Cell *36*, 540-549.

Hecht, V.C., Sullivan, L.B., Kimmerling, R.J., Kim, D.H., Hosios, A.M., Stockslager, M.A., Stevens, M.M., Kang, J.H., Wirtz, D., Vander Heiden, M.G., *et al.* (2016). Biophysical changes reduce energetic demand in growth factor-deprived lymphocytes. J Cell Biol *212*, 439-447.

Hosios, A.M., Fiske, B.P., Gui, D.Y., and Vander Heiden, M.G. (2015). Lack of Evidence for PKM2 Protein Kinase Activity. Molecular Cell *59*, 850-857.

Sullivan, L.B., Gui, D.Y., Hosios, A.M., Bush, L.N., Freinkman, E., and Vander Heiden, M.G. (2015). Supporting Aspartate Biosynthesis Is an Essential Function of Respiration in Proliferating Cells. Cell *162*, 552-563.

Lunt, S.Y., Muralidhar, V., Hosios, A.M., Israelsen, W.J., Gui, D.Y., Newhouse, L., Ogrodzinski, M., Hecht, V., Xu, K., Acevedo, P.N., *et al.* (2015). Pyruvate kinase isoform expression alters nucleotide synthesis to impact cell proliferation. Molecular Cell *57*, 95-107.

Son, S., Stevens, M.M., Chao, H.X., Thoreen, C., Hosios, A.M., Schweitzer, L.D., Weng, Y., Wood, K., Sabatini, D., Vander Heiden, M.G., *et al.* (2015). Cooperative nutrient accumulation sustains growth of mammalian cells. Sci Rep *5*, 17401.

Hosios, A.M., and Vander Heiden, M.G. (2014). Acetate metabolism in cancer cells. Cancer & Metabolism *2*, 27.

Israelsen, W.J., Dayton, T.L., Davidson, S.M., Fiske, B.P., Hosios, A.M., Bellinger, G., Li, J., Yu, Y., Sasaki, M., Horner, J.W., *et al.* (2013). PKM2 isoform-specific deletion reveals a differential requirement for pyruvate kinase in tumor cells. Cell *155*, 397-409.

Reaves, M.L., Young, B.D., Hosios, A.M., Xu, Y.F., and Rabinowitz, J.D. (2013). Pyrimidine homeostasis is accomplished by directed overflow metabolism. Nature *500*, 237-241.

Teaching Experience:

Head Teaching Assistant, General Biochemistry (7.05), MIT	Spring 2015
Teaching Assistant, Principles of Biochemical Analysis (7.51), MIT	Fall 2012

Acknowledgements

The work described in this dissertation would not have possible to accomplish without the contributions, support, dedication, and companionship of many people. I owe a tremendous debt of gratitude to each of the following individuals for the roles that they played during my time in graduate school at MIT.

At MIT, I have grown as a scientist, as a student, and as a person, and this is due in large part to the mentorship and example set by my advisor, Dr. Matthew Vander Heiden. His leadership and instruction have been instrumental to my progress and development as a graduate student, and I have learned a tremendous amount from him. Matt's constant positivity has been a crucial source of encouragement and support throughout my time at MIT, and I am grateful for his prioritizing my personal happiness and success both in and out of lab. Matt is an upstanding colleague and mentor; he is both an incredibly imaginative and a careful scientist, and I will strive to emulate the example he has set. No scientific problem is too large or too small to discuss with him, and his eagerness to engage with all scientists and their work has set a standard I hope to follow.

I am also deeply grateful for the roles that Dr. Angelika Amon and Dr. David Sabatini played as members of my thesis committee. My graduate research has benefited immensely from their input, and I am thankful for their advice and suggestions as I have considered my next steps after graduating.

I have been extremely lucky to have had the opportunity to work with a great number of talented graduate students, post-doctoral fellows, undergraduate students, and technicians in the Vander Heiden lab. The lab environment has always been a pleasure to work in, and I am appreciative of the friendship and camaraderie I have experienced there. I am particularly indebted to Dr. Caroline Lewis, Alba Luengo, and Dan Gui who have been close friends throughout my time at MIT. The lab has not only been a supportive and fun environment but has also helped to shape me as a scientist, and I know that I have benefited intellectually from my peers. I have been fortunate to share my time in the lab with: Dr. Laura Danai, Dr. Shawn Davidson, Emily Dennstedt, Frances Diehl, Dr. Brian Fiske, Dan Gui, Dr. William Israelsen, Zachary Johnson, Mitali Kini, Dr. Allison Lau, Dr. Caroline Lewis, Zhaoqi Li, Dr. Evan Lien, Alba Luengo, Dr. Sophia Lunt, Dr. Katherine Mattaini, Dr. Jared Mayers, Dr. Alexander Muir, Dr. Vinayak Muralidhar, Anna Nguyen, Dr. Benjamin Olenchock, Dr. Daniel Schmidt, Dr. Lucas Sullivan, Mark Sullivan, Sara Tollestrup, Meghan Torrence, Marit van Gorsel, Dr. Natalie Vokes, and Amelia Yu.

My research experiences have also been greatly enriched through collaborations both within MIT and outside of it, and I am thankful to have been able to work with Dr. Vivian Hecht from Dr. Scott Manalis's Lab at MIT; Brian Ji and Dr. Purutosham Dixit from Dr. Dennis Vitkup's Lab at Columbia University; Dr. Matthew Steinhauser at Harvard Medical School; and Marc Johnson from Dr. Jeff Rathmell's Lab at Vanderbilt University. Vivian Hecht played a role integral to the project described in Chapter 2, which would not have been possible without her enthusiastic efforts.

I am fortunate to have made truly wonderful friends during my time in graduate school. They have been a constant source of support, compassion, and fun, and I couldn't imagine my experience at MIT without them. Bridget Begg, Forrest Brookes, Alex Godfrey, Sean McGeary, and Cory Pender have been exceptional friends and my cheerleaders throughout, and I cherish the memories we've shared over the past several years. These friends have been great role models as we've grown together, and I have learned from and admire each of them. Audra Amasino, Dr. Douglas Cattie, and Steven Sando have been wonderful friends during this time as well. Finally, my friends from outside of MIT, Hila Calev, Miranda

Table of Contents

Chapter 1: The metabolic requirements of proliferating cells

Introduction to proliferative metabolism

Proliferation, the growth and division of cells, imposes a substantial biosynthetic requirement upon them. In order to replicate, a cell must acquire or newly synthesize each of its components, effectively doubling its mass throughout the cell cycle. All cells, whether they are proliferating or not, require a source of energy and reducing power to maintain homeostasis and combat cellular stress. Proliferating cells must also synthesize their macromolecular contents: DNA, RNA, proteins, and lipids. To meet this demand, proliferating cells carry out diverse metabolic reactions to generate the precursors for these molecules (Lunt and Vander Heiden, 2011). The reactions that compose the metabolic network have been biochemically characterized and a large number of metabolites and enzymes are known. Nevertheless, mammalian cells grow in complex environments and are exposed to many nutrients, so which nutrients are used and how these contribute to macromolecule precursors cannot be discerned from the metabolic network alone. Current studies seek to understand how metabolism supports proliferation in diverse cell types with the goal of using this knowledge to alter proliferation.

The majority of cells in an adult individual are non-proliferating, but mammalian cells can proliferate in a variety of contexts. For example, proliferation is regulated in developing embryos, stem cells, and immune cells. By contrast, cancer is a disease of uncontrolled proliferation. These examples of proliferating cells have many metabolic requirements in common but exhibit differences as well, and there is growing interest in exploiting these differences for cancer therapy (Tennant et al., 2010; Vander Heiden, 2011; Weinberg and Chandel, 2015). Several drugs currently used to treat diverse cancers have metabolic targets and many metabolic enzymes are emerging as potential drug targets. Inhibition of crucial metabolic processes has the potential to stop proliferation, and therefore an understanding of how metabolism supports proliferation is required.

In this chapter, I will describe the metabolic requirements of proliferating cells and give examples of how they are met, discussing in particular which nutrients and which metabolic pathways support macromolecule synthesis. This will provide a framework to understand how metabolism is altered to support proliferation in a variety of contexts, including cancer.

The mammalian metabolic network

The metabolic network is composed of reactions that enable cells to derive energy, reducing power, and biosynthetic precursors from the nutrients they consume. Many metabolic reactions are important to mammalian physiology but are dispensable for the growth and proliferation of individual cells. The following discussion pertains to those reactions required to synthesize macromolecule precursors necessary for proliferation of individual cells. The core component of this metabolic network is central carbon metabolism, composed of glycolysis and the tricarboxylic acid (TCA) cycle. Glycolytic and TCA cycle intermediates serve as substrates for anabolic pathways that synthesize macromolecule precursors (**Figure 1**). Both of these pathways, in particular the TCA cycle when it is coupled to oxidative phosphorylation, also provide cells with energy in the form of adenosine triphosphate (ATP). Catabolic reactions break down macromolecules to replenish glycolysis and the TCA cycle, allowing cells to derive energy from the degradation of macromolecule precursors.

Glucose is a critical source of energy and biosynthetic material for many cell types, and it is primarily catabolized by glycolysis to yield ATP and pyruvate. Pyruvate can undergo additional oxidation to acetyl-CoA, which is ultimately oxidized to carbon dioxide in the TCA cycle, enabling cells to generate substantial additional ATP via oxidative phosphorylation. The TCA cycle has two metabolic roles: to oxidize acetyl-CoA and to supply four- and five-carbon molecules for biosynthesis. Importantly, these molecules, which are depleted by biosynthesis, facilitate the oxidation of acetyl-CoA, and sustained TCA-cycle activity therefore requires that they be replaced. Anaplerotic reactions replenish these intermediates

12
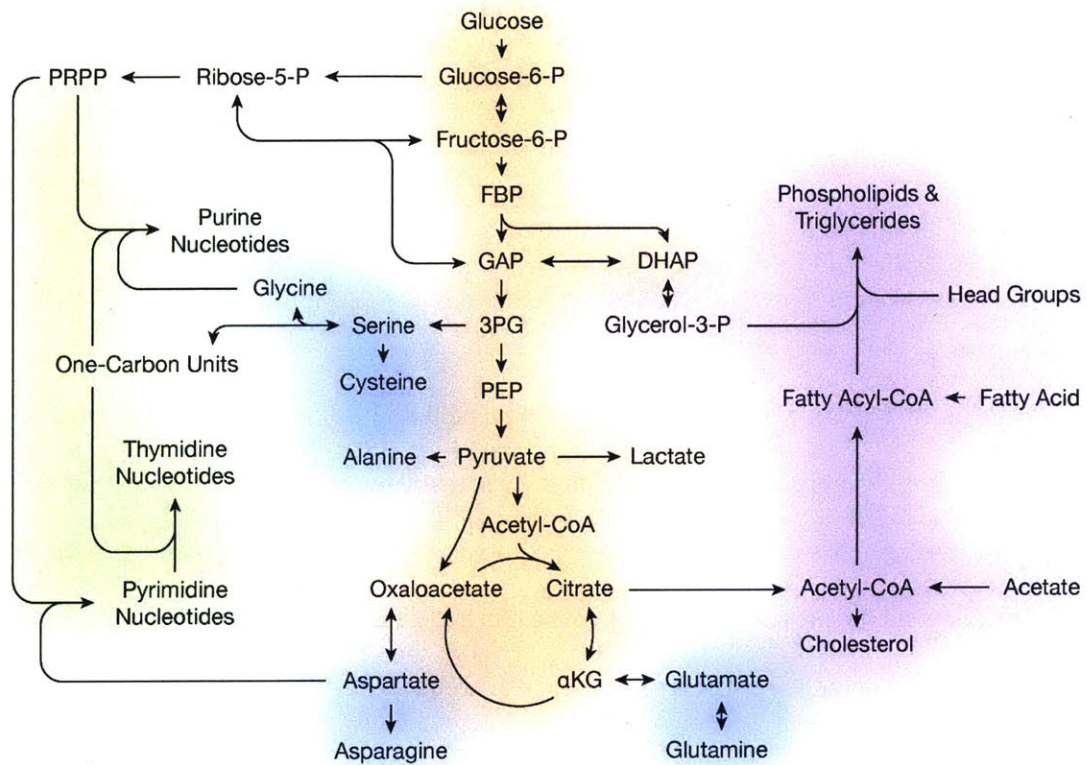
Figure 1: The mammalian metabolic network synthesizes macromolecule precursors from glucose and other sources.

Major metabolic pathways that enable synthesis of amino acids (blue), lipids (purple), and nucleotides (green) are outlined, indicating the starting materials that supply carbon atoms to synthesize macromolecule precursors. Central carbon metabolism (glycolysis and the TCA cycle) is highlighted in orange. 3PG, 3-phosphoglycerate; αKG, alpha-ketoglutarate; CoA, co-enzyme A; DHAP, dihydroxyacetone-phosphate; FBP, fructose-1,6-bisphosphate; GAP, glyceraldehyde-3-phosphate; P, phosphate; PEP, phosphoenolpyruvate; PRPP, phosphoribosyl pyrophosphate.

by amino acid catabolism or pyruvate carboxylation. Glutamine catabolism (glutaminolysis) is the primary anaplerotic reaction for mammalian cells proliferating *in vitro*, and glutamine is the most consumed amino acid by these cells (DeBerardinis et al., 2007; Jain et al., 2012). Glucose and glutamine are the most consumed nutrients by cells in culture and are among the most abundant nutrients in human plasma. While they do not supply the majority of biosynthetic material to cells (Hosios et al., 2016), they are important sources of energy and biosynthetic material for cells, and substantial work has focussed on how their metabolism supports proliferation.

Aerobic glycolysis

Pyruvate has two primary fates in mammals: it can be fermented to lactate and excreted or oxidized to carbon dioxide in the TCA cycle. The latter process requires oxygen to serve as an electron acceptor, and when oxygen is scarce, fermentation is favored. As a result, in many cell types the fate of pyruvate is dependent on the presence of oxygen (Wheaton and Chandel, 2011). Proliferating cells, however, carry out fermentation regardless of oxygen availability. This phenomenon, termed aerobic glycolysis, was first described by Otto Warburg (Warburg, 1924; Warburg, 1956). Warburg studied fermentation using tissue slices and observed that, unlike normal tissue, tumors fermented glucose to lactate in the presence of oxygen. His finding was subsequently confirmed *in vivo* by Carl and Gerty Cori. They studied blood that had passed through tumor-bearing tissue and noted a decrease in glucose and a corresponding increase in lactate relative to normal blood (Cori and Cori, 1925). In his work, Warburg noted that fermentation in the presence of oxygen is not unique to tumors. Proliferating yeast, for example, ferment glucose to ethanol in the presence of oxygen and only oxidize ethanol when glucose is exhausted (Lemoigne et al., 1954). Non-transformed mammalian cells also carry out aerobic glycolysis when rapidly proliferating. Compared to their resting state, lymphocytes and thymocytes stimulated to proliferate *in vitro* consume increased amounts of glucose and convert a greater portion to lactate (Brand, 1985; Brand et al., 1986; Hume et al., 1978). Similar findings were obtained in fibroblasts from several species and in proliferating cells derived from chicken embryos (Steck et al., 1968; Wang et al., 1976).

14

Transformation with Rous sarcoma virus did not enhance glycolytic rate in these embryonic cells, indicating that aerobic glycolysis is a feature of proliferating cells independent of oncogenic transformation. Warburg postulated that aerobic glycolysis was necessitated by mitochondrial defects, but work since then has demonstrated intact mitochondrial metabolism in many tumor cells (Zu and Guppy, 2004). In fact, mitochondrial metabolism is thought to be essential for mammalian cell proliferation and tumor formation (Sullivan et al., 2015; Tan et al., 2015), and the mitochondrial inhibitor metformin has antitumor effects in some contexts (Luengo et al., 2014; Wheaton et al., 2014).

Aerobic glycolysis may be beneficial to cells. Fermentation is seemingly wasteful, as complete oxidation of pyruvate generates more ATP, but producing lactate may allow cells to maximize their glycolytic rate. Glycolysis converts NAD^+ to NADH and cannot proceed without the regeneration of NAD^+. In the cytosol, this is accomplished by lactate dehydrogenase (LDH), a highly expressed and very efficient enzyme (Wuntch et al., 1970). Oxidative phosphorylation in the mitochondria also serves to regenerate NAD^+; however, multiple enzymatic steps are required to transport cytosolic NADH into the mitochondria. Notably, oxidative phosphorylation often does not proceed at its maximal rate and may be limited by ATP turnover (Krebs, 1959). LDH could, therefore, provide an efficient means of regenerating NAD^+ when cells are not ATP-limited or when mitochondrial regeneration of NAD^+ is limiting (Sullivan et al., 2015).

A high glycolytic rate can provide several advantages to proliferating cells. Glycolysis can be an important source of energy for cells, generating two molecules of ATP per molecule of glucose. Nonetheless, glycolysis supplies a minority of cellular ATP for a wide variety of cells *in vitro* (Fan et al., 2013; Zu and Guppy, 2004), but may play a greater role when oxidative phosphorylation is impaired. Furthermore, ATP generation is hypothesized to not be rate limiting for proliferation (Racker, 1976). An alternative hypothesis is that high glycolytic flux is necessary to sustain the biosynthetic reactions required for proliferation (Hsu and Sabatini, 2008; Hume and Weidemann, 1979; Pavlova and Thompson, 2016; Vander Heiden et al., 2009). Glycolytic intermediates serve as precursors for amino acids, nucleotides, and lipids (**Figure 1**), linking glycolysis to macromolecule biosynthesis. Hume and

Weidemann (1979) speculated that aerobic glycolysis maintains increased concentrations of glycolytic intermediates necessary to drive synthesis of macromolecule precursors, and they observed that mitogen-activated thymocytes increase incorporation of glucose carbon into macromolecules. Newsholme *et al.* postulated that rapid glycolytic flux was important to the regulation of biosynthetic pathways that branch from glycolysis (Newsholme et al., 1985b). In their model of metabolic control, low flux pathways (biosynthesis) branch from a high flux pathway (glycolysis), and as a result, the cells can activate biosynthetic pathways when needed. Since biosynthetic reactions are slow relative to glycolysis, they cannot substantially deplete glycolytic intermediates, which would ultimately reduce biosynthesis.

Aerobic glycolysis is a feature of proliferative metabolism, but how rapid flux through this pathway supports proliferation remains subject to debate. Understanding the effect of glycolytic rate on the rates of biosynthesis, ATP production, and lactate excretion will be critical to provide a definitive explanation.

Glutaminolysis

In addition to enhanced glycolysis, many proliferating cells catabolize glutamine. In the studies described above, thymocytes and lymphocytes stimulated to proliferate *in vitro* also consume more glutamine than non-proliferating cells (Brand, 1985; Brand et al., 1986; Newsholme et al., 1985b). These proliferating cells displayed elevated activity of enzymes that facilitate entry of glutamine carbon into the TCA cycle (glutaminolysis). Newsholme *et al.* hypothesized that high glutaminolytic flux is required for the same purpose as high glycolytic flux, to supply material to low-flux biosynthetic pathways (Newsholme et al., 1985a, b). Indeed, glutamine can be used to make several other amino acids, as well as other macromolecule precursors (discussed in detail below). Glutamine can serve as a source of both carbon and nitrogen for biosynthesis (Hosios et al., 2016), but its use exceeds the cellular demand for nitrogen in culture, indicating its importance for anaplerosis and energy generation (Altman et al., 2016; DeBerardinis and Cheng, 2010; DeBerardinis et al., 2007). Consistent with this, a large fraction of ATP is generated by oxidation of glutamine (Fan et al., 2013). Importantly, anaplerosis must be balanced by

16

cataplerosis (withdrawal of TCA cycle intermediates), and glutamine carbon leaves the TCA cycle through amino acid biosynthesis and malic enzyme activity (Coloff et al., 2016; DeBerardinis et al., 2007). Collectively, these findings underscore the importance of glutamine utilization for biosynthesis and energy generation.

Glutaminolysis has consequently become an appealing pathway to target for cancer therapy (Altman et al., 2016; Daye and Wellen, 2012; DeBerardinis and Cheng, 2010; Vander Heiden, 2011); however, recent work has called into question how effective this may be *in vivo*. Glutamine can be catabolized in some Myc-driven cancer models and inhibiting glutaminolysis in this context impairs growth (Xiang et al., 2015; Yuneva et al., 2012). However, metabolic tracer studies of non-small cell lung cancer (NSCLC) metabolism *in vivo* detected minimal glutamine entry into the TCA cycle, contrary to what has been observed for cells in culture (Davidson et al., 2016). NSCLC *in vivo* and in some contexts *in vitro* predominantly uses glucose a source of anaplerotic carbon, supplied by pyruvate carboxylase (Hensley et al., 2016; Sellers et al., 2015), and similar results have been obtained in glioblastoma models (Marin-Valencia et al., 2012; Mashimo et al., 2014; Tardito et al., 2015). A definitive explanation for the discrepancy between glutamine metabolism *in vivo* and *in vitro* is lacking, although nutrient environment is an intriguing possibility, given that lung cancer cell lines use glutamine differently if grown *in vitro* or as tumors (Davidson et al., 2016).

Glutamine is a significant nutrient source at least in some contexts, and glutaminolysis can fuel energetic reactions and supply carbon and nitrogen for biosynthesis. In addition to aerobic glycolysis, this pathway can be another means by which proliferating cells meet their metabolic requirements. Although in many contexts *in vivo* glutamine is not a major source of TCA cycle anaplerosis, studies of glutaminolysis have revealed the importance of anaplerotic reactions to biosynthesis and proliferation. Anaplerosis, therefore, appears to be a vulnerability of proliferating cells, and future studies should seek to identify anaplerotic reactions used by cells that rely less on glutamine.

Defining the macromolecular components of a cell

Cell composition

Regardless of which nutrient sources contribute to the mass acquired by proliferating cells, all cells must synthesize DNA, RNA, protein, and lipids, duplicating each component as they grow. These macromolecule classes are present in different quantities within a cell, and a cell's composition dictates its biosynthetic demands. An assessment of the metabolic requirements of proliferation therefore requires an understanding of cell composition.

Data regarding the composition of mammalian cells is minimal and has been calculated for only a small number of cell lines. Two approaches have been used to determine mammalian cell composition. In the first, cells are lysed and macromolecules are quantified using assays specific to each macromolecule (for example, Biuret assay to quantify protein) (Bonarius et al., 1996; Xie and Wang, 1994). Alternatively, cells are assayed by infrared spectroscopy and the relative contributions of macromolecule classes to the spectrum is calculated (Mourant et al., 2005). While there is some variability among these techniques, it is agreed that protein comprises the majority of cell mass, followed by lipids, RNA, and DNA (**Figure 2**). In rat liver and in early mouse embryos, ribosomes were found to comprise 60-80% of total cellular RNA, which is similar to what has been observed in *E. coli* (Blobel and Potter, 1967; Ecker and Kokaisl, 1969; Piko and Clegg, 1982). Ribosome content partly determines protein synthesis rate, and together these are major determinants of cell size.

Importantly, cell composition is not fixed and can vary across conditions and among cell types (Dolfi et al., 2013). Cell composition and growth rate are critical determinants of the metabolic demands of macromolecule synthesis. Although nutrient consumption rates correlate poorly with cell proliferation rate alone (Jain et al., 2012), they correlate more closely with the acquisition of new cell mass when composition is taken into account (Dolfi et al., 2013).
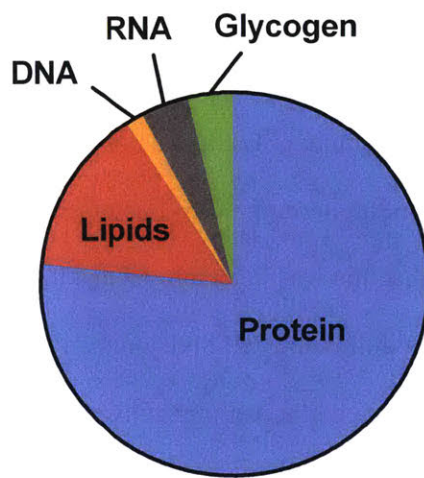
Figure 2: The composition of mammalian cell mass, adapted from Xie and Wang (1994).

Coordinating growth and proliferation

As a cell proliferates, it must coordinate the acquisition of new cell mass with cell division, and the mechanism by which these processes are linked has been the subject of extensive research. The ability to sense size would be advantageous to a cell, preventing division until sufficient new mass is accumulated. The cell cycle can be thought of as two distinct, but coordinated, cycles: the growth cycle (acquisition of new cell mass) and the DNA division cycle (DNA replication and cell division). Hartwell and colleagues provided evidence for this model by decoupling the cycles in the budding yeast *Saccharomyces cerevisiae* (Johnston et al., 1977). They noted that abnormally small cells took longer to initiate DNA replication and cell division, waiting until they reached a critical size. This suggests that a mechanism exists to control cell size, and that growth, and not DNA replication or cell division, is rate limiting for proliferation. Killander and Zetterberg (1965) obtained similar results with mouse fibroblasts, where time to initiation of DNA replication was inversely related to size following division. Fibroblast sizes were more variable immediately following cell division than by the time DNA replication began, suggesting that DNA replication is initiated at a constant cell size. This implies that sensors exist to couple growth to initiation of DNA replication; in other words, cells possess a mechanism to ensure that a new cell cycle does not occur until they have acquired the components required to generate a new cell. The existence of means for size control is intuitive. Small random asymmetry in cell division can create variability in cell size throughout a population. If no mechanism for size control existed, over time increasingly small and large cells would be generated by chance (i.e. the variance of cell sizes would increase over time). However, this is not observed, suggesting that size is regulated.

Genetic studies in yeast have implicated several proteins in size sensing. In the fission yeast *Schizosaccharomyces pombe*, cell size is sensed physically. As the cell elongates, membrane bound Pom1 kinase is separated in space from its cytosolic substrates, resulting in the inhibition of Wee1, a protein that prevents the G2/M transition (Moseley et al., 2009). In *S. cerevisiae*, biosynthesis itself is sensed and cells must acquire sufficient mass to pass Start in the cell cycle. One size-determining mechanism senses protein synthesis rate (Turner et al., 2012); the short-lived cyclin Cln3 is synthesized at rates closely

20

linked to cell size, allowing its synthesis to serve as a readout of cell size. Cln3 acts to relieve inhibition of the G1/S transition by Whi5, allowing cells to proceed with DNA replication and cell division once a minimum size is reached. Recent work, however, has argued that the more relevant parameter is dilution of Whi5 as cell size increases (Schmoller et al., 2015). Protein synthesis appears to be an important input to cell size control in mammalian cells as well. The mammalian target of rapamycin complex 1 (mTORC1) has been shown to control cell size through its dual effects on protein synthesis rate (Fingar et al., 2002).Ribosome biogenesis itself plays also a role in determining the size of both yeast and mammalian cells (reviewed in Jorgensen and Tyers, 2004).

Whether mammalian cell size is sensed as strictly as in yeast has been the subject of intense debate (Conlon and Raff, 2003; Cooper, 2004; Sveiczer et al., 2004; reviewed in Jorgensen and Tyers, 2004). Central to this debate is the question of whether the mass of a mammalian cell increases linearly or exponentially with time. Exponential mass increase requires that larger cells gain mass more rapidly, which might be expected if newly synthesized mass itself has the ability to produce new mass (i.e. contains ribosomes). An understanding of size sensing in mammalian cells is complicated by the fact that different cell types could acquire mass differently and that this can also be growth-factor controlled. Hepatocytes in re-fed mice, for example, acquire mass at a linear rate independent of their size (Conlon and Raff, 2003). Conversely, Dolznig et al. demonstrated that for chick erythroblasts and mouse fibroblasts whose size could be genetically manipulated, larger cells synthesize protein more quickly and spend less time in G1 (Dolznig et al., 2004). Any model to explain mammalian cell size control must also account for differences in cell size, addressing why the size threshold differs between cell types.

Collectively, size control mechanisms allow proliferating cells to sense their composition by providing a readout of macromolecule synthesis. This allows the macromolecular requirements for proliferation to be met before a cell commits to dividing. Mammalian cells use a variety of biosynthetic pathways to meet this demand by making use of the available nutrients, and regulatory mechanisms link this biosynthesis to cues promoting growth and division.

Nutrient sources contributing to macromolecule precursors

Nutrient environment, cell type, and growth signals can each influence how a cell generates the macromolecule precursors it requires to proliferate. Both *in vivo* and *in vitro*, mammalian cells are exposed to complex nutrient environments (Mayers and Vander Heiden, 2015), and multiple pathways exist to generate amino acids, nucleotides, and lipids. As a result, the nutrients that contribute to synthesis of a given macromolecule can vary substantially. The pathways proliferating cells commonly use to generate these precursors are described below.

Amino acids

Protein represents the largest fraction of cell mass, and acquisition of amino acids is therefore the primary biosynthetic requirement of cells. Cells can acquire amino acids through a variety of means, and cell type, environment, and genetics determine which pathways are used. Mammalian cells can synthesize non-essential amino acids *de novo* but must obtain essential amino acids from the extracellular environment (**Figure 3**). In nutrient rich conditions, uptake of essential amino acids is correlated with protein synthesis rates, indicating that these amino acids are not catabolized and only supply material for protein synthesis (Dolfi et al., 2013; Hosios et al., 2016). Human plasma contains each of the twenty amino acids at concentrations ranging from 10-600 µM (see Appendix A). Some amino acid concentrations are much less in other bodily fluids, such as cerebrospinal fluid (McGale et al., 1977), and the availability of essential amino acids may limit proliferation of cells in these contexts. Free amino acids supplied by plasma can be derived from the diet as well as protein breakdown or synthesis in the liver (Mayers et al., 2014), and cells in the tumor microenvironment can be exposed to free amino acids generated by local protein breakdown (Hirayama et al., 2009; Kamphorst et al., 2015).

In some contexts, cells synthesize amino acids to fulfill their requirement for protein synthesis, and glucose is the source for several of these non-essential amino acids (**Figure 3**). Mammalian cells with high glycolytic flux excrete alanine in addition to lactate, albeit at lower rates (DeBerardinis et al., 2007;
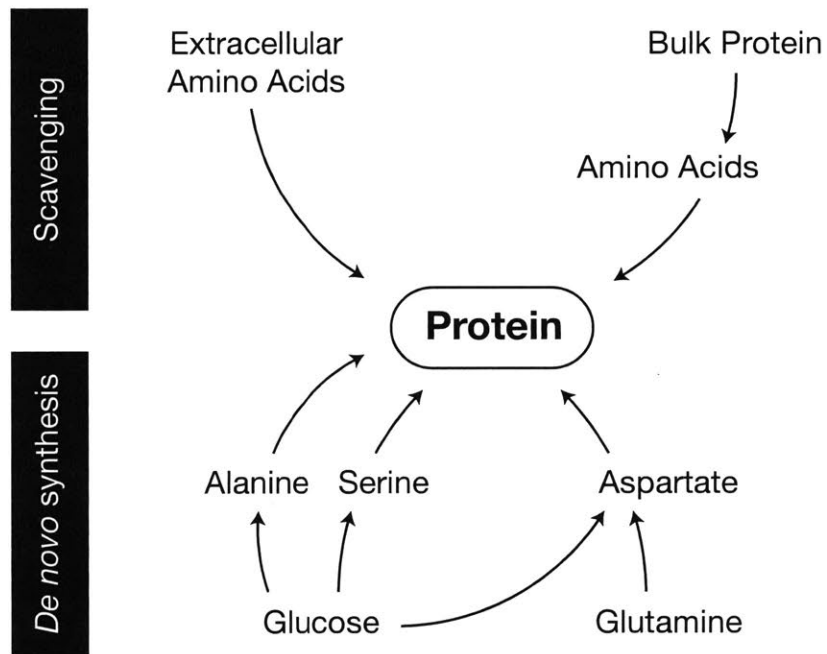
Figure 3: Selected de novo and scavenging pathways contributing amino acids for protein synthesis.

Jain et al., 2012). Proliferating cells are therefore rarely limited for alanine, and most media formulations

exclude this amino acid. Alanine is not always synthesized in excess of a cell's needs, however, and

Chuang *et al.* (1990) observed enhanced lymphocyte proliferation when alanine was added to their

growth medium. Sousa *et al.* (2016) found that pancreatic cancer cells consume alanine produced by

pancreatic stellate cells when grown in a minimal medium *in vitro*, indicating the potential for a metabolic

interaction *in vivo*. Another pathway supported by rapid glycolytic flux is the serine biosynthesis

pathway. Serine is generated from glycolytic intermediates through several reactions, the first of which is

catalyzed by phosphoglycerate dehydrogenase (PHGDH). Even though serine can be acquired from

exogenous sources, *de novo* synthesis is advantageous in some contexts. For example, PHGDH

expression is elevated in some cancers (Locasale et al., 2011; Pollari et al., 2011; Possemato et al., 2011)

and this correlates with an increased rate of serine synthesis. Overexpression of this enzyme is growth

promoting, although the mechanism remains debated (DeNicola et al., 2015; Locasale et al., 2011;

Possemato et al., 2011). Intracellular serine is derived from both *de novo* synthesis and consumed serine,

and whether the source influences serine's fate is unclear. Serine can provide carbon for nucleotide

biosynthesis (discussed further below) and is catabolized to produce glycine. Glycine can also be derived

from exogenous sources, but many cells in culture rapidly consume serine to produce glycine and only

use exogenous glycine when their serine supply is exhausted (Labuschagne et al., 2014). Some cells are

sensitive to deprivation of serine and glycine (Maddocks et al., 2013), indicating that both amino acid

consumption and *de novo* synthesis are required to fulfill the biosynthetic requirement for these amino

acids and maximize proliferation.

Serine serves a further role in protein synthesis as it can also be used to synthesize cysteine via

the transsulfuration pathway. Cysteine can therefore be obtained exogenously or by *de novo* synthesis

from glucose or exogenous serine. The transsulfuration pathway combines serine with homocysteine to

produce cystathionine, which is cleaved by cystathionase to generate cysteine. Not all proliferating cells

are capable of *de novo* cysteine synthesis, and some are auxotrophic for this amino acid, requiring an

exogenous source. Cystathionase activity is not detected in fetal tissue, for example, and appears only

after birth in mammals (Gaull et al., 1972). Cells in culture exhibit variable dependence on this pathway, and in some cases cysteine deprivation can be rescued with cystathionine or homocysteine, depending on which enzymes they express (Eagle et al., 1966). As a result, cell type and gene expression play significant roles in determining how a cell obtains the cysteine it requires for protein synthesis.

When glutamine is used by proliferating cells, it can supply carbon and nitrogen for synthesis of glutamate, aspartate, asparagine, and proline, fulfilling a substantial amino acid requirement in these cells (Hosios et al., 2016). Glutaminolysis is sufficient to sustain biosynthesis of these amino acids, and they are often excluded from culture media (DeBerardinis and Cheng, 2010; Eagle et al., 1956b). Glutaminase activity produces glutamate, which can serve as a nitrogen donor for transamination reactions in the biosynthesis of other amino acids, such as serine and alanine. In their study of pancreatic cancer cell metabolism, Sousa *et al.* (2016) observed that providing cells with alanine promoted serine biosynthesis, and this is likely because alanine production as a major fate of glutamate nitrogen was blocked. Amino acid synthesis downstream of glutamine has other advantages as well. For example, proline synthesis from glutamine is upregulated by oncogenic signalling to promote proliferation of lymphoma cells (Liu et al., 2015).

Unlike other amino acids, which can be used by cells when supplied exogenously, aspartate is necessarily synthesized *de novo*: most cells (except in the prostate and nervous system) lack high-affinity transporters for aspartate, and plasma aspartate concentrations (typically 20 µM or less) are insufficient to enable its consumption (Birsoy et al., 2015; Franklin et al., 2006). Supraphysiological concentrations of aspartate are needed to rescue proliferation of cells incapable of synthesizing it *de novo* (Sullivan et al., 2015). Aspartate can be synthesized from glutamine carbon, but as discussed above, glutaminolysis is not observed in all proliferating cells. In cases where glutamine is not used, glucose provides carbon to the TCA cycle via pyruvate carboxylase and pyruvate dehydrogenase (Davidson et al., 2016; Hensley et al., 2016; Sellers et al., 2015). In this context, amino acids other than glutamine can provide nitrogen atoms to glutamate to support transamination reactions (Mayers et al., 2016).

While an exogenous supply of many non-essential amino acids is dispensable for proliferation, proliferating cells can become auxotrophic for asparagine or arginine. In some contexts, cells are unable to synthesize sufficient quantities of these amino acids to meet their biosynthetic demands, and depletion of these amino acids can impair proliferation. Asparaginase is a bacterial enzyme used to treat patients with acute lymphoblastic leukemia (Masetti and Pession, 2009). The enzyme hydrolyzes plasma asparagine, thereby starving cells of this amino acid, arguing that cells sensitive to this treatment are asparagine auxotrophs. Why cells have impaired asparagine synthesis is unclear, but this may help to preserve intracellular aspartate pools. Studies have also identified a variety of tumors that are arginine auxotrophs. This amino acid is non-essential for adult humans, but some cells are unable to synthesize arginine *de novo*. As with cysteine, some cells auxotrophic for arginine can proliferate in its absence if provided with either of its precursors, citrulline and ornithine, which are present in plasma at levels comparable to other amino acids (see Appendix A) (Morgan et al., 1958). Some cancers are unable to synthesize arginine because they have lost expression of argininosuccinate synthase (ASS), an enzyme required for arginine synthesis. ASS consumes aspartate, and loss of its expression may serve as a means of preserving cellular aspartate pools (Rabinovich et al., 2015). Cancers lacking fumarate hydratase have high levels of fumarate, which can drive ASS in reverse, consuming arginine and effectively making cells arginine auxotrophs. Arginine deiminase, an enzyme that can deplete extracellular arginine, is being tested for efficacy against these cancers (Phillips et al., 2013).

In addition to *de novo* synthesis and consumption of exogenous amino acids, proliferating cells can consume and hydrolyze extracellular protein as a source of amino acids. Macropinocytosis, the non-specific uptake of protein, provides a source of amino acids to cells and enables them to survive starvation of individual essential amino acids when protein is abundant (Commisso et al., 2013; Kamphorst et al., 2015). The lysosome degrades consumed protein to produce individual amino acids, which can then be used by cells for biosynthesis. Although this process is non-specific, the high abundance of albumin in plasma and interstitial fluid makes it a primary substrate of this pathway (Commisso et al., 2013).

Proliferating cells have a considerable requirement for protein synthesis and as a result must

acquire amino acids necessary to meet this demand in order to grow and divide. Essential amino acids are

consumed from the extracellular environment or could be obtained by macropinocytosis, whereas non-

essential amino acids can also be acquired by *de novo* synthesis from glucose or glutamine. Cell type and

extracellular environment both influence how amino acids are acquired, and this can affect both protein

synthesis as well as other biosynthetic reactions requiring amino acids.

Lipids

Lipids are a diverse class of non-polar molecules, and their synthesis imposes a complex

biosynthetic demand for proliferating cells (Baenke et al., 2013). Lipids comprise 50% of membrane

mass, where they enable the separation of organelle contents and the intracellular and extracellular

environments, and they are also critical components of multiple signalling pathways. Synthesizing

membranes of the correct composition is critical for cell function (Simons and Sampaio, 2011; Thibault et

al., 2012). In mammalian cells, membrane lipids primarily comprise cholesterol, phospholipids, and

sphingolipids. Fatty acids are core components of these latter two classes and are also present in cells as

triglycerides. Each lipid species can be acquired exogenously or synthesized *de novo*, and nutrient supply

and growth conditions influence how cells meet this biosynthetic demand **(Figure 4)**.

A large fraction of cellular lipids are derived from the extracellular environment (Hosios et al.,

2016; Yao et al., 2016). Early work with proliferating lymphocytes demonstrated that exogenously

supplied free fatty acids are incorporated into the lipid pool in these cells (Ardawi and Newsholme, 1984).

Circulating free fatty acid levels increase when esterified fatty acids stored in adipose tissue are

hydrolyzed (Duncan et al., 2007). Breast and ovarian cancer cells stimulate lipolysis in co-cultured

adipocytes and can consume the released fatty acids (Balaban et al., 2017; Nieman et al., 2011). In other

contexts, fatty acid transport promotes cancer cell proliferation, and recent work has shown that

expression of the fatty acid receptor (and transporter) CD36 facilitates metastasis (Pascual et al., 2017).

Free fatty acids are not the only source of exogenous fatty acids. Kamphorst *et al.* (2013) observed that
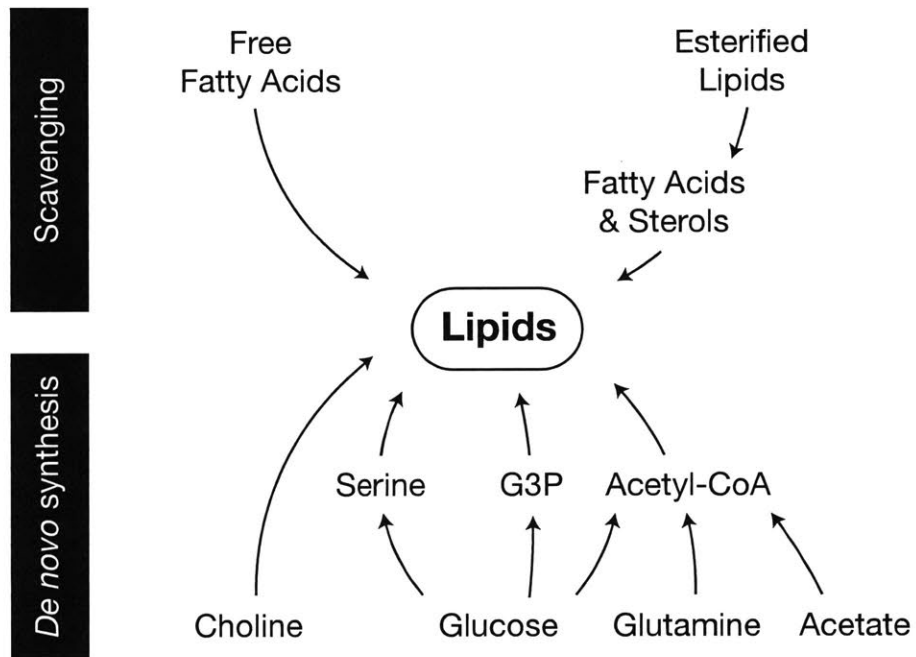
Figure 4: De novo and scavenging pathways contributing to the cellular lipid pool.

hypoxic cells and cells expressing activated Ras mutants utilize lysophospholipids present in serum as a source of unsaturated fatty acids. Lipids are carried through plasma bound to albumin or in lipoproteins, and cells can use free fatty acids and esterified lipids from these complexes as well. Lymphocytes and fibroblasts express lipoprotein lipase, allowing them to consume and hydrolyze triglycerides as a source of fatty acids for biosynthesis (Calder et al., 1994; Oram et al., 1980), and some cancers express other lipases to utilize exogenous esterified lipids (Zaidi et al., 2013).

Although a large portion of cellular lipids originate from exogenous sources (Hosios et al., 2016; Yao et al., 2016), lipids synthesized *de novo* are derived mainly from glucose carbon (Kamphorst et al., 2013). Active lipogenesis was first observed in tumor tissue slices by Medes *et al.* (1953), who noted that hepatomas incorporated more glucose into lipids than adjacent liver tissue. Pyruvate generated by glycolysis is decarboxylated by pyruvate dehydrogenase (PDH) in the mitochondria to produce acetyl-CoA, the basic component of lipids. Citrate synthase combines this acetyl-CoA with oxaloacetate to produce citrate, which can be exported from the mitochondria and cleaved by ATP-citrate lyase (ACLY) to generate cytosolic acetyl-CoA. In the cytosol, acetyl-CoA is used for *de novo* synthesis of palmitate (by fatty acid synthase, FASN) and cholesterol. Acetyl-CoA is also used for fatty acid elongation, and cellular fatty acids are diversified through elongation and desaturation reactions. Sterols can be esterified to fatty acids, increasing their complexity as well. Many cancers upregulate enzymes required for *de novo* lipid synthesis, and there is current interest in targeting these enzymes, in particular FASN, therapeutically (reviewed in Svensson and Shaw, 2017).

Glucose is not always the primary source of lipogenic acetyl-CoA. When cells are subject to mitochondrial inhibition, either as a result of hypoxia or genetic alterations, glutamine can serve as a source of acetyl-CoA for *de novo* lipid synthesis (Metallo et al., 2012; Mullen et al., 2012; Wise et al., 2011). Reductive carboxylation of glutamine-derived α-ketoglutarate by isocitrate dehydrogenase (IDH) produces citrate, which can be cleaved by ACLY to generate acetyl-CoA. PDH flux is reduced in hypoxic cells, decreasing the availability of glucose-derived acetyl-CoA (Kim et al., 2006). The hypoxia-sensing pathway in mammals, requiring hypoxia inducible factor (HIF), contribute to this metabolic change, and

constitutive HIF activation in some cancers allows them to derive lipids from glutamine when oxygen is abundant (Gameiro et al., 2013; Metallo et al., 2012). Cells proliferating with ample oxygen can also derive acetyl-CoA from glutamine, but it is not the primary contributor to lipid synthesis in this context. Mammalian cells express three IDH isoforms, and reductive carboxylation can be carried out by IDH1 and IDH2, which localize to the cytosol and mitochondria respectively. Some controversy exists as to which isoform primarily enables glutamine-derived lipogenesis; studies have argued for IDH1 (Metallo et al., 2012), IDH2 (Wise et al., 2011), or neither being predominant (Filipp et al., 2012; Mullen et al., 2012). Of note, it remains unclear whether reductive carboxylation flux is enhanced when mitochondria are impaired or if its relative contribution to lipogenesis increases due to a paucity of glucose-derived acetyl-CoA, although some have argued that decreased citrate levels are a determining factor (Fendt et al., 2013; Gameiro et al., 2013).

Free acetate can also serve as an additional lipogenic substrate for proliferating cells. Acetate can contribute to lipogenic acetyl-CoA when oxygen is abundant, but its contribution is increased in low oxygen (Comerford et al., 2014; Kamphorst et al., 2014; Schug et al., 2015). Similar to glutamine, it is unknown if active upregulation causes this increase in relative contribution or if it is the result of the lower relative contribution of glucose. Acetyl-CoA synthetases (ACSS) are required to convert acetate to acetyl-CoA, and cytosolic ACSS2 is the primary enzyme that supplies acetate for lipid biosynthesis (Comerford et al., 2014). Acetate concentration determines how much this substrate is used for lipogenesis (Kamphorst et al., 2014), and it is present in human plasma at 50-200 μM (Hosios and Vander Heiden, 2014; Schug et al., 2016), which is lower than concentrations often used experimentally. Free acetate in cells is predominantly generated by protein deacetylation, and a major role of ACSS is to salvage this acetate (Bulusu et al., 2017), raising the possibility that utilization of exogenous tracer acetate for biosynthesis is, in part, a readout of exchange between extracellular and intracellular acetate pools. Exchange explains labeling from tracer acetate when cells do not net consume acetate. Other nutrients, such as ketogenic amino acids, can provide acetyl-CoA for lipid biosynthesis, but this is not often seen in proliferating cells *in vitro*. Recent work, for example, demonstrated that 3T3-L1 cells begin to use branch

30

chain amino acid carbon for fatty acid synthesis following *in vitro* differentiation into adipocytes (Green et al., 2016). Ketone bodies have also been observed to contribute to lipid pools in some contexts, such as in brains of neonatal rodents (Patel and Owen, 1976).

Cells can acquire fatty acids from different sources; however additional molecules are required to synthesize the complex lipid species required by cells to proliferate. Fatty acids are esterified to glycerol-3-phosphate (G3P) to produce phospholipids and triglycerides, for membrane biogenesis and lipid storage respectively. G3P is generated by the phosphorylation of exogenous glycerol or by the reduction of the glycolytic intermediate dihydroxyacetone-phosphate, and proliferating cells may obtain glycerol from both sources (Harding et al., 1975). Phospholipids also contain polar head groups (choline, ethanolamine, serine, and inositol), which can also be scavenged or synthesized *de novo*. The sources of serine can vary (see above), and phosphatidylethanolamine (PE) can be synthesized from phosphatidylserine by decarboxylation. Conversely, choline, the most common phospholipid head group, is typically essential for cultured cells (van Meer et al., 2008; Yamamoto and Niwa, 1993). In the body, it is commonly obtained from the diet or methylation of PE to phosphatidylcholine (PC), but this reaction is insufficient to sustain cell-autonomous proliferation in culture. PC is readily produced by the liver, and choline may therefore rarely be limiting for cells in tissues. Inositol can be synthesized from glucose, and proliferating cells exhibit variable dependence on an exogenous supply of this nutrient (Eagle et al., 1956a).

A final important class of lipids derived from fatty acids is sphingolipids. Sphingolipids are synthesized at a minimum from palmitate and serine but can gain additional complexity from the addition of a second fatty acid, phosphate, and/or polar head groups. These molecules have important functions in cell signalling (Merrill, 2002), and inability to synthesize these molecules can impair proliferation through downstream signalling pathways (Lee et al., 2011).

Lipids can be obtained from both exogenous sources and *de novo* synthesis. For many cells proliferating in culture, *de novo* lipid synthesis is sufficient to fully support proliferation, as these cells can grow in lipid-free conditions. Conversely, lipids are abundant in the plasma, and proliferating cells are thought to rarely be deficient for lipids in animals. Therefore, which sources contribute to cellular

lipid mass and how *de novo* synthesis supports proliferation is still an open question. Understanding the interplay of consumed and synthesized lipids will provide insight into how cells acquire the mass they need to proliferate.

Nucleic acids

Nucleic acids are another integral biosynthetic requirement of proliferating cells. DNA is necessarily synthesized during the cell division cycle, and RNA, the majority of which is ribosomal, is important for synthesis of protein required to complete the cell growth cycle. Nucleotides are the precursors for nucleic acid synthesis but also serve as cofactors for many redox, energetic, and biosynthetic reactions. As with amino acids and lipids, nucleotides can be derived from *de novo* synthesis or an exogenous supply (**Figure 5**). Many extant cancer therapies target *de novo* nucleotide synthesis pathways, and their ability to impair the proliferation of both cancer and normal cells underscores the essentiality of *de novo* nucleotide synthesis (Martinez-Outschoorn et al., 2017; Vander Heiden, 2011). All nucleotides are composed of a purine or pyrimidine base joined to ribose (or deoxyribose), which is derived from ribose-5-phosphate (R5P). Free ribose can be scavenged and phosphorylated by only a minority of cell types, and R5P is therefore synthesized from glucose by most cells (Agranoff and Brady, 1956; Eagle et al., 1958). R5P can be generated through either the oxidative or non-oxidative pentose phosphate pathways, and recent work has identified cues, such as increased p53 and mTORC1 activity, that can enhance flux through these pathways (Bensaad et al., 2006; Duvel et al., 2010). The oxidative pathway is expected to be the primary source of R5P for biosynthesis in most proliferating cells (Lee et al., 1998; Reitzer et al., 1980).

Nucleotide base biosynthesis is closely linked to amino acid metabolism, requiring both amino acids themselves and one-carbon units generated by their catabolism (**Figures 1,5**). Purine bases incorporate glycine, derive additional carbon atoms from carbon dioxide and the one-carbon pool, and obtain their remaining nitrogen atoms from aspartate and glutamine. Pyrimidine bases are synthesized from aspartate, with additional nitrogen atoms from glutamine and a carbon atom from carbon dioxide.

32
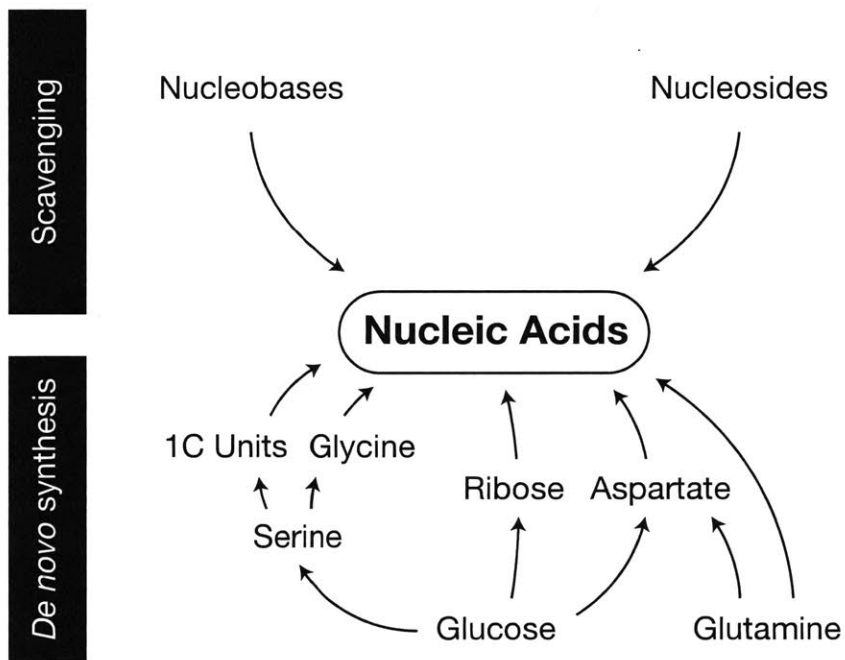
Figure 5: De novo and salvage pathways that generate nucleotides for nucleic acid synthesis.

Thymidine nucleotide synthesis requires another one-carbon unit. Consequently, the modes of acquiring amino acids described above have a direct impact on nucleotide biosynthesis as well, dictating whether purine and pyrimidine bases derive entirely from glucose or incorporate material from exogenous amino acids.

One-carbon units, individual carbon atoms covalently linked to a folate cofactor, are required for both purine and pyrimidine biosynthesis pathways. Proliferating cells primarily catabolize serine for one-carbon units to sustain nucleotides synthesis (Labuschagne et al., 2014; Mattaini et al., 2016). As with protein synthesis, this serine can be derived from glycolytic carbon or from an exogenous source (Maddocks et al., 2013). Recent work has highlighted the importance of mitochondrial function in one-carbon metabolism, and Lewis *et al.* (2014) demonstrated that serine is catabolized in the mitochondria to yield one-carbon units for nucleotide synthesis. When mitochondria are inhibited, however, the cytosol becomes the more important source of one-carbon units (Bao et al., 2016). Many cells use serine catabolism as a source of glycine as well. Glycine catabolism may also serve as a source of one-carbon units in some contexts, but this is likely not used to sustain nucleotide biosynthesis in most proliferating cells (Fan et al., 2014; Jain et al., 2012). Jain *et al.* surveyed nutrient consumption across the NCI-60 panel of cell lines, and observed that glycine consumption was most strongly correlated with proliferation rate. Importantly, they observed only direct incorporation of glycine into purines with no contribution to the one-carbon pool. Subsequent work has argued that glycine consumption correlates best with DNA synthesis rate rather than the acquisition of cell mass (Dolfi et al., 2013), underscoring the importance of glycine metabolism to nucleotide synthesis.

Serine sits at the intersection of multiple biosynthetic pathways, and how proliferating cells acquire this amino acid informs how they generate many macromolecule precursors. In addition to serine and glycine, aspartate is also required for synthesis of both purines and pyrimidines. As discussed above, aspartate must be synthesized *de novo*, and limitation for this amino acid impairs both nucleic acid and protein biosynthesis. Aspartate synthesis critically depends upon sustained mitochondrial activity, and cells are unable to proliferate due to aspartate auxotrophy when mitochondria are inhibited (Birsoy et al.,

2015; Sullivan et al., 2015). Interestingly, Sullivan *et al.* observed that aspartate is limiting for nucleotide synthesis sooner than for protein synthesis, and cells unable to synthesize aspartate take longer to arrest growth when adenine and uracil are supplied exogenously.

This result demonstrates that although cells can generate nucleotides from *de novo* synthesis pathways, they can use nucleosides or nucleobases provided in the extracellular environment. Indeed, mammalian cells possess salvage pathways that can generate nucleotides to support proliferation in some contexts. Tissues capable of salvage are resistant to nucleotide synthesis inhibitors, which can otherwise hinder proliferation (DeLapp and Karasek, 1976). Nevertheless, the concentrations of nucleosides and their bases in human plasma are rarely greater than ~10 µM (reviewed in Traut, 1994), raising the possibility that some cells *in vivo* cannot sustain proliferation through nucleotide salvage alone. This is corroborated by the insufficiency of circulating nucleosides to rescue proliferation in many cases when cells *in vivo* are treated with nucleotide synthesis inhibitors. Consequently, *de novo* biosynthesis is an essential source of nucleotides for many proliferating cells. These synthetic pathways depend on a source of ribose, amino acids, and one-carbon units, and different cell types in different contexts appear to meet these requirements differently.

Nutrient consumption

Before nutrients can be used to synthesize macromolecule precursors, they must be taken up from the extracellular environment. Mammalian cells express a wide number of solute carrier (SLC) proteins that transport specific molecules or groups of related molecules across the plasma membrane. Proliferating cells often upregulate specific SLC proteins, enhancing their ability to acquire the material needed to synthesize new cell mass. Protein systems that enable transport of glucose, amino acids, and other nutrients are described below.

Glucose is transported into cells by GLUT (SLC2 family) proteins, which allow glucose to cross the cell membrane but cannot concentrate it in cells. Glucose import is driven by abundant intracellular hexokinase activity that phosphorylates consumed glucose, trapping it within cells. This ensures that the glucose concentration is considerably lower inside cells than outside. Hexokinase activity is increased in proliferating cells, such as mitogen-stimulated lymphocytes (Brand, 1985), to enable rapid glycolytic flux. Similarly, elevated expression of hexokinase and glucose transporters is important for the rapid proliferation of cancer cells (reviewed in Vander Heiden, 2011). GLUT1 (SLC2A1) is a widely expressed high-affinity glucose transporter that is expressed by many proliferating cells to obtain glucose for glycolytic and biosynthetic metabolism. This transporter is commonly expressed in proliferating cells, such as cancer and fetal cells (Mueckler and Thorens, 2013; Yamamoto et al., 1990), and its expression is downstream of growth factor receptors and is induced in growth factor-stimulated lymphocytes (Rathmell et al., 2000; Vander Heiden et al., 2001).

To obtain the amino acids required for biosynthesis of protein, nucleotides, and lipids, cells express members of several SLC families. Within these families, a given transporter often acts on multiple amino acid substrates, and multiple transporters can transport any given amino acid. Unlike GLUT proteins, these transporters typically transport multiple molecules simultaneously. In cases where amino acid import is coupled to ion transport, the process becomes energetically favourable, and amino acids can be concentrated in cells. Many members of the amino acid transporter families SLC1, SLC7, SLC36, and SLC38 co-transport sodium, potassium, or a proton to drive amino acid transport. Some amino acid transporters (including both those that do and do not co-transport ions) are obligate amino acid exchangers, importing one amino acid while concomitantly exporting another. These transporters cannot *net* import amino acids and instead serve to equilibrate the amino acid pools inside and outside the cell(Zerangue and Kavanaugh, 1996), which can ensure that all amino acids are available for protein biosynthesis (Pochini et al., 2014). Proliferating cells employ a variety of amino acid transporters to meet their biosynthetic requirements, and both cancer cells and dividing lymphocytes increase their capacity for amino acid transport (Segel and Lichtman, 1981; reviewed in Bhutia et al., 2015).

36

Other macromolecule precursors have specific transporters as well. Two classes of transporters are responsible for nucleoside salvage: equilibrative nucleoside transporters (ENT, SLC29) and concentrative nucleoside transporters (CNT, SLC28) (Young et al., 2013). Like GLUT proteins, ENT proteins allow nucleosides and nucleobases to cross membranes but cannot concentrate them within cells. CNT proteins typically have higher affinity for their substrates and couple nucleoside import to sodium import, allowing them to concentrate nucleosides in cells. Many proliferating cells express ENT and CNT proteins, and their expression can increase in cells exposed to proliferative stimuli (Pastor-Anglada et al., 2007).

Pyruvate and lactate are transported by monocarboxylate transporters 1-4 (MCT, SLC16), which co-transport a proton with their substrates (Halestrap, 2013). Whether these substrates are imported or exported depends on their intracellular and extracellular concentrations as well as the pH of each compartment. Consequently, MCT expression may support proliferation by allowing cells to consume these molecules as nutrients or to excrete them as waste products. For example, MCT proteins export the large amounts of lactate generated by aerobic glycolysis, enabling this growth-supporting pathway. MCT1 and 4 are upregulated in many cancers, and MCT inhibitors can have antiproliferative effects in both cancer and normal cells (Halestrap, 2013; Murray et al., 2005). MCT1 may also transport acetate, when it is available, to support proliferation (Schug et al., 2016).

Lipids are imported by a variety of mechanisms, either as single molecules or in bulk. Fatty acid translocase (CD36) binds individual fatty acids, allowing cells to consume them from the extracellular environment (Goldberg et al., 2009), and SLC27 family members have also been implicated in fatty acid uptake (Anderson and Stahl, 2013). Plasma lipids are typically albumin-bound or contained within lipoproteins (large complexes of triglycerides, cholesterol, and proteins), and lipases are required to liberate lipoprotein lipids to enable transport of individual molecules by CD36 (Goldberg et al., 2009). Alternatively, whole lipoproteins can bind to plasma membrane receptors and be taken up by receptor-mediated endocytosis.

Transporters play an important role in determining which nutrients proliferating cells use to synthesize macromolecule precursors. These proteins have different substrates and varying affinities for them, so which transporters are expressed can influence which nutrients are consumed. Additionally, nutrients are present at different concentrations in the extracellular space, and both the relative affinities of a given transporter for the available nutrients and the concentrations of those nutrients will dictate which molecules are efficiently transported. Transporters collectively dictate which nutrients are available to biosynthetic pathways and, therefore, influence how cells derive the macromolecule precursors needed to synthesize new cell mass.

Regulation of biosynthesis and metabolism

The pathways a cell uses to generate new cell mass are not fixed, nor are they necessarily constitutively active. Proliferating cells possess a variety of mechanisms to regulate their biosynthetic pathways, whose flux can vary dependent on progress through the cell cycle, the activities of signal transduction pathways, and the availability of macromolecule precursors.

Coordination with the cell cycle

Acquisition of new cell mass (growth) and cell division must both occur during the cell cycle for cells to proliferate successfully. The cell cycle consists of two growth phases in which cell mass accumulates (G1 and G2), a DNA replication phase (S), and a phase of physical cell division (M). A cell's metabolic requirements, as a result, are not necessarily constant throughout this cycle. This has been best studied in *S. cerevisiae* (Cai and Tu, 2012; Futcher, 2006). When grown in nutrient-limited conditions, yeast undergo a metabolic cycle that is coordinated with cell division (Tu et al., 2005). The metabolic cycle consists of oxidative and reductive phases, defined respectively by periods of high and low oxygen consumption and low and high fermentation. McKnight and colleagues demonstrated that

DNA replication is confined to the reductive phase of the metabolic cycle possibly to reduce the risk of oxidative DNA damage that is more likely to occur when oxygen consumption is high (Chen et al., 2007). They subsequently observed that intracellular levels of metabolites peak at different points during the metabolic cycle: glycolytic intermediates and nucleotides were more abundant during the reductive phase, and TCA cycle intermediates were elevated during the oxidative phase (Tu et al., 2007). Yeast cells also coordinate carbohydrate storage with their cell cycle. Cdk1 activity, which controls cell cycle progression in yeast, is required for liquidation of sugar stores to fuel biosynthesis at defined points in the cell cycle (Ewald et al., 2016; Zhao et al., 2016).

Mammalian cells also coordinate metabolic pathway activities with cell cycle progression. As in yeast, oxygen consumption can vary over the course of the mammalian cell cycle and was observed to peak in late S phase in CHO cells (Lai et al., 1982). Synthesis of macromolecule precursors and of macromolecules themselves is also not constant throughout the mammalian cell cycle (Kaplon et al., 2015). E2F, for example, is activated prior to the G1/S transition to regulate transcription of cell cycle genes, but its other targets include several metabolic enzymes. Metabolism can also be regulated non-transcriptionally. Studying HeLa cells *in vitro*, Colombo *et al.* (2011) observed that levels of glutaminase and phosphofructokinase peaked during G1, and this resulted in increased glutaminolysis and glycolysis, respectively. Degradation of these proteins is subject to cell cycle control, ensuring that levels of these enzymes and flux through their respective pathways decrease after cells exit G1. Many mammalian studies have relied on metabolic perturbations to synchronize the cell cycle of a population; however, these methods also alter metabolism to exert their effects on cell cycle progression. Alternative modes of synchronization will be required to delineate how metabolism varies throughout the cell cycle.

Regulation that coordinates metabolism with the cell cycle could be important to provide cells with the different macromolecule precursors required at specific times during the cell cycle. The yeast metabolic cycle, for example, enhances amino acid biosynthesis and ribosome biogenesis for protein synthesis during G1 and produces nucleotides for DNA synthesis during S phase (Cai and Tu, 2012).

Further work is needed to better understand regulation of metabolism through the mammalian cell cycle and the advantages this can provide to proliferating cells.

Growth factors and signalling pathways

Many signal transduction pathways link metabolic regulation to proliferation. In mammalian cells, these signalling pathways can be activated either by exogenous growth factors or by oncogenic mutations, inducing cell proliferation and an associated metabolic program. This regulation ensures that cells acquire the macromolecule precursors necessary to generate new mass to enable their proliferation. Extensive research in cancer metabolism has characterized metabolic alterations associated with the activation of specific signalling pathways, and this body of work is reviewed in detail elsewhere (Cairns et al., 2011; Iurlaro et al., 2014; Lunt and Vander Heiden, 2011; Vander Heiden and DeBerardinis, 2017). Signal transduction pathways can both enhance synthesis of macromolecule precursors and can also influence how cells obtain nutrients to fuel biosynthesis. Several examples are discussed below.

The PI3K/AKT/mTOR pathway controls a variety of metabolic processes used by proliferating cells. This pathway is regulated by growth factors in normal proliferating cells but is also activated by mutations in numerous cancers. AKT activation is sufficient to enhance glycolytic flux in mammalian cells, and this occurs both through increased expression of glucose transporters as well as post-translational regulation of glycolytic enzymes (reviewed in Cairns et al., 2011). As discussed, glycolytic flux itself may facilitate the synthesis of macromolecule precursors (Lunt and Vander Heiden, 2011; Newsholme et al., 1985b; Vander Heiden et al., 2009). mTORC1 activity downstream of AKT broadly regulates protein synthesis and other anabolic processes, but also controls biosynthetic metabolic pathways, such as *de novo* lipid and nucleotide synthesis (Duvel et al., 2010; Shimobayashi and Hall, 2014).

Activation of RAS signalling promotes proliferation as well as a variety of metabolic alterations. Like AKT signalling, RAS promotes glycolytic flux by increasing GLUT1 expression (Chen et al., 2001). Oncogenic RAS also increases the uptake of some extracellular lipids (Kamphorst et al., 2013) and may

40

enhance the ability of cells to scavenge bulk protein from the extracellular environment (Commisso et al., 2013; Pavlova and Thompson, 2016), potentially altering the sources of lipid and protein mass in cells. MYC, a transcription factor downstream of RAS and AKT, promotes cell proliferation and is activated in many cancers. MYC increases glutamine utilization in some contexts, allowing this nutrient to make a greater contribution to biosynthesis of macromolecule precursors (Altman et al., 2016; Yuneva et al., 2012).

These examples demonstrate that signalling pathways link proliferation and metabolism in multiple ways. Their activation causes cells to proliferate and to activate metabolic pathways to synthesize new cell mass. Additionally, specific signalling pathways can influence how cells synthesize macromolecule precursors, determining which nutrients are consumed and used for energy and biosynthesis.

Metabolite sensing

Signalling pathways allow cells to integrate extracellular signals and to produce intracellular responses. These signals include growth factors that induce cells to proliferate, and aberrant activation of cell signalling results in dysregulated proliferation in the context of cancer. Signalling pathways must also be able to sense nutrients: when cells are deprived of essential nutrients, they cease to proliferate, and when they are deprived of non-essential nutrients, they activate compensatory *de novo* synthesis pathways. These responses are necessary to ensure that cells do not proliferate unless they are able to obtain the macromolecule precursors necessary to synthesize new cell mass.

In mammalian cells, two systems are used to sense the presence of amino acids: mTORC1 and the amino acid response pathway (AAR). mTORC1 senses amino acid sufficiency; when amino acids are abundant, this kinase activates downstream biosynthetic pathways (such as protein synthesis) to generate new cell mass. Importantly, mTORC1 activity requires both adequate nutrients and upstream growth factors, allowing it to sense when conditions are appropriate to support proliferation (Laplante and Sabatini, 2012). Consequently, deprivation of amino acids in culture or fasting *in vivo* inhibits protein

synthesis downstream of mTORC1. Withdrawal of any single amino acid *in vitro* is sufficient to reduce activity of this pathway; however, depletion of leucine or arginine is particularly potent (Hara et al., 1998). Amino acid deprivation activates the AAR in both mammalian and yeast cells: uncharged tRNAs stimulate the kinase GCN2, resulting in the translation of transcription factor ATF4 (Kilberg et al., 2009). ATF4 has diverse transcriptional targets, which include amino acid transporters and enzymes involved in *de novo* amino acid synthesis. Activation of the AAR, therefore, allows cells to adapt to amino acid-depleted conditions and alter how they obtain this class of macromolecule precursors (Harding et al., 2003).

Lipids are sensed by SREBP proteins, a well-characterized set of transcription factors that enhance transcription of lipid biosynthesis genes when lipid abundance is reduced (Goldstein et al., 2006; Ye and DeBose-Boyd, 2011). SREBP1 isoforms preferentially promote expression of fatty acid synthesis genes and the mechanism of their activation is not fully understood; SREBP2, by contrast, senses cholesterol, and it more strongly enhances expression of sterol synthesis genes. These transcription factors are retained in the endoplasmic reticulum when lipids are abundant, but in conditions of lipid starvation, proteolytic cleavage liberates the transcription-activating portion of the protein. This allows cells to activate *de novo* lipid synthesis when extracellular lipids are not available.

Currently no detailed mechanisms have been described by which cells can sense nucleotide sufficiency. Since nucleotides can be derived from salvage as well as *de novo* synthesis, it is possible that there is crosstalk between these metabolic pathways. For example, inhibition of deoxyribonucleotide (dNTP) biosynthesis (but not DNA synthesis) increases expression of nucleoside transporters, suggesting that dNTP levels might be sensed by cells (Pressacco et al., 1995). Enzymes of *de novo* nucleotide biosynthesis pathways are subject to end-product feedback inhibition (Lane and Fan, 2015), providing a means of inhibiting synthesis when nucleotides are abundant.

To successfully grow and proliferate, a cell must acquire new protein, lipid, and nucleic acid mass, requiring specific nutrients to synthesize macromolecule precursors. Signalling pathways that sense these molecules allow cells to activate the appropriate *de novo* synthesis pathways and transporters when

42

their levels are insufficient to support biosynthesis. The metabolism of proliferating cells, therefore, is closely linked to proliferative cues themselves. Signalling pathways that stimulate proliferation also induce biosynthesis to support the required acquisition of new cell mass, and nutrient sensing provides feedback to ensure that biosynthesis keeps up with the demands of proliferation, allowing cells to grow and proliferate in concert.

Pyruvate kinase M2

One mechanism by which proliferating cells control biosynthetic flux depends upon the activity of the final step in glycolysis, catalyzed by pyruvate kinase. Pyruvate kinase is a highly regulated enzyme that plays a critical role in cellular metabolism. Mammals express four isoforms of this enzyme: PKL, PKR, PKM1, and PKM2. PKL and PKR are expressed from the *PKLR* gene, and their expression is largely confined to the liver and erythrocytes, respectively. PKM1 and PKM2 are encoded by *PKM* and their differential expression is the result of a mutually exclusive splicing event. The region coded by the alternately spliced exon confers unique biochemical properties to PKM1 and PKM2 (Noguchi et al., 1986), and which isoform is expressed profoundly influences cellular metabolism and proliferation (Israelsen and Vander Heiden, 2015; Mazurek et al., 2002).

Biochemistry

Pyruvate kinase carries out the last reaction in glycolysis, transferring a phosphate group from phosphoenolpyruvate (PEP) to adenosine diphosphate (ADP) to produce pyruvate and ATP (**Figure 6**). Completion of this step allows a cell to net generate two molecules of ATP per molecule of glucose metabolized. This reaction is highly energetically favourable and PEP dephosphorylation provides sufficient energy to drive ADP phosphorylation, which is otherwise unfavourable (Mazurek et al., 2002).
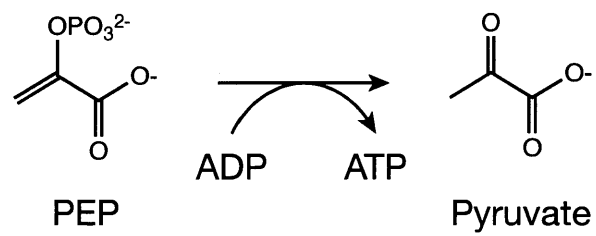
Figure 6: The reaction catalyzed by pyruvate kinase.

Pyruvate kinase transfers a phosphate from phosphoenolpyruvate (PEP) to adenosine diphosphate (ADP), yielding pyruvate and adenosine triphosphate (ATP).

Pyruvate kinases typically exist as monomers, dimers, and tetramers that are dimers of dimers, although whether the dimer is biologically relevant has been questioned (Anastasiou et al., 2012). Mammalian pyruvate kinases can form homo- and hetero-tetramers, and the distribution of complex compositions depends on the relative expression of each pyruvate kinase isoform (Cardenas and Dyson, 1978). PKM1 is a constitutive tetramer, but PKM2 can exist in different oligomeric states. PKM2 but not PKM1 tetramers exhibit positive cooperativity for PEP, allowing enzyme activity to be quite sensitive to PEP levels (Sparmann et al., 1973). Importantly, tetrameric pyruvate kinase is more active than monomeric pyruvate kinase (Ashizawa et al., 1991a), and inputs that regulate pyruvate kinase activity often enhance or weaken tetramer stability.

Most pyruvate kinases are allosterically activated by the upstream glycolytic intermediate fructose-1,6-bisphosphate (FBP) (Israelsen and Vander Heiden, 2015). This establishes feed-forward regulation in which this later glycolytic enzyme is more active when early glycolytic metabolites accumulate. In *S. cerevisiae*, for example, acute glucose starvation depletes cellular FBP, and this inhibits Cdc19 (yeast pyruvate kinase), resulting in a dramatic spike in PEP levels (Xu et al., 2012). In mammals, PKL, PKR, and PKM2 all bind to and are activated by FBP. Four molecules of FBP bind tetrameric PKM2 and serve to strengthen interactions at the dimer-dimer interface, stabilizing the enzyme in its most active oligomeric state (Anastasiou et al., 2012; Dombrauckas et al., 2005). When mammalian cells are acutely starved of glucose, FBP levels drop, and PKM2 rapidly dissociates into monomers, similar to what happens in yeast (Ashizawa et al., 1991b). By contrast, PKM1 is unable to bind FBP but is a constitutive tetramer with high activity. FBP binds stably to PKM2 tetramers and very slowly dissociates from this complex, but this dissociation is accelerated in the presence of phosphotyrosine-containing peptides (Christofk et al., 2008b). Growth factor (and oncogenic) signalling often increases tyrosine phosphorylation, and proliferative cues could, therefore, reduce pyruvate kinase activity in PKM2-expressing cells. PKM2 is also able to bind other allosteric effectors. Each PKM2 monomer contains an amino acid-binding pocket, which is distinct from the FBP binding site and exerts allosteric control on enzyme activity (Israelsen and Vander Heiden, 2015). Serine binds this site to activate PKM2, and

phenylalanine and alanine inhibit PKM2 by binding that site as well (Chaneton et al., 2012; Eigenbrodt et al., 1983; Sparmann et al., 1973). Succinylaminoimidazolecarboxamide ribose-5'-phosphate (SAICAR), a purine nucleotide precursor, is a recently identified allosteric activator of PKM2 (Keller et al., 2012), although its binding site has yet to be characterized. SAICAR levels were reported to rise after cells were starved of glucose, perhaps maintaining PKM2 activity when FBP is depleted. PKM2 can also be regulated by post-translational modifications. Tetramer formation is directly inhibited by lysine-305 acetylation, and FBP binding is blocked by acetylation of lysine-433 or phosphorylation of tyrosine-105 (Hitosugi et al., 2009; Lv et al., 2013; Wang et al., 2015).

PKM2 is a highly regulated enzyme, while PKM1 is less regulated and maintains constant high activity. The allosteric effectors of PKM2 link the enzyme's activity to multiple inputs including glucose availability, amino acid levels, nucleotide synthesis, and proliferative signalling. PKM2 activity is therefore intimately linked to cellular metabolism, particularly in proliferating cells. PKM2 plays a critical role in allowing cells to synthesize macromolecular precursors needed to proliferate, and the enzyme's unique biochemical properties appear to link PKM2 activity to cellular biosynthesis.

Role in cellular metabolism

PKM2 is expressed in cells with proliferative potential: in embryonic tissues, in tumors, and in cells proliferating *in vitro*. As a result, PKM2 is hypothesized to enable proliferative metabolism and biosynthesis (Mazurek et al., 2002). PKM2 is expressed in a variety of non-proliferating adult tissues as well and may promote glycolytic metabolism in these tissues (Dayton et al., 2016; Imamura and Tanaka, 1972). In either context, *PKM* isoform expression can influence cellular metabolism. Christofk *et al.* (2008a), for example, observed that, despite having similar glycolytic rates, cell lines engineered to exclusively express PKM2 produced more lactate and consumed less oxygen than those expressing only PKM1. This indicates that PKM2 facilitates aerobic glycolysis by influencing the fate of pyruvate, although how this occurs remains to be determined.

Beyond its effect on aerobic glycolysis, PKM2 expression has been observed to favor

biosynthesis of new cell mass in proliferating cells, and this is dependent upon regulation of PKM2 by its

allosteric effectors. Manipulations that increase phosphotyrosine peptide levels suppress PKM2 activity

and increase the flux of glucose carbon to lipid synthesis (Christofk et al., 2008b). PKM2 inhibition can

also increase the production of serine from glycolytic intermediates (Chaneton et al., 2012), and chemical

activators of PKM2 reduce serine biosynthesis, rendering cells auxotrophic for serine (Kung et al., 2012).

Because serine is itself a PKM2 activator, PKM2 will be less active in conditions of serine deprivation,

leading to increased *de novo* synthesis of this amino acid. Changes in PKM2 activity may also alter the

availability of glycolytic intermediates that feed other biosynthetic pathways (Anastasiou et al., 2012;

Hitosugi et al., 2009; Lunt et al., 2015; Mazurek et al., 2002). Treatment with a PKM2 activator or

overexpression of PKM1 reduces *de novo* nucleotide synthesis in primary MEFs, inhibiting their

proliferation (Lunt et al., 2015). An exogenous source of nucleosides rescues proliferation in these cells,

indicating that PKM2 plays a metabolic role to support proliferation. The mechanism connecting PKM2

to nucleotide auxotrophy remains unknown; however, allosteric regulation by SAICAR supports the link

between regulation of PKM2 activity and nucleotide biosynthesis.

Expressing PKM2 alters cell metabolism and facilitates increased biosynthetic flux. Regulation of

this enzyme's activity by allosteric effectors is essential, and the ability of these effectors to reduce

pyruvate kinase activity enables biosynthesis of macromolecule precursors. Because PKM1 has

constitutive activity, it is unable to fulfill this role. This model is consistent with the fact that PKM2 is the

predominant isoform expressed in proliferating tissues and provides a framework to consider the role that

PKM2 may play in cancer.

Role in cancer

PKM2 is expressed universally in cancers, and its expression enhances the production of

macromolecular precursors, suggesting that PKM2 expression allows for enhanced proliferation. In

support of this notion, proliferative signalling promotes splicing of the *PKM* transcript to generate PKM2-

encoding mRNA (David et al., 2010). Xenograft tumors derived from cell lines expressing exclusively PKM1 grow more slowly than those expressing PKM2, demonstrating that pyruvate kinase isoform can influence proliferation (Christofk et al., 2008a). Importantly, suppression of PKM1, rather than expression of PKM2, is growth-promoting: cells that express both PKM1 and PKM2 exhibit the same proliferation defect as those expressing exclusively PKM1, and PKM2 activators can also inhibit proliferation (Anastasiou et al., 2012; Lunt et al., 2015).

PKM2 may not be essential for proliferation. Indeed, knockdown of PKM2 or both PKM1 and PKM2 does not impair the growth of xenograft tumors (Cortes-Cros et al., 2013). Genetic deletion of the PKM2-specific exon similarly does not prevent or slow tumor growth in genetically engineered breast cancer mouse models (Israelsen et al., 2013). In this mouse model, PKM2 deletion results in reduced pyruvate kinase activity, and this residual activity stems from low levels of PKM1 expression that is largely confined to non-proliferating regions within the tumor. In fact tumors appear to select for loss of pyruvate kinase expression(Israelsen et al., 2013). These results are consistent with a model wherein proliferating cells express PKM2 because it can be allosterically inhibited; the resulting low pyruvate kinase activity promotes anabolic metabolism to enable rapid proliferation.

Some have argued that PKM2 instead is growth-promoting because of an essential non-metabolic role as a protein kinase (see Chapter 3). We have failed to reproduce this activity in a biochemical assay and do not expect it to be the primary function of PKM2 (Hosios et al., 2015). That PKM2 is essential neither for tumor formation nor for viability and development of normal mice argues against an essential role in proliferation (Dayton et al., 2016; Israelsen et al., 2013). Furthermore, when PKM2 loss is growth-inhibiting, it can often be explained by the resulting metabolic alterations (Lunt et al., 2015; Wang et al., 2014). The findings discussed above collectively imply that PKM2 plays an integral part in the metabolic program that supports rapid proliferation in mammals. PKM2 is linked to both aerobic glycolysis and anabolic pathways, and expression and regulation of this pyruvate kinase isoform enables cells to acquire the macromolecule precursors they need to generate new cell mass.

Energy and redox reactions impotant for biosynthesis

In addition the substrates used to generate cell mass, biosynthesis is also dependent on energy and cofactor recycling to enable reduction-oxidation (redox) reactions. The nutrients that cells consume not only provide biosynthetic material but must also fuel catabolic reactions that generate energy, collectively enabling anabolism. Many of these biosynthetic reactions are energetically unfavourable and must be driven by coupling them to ATP hydrolysis. Nucleic acid and protein synthesis, for example, both require this energy to drive polymerization, and *de novo* synthesis of nucleotides, lipids, and some amino acids also use ATP (Lunt and Vander Heiden, 2011). Cells can derive ATP from glycolysis and oxidative phosphorylation, and there have been considerable efforts to quantify the relative contributions of these pathways to ATP production *in vitro* (Fan et al., 2013; Zu and Guppy, 2004). Many cells derive a majority of their ATP from oxidative phosphorylation. This is true even for cells cultured in low (1-2%) oxygen, as this only partially reduces their oxygen consumption. In some contexts *in vivo*, oxygen tension is even lower, and cells might depend more on glycolysis in this case. In addition to biosynthetic reactions, ATP hydrolysis also drives homeostatic functions such as protein turnover and the maintenance of ion gradients across membranes. These costs are thought to represent a major use of ATP, and the proportion used for biosynthesis varies with proliferation rate (Kilburn et al., 1969).

Biosynthetic pathways also make use of redox reactions, and nicotinamide adenine dinucleotide cofactors (NAD(H) and NADP(H)) provide or remove electrons for these reactions (Lunt and Vander Heiden, 2011). NADPH is used in reduction reactions to synthesize lipids, deoxynucleotides, and proline. NAD^+ is directly used to oxidize precursors of some nucleotides, serine, and aspartate (Birsoy et al., 2015; Lunt and Vander Heiden, 2011; Sullivan et al., 2015). As discussed, LDH activity and oxidative phosphorylation both sustain NAD^+ levels in cells. Many reactions can generate NADPH, and both the oxidative pentose phosphate pathway and mitochondrial reactions contribute to its synthesis (Fan et al., 2014; Lewis et al., 2014).

Reactions that provide energy and redox cofactors are critical to biosynthesis even though they do not directly contribute new cell mass. Proliferating cells must abundantly re-generate these cofactors by metabolizing products of consumed nutrients. Therefore proliferative metabolism enhances biosynthesis both by providing the carbon and nitrogen for macromolecule precursors and by providing energy and by recycling redox cofactors that enable synthesis reactions.

Summary

Synthesizing the components of a new cell is a complicated task. Proliferating cells meet the requirement to double in mass by engaging a complex network of metabolic reactions that enable them to synthesize the precursors of protein, lipids, and nucleic acids. High flux through glycolytic reactions is a feature of this metabolic program, providing several advantages to proliferating cells: it is the source of material for *de novo* synthesis of many macromolecule precursors and also generates energy to fuel biosynthetic reactions. Differential expression of glucose transporters and glycolytic enzymes, such as pyruvate kinase, downstream of proliferative cues mechanistically links the choice to proliferate to the induction of aerobic glycolysis. A definitive explanation for the resulting high flux from glucose to lactate is lacking. The preferential expression of PKM2 as opposed to PKM1 is one factor, influencing the metabolic fate of pyruvate to enable aerobic glycolysis and biosynthesis. Loss of PKM1 expression aids proliferation *in vivo*, and further work is required to understand why high pyruvate kinase activity suppresses growth.

Glycolytic regulation and its links to anabolism, in part, inform how a cell obtains a sufficient amount of material to proliferate. Amino acids, lipids, and nucleotides can each be obtained from different sources and myriad factors determine how cells obtain macromolecule precursors. Many of these components are freely available to cells, although their abundance varies, and in some contexts, cells degrade extracellular macromolecules to obtain amino acids and lipids. *De novo* biosynthetic pathways

allow cells to synthesize complex precursors from the nutrients that are available to them. The source of these precursors may be fixed, but often cells have multiple mechanisms to generate them. For example, nucleotide ribose necessarily derives from glucose, but aspartate may be synthesized from glucose or glutamine carbon, or potentially from other anaplerotic substrates. Many factors, among them nutrient environment and gene expression, dictate which sources of cell mass are used. Interestingly, proliferating cells often make use of both exogenously supplied material as well as *de novo* biosynthetic pathways. Serine and lipids, for example, are both actively synthesized and scavenged by many proliferating cells (Kamphorst et al., 2013; Mattaini et al., 2016; Possemato et al., 2011). The requirement for these components could be met by either means, and why both pathways are engaged is unknown. This might allow cells to generate these components more abundantly or could provide other advantages to proliferating cells.

Further work is required to fully understand how the sources of macromolecule mass are determined. Nutrient transporter expression is likely a major contributor as these proteins determine what a cell can consume from the environment. Amino acid transporters, in particular, have been well characterized in recombinant systems *in vitro*, but what they transport in physiological conditions is less well understood. Extracellular environment also plays an important role as well. Glutamine, for example, is universally catabolized by cells proliferating in culture, but this is often not the case *in vivo*. Nutrient environment, genetics, and interactions with other cells in the body might account for this difference.

Which nutrients contribute to proliferating cell mass, how this is determined, and how this enables proliferation is far from being completely understood; however, in recent years our knowledge of which metabolic pathways critically support proliferation has greatly expanded. The work described in the following chapters seeks to provide a framework to address how metabolism contributes to rapid proliferation, both by broadly examining how new cell mass is acquired and by exploring the functions of specific metabolic pathways.

References

Agranoff, B.W., and Brady, R.O. (1956). Purification and properties of calf liver ribokinase. J Biol Chem *219*, 221-229.

Altman, B.J., Stine, Z.E., and Dang, C.V. (2016). From Krebs to clinic: glutamine metabolism to cancer therapy. Nature reviews Cancer *16*, 619-634.

Anastasiou, D., Yu, Y., Israelsen, W.J., Jiang, J.K., Boxer, M.B., Hong, B.S., Tempel, W., Dimov, S., Shen, M., Jha, A., *et al.* (2012). Pyruvate kinase M2 activators promote tetramer formation and suppress tumorigenesis. Nat Chem Biol *8*, 839-847.

Anderson, C.M., and Stahl, A. (2013). SLC27 fatty acid transport proteins. Mol Aspects Med *34*, 516-528.

Ardawi, M.S., and Newsholme, E.A. (1984). Metabolism of ketone bodies, oleate and glucose in lymphocytes of the rat. The Biochemical journal *221*, 255-260.

Ashizawa, K., McPhie, P., Lin, K.H., and Cheng, S.Y. (1991a). An in vitro novel mechanism of regulating the activity of pyruvate kinase M2 by thyroid hormone and fructose 1, 6-bisphosphate. Biochemistry *30*, 7105-7111.

Ashizawa, K., Willingham, M.C., Liang, C.M., and Cheng, S.Y. (1991b). In vivo regulation of monomer-tetramer conversion of pyruvate kinase subtype M2 by glucose is mediated via fructose 1,6-bisphosphate. J Biol Chem *266*, 16842-16846.

Baenke, F., Peck, B., Miess, H., and Schulze, A. (2013). Hooked on fat: the role of lipid synthesis in cancer metabolism and tumour development. Dis Model Mech *6*, 1353-1363.

Balaban, S., Shearer, R.F., Lee, L.S., van Geldermalsen, M., Schreuder, M., Shtein, H.C., Cairns, R., Thomas, K.C., Fazakerley, D.J., Grewal, T., *et al.* (2017). Adipocyte lipolysis links obesity to breast cancer growth: adipocyte-derived fatty acids drive breast cancer cell proliferation and migration. Cancer & metabolism *5*, 1.

Bao, X.R., Ong, S.E., Goldberger, O., Peng, J., Sharma, R., Thompson, D.A., Vafai, S.B., Cox, A.G., Marutani, E., Ichinose, F., *et al.* (2016). Mitochondrial dysfunction remodels one-carbon metabolism in human cells. eLife *5*.

Bensaad, K., Tsuruta, A., Selak, M.A., Vidal, M.N., Nakano, K., Bartrons, R., Gottlieb, E., and Vousden, K.H. (2006). TIGAR, a p53-inducible regulator of glycolysis and apoptosis. Cell *126*, 107-120.

Bhutia, Y.D., Babu, E., Ramachandran, S., and Ganapathy, V. (2015). Amino Acid transporters in cancer and their relevance to "glutamine addiction": novel targets for the design of a new class of anticancer drugs. Cancer Res *75*, 1782-1788.

Birsoy, K., Wang, T., Chen, W.W., Freinkman, E., Abu-Remaileh, M., and Sabatini, D.M. (2015). An Essential Role of the Mitochondrial Electron Transport Chain in Cell Proliferation Is to Enable Aspartate Synthesis. Cell *162*, 540-551.

Blobel, G., and Potter, V.R. (1967). Studies on free and membrane-bound ribosomes in rat liver. I. Distribution as related to total cellular RNA. J Mol Biol *26*, 279-292.

Bonarius, H.P., Hatzimanikatis, V., Meesters, K.P., de Gooijer, C.D., Schmid, G., and Tramper, J. (1996). Metabolic flux analysis of hybridoma cells in different culture media using mass balances. Biotechnology and bioengineering *50*, 299-318.

Brand, K. (1985). Glutamine and glucose metabolism during thymocyte proliferation. Pathways of glutamine and glutamate metabolism. The Biochemical journal *228*, 353-361.

Brand, K., Leibold, W., Luppa, P., Schoerner, C., and Schulz, A. (1986). Metabolic alterations associated with proliferation of mitogen-activated lymphocytes and of lymphoblastoid cell lines: evaluation of glucose and glutamine metabolism. Immunobiology *173*, 23-34.

Bulusu, V., Tumanov, S., Michalopoulou, E., van den Broek, N.J., MacKay, G., Nixon, C., Dhayade, S., Schug, Z.T., Vande Voorde, J., Blyth, K., *et al.* (2017). Acetate Recapturing by Nuclear Acetyl-CoA Synthetase 2 Prevents Loss of Histone Acetylation during Oxygen and Serum Limitation. Cell reports *18*, 647-658.

Cai, L., and Tu, B.P. (2012). Driving the cell cycle through metabolism. Annual review of cell and developmental biology *28*, 59-87.

Cairns, R.A., Harris, I.S., and Mak, T.W. (2011). Regulation of cancer cell metabolism. Nature reviews Cancer *11*, 85-95.

Calder, P.C., Yaqoob, P., and Newsholme, E.A. (1994). Triacylglycerol metabolism by lymphocytes and the effect of triacylglycerols on lymphocyte proliferation. The Biochemical journal *298 Pt 3*, 605-611.

Cardenas, J.M., and Dyson, R.D. (1978). Mammalian pyruvate kinase hybrid isozymes: tissue distribution and physiological significance. J Exp Zool *204*, 361-367.

Chaneton, B., Hillmann, P., Zheng, L., Martin, A.C., Maddocks, O.D., Chokkathukalam, A., Coyle, J.E., Jankevics, A., Holding, F.P., Vousden, K.H., *et al.* (2012). Serine is a natural ligand and allosteric activator of pyruvate kinase M2. Nature *491*, 458-462.

Chen, C., Pore, N., Behrooz, A., Ismail-Beigi, F., and Maity, A. (2001). Regulation of glut1 mRNA by hypoxia-inducible factor-1. Interaction between H-ras and hypoxia. J Biol Chem *276*, 9519-9525.

Chen, Z., Odstrcil, E.A., Tu, B.P., and McKnight, S.L. (2007). Restriction of DNA replication to the reductive phase of the metabolic cycle protects genome integrity. Science *316*, 1916-1919.

Christofk, H.R., Vander Heiden, M.G., Harris, M.H., Ramanathan, A., Gerszten, R.E., Wei, R., Fleming, M.D., Schreiber, S.L., and Cantley, L.C. (2008a). The M2 splice isoform of pyruvate kinase is important for cancer metabolism and tumour growth. Nature *452*, 230-233.

Christofk, H.R., Vander Heiden, M.G., Wu, N., Asara, J.M., and Cantley, L.C. (2008b). Pyruvate kinase M2 is a phosphotyrosine-binding protein. Nature *452*, 181-186.

Chuang, J.C., Yu, C.L., and Wang, S.R. (1990). Modulation of human lymphocyte proliferation by amino acids. Clin Exp Immunol *81*, 173-176.

Coloff, J.L., Murphy, J.P., Braun, C.R., Harris, I.S., Shelton, L.M., Kami, K., Gygi, S.P., Selfors, L.M., and Brugge, J.S. (2016). Differential Glutamate Metabolism in Proliferating and Quiescent Mammary Epithelial Cells. Cell metabolism *23*, 867-880.

Colombo, S.L., Palacios-Callender, M., Frakich, N., Carcamo, S., Kovacs, I., Tudzarova, S., and Moncada, S. (2011). Molecular basis for the differential use of glucose and glutamine in cell proliferation as revealed by synchronized HeLa cells. Proceedings of the National Academy of Sciences of the United States of America *108*, 21069-21074.

Comerford, S.A., Huang, Z., Du, X., Wang, Y., Cai, L., Witkiewicz, A.K., Walters, H., Tantawy, M.N., Fu, A., Manning, H.C., *et al.* (2014). Acetate dependence of tumors. Cell *159*, 1591-1602.

Commisso, C., Davidson, S.M., Soydaner-Azeloglu, R.G., Parker, S.J., Kamphorst, J.J., Hackett, S., Grabocka, E., Nofal, M., Drebin, J.A., Thompson, C.B., *et al.* (2013). Macropinocytosis of protein is an amino acid supply route in Ras-transformed cells. Nature *497*, 633-637.

Conlon, I., and Raff, M. (2003). Differences in the way a mammalian cell and yeast cells coordinate cell growth and cell-cycle progression. J Biol *2*, 7.

Cooper, S. (2004). Control and maintenance of mammalian cell size. BMC Cell Biol *5*, 35.

Cori, C.F., and Cori, G.T. (1925). The carobohydrate metabolism of tumors II: Changes in the sugar, lactic acid, and CO_2-combining power of blood passing through a tumor. Journal of Biological Chemistry *65*, 397-405.

Cortes-Cros, M., Hemmerlin, C., Ferretti, S., Zhang, J., Gounarides, J.S., Yin, H., Muller, A., Haberkorn, A., Chene, P., Sellers, W.R., *et al.* (2013). M2 isoform of pyruvate kinase is dispensable for tumor maintenance and growth. Proceedings of the National Academy of Sciences of the United States of America *110*, 489-494.

David, C.J., Chen, M., Assanah, M., Canoll, P., and Manley, J.L. (2010). HnRNP proteins controlled by c-Myc deregulate pyruvate kinase mRNA splicing in cancer. Nature *463*, 364-368.

Davidson, S.M., Papagiannakopoulos, T., Olenchock, B.A., Heyman, J.E., Keibler, M.A., Luengo, A., Bauer, M.R., Jha, A.K., O'Brien, J.P., Pierce, K.A., *et al.* (2016). Environment impacts the metabolic dependencies of Ras-driven non-small cell lung cancer. Cell metabolism *In Press*.

Daye, D., and Wellen, K.E. (2012). Metabolic reprogramming in cancer: unraveling the role of glutamine in tumorigenesis. Seminars in cell & developmental biology *23*, 362-369.

Dayton, T.L., Gocheva, V., Miller, K.M., Israelsen, W.J., Bhutkar, A., Clish, C.B., Davidson, S.M., Luengo, A., Bronson, R.T., Jacks, T., *et al.* (2016). Germline loss of PKM2 promotes metabolic distress and hepatocellular carcinoma. Genes Dev *30*, 1020-1033.

DeBerardinis, R.J., and Cheng, T. (2010). Q's next: the diverse functions of glutamine in metabolism, cell biology and cancer. Oncogene *29*, 313-324.

DeBerardinis, R.J., Mancuso, A., Daikhin, E., Nissim, I., Yudkoff, M., Wehrli, S., and Thompson, C.B. (2007). Beyond aerobic glycolysis: transformed cells can engage in glutamine metabolism that exceeds the requirement for protein and nucleotide synthesis. Proceedings of the National Academy of Sciences of the United States of America *104*, 19345-19350.

DeLapp, N.W., and Karasek, M.A. (1976). Importance of pyrimidine nucleotide salvage pathways for DNA synthesis in skin. J Invest Dermatol *66*, 306-312.

DeNicola, G.M., Chen, P.H., Mullarky, E., Sudderth, J.A., Hu, Z., Wu, D., Tang, H., Xie, Y., Asara, J.M., Huffman, K.E., *et al.* (2015). NRF2 regulates serine biosynthesis in non-small cell lung cancer. Nat Genet *47*, 1475-1481.

Dolfi, S.C., Chan, L.L., Qiu, J., Tedeschi, P.M., Bertino, J.R., Hirshfield, K.M., Oltvai, Z.N., and Vazquez, A. (2013). The metabolic demands of cancer cells are coupled to their size and protein synthesis rates. Cancer & metabolism *1*, 20.

Dolznig, H., Grebien, F., Sauer, T., Beug, H., and Mullner, E.W. (2004). Evidence for a size-sensing mechanism in animal cells. Nature cell biology *6*, 899-905.

Dombrauckas, J.D., Santarsiero, B.D., and Mesecar, A.D. (2005). Structural basis for tumor pyruvate kinase M2 allosteric regulation and catalysis. Biochemistry *44*, 9417-9429.

Duncan, R.E., Ahmadian, M., Jaworski, K., Sarkadi-Nagy, E., and Sul, H.S. (2007). Regulation of lipolysis in adipocytes. Annu Rev Nutr *27*, 79-101.

Duvel, K., Yecies, J.L., Menon, S., Raman, P., Lipovsky, A.I., Souza, A.L., Triantafellow, E., Ma, Q., Gorski, R., Cleaver, S., *et al.* (2010). Activation of a metabolic gene regulatory network downstream of mTOR complex 1. Molecular cell *39*, 171-183.

Eagle, H., Barban, S., Levy, M., and Schulze, H.O. (1958). The utilization of carbohydrates by human cell cultures. J Biol Chem *233*, 551-558.

Eagle, H., Oyama, V.I., Levy, M., and Freeman, A. (1956a). Myo-inositol as an essential growth factor for normal and malignant human cells in tissue culture. Science *123*, 845-847.

Eagle, H., Oyama, V.I., Levy, M., Horton, C.L., and Fleischman, R. (1956b). The growth response of mammalian cells in tissue culture to L-glutamine and L-glutamic acid. J Biol Chem *218*, 607-616.

Eagle, H., Washington, C., and Friedman, S.M. (1966). The synthesis of homocystine, cystathionine, and cystine by cultured diploid and heteroploid human cells. Proceedings of the National Academy of Sciences of the United States of America *56*, 156-163.

Ecker, R.E., and Kokaisl, G. (1969). Synthesis of protein, ribonucleic acid, and ribosomes by individual bacterial cells in balanced growth. J Bacteriol *98*, 1219-1226.

Eigenbrodt, E., Leib, S., Kramer, W., Friis, R.R., and Schoner, W. (1983). Structural and kinetic differences between the M2 type pyruvate kinases from lung and various tumors. Biomed Biochim Acta *42*, S278-282.

Ewald, J.C., Kuehne, A., Zamboni, N., and Skotheim, J.M. (2016). The Yeast Cyclin-Dependent Kinase Routes Carbon Fluxes to Fuel Cell Cycle Progression. Molecular cell *62*, 532-545.

Fan, J., Kamphorst, J.J., Mathew, R., Chung, M.K., White, E., Shlomi, T., and Rabinowitz, J.D. (2013). Glutamine-driven oxidative phosphorylation is a major ATP source in transformed mammalian cells in both normoxia and hypoxia. Mol Syst Biol *9*, 712.

Fan, J., Ye, J., Kamphorst, J.J., Shlomi, T., Thompson, C.B., and Rabinowitz, J.D. (2014). Quantitative flux analysis reveals folate-dependent NADPH production. Nature *510*, 298-302.

Fendt, S.M., Bell, E.L., Keibler, M.A., Olenchock, B.A., Mayers, J.R., Wasylenko, T.M., Vokes, N.I., Guarente, L., Vander Heiden, M.G., and Stephanopoulos, G. (2013). Reductive glutamine metabolism is a function of the alpha-ketoglutarate to citrate ratio in cells. Nat Commun *4*, 2236.

Filipp, F.V., Scott, D.A., Ronai, Z.A., Osterman, A.L., and Smith, J.W. (2012). Reverse TCA cycle flux through isocitrate dehydrogenases 1 and 2 is required for lipogenesis in hypoxic melanoma cells. Pigment Cell Melanoma Res *25*, 375-383.

Fingar, D.C., Salama, S., Tsou, C., Harlow, E., and Blenis, J. (2002). Mammalian cell size is controlled by mTOR and its downstream targets S6K1 and 4EBP1/eIF4E. Genes Dev *16*, 1472-1487.

Franklin, R.B., Zou, J., Yu, Z., and Costello, L.C. (2006). EAAC1 is expressed in rat and human prostate epithelial cells; functions as a high-affinity L-aspartate transporter; and is regulated by prolactin and testosterone. BMC Biochem *7*, 10.

Futcher, B. (2006). Metabolic cycle, cell cycle, and the finishing kick to Start. Genome Biol *7*, 107.

Gameiro, P.A., Yang, J., Metelo, A.M., Perez-Carro, R., Baker, R., Wang, Z., Arreola, A., Rathmell, W.K., Olumi, A., Lopez-Larrubia, P., *et al.* (2013). In vivo HIF-mediated reductive carboxylation is regulated by citrate levels and sensitizes VHL-deficient cells to glutamine deprivation. Cell metabolism *17*, 372-385.

Gaull, G., Sturman, J.A., and Raiha, N.C. (1972). Development of mammalian sulfur metabolism: absence of cystathionase in human fetal tissues. Pediatr Res *6*, 538-547.

Goldberg, I.J., Eckel, R.H., and Abumrad, N.A. (2009). Regulation of fatty acid uptake into tissues: lipoprotein lipase- and CD36-mediated pathways. Journal of lipid research *50 Suppl*, S86-90.

Goldstein, J.L., DeBose-Boyd, R.A., and Brown, M.S. (2006). Protein sensors for membrane sterols. Cell *124*, 35-46.

Green, C.R., Wallace, M., Divakaruni, A.S., Phillips, S.A., Murphy, A.N., Ciaraldi, T.P., and Metallo, C.M. (2016). Branched-chain amino acid catabolism fuels adipocyte differentiation and lipogenesis. Nat Chem Biol *12*, 15-21.

Halestrap, A.P. (2013). The SLC16 gene family - structure, role and regulation in health and disease. Mol Aspects Med *34*, 337-349.

Hara, K., Yonezawa, K., Weng, Q.P., Kozlowski, M.T., Belham, C., and Avruch, J. (1998). Amino acid sufficiency and mTOR regulate p70 S6 kinase and eIF-4E BP1 through a common effector mechanism. J Biol Chem *273*, 14484-14494.

Harding, H.P., Zhang, Y., Zeng, H., Novoa, I., Lu, P.D., Calfon, M., Sadri, N., Yun, C., Popko, B., Paules, R., *et al.* (2003). An integrated stress response regulates amino acid metabolism and resistance to oxidative stress. Molecular cell *11*, 619-633.

Harding, J.W., Jr., Pyeritz, E.A., Morris, H.P., and White, H.B., 3rd (1975). Proportional activities of glycerol kinase and glycerol 3-phosphate dehydrogenase in rat hepatomas. The Biochemical journal *148*, 545-550.

Hensley, C.T., Faubert, B., Yuan, Q., Lev-Cohain, N., Jin, E., Kim, J., Jiang, L., Ko, B., Skelton, R., Loudat, L., *et al.* (2016). Metabolic Heterogeneity in Human Lung Tumors. Cell *164*, 681-694.

Hirayama, A., Kami, K., Sugimoto, M., Sugawara, M., Toki, N., Onozuka, H., Kinoshita, T., Saito, N., Ochiai, A., Tomita, M., *et al.* (2009). Quantitative metabolome profiling of colon and stomach cancer microenvironment by capillary electrophoresis time-of-flight mass spectrometry. Cancer Res *69*, 4918-4925.

Hitosugi, T., Kang, S., Vander Heiden, M.G., Chung, T.W., Elf, S., Lythgoe, K., Dong, S., Lonial, S., Wang, X., Chen, G.Z., *et al.* (2009). Tyrosine phosphorylation inhibits PKM2 to promote the Warburg effect and tumor growth. Sci Signal *2*, ra73.

Hosios, A.M., Fiske, B.P., Gui, D.Y., and Vander Heiden, M.G. (2015). Lack of Evidence for PKM2 Protein Kinase Activity. Molecular cell *59*, 850-857.

Hosios, A.M., Hecht, V.C., Danai, L.V., Johnson, M.O., Rathmell, J.C., Steinhauser, M.L., Manalis, S.R., and Vander Heiden, M.G. (2016). Amino Acids Rather than Glucose Account for the Majority of Cell Mass in Proliferating Mammalian Cells. Dev Cell *36*, 540-549.

Hosios, A.M., and Vander Heiden, M.G. (2014). Acetate metabolism in cancer cells. Cancer & metabolism *2*, 27.

Hsu, P.P., and Sabatini, D.M. (2008). Cancer cell metabolism: Warburg and beyond. Cell *134*, 703-707.

Hume, D.A., Radik, J.L., Ferber, E., and Weidemann, M.J. (1978). Aerobic glycolysis and lymphocyte transformation. The Biochemical journal *174*, 703-709.

Hume, D.A., and Weidemann, M.J. (1979). Role and regulation of glucose metabolism in proliferating cells. J Natl Cancer Inst *62*, 3-8.

Imamura, K., and Tanaka, T. (1972). Multimolecular forms of pyruvate kinase from rat and other mammalian tissues. I. Electrophoretic studies. J Biochem *71*, 1043-1051.

Israelsen, W.J., Dayton, T.L., Davidson, S.M., Fiske, B.P., Hosios, A.M., Bellinger, G., Li, J., Yu, Y., Sasaki, M., Horner, J.W., *et al.* (2013). PKM2 isoform-specific deletion reveals a differential requirement for pyruvate kinase in tumor cells. Cell *155*, 397-409.

Israelsen, W.J., and Vander Heiden, M.G. (2015). Pyruvate kinase: Function, regulation and role in cancer. Seminars in cell & developmental biology *43*, 43-51.

Iurlaro, R., Leon-Annicchiarico, C.L., and Munoz-Pinedo, C. (2014). Regulation of cancer metabolism by oncogenes and tumor suppressors. Methods Enzymol *542*, 59-80.

Jain, M., Nilsson, R., Sharma, S., Madhusudhan, N., Kitami, T., Souza, A.L., Kafri, R., Kirschner, M.W., Clish, C.B., and Mootha, V.K. (2012). Metabolite profiling identifies a key role for glycine in rapid cancer cell proliferation. Science *336*, 1040-1044.

Johnston, G.C., Pringle, J.R., and Hartwell, L.H. (1977). Coordination of growth with cell division in the yeast Saccharomyces cerevisiae. Exp Cell Res *105*, 79-98.

Jorgensen, P., and Tyers, M. (2004). How cells coordinate growth and division. Curr Biol *14*, R1014-1027.

Kamphorst, J.J., Chung, M.K., Fan, J., and Rabinowitz, J.D. (2014). Quantitative analysis of acetyl-CoA production in hypoxic cancer cells reveals substantial contribution from acetate. Cancer & metabolism *2*, 23.

Kamphorst, J.J., Cross, J.R., Fan, J., de Stanchina, E., Mathew, R., White, E.P., Thompson, C.B., and Rabinowitz, J.D. (2013). Hypoxic and Ras-transformed cells support growth by scavenging unsaturated fatty acids from lysophospholipids. Proceedings of the National Academy of Sciences of the United States of America *110*, 8882-8887.

Kamphorst, J.J., Nofal, M., Commisso, C., Hackett, S.R., Lu, W., Grabocka, E., Vander Heiden, M.G., Miller, G., Drebin, J.A., Bar-Sagi, D., *et al.* (2015). Human pancreatic cancer tumors are nutrient poor and tumor cells actively scavenge extracellular protein. Cancer Res *75*, 544-553.

Kaplon, J., van Dam, L., and Peeper, D. (2015). Two-way communication between the metabolic and cell cycle machineries: the molecular basis. Cell Cycle *14*, 2022-2032.

Keller, K.E., Tan, I.S., and Lee, Y.S. (2012). SAICAR stimulates pyruvate kinase isoform M2 and promotes cancer cell survival in glucose-limited conditions. Science *338*, 1069-1072.

Kilberg, M.S., Shan, J., and Su, N. (2009). ATF4-dependent transcription mediates signaling of amino acid limitation. Trends Endocrinol Metab *20*, 436-443.

Kilburn, D.G., Lilly, M.D., and Webb, F.C. (1969). The energetics of mammalian cell growth. J Cell Sci *4*, 645-654.

Killander, D., and Zetterberg, A. (1965). A quantitative cytochemical investigation of the relationship between cell mass and initiation of DNA synthesis in mouse fibroblasts in vitro. Exp Cell Res *40*, 12-20.

Kim, J.W., Tchernyshyov, I., Semenza, G.L., and Dang, C.V. (2006). HIF-1-mediated expression of pyruvate dehydrogenase kinase: a metabolic switch required for cellular adaptation to hypoxia. Cell metabolism *3*, 177-185.

Krebs, H. (1959). Chairman's Introductory Address: Rate-Limiting Factors in Cell Respiration. In Ciba Foundation Symposium — Regulation of Cell Metabolism (John Wiley & Sons, Ltd), pp. 1-16.

Kung, C., Hixon, J., Choe, S., Marks, K., Gross, S., Murphy, E., DeLaBarre, B., Cianchetta, G., Sethumadhavan, S., Wang, X., *et al.* (2012). Small molecule activation of PKM2 in cancer cells induces serine auxotrophy. Chem Biol *19*, 1187-1198.

Labuschagne, C.F., van den Broek, N.J., Mackay, G.M., Vousden, K.H., and Maddocks, O.D. (2014). Serine, but not glycine, supports one-carbon metabolism and proliferation of cancer cells. Cell reports *7*, 1248-1258.

Lai, C.S., Hopwood, L.E., Hyde, J.S., and Lukiewicz, S. (1982). ESR studies of O2 uptake by Chinese hamster ovary cells during the cell cycle. Proceedings of the National Academy of Sciences of the United States of America *79*, 1166-1170.

Lane, A.N., and Fan, T.W. (2015). Regulation of mammalian nucleotide metabolism and biosynthesis. Nucleic Acids Res *43*, 2466-2485.

Laplante, M., and Sabatini, D.M. (2012). mTOR signaling in growth control and disease. Cell *149*, 274-293.

Lee, W.N., Boros, L.G., Puigjaner, J., Bassilian, S., Lim, S., and Cascante, M. (1998). Mass isotopomer study of the nonoxidative pathways of the pentose cycle with [1,2-13C2]glucose. Am J Physiol *274*, E843-851.

Lee, Y.S., Choi, K.M., Choi, M.H., Ji, S.Y., Lee, S., Sin, D.M., Oh, K.W., Lee, Y.M., Hong, J.T., Yun, Y.P., *et al.* (2011). Serine palmitoyltransferase inhibitor myriocin induces growth inhibition of B16F10 melanoma cells through G(2) /M phase arrest. Cell Prolif *44*, 320-329.

Lemoigne, M., Aubert, J.P., and Millet, J. (1954). [Ethyl alcohol production and growth of baker's yeast cultured under aerobic conditions]. Ann Inst Pasteur (Paris) *87*, 427-439.

Lewis, C.A., Parker, S.J., Fiske, B.P., McCloskey, D., Gui, D.Y., Green, C.R., Vokes, N.I., Feist, A.M., Vander Heiden, M.G., and Metallo, C.M. (2014). Tracing compartmentalized NADPH metabolism in the cytosol and mitochondria of mammalian cells. Molecular cell *55*, 253-263.

Liu, W., Hancock, C.N., Fischer, J.W., Harman, M., and Phang, J.M. (2015). Proline biosynthesis augments tumor cell growth and aerobic glycolysis: involvement of pyridine nucleotides. Sci Rep *5*, 17206.

Locasale, J.W., Grassian, A.R., Melman, T., Lyssiotis, C.A., Mattaini, K.R., Bass, A.J., Heffron, G., Metallo, C.M., Muranen, T., Sharfi, H., *et al.* (2011). Phosphoglycerate dehydrogenase diverts glycolytic flux and contributes to oncogenesis. Nat Genet *43*, 869-874.

Luengo, A., Sullivan, L.B., and Heiden, M.G. (2014). Understanding the complex-I-ty of metformin action: limiting mitochondrial respiration to improve cancer therapy. BMC Biol *12*, 82.

Lunt, S.Y., Muralidhar, V., Hosios, A.M., Israelsen, W.J., Gui, D.Y., Newhouse, L., Ogrodzinski, M., Hecht, V., Xu, K., Acevedo, P.N., *et al.* (2015). Pyruvate kinase isoform expression alters nucleotide synthesis to impact cell proliferation. Molecular cell *57*, 95-107.

Lunt, S.Y., and Vander Heiden, M.G. (2011). Aerobic glycolysis: meeting the metabolic requirements of cell proliferation. Annual review of cell and developmental biology *27*, 441-464.

Lv, L., Xu, Y.P., Zhao, D., Li, F.L., Wang, W., Sasaki, N., Jiang, Y., Zhou, X., Li, T.T., Guan, K.L., *et al.* (2013). Mitogenic and oncogenic stimulation of K433 acetylation promotes PKM2 protein kinase activity and nuclear localization. Molecular cell *52*, 340-352.

Maddocks, O.D., Berkers, C.R., Mason, S.M., Zheng, L., Blyth, K., Gottlieb, E., and Vousden, K.H. (2013). Serine starvation induces stress and p53-dependent metabolic remodelling in cancer cells. Nature *493*, 542-546.

Marin-Valencia, I., Yang, C., Mashimo, T., Cho, S., Baek, H., Yang, X.L., Rajagopalan, K.N., Maddie, M., Vemireddy, V., Zhao, Z., *et al.* (2012). Analysis of tumor metabolism reveals mitochondrial glucose oxidation in genetically diverse human glioblastomas in the mouse brain in vivo. Cell metabolism *15*, 827-837.

Martinez-Outschoorn, U.E., Peiris-Pages, M., Pestell, R.G., Sotgia, F., and Lisanti, M.P. (2017). Cancer metabolism: a therapeutic perspective. Nat Rev Clin Oncol *14*, 11-31.

Masetti, R., and Pession, A. (2009). First-line treatment of acute lymphoblastic leukemia with pegasparaginase. Biologics *3*, 359-368.

Mashimo, T., Pichumani, K., Vemireddy, V., Hatanpaa, K.J., Singh, D.K., Sirasanagandla, S., Nannepaga, S., Piccirillo, S.G., Kovacs, Z., Foong, C., *et al.* (2014). Acetate is a bioenergetic substrate for human glioblastoma and brain metastases. Cell *159*, 1603-1614.

Mattaini, K.R., Sullivan, M.R., and Vander Heiden, M.G. (2016). The importance of serine metabolism in cancer. J Cell Biol *214*, 249-257.

Mayers, J.R., Torrence, M.E., Danai, L.V., Papagiannakopoulos, T., Davidson, S.M., Bauer, M.R., Lau, A.N., Ji, B.W., Dixit, P.D., Hosios, A.M., *et al.* (2016). Tissue of origin dictates branched-chain amino acid metabolism in mutant Kras-driven cancers. Science *353*, 1161-1165.

Mayers, J.R., and Vander Heiden, M.G. (2015). Famine versus feast: understanding the metabolism of tumors in vivo. Trends Biochem Sci *40*, 130-140.

Mayers, J.R., Wu, C., Clish, C.B., Kraft, P., Torrence, M.E., Fiske, B.P., Yuan, C., Bao, Y., Townsend, M.K., Tworoger, S.S., *et al.* (2014). Elevation of circulating branched-chain amino acids is an early event in human pancreatic adenocarcinoma development. Nat Med *20*, 1193-1198.

Mazurek, S., Grimm, H., Boschek, C.B., Vaupel, P., and Eigenbrodt, E. (2002). Pyruvate kinase type M2: a crossroad in the tumor metabolome. Br J Nutr *87 Suppl 1*, S23-29.

McGale, E.H., Pye, I.F., Stonier, C., Hutchinson, E.C., and Aber, G.M. (1977). Studies of the inter-relationship between cerebrospinal fluid and plasma amino acid concentrations in normal individuals. J Neurochem *29*, 291-297.

Medes, G., Thomas, A., and Weinhouse, S. (1953). Metabolism of neoplastic tissue. IV. A study of lipid synthesis in neoplastic tissue slices in vitro. Cancer Res *13*, 27-29.

Merrill, A.H., Jr. (2002). De novo sphingolipid biosynthesis: a necessary, but dangerous, pathway. J Biol Chem *277*, 25843-25846.

Metallo, C.M., Gameiro, P.A., Bell, E.L., Mattaini, K.R., Yang, J., Hiller, K., Jewell, C.M., Johnson, Z.R., Irvine, D.J., Guarente, L., *et al.* (2012). Reductive glutamine metabolism by IDH1 mediates lipogenesis under hypoxia. Nature *481*, 380-384.

Morgan, J.F., Morton, H.J., and Pasieka, A.E. (1958). The arginine requirement of tissue cultures. I. Interrelationships between arginine and related compounds. J Biol Chem *233*, 664-667.

Moseley, J.B., Mayeux, A., Paoletti, A., and Nurse, P. (2009). A spatial gradient coordinates cell size and mitotic entry in fission yeast. Nature *459*, 857-860.

Mourant, J.R., Short, K.W., Carpenter, S., Kunapareddy, N., Coburn, L., Powers, T.M., and Freyer, J.P. (2005). Biochemical differences in tumorigenic and nontumorigenic cells measured by Raman and infrared spectroscopy. Journal of biomedical optics 10, 031106.

Mueckler, M., and Thorens, B. (2013). The SLC2 (GLUT) family of membrane transporters. Mol Aspects Med 34, 121-138.

Mullen, A.R., Wheaton, W.W., Jin, E.S., Chen, P.H., Sullivan, L.B., Cheng, T., Yang, Y., Linehan, W.M., Chandel, N.S., and DeBerardinis, R.J. (2012). Reductive carboxylation supports growth in tumour cells with defective mitochondria. Nature 481, 385-388.

Murray, C.M., Hutchinson, R., Bantick, J.R., Belfield, G.P., Benjamin, A.D., Brazma, D., Bundick, R.V., Cook, I.D., Craggs, R.I., Edwards, S., et al. (2005). Monocarboxylate transporter MCT1 is a target for immunosuppression. Nat Chem Biol 1, 371-376.

Newsholme, E.A., Crabtree, B., and Ardawi, M.S. (1985a). Glutamine metabolism in lymphocytes: its biochemical, physiological and clinical importance. Q J Exp Physiol 70, 473-489.

Newsholme, E.A., Crabtree, B., and Ardawi, M.S. (1985b). The role of high rates of glycolysis and glutamine utilization in rapidly dividing cells. Bioscience reports 5, 393-400.

Nieman, K.M., Kenny, H.A., Penicka, C.V., Ladanyi, A., Buell-Gutbrod, R., Zillhardt, M.R., Romero, I.L., Carey, M.S., Mills, G.B., Hotamisligil, G.S., et al. (2011). Adipocytes promote ovarian cancer metastasis and provide energy for rapid tumor growth. Nat Med 17, 1498-1503.

Noguchi, T., Inoue, H., and Tanaka, T. (1986). The M1- and M2-type isozymes of rat pyruvate kinase are produced from the same gene by alternative RNA splicing. J Biol Chem 261, 13807-13812.

Oram, J.F., Shafrir, E., and Bierman, E.L. (1980). Triacylglycerol metabolism and triacylglycerol lipase activities of cultured human skin fibroblasts. Biochim Biophys Acta 619, 214-227.

Pascual, G., Avgustinova, A., Mejetta, S., Martin, M., Castellanos, A., Attolini, C.S., Berenguer, A., Prats, N., Toll, A., Hueto, J.A., et al. (2017). Targeting metastasis-initiating cells through the fatty acid receptor CD36. Nature 541, 41-45.

Pastor-Anglada, M., Errasti-Murugarren, E., Aymerich, I., and Casado, F.J. (2007). Concentrative nucleoside transporters (CNTs) in epithelia: from absorption to cell signaling. J Physiol Biochem 63, 97-110.

Patel, M.S., and Owen, O.E. (1976). Lipogenesis from ketone bodies in rat brain. Evidence for conversion of acetoacetate into acetyl-coenzyme A in the cytosol. The Biochemical journal 156, 603-607.

Pavlova, N.N., and Thompson, C.B. (2016). The Emerging Hallmarks of Cancer Metabolism. Cell metabolism 23, 27-47.

Phillips, M.M., Sheaff, M.T., and Szlosarek, P.W. (2013). Targeting arginine-dependent cancers with arginine-degrading enzymes: opportunities and challenges. Cancer Res Treat 45, 251-262.

Piko, L., and Clegg, K.B. (1982). Quantitative changes in total RNA, total poly(A), and ribosomes in early mouse embryos. Dev Biol 89, 362-378.

Pochini, L., Scalise, M., Galluccio, M., and Indiveri, C. (2014). Membrane transporters for the special amino acid glutamine: structure/function relationships and relevance to human health. Front Chem *2*, 61.

Pollari, S., Kakonen, S.M., Edgren, H., Wolf, M., Kohonen, P., Sara, H., Guise, T., Nees, M., and Kallioniemi, O. (2011). Enhanced serine production by bone metastatic breast cancer cells stimulates osteoclastogenesis. Breast Cancer Res Treat *125*, 421-430.

Possemato, R., Marks, K.M., Shaul, Y.D., Pacold, M.E., Kim, D., Birsoy, K., Sethumadhavan, S., Woo, H.K., Jang, H.G., Jha, A.K., *et al.* (2011). Functional genomics reveal that the serine synthesis pathway is essential in breast cancer. Nature *476*, 346-350.

Pressacco, J., Wiley, J.S., Jamieson, G.P., Erlichman, C., and Hedley, D.W. (1995). Modulation of the equilibrative nucleoside transporter by inhibitors of DNA synthesis. Br J Cancer *72*, 939-942.

Rabinovich, S., Adler, L., Yizhak, K., Sarver, A., Silberman, A., Agron, S., Stettner, N., Sun, Q., Brandis, A., Helbling, D., *et al.* (2015). Diversion of aspartate in ASS1-deficient tumours fosters de novo pyrimidine synthesis. Nature *527*, 379-383.

Racker, E. (1976). Why do tumor cells have a high aerobic glycolysis? J Cell Physiol *89*, 697-700.

Rathmell, J.C., Vander Heiden, M.G., Harris, M.H., Frauwirth, K.A., and Thompson, C.B. (2000). In the absence of extrinsic signals, nutrient utilization by lymphocytes is insufficient to maintain either cell size or viability. Molecular cell *6*, 683-692.

Reitzer, L.J., Wice, B.M., and Kennell, D. (1980). The pentose cycle. Control and essential function in HeLa cell nucleic acid synthesis. J Biol Chem *255*, 5616-5626.

Schmoller, K.M., Turner, J.J., Koivomagi, M., and Skotheim, J.M. (2015). Dilution of the cell cycle inhibitor Whi5 controls budding-yeast cell size. Nature *526*, 268-272.

Schug, Z.T., Peck, B., Jones, D.T., Zhang, Q., Grosskurth, S., Alam, I.S., Goodwin, L.M., Smethurst, E., Mason, S., Blyth, K., *et al.* (2015). Acetyl-CoA synthetase 2 promotes acetate utilization and maintains cancer cell growth under metabolic stress. Cancer cell *27*, 57-71.

Schug, Z.T., Vande Voorde, J., and Gottlieb, E. (2016). The metabolic fate of acetate in cancer. Nature reviews Cancer *16*, 708-717.

Segel, G.B., and Lichtman, M.A. (1981). Amino acid transport in human lymphocytes: distinctions in the enhanced uptake with PHA treatment or amino acid deprivation. J Cell Physiol *106*, 303-308.

Sellers, K., Fox, M.P., Bousamra, M., 2nd, Slone, S.P., Higashi, R.M., Miller, D.M., Wang, Y., Yan, J., Yuneva, M.O., Deshpande, R., *et al.* (2015). Pyruvate carboxylase is critical for non-small-cell lung cancer proliferation. The Journal of clinical investigation *125*, 687-698.

Shimobayashi, M., and Hall, M.N. (2014). Making new contacts: the mTOR network in metabolism and signalling crosstalk. Nat Rev Mol Cell Biol *15*, 155-162.

Simons, K., and Sampaio, J.L. (2011). Membrane organization and lipid rafts. Cold Spring Harb Perspect Biol *3*, a004697.

Sousa, C.M., Biancur, D.E., Wang, X., Halbrook, C.J., Sherman, M.H., Zhang, L., Kremer, D., Hwang, R.F., Witkiewicz, A.K., Ying, H., *et al.* (2016). Pancreatic stellate cells support tumour metabolism through autophagic alanine secretion. Nature *536*, 479-483.

Sparmann, G., Schulz, J., and Hofmann, E. (1973). Effects of L-alanine and fructose (1,6-diphosphate) on pyruvate kinase from ehrlich ascites tumour cells. FEBS Lett *36*, 305-308.

Steck, T.L., Kaufman, S., and Bader, J.P. (1968). Glycolysis in chick embryo cell cultures transformed by Rous sarcoma virus. Cancer Res *28*, 1611-1619.

Sullivan, L.B., Gui, D.Y., Hosios, A.M., Bush, L.N., Freinkman, E., and Vander Heiden, M.G. (2015). Supporting Aspartate Biosynthesis Is an Essential Function of Respiration in Proliferating Cells. Cell *162*, 552-563.

Sveiczer, A., Novak, B., and Mitchison, J.M. (2004). Size control in growing yeast and mammalian cells. Theor Biol Med Model *1*, 12.

Svensson, R.U., and Shaw, R.J. (2017). Lipid Synthesis Is a Metabolic Liability of Non-Small Cell Lung Cancer. Cold Spring Harb Symp Quant Biol.

Tan, A.S., Baty, J.W., Dong, L.F., Bezawork-Geleta, A., Endaya, B., Goodwin, J., Bajzikova, M., Kovarova, J., Peterka, M., Yan, B., *et al.* (2015). Mitochondrial genome acquisition restores respiratory function and tumorigenic potential of cancer cells without mitochondrial DNA. Cell metabolism *21*, 81-94.

Tardito, S., Oudin, A., Ahmed, S.U., Fack, F., Keunen, O., Zheng, L., Miletic, H., Sakariassen, P.O., Weinstock, A., Wagner, A., *et al.* (2015). Glutamine synthetase activity fuels nucleotide biosynthesis and supports growth of glutamine-restricted glioblastoma. Nature cell biology *17*, 1556-1568.

Tennant, D.A., Duran, R.V., and Gottlieb, E. (2010). Targeting metabolic transformation for cancer therapy. Nature reviews Cancer *10*, 267-277.

Thibault, G., Shui, G., Kim, W., McAlister, Graeme C., Ismail, N., Gygi, Steven P., Wenk, Markus R., and Ng, Davis T.W. (2012). The Membrane Stress Response Buffers Lethal Effects of Lipid Disequilibrium by Reprogramming the Protein Homeostasis Network. Molecular cell *48*, 16-27.

Traut, T.W. (1994). Physiological concentrations of purines and pyrimidines. Mol Cell Biochem *140*, 1-22.

Tu, B.P., Kudlicki, A., Rowicka, M., and McKnight, S.L. (2005). Logic of the yeast metabolic cycle: temporal compartmentalization of cellular processes. Science *310*, 1152-1158.

Tu, B.P., Mohler, R.E., Liu, J.C., Dombek, K.M., Young, E.T., Synovec, R.E., and McKnight, S.L. (2007). Cyclic changes in metabolic state during the life of a yeast cell. Proceedings of the National Academy of Sciences of the United States of America *104*, 16886-16891.

Turner, J.J., Ewald, J.C., and Skotheim, J.M. (2012). Cell size control in yeast. Curr Biol *22*, R350-359.

van Meer, G., Voelker, D.R., and Feigenson, G.W. (2008). Membrane lipids: where they are and how they behave. Nat Rev Mol Cell Biol *9*, 112-124.

Vander Heiden, M.G. (2011). Targeting cancer metabolism: a therapeutic window opens. Nat Rev Drug Discov *10*, 671-684.

Vander Heiden, M.G., Cantley, L.C., and Thompson, C.B. (2009). Understanding the Warburg effect: the metabolic requirements of cell proliferation. Science *324*, 1029-1033.

Vander Heiden, M.G., and DeBerardinis, R.J. (2017). Understanding the Intersections between Metabolism and Cancer Biology. Cell *168*, 657-669.

Vander Heiden, M.G., Plas, D.R., Rathmell, J.C., Fox, C.J., Harris, M.H., and Thompson, C.B. (2001). Growth factors can influence cell growth and survival through effects on glucose metabolism. Mol Cell Biol *21*, 5899-5912.

Wang, P., Sun, C., Zhu, T., and Xu, Y. (2015). Structural insight into mechanisms for dynamic regulation of PKM2. Protein Cell *6*, 275-287.

Wang, T., Marquardt, C., and Foker, J. (1976). Aerobic glycolysis during lymphocyte proliferation. Nature *261*, 702-705.

Wang, Y.H., Israelsen, W.J., Lee, D., Yu, V.W., Jeanson, N.T., Clish, C.B., Cantley, L.C., Vander Heiden, M.G., and Scadden, D.T. (2014). Cell-state-specific metabolic dependency in hematopoiesis and leukemogenesis. Cell *158*, 1309-1323.

Warburg, O. (1924). Über den Stoffwechsel der Carcinomzelle. Naturwissenschaften *12*, 1131-1137.

Warburg, O. (1956). On the origin of cancer cells. Science *123*, 309-314.

Weinberg, S.E., and Chandel, N.S. (2015). Targeting mitochondria metabolism for cancer therapy. Nat Chem Biol *11*, 9-15.

Wheaton, W.W., and Chandel, N.S. (2011). Hypoxia. 2. Hypoxia regulates cellular metabolism. Am J Physiol Cell Physiol *300*, C385-393.

Wheaton, W.W., Weinberg, S.E., Hamanaka, R.B., Soberanes, S., Sullivan, L.B., Anso, E., Glasauer, A., Dufour, E., Mutlu, G.M., Budigner, G.S., *et al.* (2014). Metformin inhibits mitochondrial complex I of cancer cells to reduce tumorigenesis. eLife *3*, e02242.

Wise, D.R., Ward, P.S., Shay, J.E., Cross, J.R., Gruber, J.J., Sachdeva, U.M., Platt, J.M., DeMatteo, R.G., Simon, M.C., and Thompson, C.B. (2011). Hypoxia promotes isocitrate dehydrogenase-dependent carboxylation of alpha-ketoglutarate to citrate to support cell growth and viability. Proceedings of the National Academy of Sciences of the United States of America *108*, 19611-19616.

Wuntch, T., Chen, R.F., and Vesell, E.S. (1970). Lactate dehydrogenase isozymes: kinetic properties at high enzyme concentrations. Science *167*, 63-65.

Xiang, Y., Stine, Z.E., Xia, J., Lu, Y., O'Connor, R.S., Altman, B.J., Hsieh, A.L., Gouw, A.M., Thomas, A.G., Gao, P., *et al.* (2015). Targeted inhibition of tumor-specific glutaminase diminishes cell-autonomous tumorigenesis. The Journal of clinical investigation *125*, 2293-2306.

Xie, L., and Wang, D.I. (1994). Applications of improved stoichiometric model in medium design and fed-batch cultivation of animal cells in bioreactor. Cytotechnology *15*, 17-29.

Xu, Y.F., Zhao, X., Glass, D.S., Absalan, F., Perlman, D.H., Broach, J.R., and Rabinowitz, J.D. (2012). Regulation of yeast pyruvate kinase by ultrasensitive allostery independent of phosphorylation. Molecular cell *48*, 52-62.

Yamamoto, K., and Niwa, A. (1993). Amino acid and vitamin requirements in mammalian cultured cells. Amino Acids *5*, 1-16.

Yamamoto, T., Seino, Y., Fukumoto, H., Koh, G., Yano, H., Inagaki, N., Yamada, Y., Inoue, K., Manabe, T., and Imura, H. (1990). Over-expression of facilitative glucose transporter genes in human cancer. Biochem Biophys Res Commun *170*, 223-230.

Yao, C.H., Fowle-Grider, R., Mahieu, N.G., Liu, G.Y., Chen, Y.J., Wang, R., Singh, M., Potter, G.S., Gross, R.W., Schaefer, J., *et al.* (2016). Exogenous Fatty Acids Are the Preferred Source of Membrane Lipids in Proliferating Fibroblasts. Cell Chem Biol *23*, 483-493.

Ye, J., and DeBose-Boyd, R.A. (2011). Regulation of cholesterol and fatty acid synthesis. Cold Spring Harb Perspect Biol *3*.

Young, J.D., Yao, S.Y., Baldwin, J.M., Cass, C.E., and Baldwin, S.A. (2013). The human concentrative and equilibrative nucleoside transporter families, SLC28 and SLC29. Mol Aspects Med *34*, 529-547.

Yuneva, M.O., Fan, T.W., Allen, T.D., Higashi, R.M., Ferraris, D.V., Tsukamoto, T., Mates, J.M., Alonso, F.J., Wang, C., Seo, Y., *et al.* (2012). The metabolic profile of tumors depends on both the responsible genetic lesion and tissue type. Cell metabolism *15*, 157-170.

Zaidi, N., Lupien, L., Kuemmerle, N.B., Kinlaw, W.B., Swinnen, J.V., and Smans, K. (2013). Lipogenesis and lipolysis: the pathways exploited by the cancer cells to acquire fatty acids. Prog Lipid Res *52*, 585-589.

Zerangue, N., and Kavanaugh, M.P. (1996). ASCT-1 is a neutral amino acid exchanger with chloride channel activity. J Biol Chem *271*, 27991-27994.

Zhao, G., Chen, Y., Carey, L., and Futcher, B. (2016). Cyclin-Dependent Kinase Co-Ordinates Carbohydrate Metabolism and Cell Cycle in S. cerevisiae. Molecular cell *62*, 546-557.

Zu, X.L., and Guppy, M. (2004). Cancer metabolism: facts, fantasy, and fiction. Biochem Biophys Res Commun *313*, 459-465.

Chapter 2: Amino acids rather than glucose account for the majority of cell mass in proliferating mammalian cells

Authors: Aaron M. Hosios[1,2], Vivian C. Hecht[1,3], Laura V. Danai[1,2], Marc O. Johnson[4], Jeffrey C. Rathmell[4], Matthew L. Steinhauser[5,6,7], Scott R. Manalis[1,3], Matthew G. Vander Heiden[1,2,8]

Affiliations:
[1] Koch Institute for Integrative Cancer Research, Massachusetts Institute of Technology, Cambridge, MA 02139, USA.
[2] Department of Biology, Massachusetts Institute of Technology, Cambridge, MA 02139, USA.
[3] Department of Biological Engineering, Massachusetts Institute of Technology, Cambridge, MA 02139, USA.
[4] Department of Pathology, Microbiology, and Immunology, Vanderbilt University Medical Center, Nashville, TN 37232, USA
[5] Department of Medicine, Division of Genetics, Brigham and Women's Hospital, Boston, MA 02115, USA
[6] Department of Medicine, Division of Cardiovascular Medicine, Brigham and Women's Hospital, Boston, MA 02115, USA
[7] Harvard Medical School, Boston, MA 02115, USA
[8] Department of Medical Oncology, Dana-Farber Cancer Institute, Boston, MA 02115, USA

Abstract

Cells must duplicate their mass in order to proliferate. Glucose and glutamine are the major nutrients consumed by proliferating mammalian cells, but the extent to which these and other nutrients contribute to cell mass is unknown. We quantified the fraction of cell mass derived from different nutrients and find that the majority of carbon mass in cells is derived from other amino acids, which are consumed at much lower rates than glucose and glutamine. While glucose carbon has diverse fates, glutamine contributes most to protein, and this suggests that glutamine's ability to replenish TCA cycle intermediates (anaplerosis) is primarily used for amino acid biosynthesis. These findings demonstrate that rates of nutrient consumption are indirectly associated with mass accumulation and suggest that high rates of glucose and glutamine consumption support rapid cell proliferation beyond providing carbon for biosynthesis.

Introduction

Rapidly proliferating cells have different metabolic needs from non-proliferating cells. During each cell cycle, proliferating cells must synthesize all of the components needed to duplicate cell mass (Lunt and Vander Heiden, 2011). One metabolic feature common to many proliferating cells is high glycolytic flux to lactate in the presence of oxygen, a phenomenon referred to as aerobic glycolysis or the Warburg effect. Why proliferating cells, including cancer cells, consume large quantities of glucose only to excrete the majority of this carbon as lactate is a subject of debate (Brand, 1985; Brand et al., 1986; DeBerardinis et al., 2008; Gatenby and Gillies, 2004; Hsu and Sabatini, 2008; Hume et al., 1978; Jiang and Deberardinis, 2012; Koppenol et al., 2011; Lunt and Vander Heiden, 2011; Newsholme et al., 1985; Vander Heiden et al., 2009; Vazquez et al., 2010). One widely held hypothesis is that high glycolytic flux allows intermediates to be shunted into anabolic pathways to support biomass accumulation (Brand, 1985; Chaneton et al., 2012; Faubert et al., 2013; Hsu and Sabatini, 2008; Hume et al., 1978; Jiang and

Deberardinis, 2012; Jiang et al., 2011; Lunt and Vander Heiden, 2011; Newsholme et al., 1985; Shestov et al., 2014; Vander Heiden et al., 2009; Wang and Green, 2012). Many proliferating mammalian cells also consume substantial quantities of glutamine, and glutamine is also hypothesized to provide material for biosynthesis (Brand, 1985; Brand et al., 1986; Daye and Wellen, 2012; DeBerardinis et al., 2007; Hsu and Sabatini, 2008; Wang and Green, 2012). Glutamine or other carbon sources can add new carbon to the tri-carboxylic acid (TCA) cycle (anaplerosis) in order for TCA cycle intermediates to be removed from the cycle and used for the production of new macromolecules in cells (Daye and Wellen, 2012; DeBerardinis and Cheng, 2010; DeBerardinis et al., 2007; Lunt and Vander Heiden, 2011; Newsholme et al., 1985; Wang and Green, 2012), although the extent to which glutamine or other nutrients contribute to biomass has not been determined.

Implicit in these hypotheses is the notion that the most consumed nutrients are also the major contributors to biosynthesis and, therefore, to cell mass. This hypothesis has not been rigorously tested, yet it forms the basis for modeling efforts to understand cancer metabolism (Cascante et al., 2002; Shestov et al., 2014; Shlomi et al., 2011). In *Escherichia coli*, the sources of cell mass and their fates have been carefully quantified (Roberts et al., 1955), and for prototrophic strains grown in defined minimal media, medium composition constrains the nutrients available to produce new biomass. This is not the case for mammalian cells; in both tissues and in cell culture mammalian cells are exposed to diverse metabolic substrates. While the relative uptake of various nutrients has been examined in several systems (Jain et al., 2012; Paredes et al., 1998), the extent to which any contributes to biomass is unknown.

Various qualitative fates of glucose and glutamine in proliferating cells have been extensively studied, and recent work has suggested that metabolism of other nutrients can be important for proliferation, although net contribution of these alternate fuels to cell mass has not been quantified (Comerford et al., 2014; Kamphorst et al., 2013; Labuschagne et al., 2014; Maddocks et al., 2013; Schoors et al., 2015; Schug et al., 2015). In this study we quantitatively determined the sources of cell mass in rapidly proliferating mammalian cells. Surprisingly, we found that glucose and glutamine, the two nutrients with the highest consumption rates, are not the major contributors of carbon to cell mass.

Instead, other amino acids, which are consumed at much lower rates, together account for the majority of carbon in cells. Examining the biosynthetic fates of these nutrients for mass acquisition provides a framework for considering how metabolism supports cell proliferation.

Results

The contribution of glucose to cell mass

To begin examining the contribution of nutrients to mammalian cell mass, we measured the consumption and excretion rates of glucose, lactate, and amino acids in H1299 and A549 non-small cell lung cancer cell lines, cells that have been shown previously to rely on aerobic glycolysis for proliferation (Christofk et al., 2008) (**Figure 1**). Similar to other mammalian cell lines (**Figure 2A**) (Jain et al., 2012), glucose, followed by glutamine, was the most consumed nutrient, and consumption of both exceeded that of serine, the third most consumed metabolite by several fold. Consistent with high aerobic glycolysis in these cells, glucose was consumed at approximately half the rate that lactate was excreted. Most lactate is derived from glucose (**Figure 2B**) (Brand, 1985; Hume et al., 1978), and two lactate molecules can be derived from one glucose molecule. Since the difference between glucose uptake and lactate excretion equals the maximum possible rate of glucose contribution to cell mass, the rate of new mass addition from glucose must be small relative to the rate of glycolysis.

To determine how different nutrients contribute carbon to cell mass, H1299 and A549 cells were grown in the presence of glucose uniformly labeled with carbon-14 ([U-^{14}C]-glucose, i.e. all carbon atoms substituted with carbon-14) until >95% of cell mass had turned over, allowing the proportion of cell dry mass derived from glucose carbon to be determined (**Figure 4**, see methods). Surprisingly, glucose carbon only contributed to around 10% of cell mass even though cells are approximately 50% carbon by dry weight (**Figure 3A,B, 4B**). To confirm that this method is capable of accounting for the contribution of glucose to cell mass, the approach was repeated in prototrophic *Saccharomyces cerevisiae* strain SK1.

70

The dry mass of this strain is also approximately 50% carbon, and when SK1 yeast were cultured in minimal medium containing glucose as the sole carbon source, this carbon could be accounted for using carbon-14 incorporation from $[U-^{14}C]$-glucose (**Figure 3C**).

Glutamine is the most abundant amino acid in plasma (McMenamy et al., 1957), and, like glucose, can be rapidly consumed by proliferating cells. To measure the contribution of glutamine to cell mass, we assessed carbon-14 labeling from $[U-^{14}C]$-glutamine (**Figure 3A,B**). Like glucose, glutamine carbon did not contribute to more than 10% of cell mass, suggesting that the majority of cellular carbon is not derived from glucose or glutamine. To ensure that low incorporation of glucose and glutamine carbon was not influenced by base medium choice, carbon-14 labeling of cells cultured in RPMI 1640 and DMEM were compared, with no differences observed (**Figure 4C**). We also confirmed that labeling was saturated during these experiments; as subsequent passaging in medium with labeled glucose or glutamine did not increase the fraction of cell mass labeled by these nutrients (**Figure 4D,E**).

To confirm these findings using an orthogonal approach, cells were grown in medium containing $[U-^{13}C]$-glucose or glutamine, such that none of the carbon in either nutrient was unlabeled. After culturing cells in this medium until >95% of cell mass was produced *de novo*, the fraction of cellular carbon labeled by carbon-13 was measured by isotope ratio mass spectrometry (IRMS), and the fractional labeling observed was consistent with values derived from carbon-14 incorporation (**Figure 4F**).

Other cell lines representing different tissues of origin, oncogenic drivers, and species also incorporated glucose and glutamine carbon to a similar extent as H1299 and A549 cells (**Table 1, Figure 3D**). This finding suggests that many immortalized cells derive substantial cell mass from a source other than glucose and glutamine. To determine if cell mass is acquired similarly by normal proliferating mammalian cells, we examined both primary embryonic fibroblasts (MEFs) and primary T cells derived from mice. Both MEFS and activated proliferating T cells exhibited comparable levels of carbon incorporation from glucose and glutamine, suggesting that a large proportion of cell mass is also derived from other nutrients in these cells (**Figure 3D,E**).
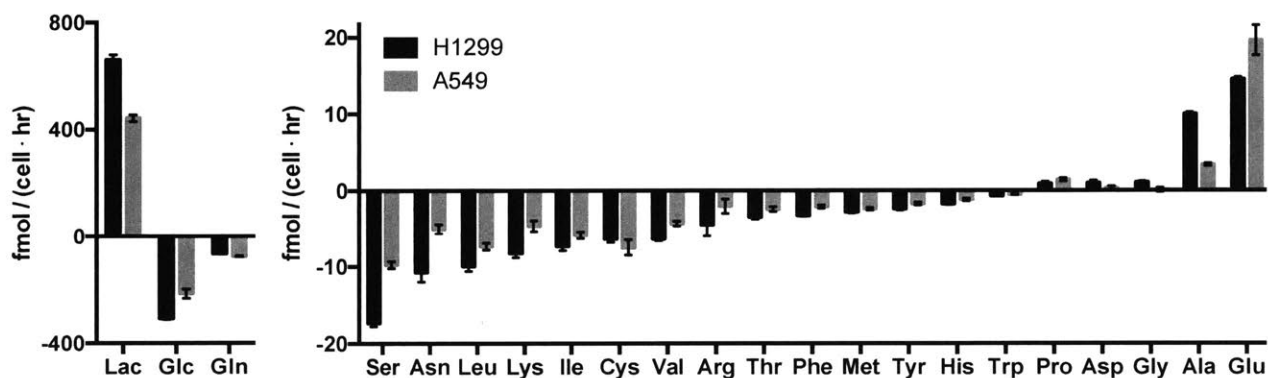
Figure 1: Rapidly proliferating mammalian cells in culture consume glucose and glutamine in excess of other nutrients.

Consumption and excretion rates of glucose, lactate, and amino acids by H1299 and A549 cells. Nutrients are ranked in descending order by absolute magnitude of their fluxes. Each bar represents the slope from a linear fit of N=3 replicate, ± standard error. Standard three-letter abbreviations are used for amino acids; Glc, glucose; Lac, lactate.
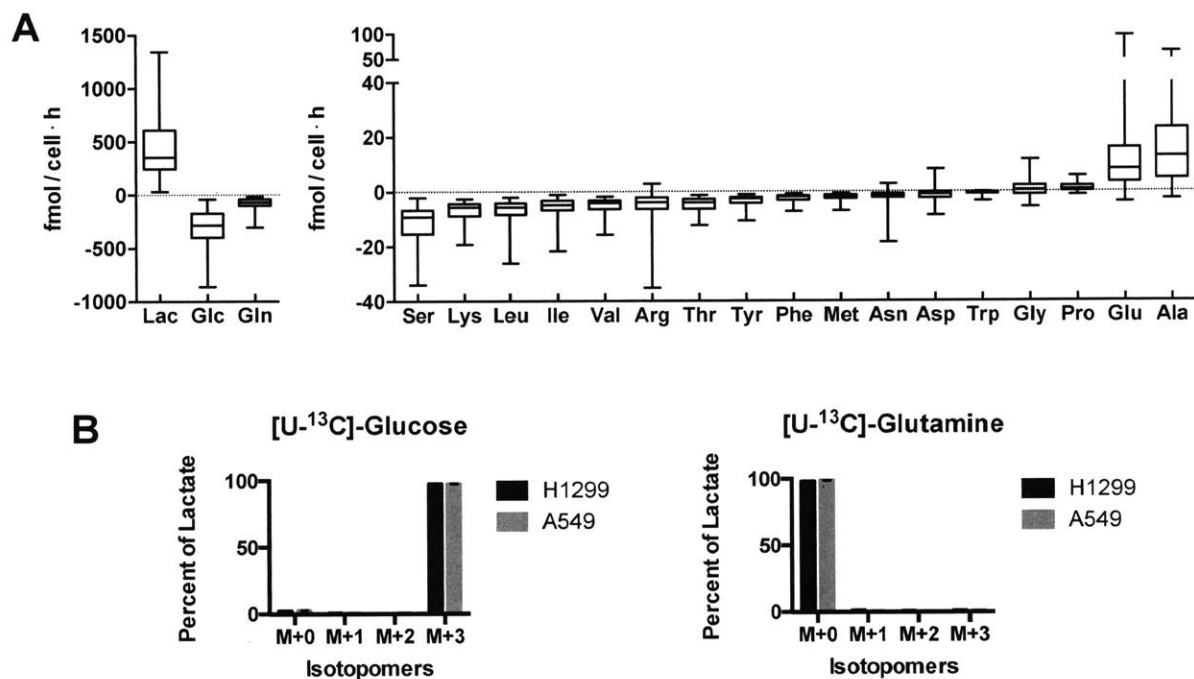
Figure 2: Rapidly proliferating cells have common metabolic features, consuming large amounts of glucose and glutamine and converting most glucose to lactate.

Rapidly proliferating cells have common metabolic features. (A) Consumption and excretion rates (CORE) of glucose, lactate, and amino acids for the NCI-60 cell lines as observed by Jain et al. (2012). Boxes indicate the mean and middle two quartiles, and whiskers indicate the minimum and maximum values. (B) Fractional labeling of lactate by H1299 and A549 cells grown in medium containing [U-^{13}C]-glucose or glutamine. Each bar represents the average of N=3, ±S.D. Standard three-letter abbreviations are used for amino acids; Glc, glucose; Lac, lactate.
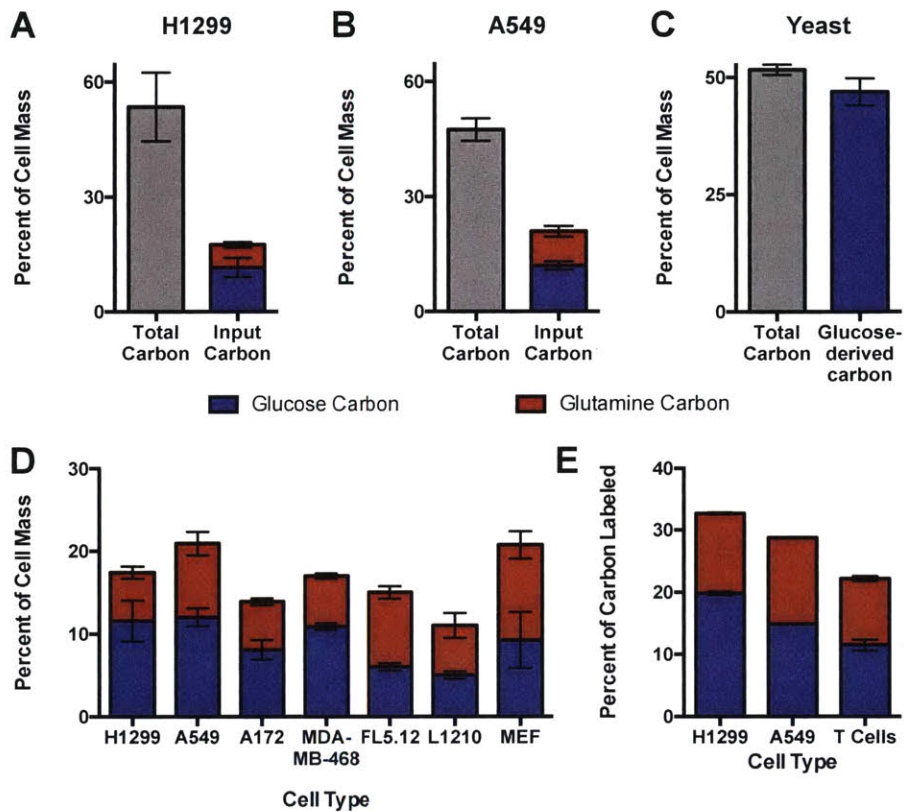
Figure 3: Neither glucose nor glutamine contributes the majority of carbon present in proliferating mammalian cells.

The fraction of cell dry mass consisting of carbon in (A) H1299 and (B) A549 cancer cells exceeds the fraction of cell mass labeled by glucose or glutamine. (C) In SK1 prototrophic yeast, the fraction of cell mass labeled by glucose as the sole carbon source is equal to the fraction of cell mass composed of carbon. (D) The contributions of glucose and glutamine to cell mass are similar across mammalian cells. (E) The fraction of cellular carbon derived from glucose or glutamine in activated primary mouse T cells. Each bar represents the average of N=3 replicates, ±S.D.
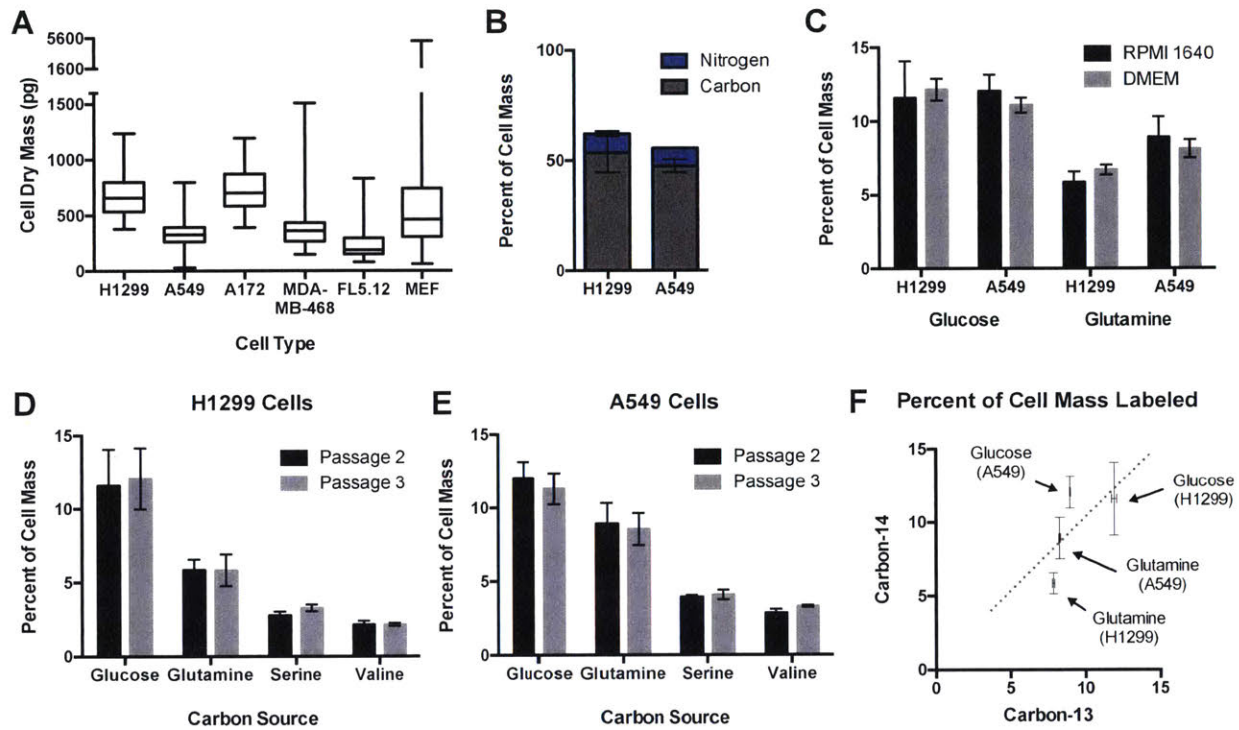
Figure 4: Validation of carbon-14 incorporation measurement to quantify nutrient contribution to cell mass.

(A) Cell dry mass of H1299, A549, A172, MDA-MB-468, FL5.12, and MEF cells as measured using a suspended microchannel resonator (SMR) (Feijo Delgado et al., 2013). (B) Carbon and nitrogen elemental composition of H1299 and A549 cell dry mass as determined by elemental analysis. (C) Incorporation of glucose and glutamine carbon into dry mass of H1299 and A549 cells cultured in DMEM with 10% FBS, or RPMI 1640 with 10% FBS. (D and E) Incorporation of carbon from glucose, glutamine, serine, or valine into H1299 and A549 cell mass after two and three passages in medium containing carbon-14-labeled nutrients. (F) Percent of cell dry mass labeled by [U-^{14}C]- or [U-^{13}C]-glucose or glutamine in H1299 and A549 cells. Carbon-14 incorporation was measured by scintillation counting and normalized relative to culture mass. Carbon-13 incorporation was measured as a fraction of total cellular carbon by EA-IRMS and was adjusted to percentage of cell mass by multiplying by the fraction of cell dry mass consisting of carbon (see 4A). The dotted line represents equal labeling by carbon-14 and carbon-13. In A, boxes indicate the mean and middle two quartiles, and whiskers indicate the minimum and maximum values measured; single cell dry masses of 60-200 cells are presented for each cell type assessed. In B-F, each point represents the average of N=3, ±S.D.
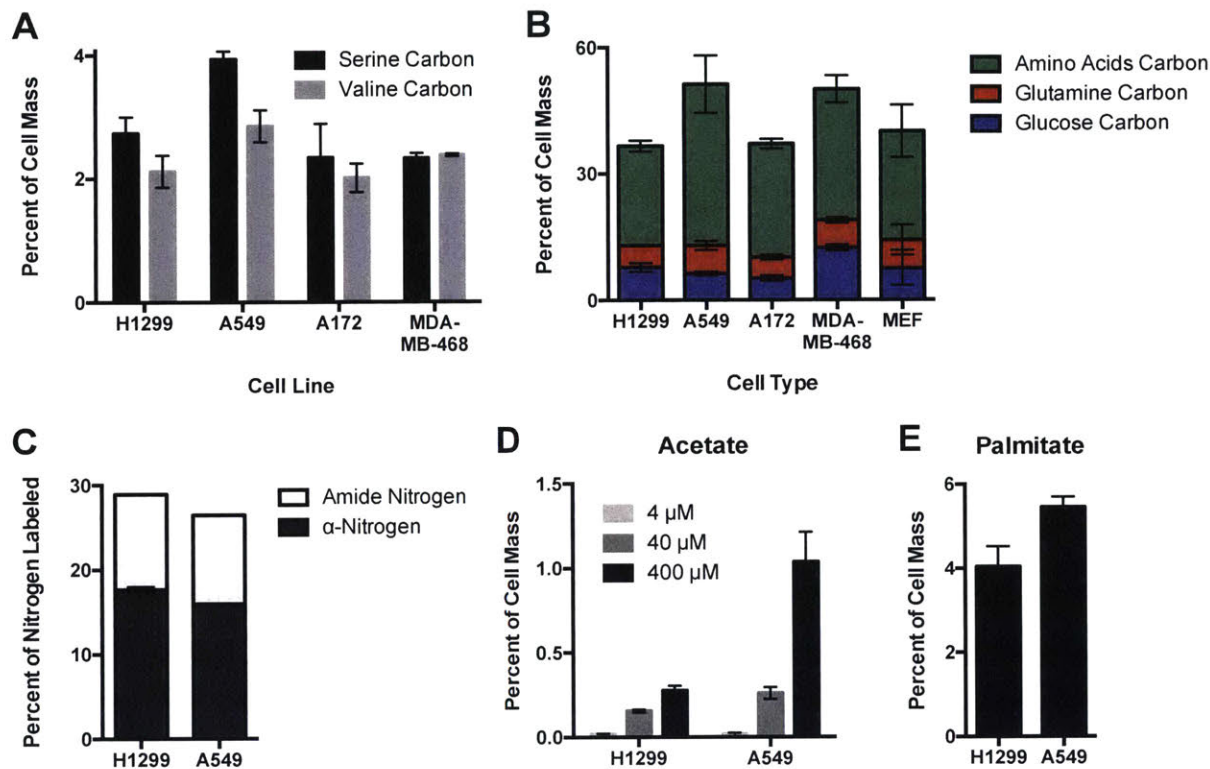
Amino acids contribute the majority of mammalian cell mass

Mammalian cells are thought to consist largely of protein (Alberts et al., 2008; Bonarius et al., 1996; Mourant et al., 2005), so we hypothesized that amino acids could be a major contributor to cell mass. Mammalian cells cannot synthesize many amino acids, and often have access to both essential and non-essential amino acids in their environment. For example, valine, an essential amino acid, must be taken up from the environment, but serine, a non-essential amino acid, may be synthesized *de novo*. Carbon from these amino acids, which have different fates in central carbon metabolism and a different ability to contribute to non-protein biomass, each labeled 2-4% of cell mass (**Figure 5A**). To examine how amino acids in general contribute to cell mass, several mammalian cell lines and primary MEFs were grown in medium containing a pool of fifteen [U-^{14}C]-amino acids (which did not include glutamine). This medium was modified from RPMI 1640 in a manner that supported normal cell proliferation in order to facilitate quantitative determination of cell labeling by these amino acids (see methods, **Figure 6A,B**). Together, amino acids were found to label the majority of carbon in cells and, together with the carbon derived from glucose and glutamine, can account for most of the carbon mass in mammalian cells (**Figure 5B**).

In addition to providing carbon, glutamine contains two nitrogen atoms and can be a nitrogen source for cultured cells (DeBerardinis and Cheng, 2010). The amide nitrogen can be transferred to asparagine and nucleotides, and the α- (amino) nitrogen can be transaminated to non-essential amino acids. Both nitrogen atoms can also be incorporated into protein as glutamine, and hydrolysis reactions allow either to be excreted as ammonia. To determine the extent to which glutamine contributes nitrogen to biomass of H1299 and A549 cells, cells were cultured in the presence of either [amide-^{15}N]- or [α-^{15}N]-glutamine, and the contribution of each to cellular nitrogen was measured by IRMS after labeling had reached steady state (**Figures 5C, 6C,D**). The amide- and α-nitrogen atoms, respectively, accounted for approximately 11% and 17% of cellular nitrogen. Interestingly, glutamine nitrogen altogether contributed less than half of the nitrogen in each of the cell lines analyzed, suggesting that the rest is derived from other sources such as amino acids.

76

Cell mass partially turns over in non-proliferating mammalian cells

We next sought to determine the extent to which glucose and amino acids contribute carbon mass to non-proliferating cells. These cells do not have the biosynthetic demand to duplicate cell mass, but are not thought to be metabolically quiescent (Lemons et al., 2010) and likely turnover some proportion of cell mass. To determine the mass contribution to quiescent cells, we examined non-transformed human mammary epithelial cells (HMECs) that reversibly arrest when epidermal growth factor (EGF) is withdrawn (**Figure 7A**) (Stampfer et al., 1993). Proliferating HMECs incorporate carbon from glucose, glutamine, serine, and valine to an extent comparable to other proliferating cells, and interestingly, labeling of non-proliferating HMECs approached similar steady state values, suggesting that most of their cell mass turns over after several weeks (**Figure 8A,B**). We also determined the contributions of these nutrients to carbon cell mass of post-mitotic cells: primary hepatocytes cultured *ex vivo*, as well as myocytes and adipocytes differentiated *in vitro* from C2C12 and 3T3-L1 cells, respectively. Similar to HMECs, hepatocytes, myocytes, and adipocytes were labeled by each of the tracers used, indicating some cell mass turnover (**Figures 8C-G, 7B-E**). However, in most cases labeling approached steady state values lower than those observed for proliferating cells. This suggests that, in contrast to the HMECs, only a fraction of cell mass in these differentiated cells is turned over. Importantly, undifferentiated C2C12 myoblasts and undifferentiated 3T3-L1 pre-adipocytes incorporated glucose and amino acids to an extent similar to other proliferating cells (**Figure 8D,F**). Like hepatocytes and myocytes, adipocytes incorporated amino acids at levels lower than proliferating cells (**Figure 8G**). Glucose, however, labeled a substantial portion of adipocyte cell mass, consistent with their role in lipid storage (**Figure 7E**). The non-proliferating cells analyzed illustrate that different cell types use different metabolic programs. Hepatocytes and myocytes partially turn over cell mass, using glucose and amino acids to similar extents. Adipocytes are metabolically specialized, incorporating large amounts of glucose carbon, and HMECs abundantly incorporate amino acids into cell mass regardless of their proliferation status.

Figure 5: Amino acids contribute the majority of cell mass for proliferating mammalian cells.

(A) Serine and valine carbon each contribute 2-4% of cell dry mass in mammalian cells. (B) A pooled mixture of fifteen amino acids can label the majority of cellular carbon in proliferating mammalian cells. Amino acid mass contribution was determined by culturing cells in modified RPMI (Table 2, Figure 6A) with [U-^{14}C]-amino acids. Mass contribution of glucose and glutamine as determined in D are also presented for comparison. (C) The fraction of cellular nitrogen derived from glutamine α- and amide-nitrogen atoms. (D) Acetate carbon is a minor contributor to cell mass, and the net contribution is dependent on acetate concentration. (E) Contribution of serum palmitate to cell mass as determined by incorporation of [U-^{14}C]-palmitate. Each bar represents the average of N=3 replicates, ±S.D.
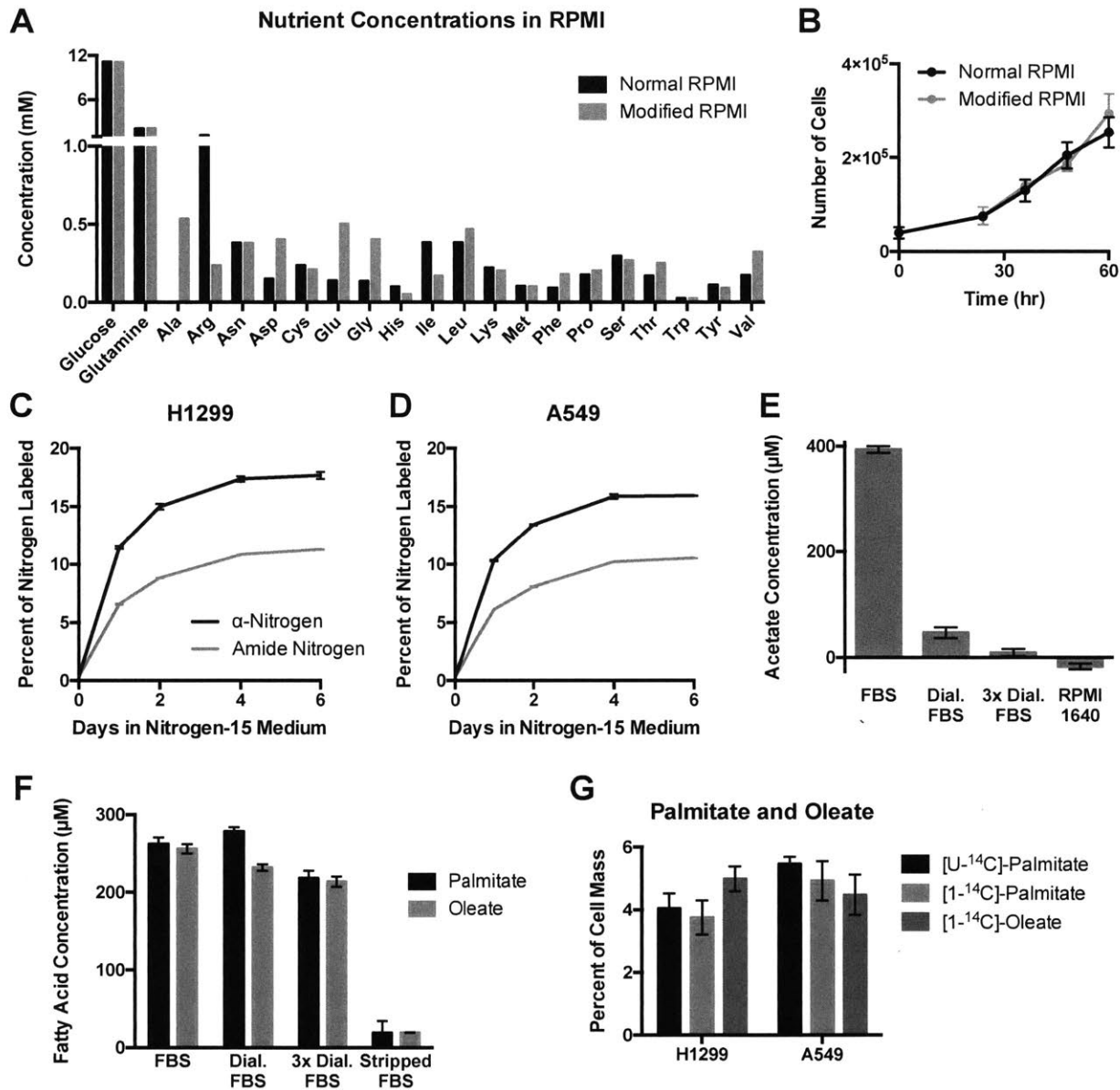
Figure 6. Validation of culture conditions to determine amino acid, lipid, and acetate incorporation.

(A) Concentrations of glucose and amino acids in normal RPMI 1640 and modified medium used to measure incorporation of amino acids into cell mass (see Table 2). (B) Growth of A549 cells in normal RPMI 1640 medium and in medium with modified amino acid concentrations. Nitrogen-15 incorporation into (C) H1299 and (D) A549 cells from [amide-15N]- or [α-15N]-glutamine. Concentrations of (E) acetate and (F) palmitate and oleate in FBS, commercial dialyzed FBS (dial. FBS), FBS dialyzed three times against saline (3x dial. FBS), FBS extracted with 2:1 diisopropyl-ether:butanol (stripped FBS), and RPMI 1640 medium (without serum). (G) The fraction of H1299 and A549 cell dry mass derived from serum palmitate and oleate. The amount of carbon labeled by [1-14C]-palmitate and [1-14C]-oleate was multiplied by 16 and 18, respectively, to estimate the contribution from the full-length fatty acid. This calculation makes the assumption that like palmitate, oleate is also fully incorporated into cell mass. Each point represents the average of N=3, ±S.D.
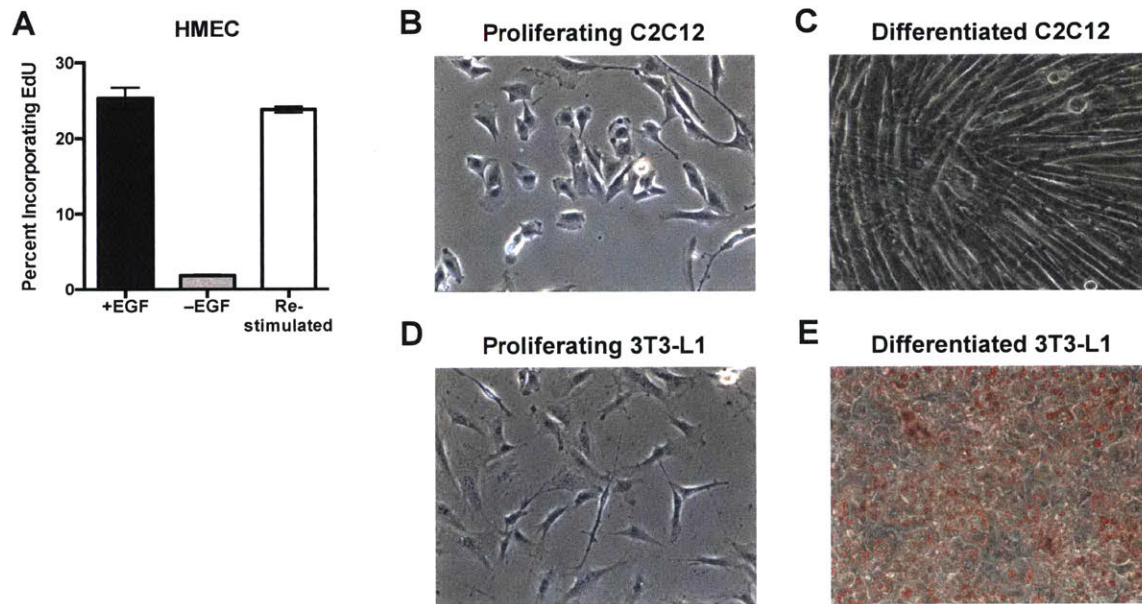
Figure 7: Validation of non-proliferating cell models.

(A) Human mammary epithelial cell (HMEC) proliferation is reversibly arrested when epidermal growth factor (EGF) is withdrawn, as measured by 5-ethynyl-2-deoxyuridine (EdU) incorporation. N=3, ±S.D. Representative phase contrast images of (B) proliferating C2C12 myoblasts, (C) differentiated C2C12 myocytes, (D) proliferating 3T3-L1 fibroblasts, and (E) 3T3-L1 differentiated into adipocytes. Cells in (D) and (E) are stained with oil red O.
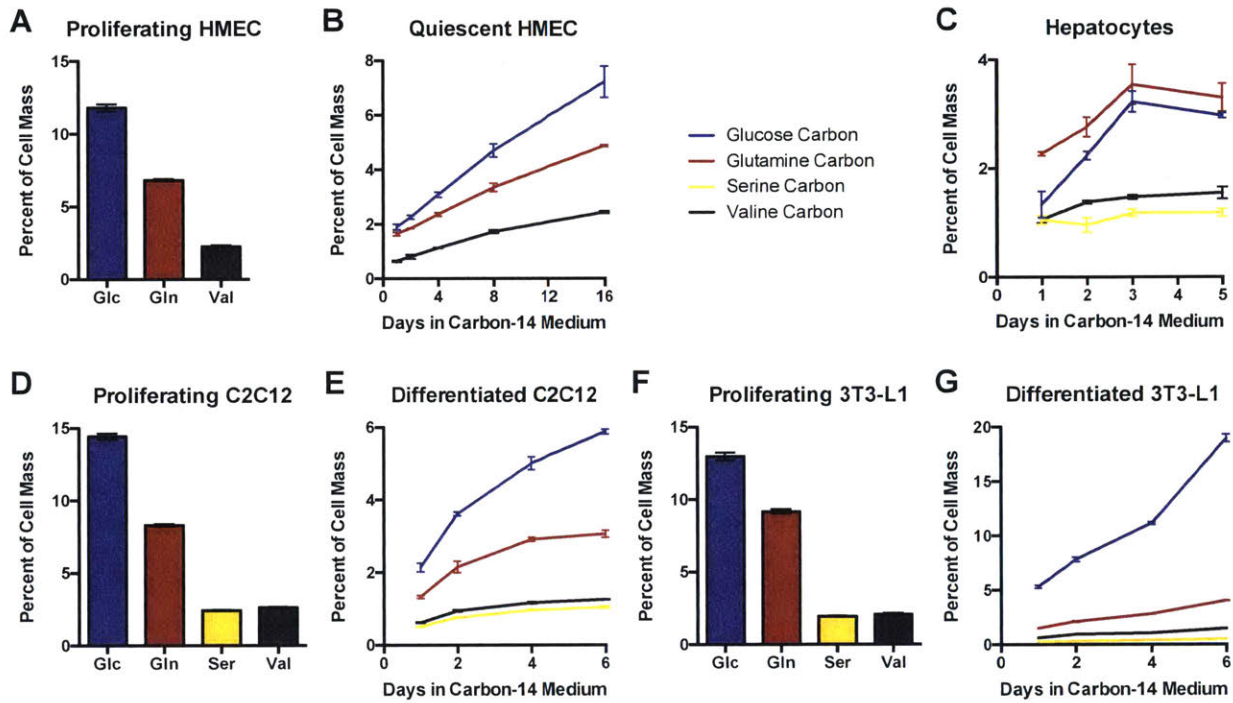
Figure 8: Carbon contribution to non-proliferating cell mass.

Using carbon-14 tracers, carbon from glucose (Glc), glutamine (Gln), serine (Ser), and valine (Val) was traced into cell mass of: (A) proliferating human mammary epithelial cells (HMEC), (B) arrested HMEC, (C) primary hepatocytes, (D) proliferating C2C12 myoblasts, (E) differentiated C2C12 myocytes, (F) proliferating 3T3-L1 fibroblasts, and (G) 3T3-L1 differentiated into adipocytes. Carbon incorporation into proliferating cells is shown at steady state, whereas incorporation over time is shown for non-proliferating cells. Each bar represents the average of N=3 replicates, ±S.D.

Fatty acids and acetate are minor sources contributing to cell mass

The large contribution of amino acids to cell mass despite relatively low uptake suggests that other nutrients consumed at low rates might contribute to cell mass. For instance, acetate can play a role in fueling cell proliferation (Comerford et al., 2014; Schug et al., 2015). Acetate is absent from tissue culture base media, so we measured acetate levels in fetal bovine serum (FBS) and in the dialyzed FBS used in our labeling studies (**Figure 6E**). In bovine serum, acetate was approximately 400 μM, and in tissue culture medium containing 10% FBS or 10% dialyzed FBS, acetate levels were approximately 40 μM or 4 μM, respectively. Carbon from acetate did not label cells appreciably when cultured in medium with 10% serum, but began to approach 1% of cell dry mass when 400 μM acetate was present in the medium (**Figure 5D**), a concentration higher than what is typically observed in human serum (Richards et al., 1976; Tollinger et al., 1979).

Cells can also scavenge serum fatty acids as another potential source of mass (Bailey et al., 1972; Kamphorst et al., 2013; Schoors et al., 2015). Quantitative assessment of total fatty acid contribution is complicated by the fact that the fatty acid composition of serum is complex and cannot be recapitulated using isotope labeled tracers. However, to assess the magnitude of individual fatty acid contribution, we examined the incorporation of palmitate (C16:0) into cell mass. Palmitate is the most abundant fatty acid in both serum and in cell membranes (Kilsdonk et al., 1992; Raatz et al., 2001; Vajreswari et al., 1990). Palmitate is present at around 260 μM in FBS (**Figure 6F**), however this value includes both free fatty acid and esterified palmitate in lipids. [U-^{14}C]-palmitate provided as a free fatty acid labeled approximately 5% of H1299 and A549 cell mass when considered in relation to total palmitate (free fatty acid and esterified) in media (**Figure 5E**). These data indicate that exogenous lipids can also be a contributor to mass; however this assessment may overestimate the contribution because most serum fatty acids are esterified in lipids such as triglycerides (Raatz et al., 2001). Esterified fatty acids taken up by cells are first hydrolyzed by lipases to generate free fatty acids that mix with free fatty acid pools in cells (Walther and Farese, 2012). However, the amount of carbon incorporated from [1-^{14}C]-palmitate was one sixteenth of that incorporated from [U-^{14}C]-palmitate (**Figure 6G**). Because the labeled carbon atom in

[1-^{14}C]-palmitate is the first carbon lost during fatty acid oxidation, these data suggest that each molecule

of palmitate acquired by cells is either completely catabolized or completely incorporated into cell mass.

Based on similar assumptions, carbon from [1-^{14}C]-oleate (C18:1), the second most abundant serum fatty

acid (**Figure S3F**) (Raatz et al., 2001), also could account for approximately 5% of cell mass (**Figure**

6G).

Serum provides the majority of cellular lipids

Lipids can be scavenged from the environment or synthesized *de novo*, with glucose and

glutamine serving as potential substrates for *de novo* biosynthesis (Kamphorst et al., 2013; Metallo et al.,

2012; Mullen et al., 2012). To understand the contributions of glucose and glutamine specifically to

lipids, we adapted a bi-phasic extraction protocol to separate and recover lipids (and other non-polar

compounds) as well as the other major macromolecule classes: RNA, DNA, protein, and polar

metabolites (**Figure 9A**). This approach can quantitatively recover these macromolecules from a cell

lysate with high purity, as validated using radioactive standards that were isolated by orthogonal means

(**Figure 9B,C**). Fractionation of radiolabeled cells using this approach also yields full recovery of input

radioactivity (**Figure 10A**). Consistent with previous studies (Kamphorst et al., 2013; Metallo et al.,

2012; Mullen et al., 2012), carbon-14 from both glucose and glutamine was recovered in the lipid fraction

of H1299, A549, and A172 cells, with greater glucose contribution to lipids than glutamine (**Figure 9D**).

Substantial amounts of glucose carbon were recovered in each of the macromolecule fractions

investigated, but the largest proportion of glucose was diverted to the non-polar fraction suggesting that

glucose is a major source of material for *de novo* lipogenesis.

To assess the contribution of lipid biosynthesis from glucose relative to lipid scavenging from the

environment, we measured the increase in glucose incorporation into the lipid fraction when proliferating

cells were deprived of exogenous lipids. To do this, cells were cultured in serum stripped of lipids by

non-denaturing organic extraction (**Figure 6F**). Any increase in glucose contribution to fatty acids under

these conditions should reflect the contribution of exogenous lipids to mass when cells are cultured in
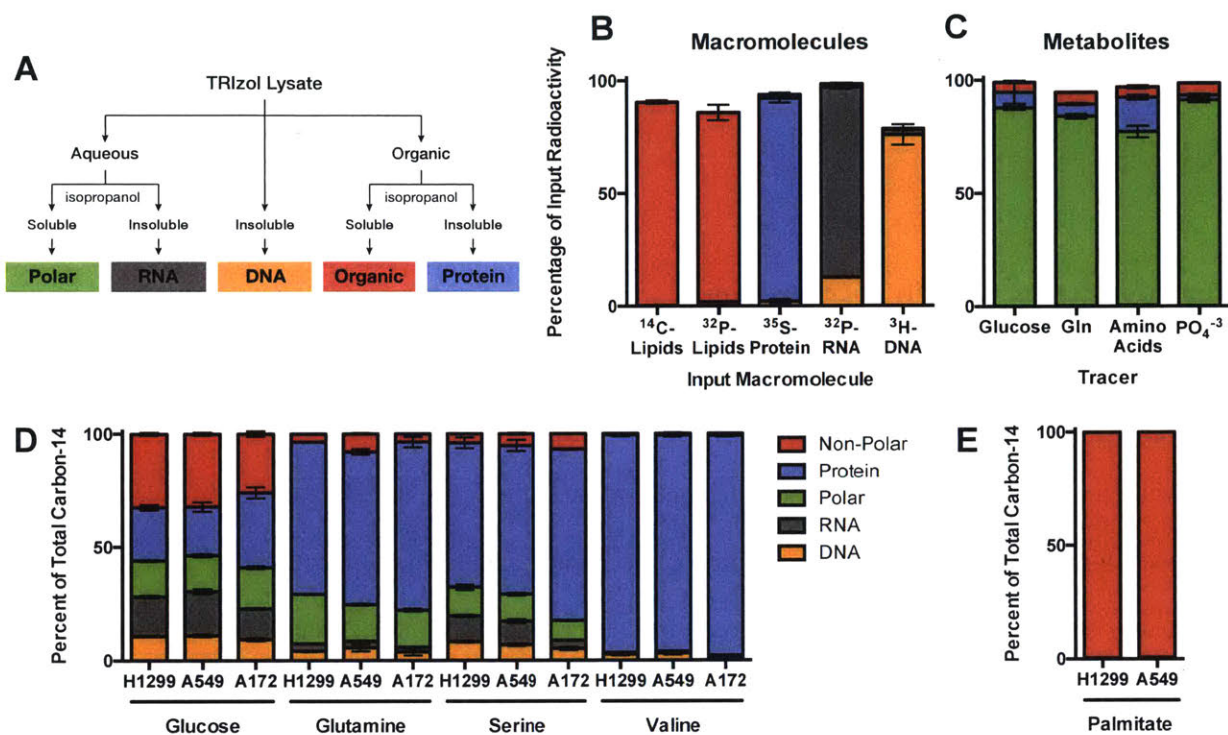
Figure 9: Glucose, glutamine, and other amino acids have diverse biosynthetic fates.

(A) Scheme used to fractionate cells into different macromolecular classes based on differential solubility is shown. Material not precipitated from the aqueous phase is referred to as the polar fraction, and material not precipitated from the organic phase is referred to as the non-polar fraction. (B) Radioactive macromolecules were independently synthesized and purified from HEK293 cells and then used to assess yield and purity of the fractions resulting from the scheme in (A). (C) Radioactive small molecules derived from different nutrients were extracted from HEK293 cells and used to assess yield and purity of the polar fraction resulting from the scheme in (A). (D and E) The relative contributions of (D) glucose, glutamine, serine, and valine, and (E) exogenous palmitate to different macromolecule fractions were determined for H1299, A549, and A172 cells. Each bar represents the average of N=3 replicates, ±S.D.
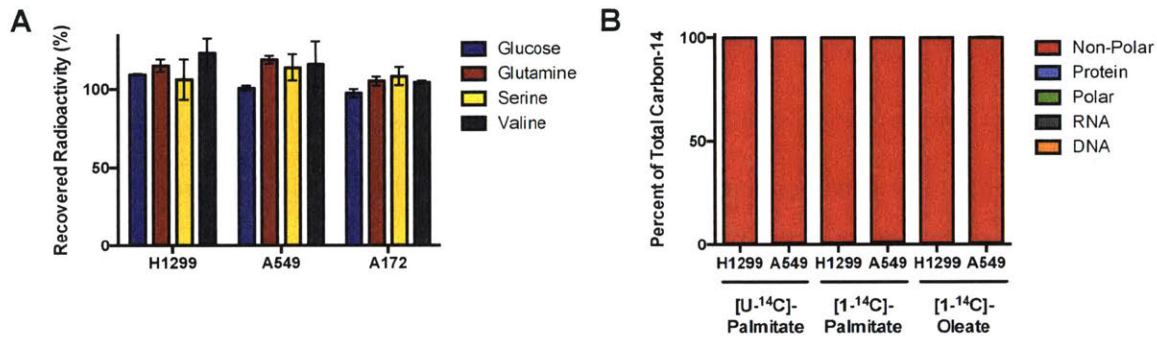
Figure 10: Recovery of input radioactivity after fractionation of cells.

(A) Recovery of input radioactivity after fractionation of H1299, A549, and A172 cells grown in the presence of [U-^{14}C]-glucose, glutamine, serine, or valine. The radioactivity recovered in the different macromolecule fractions (Figure 5A) was summed and is shown relative to the total radioactivity incorporated into parallel cultures. (B) Fate of exogenous lipids in H1299 and A549 cells. N=3, ±S.D.

lipid-replete conditions. Importantly, cell mass was not significantly changed when cells were cultured in

medium containing fatty-acid-stripped serum (**Figure 12A**). Substantially more glucose carbon was

incorporated into cell mass when cells were cultured without lipids, such that approximately half of

carbon from glucose was diverted to the non-polar fraction under these conditions (**Figure 11A,B**). These

data are consistent with cells obtaining substantial lipid mass from their environment when available

(**Figures 9E, 10B**). These data are also consistent with the observed equal contributions of [U-^{14}C]-

palmitate and [1-^{14}C]-palmitate to cell mass (**Figure 6G**). No detectable change in net glutamine carbon

contribution to cell mass was observed when cells were cultured in the absence of lipids; however, the

relative incorporation of glutamine carbon into non-polar material approximately doubled in this

condition. Finally, the difference in the proportion of cell mass derived from glucose when cells are

grown with or without serum fatty acids corresponds well with the measured contribution of palmitate

and oleate carbon to cell mass when these fatty acids are present (**Figures 5E, 6G**). This corroborates the

notion that these two fatty acids are the predominant mass contributors from exogenous lipids and argues

that lipid mass in these cells is obtained from a combination of scavenging and *de novo* synthesis from

glucose. Assuming that cellular lipids are derived from only glucose, glutamine, and extracellular lipids,

the above data suggest that 60-70% of lipid carbon is derived from exogenous sources, while 20-30% is

derived from glucose and ~5% from glutamine.

The fate of carbon incorporated into cell mass

Glucose carbon can enter many biosynthetic pathways (Hume et al., 1978; Lunt and Vander

Heiden, 2011), and glucose contributes to all macromolecular fractions (**Figure 9D**). One non-redundant

function of glucose is to provide ribose for nucleotide biosynthesis and a quarter of glucose carbon was

traced to RNA and DNA. Some amino acids might also contribute to pathways beyond protein synthesis.

To understand how cells utilize amino acids, we traced glutamine, serine, and valine carbon into

macromolecules (**Figure 9D**). Both glutamine and serine can be metabolized to other biosynthetic

precursors. Although glutamine anapleurosis for the TCA cycle is hypothesized to provide material that

can satisfy biosynthetic demands beyond protein biosynthesis (Daye and Wellen, 2012; DeBerardinis and

Cheng, 2010; DeBerardinis et al., 2007; Lunt and Vander Heiden, 2011; Metallo et al., 2012; Mullen et

al., 2012), protein was by far the major fate of glutamine carbon. Apart from a small contribution to the

non-polar fraction, minor amounts of glutamine carbon were also recovered in nucleic acids. Glutamine

carbon incorporation was 3-4 times greater than serine or valine carbon incorporation (**Figures 3,5**), but

nonetheless most glutamine carbon was recovered with the protein fraction. Because glutamine is not

over-represented in cell protein (Bonarius et al., 1996), this finding suggests that glutamine anapleurosis

provides carbon for other TCA cycle-derived amino acids. Serine carbon exhibited similar relative

incorporation into cell mass as glutamine carbon. While the majority of serine carbon was found in

protein, serine carbon was also recovered in nucleic acids in agreement with the known role of serine in

providing both one-carbon units and glycine for nucleotide biosynthesis (Labuschagne et al., 2014; Lunt

and Vander Heiden, 2011). Valine carbon was traced exclusively into protein. If glucose, glutamine, and

serine are assumed to be the sole carbon sources for nucleic acids (glycine is likely a minor contributor as

it is excreted by these cells, see **Figure 1**), these data suggest that glucose supplies 60-80% of nucleotide

carbon, and glutamine and serine supply 10-20% and ~15%, respectively.

Nutrient deprivation increases the contribution of glucose to cell mass

It is possible that under some conditions glucose and/or glutamine carbon contribute more to cell

mass. Several amino acids are non-essential for cells, and cells cultured without those amino acids may

become more dependent on glucose, glutamine, or other nutrients. To identify which amino acids or

combinations of amino acids are non-essential for cells in culture, H1299 and A549 cells were cultivated

in media lacking combinations of non-essential amino acids (**Figure 12B,C**). Two amino acids that can

be derived from glycolysis, serine and glycine, and four amino acids that can be derived from the TCA

cycle, asparagine, aspartate, glutamate, and proline can be removed from medium without stopping

proliferation of these cells. Removal of glycine or the TCA-cycle amino acids had minimal effect on

doubling times of the cells tested (**Figure 12B,C**), and removal of either the TCA-cycle amino acids or
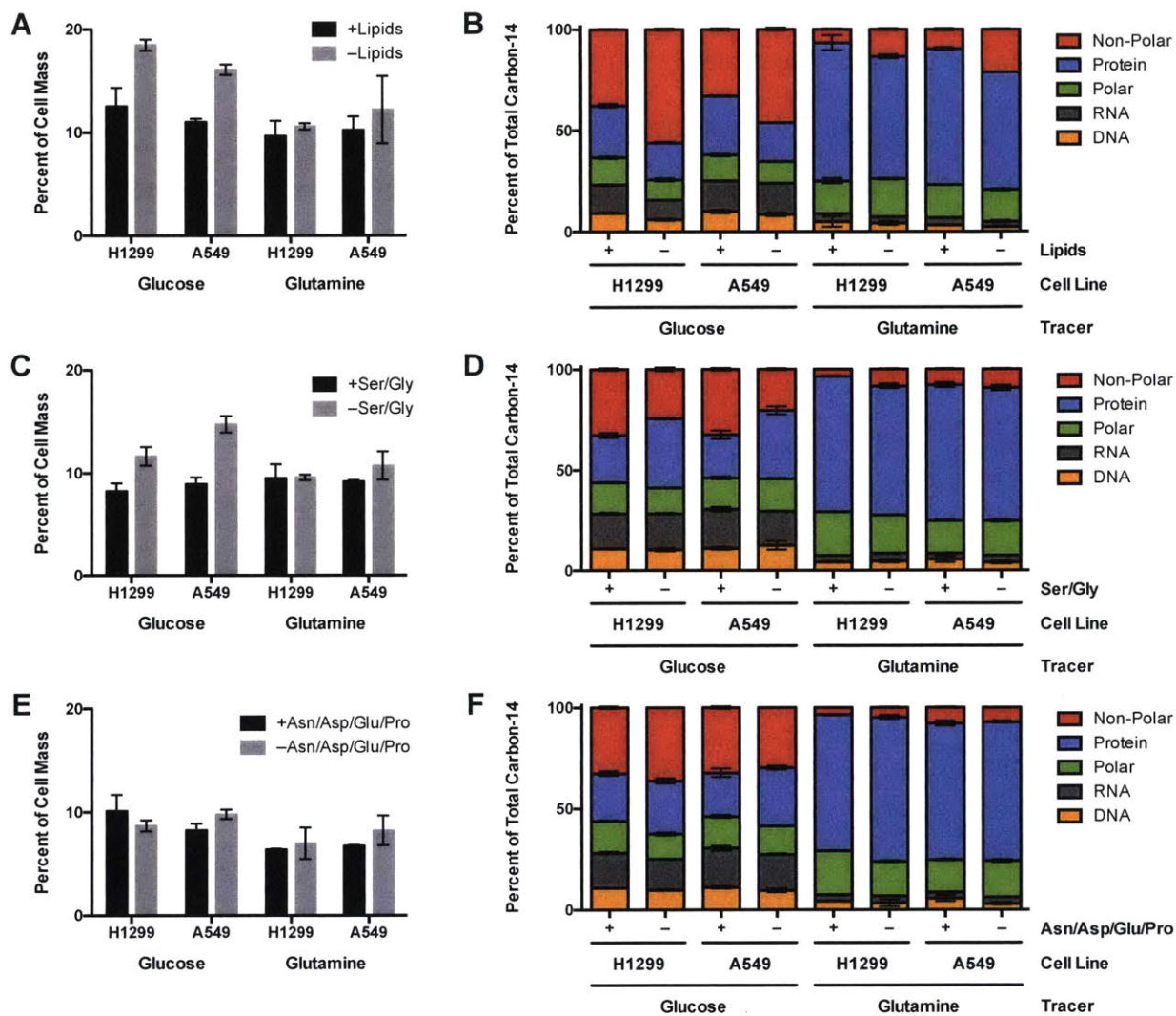
Figure 11: Glucose carbon incorporation into cell mass is increased when non-essential nutrients are absent.

Glucose and glutamine incorporation and utilization in H1299 and A549 cells grown in RPMI 1640 (A) containing normal serum or serum stripped of lipids; (B) with or without serine and glycine; or (C) with or without asparagine, aspartate, proline, and glutamate. Each bar represents the average of N=3 replicates, ±S.D.
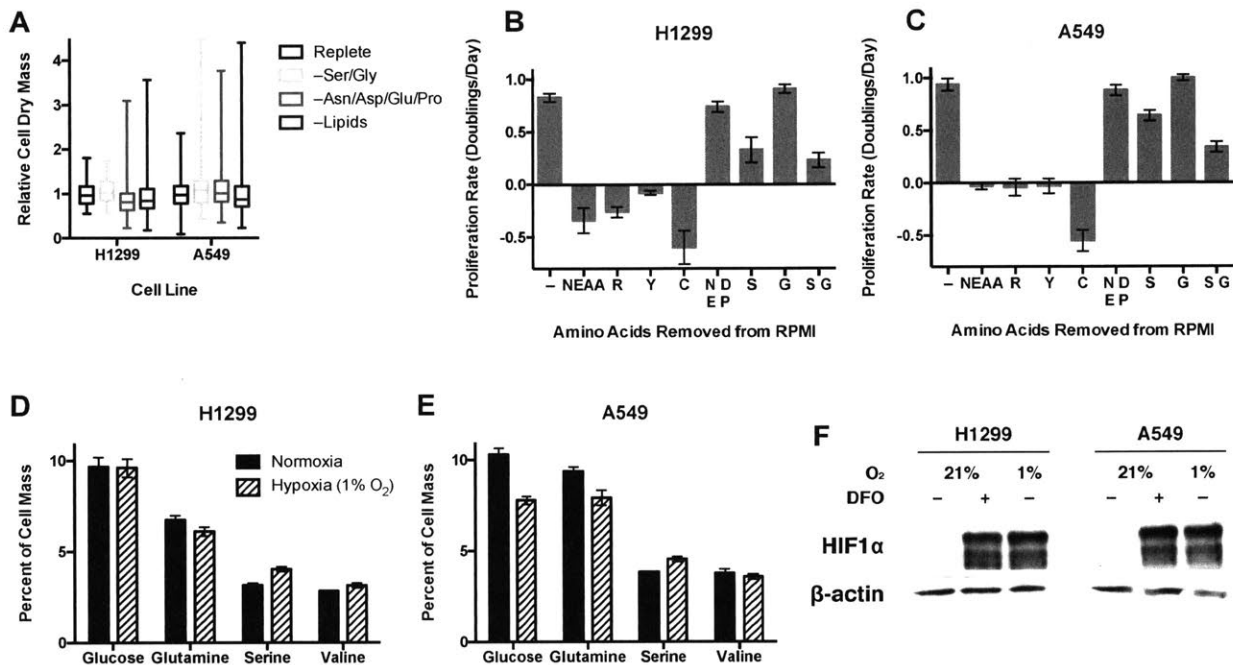
Figure 12: Identification of non-essential medium components and analysis of nutrient incorporation by hypoxic cells.

(A) Relative cell dry masses of H1299 and A549 cells cultured in RPMI 1640 with 10% dialyzed FBS (replete), medium lacking serine and glycine, medium lacking asparagine, aspartate, glutamate, and proline, or medium supplemented with 10% lipid-stripped FBS. Boxes indicate the mean and middle two quartiles, and whiskers indicate the minimum and maximum values measured; each represents single cell dry masses of 60-200 cells. Average cell mass in each condition did not differ significantly from that in replete medium according to a two-tailed Student's t-test ($p > 0.05$). Proliferation rates of (B) H1299 and (C) A549 cells in RPMI 1640 lacking all non-essential amino acids (NEAA), or specific non-essential amino acids (standard one-letter abbreviations are used). N=3, ±S.D. Carbon incorporation into proliferating (D) H1299 and (E) A549 cells cultured in 1% O2. (F) Immunoblot for HIF1α in cells cultured in 21% oxygen with or without deferoxamine (DFO, a chemical inhibitor of HIF degradation), or 1% oxygen for 4 hours. A β-actin immunoblot is shown as a loading control.

both serine and glycine did not significantly alter cell mass (**Figure 12A**). In the absence of serine and glycine cells incorporate more glucose carbon (**Figure 11C**), and the increase in incorporation is approximately two times greater than the amount of carbon incorporated from serine. More glucose carbon also contributes to protein in this condition (**Figure 11D**), but the relative fate of glucose carbon does not differ much from serine/glycine-replete conditions, most likely because serine and glycine also contribute to nucleotides and lipids (Lunt and Vander Heiden, 2011). Since serine and glycine are synthesized from glycolytic intermediates, glutamine incorporation and utilization are not changed when cells are cultured in the absence of these amino acids (**Figure 12D**).

Without the TCA-cycle amino acids asparagine, aspartate, glutamate, and proline, neither glucose nor glutamine carbon incorporation into cell mass changes (**Figure 11E**), and their relative biosynthetic fates are not altered (**Figure 11F**). This suggests that independent of the presence or absence of these four TCA-derived amino acids, glutamine provides much of the carbon for these amino acids even when they are available in the medium. Because glutamine carbon mostly contributes to protein and because its incorporation into cell mass is 3-4 times greater than that of serine or valine, these data are consistent with TCA cycle anapleurosis from glutamine producing these amino acids in greater quantities than other macromolecular precursors. Consistent with this hypothesis, based on known pathways, the contribution of glutamine carbon to RNA and DNA only occurs via glutamine-generated aspartate.

Glucose and glutamine utilization is altered in hypoxia: glucose contributes less carbon and glutamine contributes more carbon to lipogenic acetyl-CoA, and cells become increasingly dependent on scavenged lipids (Kamphorst et al., 2013; Metallo et al., 2012). In H1299 cells, glucose and glutamine incorporation was not altered when cells were cultured in 1% oxygen, whereas incorporation of both was decreased in A549 cells while serine and valine incorporation were relatively unchanged in hypoxia (**Figure 12D,E**). Importantly, HIF1α was stabilized in cells cultured in 1% oxygen confirming a normal response to low oxygen (**Figure 12F**), These results suggest that, although metabolic specific pathways are regulated by hypoxia, the incorporation of glucose and glutamine carbon into cell mass is not grossly altered.

90

Discussion

The finding that mammalian cells derive the majority of their mass from exogenously supplied amino acids provides a model for efficient cell growth. By utilizing biosynthetic end products available in the environment rather than synthesizing them *de novo*, cells will require less ATP, redox equivalents, and carbon to support cell proliferation. Consistent with this hypothesis, carbon from available fatty acids is used exclusively to generate non-polar material, and any fatty acid oxidation does not appear to provide carbon to non-lipid biomass. In some cell types, fatty acid carbon has been traced into dNTPs, but the net contribution of this carbon source has not been quantified (Schoors et al., 2015). In this study, valine carbon was only found in protein, with no evidence that catabolism of this amino acid provides carbon for non-protein biomass. Whole protein can also be scavenged as an alternative source of amino acids for cells (Commisso et al., 2013). Because we can account for protein mass in the cells from the uptake of free amino acids, protein scavenging does not appear to be a major contributor to cell carbon under the conditions tested. Nevertheless, in conditions where free amino acids are limiting, mobilizing amino acids from bulk protein may be important (Commisso et al., 2013), particularly if minimizing *de novo* amino acid biosynthesis is favored in proliferating cells.

The finding that amino acids together contribute the majority of cell mass is in agreement with the notion that cells are composed primarily of protein (Alberts et al., 2008; Dolfi et al., 2013; Mourant et al., 2005) and is consistent with genomic models of mammalian metabolism (Thiele et al., 2013). The nutrients used to support the growth of other organisms also argues that direct use of amino acids nutrients is a common means to support cell proliferation. Both fertilized bird eggs and germinating plant seeds are examples of closed systems comprised primarily of protein, amino acid, and lipid stores that support rapid gains in organismal mass in the absence of other exogenous nutrients (Boulter and Barber, 1963; Moran, 2007; Willems et al., 2014). Rapid cell proliferation in these systems is also consistent with the notion that proliferating cells avoid *de novo* biosynthesis where possible. Glycolytic flux is also crucial to development, but it may be more important for ATP and redox balance than for direct

production of biosynthetic carbon (Kučera et al., 1984), and the sugar reserves found in seeds contribute primarily to polysaccharides in seedlings (Abdul-Baki, 1969).

The observation that glucose incorporation can be increased to compensate for the absence of some nutrients implies that there is a degree of modularity in macromolecular biosynthesis. Cells are known to have increased dependence on glucose-derived serine when serine is limiting (Chaneton et al., 2012; Labuschagne et al., 2014), and when cells are grown without serine and glycine, the increase in glucose incorporation is roughly twice the amount of carbon derived from serine. Similarly, the increase in glucose incorporation in the absence of lipids corresponded closely to the contributions of palmitate and oleate to cell mass. These findings argue that cell composition and the biosynthetic components required for proliferation do not change across these conditions.

Modeling efforts have sought to explain rapid glucose and glutamine consumption by maximizing the efficiency of consumed carbon incorporation into biomass (Cascante et al., 2002; Shestov et al., 2014; Shlomi et al., 2011). However, rapid consumption of a particular nutrient need not correlate with cell mass incorporation and it appears that the large fluxes through glycolysis and glutaminolysis support proliferation in ways other than supplying carbon. Although the contribution of glucose carbon to cell mass is small, both glucose carbon and glucose metabolism are still important for proliferation. For instance, duplication of nucleic acids is needed for cell proliferation and this requires ribose from glucose or another bioavailable carbohydrate. Glucose and glutamine metabolism also have important roles in contributing non-carbon material to biosynthesis, including energy and reducing equivalents, as well as nitrogen. In many cell lines and in some tumors, glutamine is a major source of nitrogen and can provide anapleurotic TCA cycle carbon. Both glutamine nitrogen atoms contributed abundantly to cellular nitrogen, with the α-nitrogen contributing slightly more. Because the α-nitrogen is used for *de novo* amino acid synthesis that contribute to both protein and nucleic acids, while the amide-nitrogen contributes primarily to nucleic acids, the increased abundance of proteins in cells likely accounts for this difference.

The primary contribution of glutamine to biomass production in proliferating cells is to the protein fraction. Although non-glutamine amino acids are the dominant source of protein carbon mass, the

contribution of glutamine is in excess of that expected of glutamine salvage alone because glutamine atoms are incorporated into other amino acids and TCA cycle intermediates. Indeed, while glutamine may not be utilized as a TCA cycle substrate in all cells *in vivo* (Davidson et al., 2016; Marin-Valencia et al., 2012; Tardito et al., 2015; Yuneva et al., 2012), our data suggests important incorporation of glutamine-derived carbon in TCA cycle intermediates regardless of whether they are freely available in the media. Aspartate, for example, is poorly transported by cells outside of the prostate and the nervous system (Lao et al., 1993; Storck et al., 1992) and therefore must be synthesized. Glutamine is by far the most abundant amino acid in tissue culture media; facile transport of this amino acid and high glutaminase activity observed in cultured cells (DeBerardinis and Cheng, 2010) yield a rapid influx of glutamine carbon to generate glutamate and proline, which are both excreted by the cells studied. High concentrations of glutamate can enable cell growth in the absence of glutamine, indicating that, relative to glutamine, glutamate import is limited (Eagle et al., 1956). Alternatively, *de novo* synthesis of TCA-cycle amino acids may provide some benefit to proliferating mammalian cells that exceeds the cost of their synthesis. Collectively, our data argue that the importance of rapid glycolysis and glutaminolysis for proliferating cells lies in an ability to generate metabolic products beyond biomass carbon.

Materials and Methods

Cell Culture: Cells were maintained in RPMI 1640 or DMEM (without pyruvate) supplemented with 10% heat-inactivated fetal bovine serum (FBS), penicillin (100 U/mL), and streptomycin (100 µg/mL) using standard tissue culture techniques. FL5.12 cultures were always supplemented with 0.35 ng/mL IL-3 (Chemicon International). When cells were grown in the absence of specific amino acids, RPMI 1640 lacking these amino acids was supplemented with 10% heat-inactivated dialyzed FBS and all other medium components did not differ relative to normal RPMI 1640. RPMI containing modified amino acids was prepared by dissolving glucose and amino acids into RPMI 1640 base. The composition of this

medium is detailed in **Table 2** and **Figure 6A**. Medium lacking lipids was RPMI 1640 supplemented with

10% lipid-stripped heat-inactivated FBS (see below). Sodium acetate was added to RPMI 1640 at various

concentrations where indicated. Hypoxic cells were cultured in 1% O_2, 5% CO_2, and 94% N_2.

Prototrophic SK1 *S. cerevisiae* were maintained on YEPD (1% yeast extract, 2% peptone, 1% glucose)

agar plates and grown in liquid cultures of synthetic dextrose minimal medium (0.67% yeast nitrogen

base without amino acids, 2% glucose) containing glucose as the sole carbon source.

Table 1: Characteristics of the cell lines used in this study.

Cell Type	Species	Known mutations*	Notes*
H1299	Human	N-Ras^{Q61K}, p53-null	Non-small cell lung cancer, lymph-node metastasis
A549	Human	K-Ras^{G12S}	Lung adenocarcinoma
A172	Human	PTEN- and p16/p19-null	Glioblastoma
MDA-MB-468	Human	p53$^{R273H/R273H}$; pRB-, PTEN-, and SMAD4-null	Breast adenocarcinoma metastasis
HMEC, 184A1	Human	p16-null	Human mammary epithelial cells, immortalized in culture
FL5.12	Mouse		Pro-B cells immortalized in culture, IL-3 dependent
L1210	Mouse	p53$^{M240I/\Delta}$, p16/p19-null	Lymphocytic leukemia
C2C12	Mouse	n/a	Myoblast, differentiates into myocytes
3T3-L1	Mouse		Fibroblast, differentiates into adipocytes
MEF	Mouse	n/a	Primary fibroblasts
T Cell	Mouse	n/a	Primary lymphocytes activated *ex vivo*
Hepatocyte	Mouse	n/a	Primary hepatocytes, non-proliferating

* Source: American Type Culture Collection, and (Bhadury et al., 2013; McKearn et al., 1985).

Table 2: Concentrations (in mM) of glucose and amino acids in RPMI 1640, RPMI with modified amino acids, and DMEM.

Component	RPMI 1640*	Modified RPMI	DMEM*
Glucose	11.11	11.11	25
Alanine		0.534	
Arginine	1.149	0.234	.398
Asparagine	0.379	0.379	
Aspartate	0.150	0.401	
Cystine	0.208	0.208	.201

Glutamate	0.136	0.501	
Glutamine	2.055	2.055	4
Glycine	0.133	0.401	.4
Histidine	0.097	0.050	.2
Hydroxyproline	0.153		
Isoleucine	0.382	0.167	.802
Leucine	0.382	0.467	.802
Lysine	0.219	0.200	.798
Methionine	0.101	0.101	.201
Phenylalanine	0.091	0.178	.4
Proline	0.174	0.200	
Serine	0.286	0.267	.4
Threonine	0.168	0.250	.798
Tryptophan	0.025	0.025	.078
Tyrosine	0.111	0.089	.398
Valine	0.171	0.321	.803

* Source: Life Technologies.

Primary Cell Culture: Mouse embryonic fibroblasts (MEFs) were derived from C57BL/6J embryos at day E14.5. Embryos were dissected and digested in 0.25% trypsin/EDTA, and cells were passed through an 18-gauge needle and then incubated in HBSS with 5 µg/mL DNase at 37 °C. Cells were plated in DMEM with 10% heat-inactivated FBS, and non-adherent cells were washed away with PBS, leaving adherent proliferating cells referred to as MEFs in this study. Primary T cells were derived from the spleens of 6-week old C57BL/6 mice, and pan T cells were isolated using the mouse Pan T cell Isolation Kit II (Miltenyi Biotec) according to the manufacturer's protocol. Cells were resuspended in RPMI 1640 with 10% FBS and activated in CD3/CD28-coated 24-well culture plates and cultured for 48 hours before analysis. Primary hepatocytes were isolated from adult female C57BL/6J mice using the Hepatocyte Isolation System (Worthington Biochemical) according to the manufacturer's instructions. Briefly, livers were perfused with HBSS followed by collagenase, elastase, and DNase I, and hepatocytes were released by dissecting the digested livers. Cells were filtered through a 100 µm filter, washed and plated in hepatocyte adherence medium (Medium 199 with 0.1% BSA, 2% FBS, 100 nM dexamethasone, and 100 nM insulin) on plates coated with type I collagen. The following day, medium was changed to hepatocyte

basal medium (Medium 199 with 2% dialyzed FBS, 100 nM dexamethasone, and 1 nM insulin) for carbon-14 labeling.

Differentiation Models: Proliferating C2C12 and 3T3-L1 cells were maintained in DMEM with 10% FBS. Confluent C2C12 cells were differentiated for six days in DMEM with 2% horse serum refreshed daily before initiating carbon-14 labeling in that medium. Confluent 3T3-L1 cells were differentiated by incubating for two days in DMEM with 10% FBS, 0.5 mM IBMX, 4 µg/mL insulin, 2 µM rosiglitazone, and 100 nM dexamethasone, followed by two days in DMEM with 10% FBS and 4 µg/mL insulin. The resulting adipocytes were returned to DMEM with 10% FBS for one day prior to carbon-14 labeling in that medium. Adipocyte differentiation was confirmed by oil red O staining: cells were fixed with 4% formalin, washed with 60% isopropanol, air dried, and stained for 10 min in 60% isopropanol containing 0.3% oil red O. Cells were washed multiple times with water prior to imaging.

HMEC Culture and Proliferation: Human mammary epithelial cell (HMEC) line 184A1 (Stampfer et al., 1993) was maintained in RPMI 1640 supplemented with 5 µg/mL insulin, 0.5% (v/v) bovine pituitary extract, 5 µg/mL transferrin, 0.5 µg/mL hydrocortisone, 10 µM isoproterenol, and 5 ng/mL EGF. Cells were arrested by incubating in this medium lacking EGF for three days prior to carbon-14 labeling in the absence of EGF. Proliferation was assessed by incorporation of 5-ethynyl-2-deoxyuridine (EdU), a nucleotide analogue, using the Click-iT EdU Flow Cytometry Kit (Life Technologies). Cells were pulsed with 10 µM EdU for 2 hours and fixed and stained according to the manufacturer's instructions. The proportion of cells incorporating EdU was analyzed using a BD FACSCanto II using FACS Diva Software.

Measurement of nutrient consumption and excretion: Cells number was monitored and medium collected from cultures of exponentially proliferating cells. Glucose, glutamine, and lactate concentrations were measured on a YSI-7100 MBS (Yellow Springs Instruments). Medium amino acids were quantified

by gas chromatography-mass spectrometry (GC-MS, see below) by comparison to isotopically labeled internal standards of known concentrations. To calculate consumption rate per cell for a given nutrient, its concentration over time was plot relative to the area under the curve (units: cells · time) of an exponential function fit to the number of cells. Linear regression analysis was performed, and the calculated slope is the consumption rate.

Mass Spectrometry Analysis: Samples were analyzed by gas-chromatography coupled to mass spectrometry (GC-MS) as described previously (Lewis et al., 2014). Polar metabolites were extracted from medium with 15 volumes of cold acetone containing norvaline and isotopically labeled amino acid standards (Cambridge Isotopes MSK-A2-1.2) and dried under nitrogen gas. Samples were derivitized with MOX reagent (Thermo Scientific) and N-tert-butyldimethylsilyl-N-methyltrifluoroacetamide with 1% tert-butyldimethylchlorosilane (Sigma Aldrich). Fatty acids were extracted from serum with 9 volumes of 4:5 methanol:chloroform, dried under nitrogen gas, and derivitized to fatty acid methyl esters in methanol with 2% sulphuric acid. After derivitization, samples were analyzed by GC-MS, using a DB-35MS column (Agilent Technologies) in an Agilent 7890A gas chromatograph coupled to an Agilent 5975C mass spectrometer. Data were analyzed using in-house software described previously (Lewis et al., 2014).

Carbon-14 labeling studies: Unless otherwise indicated, mammalian cells were grown in RPMI 1640 containing 10% dialyzed heat-inactivated FBS supplemented with carbon-14 tracer. Media were supplemented with one of the following tracers: 0.2 µCi/mL [U-^{14}C]-glucose, 0.05 µCi/mL [U-^{14}C]-glutamine, 0.05 µCi/mL sodium [1,2-^{14}C]-acetate, 0.05 µCi/mL [U-^{14}C]-palmitic acid, or 0.05 µCi/mL L-[U-^{14}C]-amino acid mixture (all from American Radiolabeled Chemicals); or 0.05 µCi/mL [U-^{14}C]-serine, 0.05 µCi/mL [U-^{14}C]-valine, 0.05 µCi/mL [1-^{14}C]-palmitic acid, or 0.05 µCi/mL [1-^{14}C]-oleic acid (all from Perkin Elmer). Before addition to the medium, fatty acids were first conjugated to serum proteins by mixing 0.55 µCi/mL of tracer with dialyzed FBS overnight at 37 °C. To ensure labeling steady state was

reached, cells were grown in the presence of carbon-14 until >95% of cellular material had turned over. Cells were washed three times with phosphate-buffered saline (PBS) to remove unincorporated carbon-14, collected by trypsinization, and counted. Cells were lysed in ≥10 volumes Emulsifier-Safe liquid scintillation cocktail (Perkin Elmer), and incorporated carbon-14 was quantified by liquid scintillation counting by comparison to a carbon-14 standard curve. Overnight cultures of SK1 yeast grown in SD (2% glucose) with 0.2 μCi/mL [U-^{14}C]-glucose were diluted into the same medium and grown to mid-log phase. Approximately 20 million cells were washed three times with cold deionized water and lysed with cold trichloroacetic acid on ice. Incorporated carbon-14 was quantified by scintillation counting as above.

To determine the fraction of cell dry mass derived from a specific nutrient, the ratio of concentrations of carbon-14 tracer ($^{14}C_{medium}$) to carbon-12 nutrient ($^{12}C_{medium}$) in the medium was first calculated. The amount of carbon-14 present in the medium was verified by scintillation counting. The amount of carbon-14 incorporated into cells ($^{14}C_{cells}$) was divided by this ratio to determine the total amount of carbon incorporated from the nutrient, and this was converted to mass by multiplying by 12 g/mol. Finally, this number was normalized to cell mass by dividing by the number of cells in the culture (N) and the average mass of a single cell (m) (see below). The reported fraction of cell mass derived from a given nutrient is therefore equal to: $^{14}C_{cells}(^{12}C_{medium}/^{14}C_{medium})(12 \text{ g/mol})(Nm)^{-1}$.

Measurement of cell dry mass: Dry mass of individual cells was determined by a method described previously (Feijo Delgado et al., 2013). Cells were trypsinized and resuspended in PBS at a concentration of 200,000 cells/mL. The cells were then loaded into a 25 × 25 μm cross-section suspended microchannel resonator (SMR), and the buoyant mass of single cells was measured first in PBS and then in D$_2$O-PBS. Each experiment lasted around 60 min at room temperature. Dry mass values for cells grown in different conditions were compared using an unpaired Student's t-test, assuming unequal variances. Where cell dry mass was not significantly different between conditions, average cell dry mass was taken to be equal among these conditions for the calculations in the carbon-14 labeling studies.

Stable isotope labeling studies: Cells were cultured in RPMI 1640 supplemented with 10% heat-inactivated dialyzed FBS and containing either [U-^{13}C]-glucose or [U-^{13}C]-glutamine (Cambridge Isotopes Laboratories) in place of the corresponding unlabeled nutrient. After cells were cultured in this medium for 24 hours, polar metabolites were obtained by 80% methanol extraction, dried under nitrogen gas, and analyzed by GC-MS to determine lactate labeling (see above). Contribution of glucose or glutamine to total cellular carbon was measured after multiple passages in medium containing carbon-13. Contribution of glutamine to total cellular nitrogen was measured at the times indicated for cells grown in RPMI 1640 supplemented as above but containing [amide-^{15}N]- or [α-^{15}N]-glutamine (supplemented at 4% of totral glutamine). In either case, approximately ten million cells per replicate were trypsinized, washed three times with cold PBS, and dried. Carbon-13 and nitrogen-15 enrichment (i.e. ^{13}C:^{12}C and ^{15}N:^{14}N) were measured by isotope ratio mass spectrometry (IRMS) (see below).

Elemental analysis and IRMS: To determine the elemental composition of mammalian cells, approximately ten million cells per replicate were trypsinized and washed twice with cold PBS and once with 154 mM ammonium bicarbonate. Approximately 100 million SK1 yeast cells were washed three times with cold deionized water. After washing, cells were flash frozen and lyophilized. Samples of known mass (determined by analytical balance) were wrapped in tin capsules, and total carbon and nitrogen content were determined by continuous-flow direct combustion mass spectrometry on a Europa 20/20 IRMS (Sercon Limited) at the Utah State University Stable Isotope Laboratory (as in Herron et al. (2009)). This mass spectrometer was calibrated with glucose and ammonium sulfate standards. Mammalian cells labeled with carbon-13 were analyzed by this method.

For nitrogen-15 labeled cells, IRMS was conducted as previously described (Kim et al., 2014). Approximately 10 million cells for each replicate were dried and aliquoted to tin cups prior to analysis. Samples were analyzed using an elemental analyzer (Vario Pyrocube, Elementar) coupled to an IRMS

(Isoprime 100, Elementar). Prior to analysis, instrumental tuning was confirmed using urea standards and standard replicates were analyzed at regular intervals to confirm absence of instrumental drift.

Cell fractionation: Cells were lysed using the TRIzol reagent (Life Technologies) and RNA, DNA, and protein were extracted and purified by bi-phasic extraction according to the manufacturer's instructions (Chomczynski, 1993). Briefly, following initial lysis, insoluble material was considered to be DNA; RNA was precipitated from the aqueous phase, and the remaining soluble material was termed the "polar fraction"; protein was precipitated from the organic phase, and the remaining soluble material was termed the "non-polar fraction". Radioactivity in each fraction was quantified by liquid scintillation counting.

To evaluate the efficacy of this purification scheme, radioactive molecules of a defined macromolecular class were spiked into a TRIzol lysate of unlabeled HEK293 cells prior to fractionation, and radioactivity in the resulting fractions measured. For this analysis, radioactive lipids were obtained from HEK293 cells grown in medium containing [U-^{14}C]-glucose or [^{32}P]-orthophosphate (Perkin Elmer) with 2:1 chloroform:methanol extraction. Non-lipid contaminants were removed by further extracting with 0.2 volumes of saline. Radioactive protein was obtained by extensively dialyzing a RIPA lysate of HEK293 cells grown in medium containing [^{35}S]-methionine (Perkin Elmer). Radioactive DNA and RNA were respectively purified with the PureLink Genomic DNA Mini Kit (Life Technologies) and the RNeasy Mini Kit (Qiagen) from HEK293 cells grown in medium containing [methyl-^{3}H]-thymidine (Perkin Elmer) or [^{32}P]-orthophosphate. Radioactive small molecule metabolites were obtained by 80% methanol extraction of HEK293 cells grown with various carbon-14 nutrients. Yield from fractionation was assessed by comparing the sums of the quantities of radioactivity in each fraction to the amount of input radioactive tracer (**Figure 9B,C**) or to a culture grown in parallel (**Figure 10**).

Cell proliferation. One day after cells were sparsely seeded, they were washed extensively with PBS and changed into different media prior to cell counting over time. To calculate proliferation rate, cells were

100

counted over a period of 96 hours, and cell counts fit to the function $N(t) = N_0 \cdot 2^{kt}$ to determine k, the proliferation rate (in units of doublings per time).

Generation of lipid-stripped serum: Lipids were extracted from FBS without denaturing serum protein according to a previously established method (Cham and Knowles, 1976). Briefly, a 5:4:2 mixture of serum:diisopropyl-ether:n-butanol was stirred at room temperature for 30 min. Phases were separated by centrifugation, and the aqueous phase was re-extracted with an equal volume of diisopropyl ether. The resulting aqueous phase was dialyzed three times against saline at 4 °C and filter sterilized prior to use. Control (not stripped) serum was prepared by dialyzing FBS in this manner without organic extraction. Serum fatty acids were quantified by GC-MS (see above).

Measurement of acetate concentration: Polar metabolites were extracted from serum by adding four volumes of cold methanol to precipitate protein. Following centrifugation, the supernatant was dried under nitrogen gas and resuspended in ultrapure water. Acetate concentration in this extract was determined using the Acetate Colorimetric Assay Kit (Sigma Aldrich).

Immunoblot Analysis: H1299 and A549 cells were incubated for 4 hrs in hypoxia (1% O_2) or in normoxia with or without the addition of 100 μM deferoxamine (DFO) to chemically inhibit HIF1α degradation. Cells were lysed in RIPA buffer containing cOmplete Mini Protease Inhibitors (Roche) and 100 μM DFO. Samples were analyzed by SDS-PAGE and proteins were detected by immunoblot and ECL assay. Antibodies used: HIF1α (BD Biosciences, 610958) and β-actin (Abcam, 8227).

Author Contributions

A.M.H. and M.V.G.H conceived of and analyzed all experiments and wrote and edited this chapter.

L.V.D. isolated primary hepatocytes from mice. V.C.H. and S.R.M. measured single cell mass values, and

M.O.J. and J.C.R. isolated and traced the fate of carbon into primary lymphocytes.

References

Abdul-Baki, A.A. (1969). Metabolism of barley seed during early hours of germination. Plant physiology *44*, 733-738.

Alberts, B., Johnson, A., Lewis, J., Raff, M., Roberts, K., and Walter, P. (2008). Molecular Biology of the Cell, 5 edn (New York, NY: Garland Science).

Bailey, J.M., Howard, B.V., Dunbar, L.M., and Tillman, S.F. (1972). Control of lipid metabolism in cultured cells. Lipids *7*, 125-134.

Bhadury, J., Lopez, M.D., Muralidharan, S.V., Nilsson, L.M., and Nilsson, J.A. (2013). Identification of tumorigenic and therapeutically actionable mutations in transplantable mouse tumor cells by exome sequencing. Oncogenesis *2*, e44.

Bonarius, H.P., Hatzimanikatis, V., Meesters, K.P., de Gooijer, C.D., Schmid, G., and Tramper, J. (1996). Metabolic flux analysis of hybridoma cells in different culture media using mass balances. Biotechnology and bioengineering *50*, 299-318.

Boulter, D., and Barber, J.T. (1963). Amino-acid metabolism in germinating seeds of Vicia faba L. in relation to their biology. New Phytologist *62*, 301-316.

Brand, K. (1985). Glutamine and glucose metabolism during thymocyte proliferation. Pathways of glutamine and glutamate metabolism. The Biochemical journal *228*, 353-361.

Brand, K., Leibold, W., Luppa, P., Schoerner, C., and Schulz, A. (1986). Metabolic alterations associated with proliferation of mitogen-activated lymphocytes and of lymphoblastoid cell lines: evaluation of glucose and glutamine metabolism. Immunobiology *173*, 23-34.

Cascante, M., Boros, L.G., Comin-Anduix, B., de Atauri, P., Centelles, J.J., and Lee, P.W. (2002). Metabolic control analysis in drug discovery and disease. Nature biotechnology *20*, 243-249.

Cham, B.E., and Knowles, B.R. (1976). A solvent system for delipidation of plasma or serum without protein precipitation. Journal of lipid research *17*, 176-181.

Chaneton, B., Hillmann, P., Zheng, L., Martin, A.C., Maddocks, O.D., Chokkathukalam, A., Coyle, J.E., Jankevics, A., Holding, F.P., Vousden, K.H., *et al.* (2012). Serine is a natural ligand and allosteric activator of pyruvate kinase M2. Nature *491*, 458-462.

Chomczynski, P. (1993). A reagent for the single-step simultaneous isolation of RNA, DNA and proteins from cell and tissue samples. BioTechniques *15*, 532-534, 536-537.

Christofk, H.R., Vander Heiden, M.G., Harris, M.H., Ramanathan, A., Gerszten, R.E., Wei, R., Fleming, M.D., Schreiber, S.L., and Cantley, L.C. (2008). The M2 splice isoform of pyruvate kinase is important for cancer metabolism and tumour growth. Nature *452*, 230-233.

Comerford, S.A., Huang, Z., Du, X., Wang, Y., Cai, L., Witkiewicz, A.K., Walters, H., Tantawy, M.N., Fu, A., Manning, H.C., *et al.* (2014). Acetate dependence of tumors. Cell *159*, 1591-1602.

Commisso, C., Davidson, S.M., Soydaner-Azeloglu, R.G., Parker, S.J., Kamphorst, J.J., Hackett, S., Grabocka, E., Nofal, M., Drebin, J.A., Thompson, C.B., *et al.* (2013). Macropinocytosis of protein is an amino acid supply route in Ras-transformed cells. Nature *497*, 633-637.

Davidson, S.M., Papagiannakopoulos, T., Olenchock, B.A., Heyman, J.E., Keibler, M.A., Luengo, A., Bauer, M.R., Jha, A.K., O'Brien, J.P., Pierce, K.A., *et al.* (2016). Environment impacts the metabolic dependencies of Ras-driven non-small cell lung cancer. Cell metabolism *In Press*.

Daye, D., and Wellen, K.E. (2012). Metabolic reprogramming in cancer: unraveling the role of glutamine in tumorigenesis. Seminars in cell & developmental biology *23*, 362-369.

DeBerardinis, R.J., and Cheng, T. (2010). Q's next: the diverse functions of glutamine in metabolism, cell biology and cancer. Oncogene *29*, 313-324.

DeBerardinis, R.J., Lum, J.J., Hatzivassiliou, G., and Thompson, C.B. (2008). The biology of cancer: metabolic reprogramming fuels cell growth and proliferation. Cell metabolism *7*, 11-20.

DeBerardinis, R.J., Mancuso, A., Daikhin, E., Nissim, I., Yudkoff, M., Wehrli, S., and Thompson, C.B. (2007). Beyond aerobic glycolysis: transformed cells can engage in glutamine metabolism that exceeds the requirement for protein and nucleotide synthesis. Proceedings of the National Academy of Sciences of the United States of America *104*, 19345-19350.

Dolfi, S.C., Chan, L.L., Qiu, J., Tedeschi, P.M., Bertino, J.R., Hirshfield, K.M., Oltvai, Z.N., and Vazquez, A. (2013). The metabolic demands of cancer cells are coupled to their size and protein synthesis rates. Cancer & metabolism *1*, 20.

Eagle, H., Oyama, V.I., Levy, M., Horton, C.L., and Fleischman, R. (1956). The growth response of mammalian cells in tissue culture to L-glutamine and L-glutamic acid. J Biol Chem *218*, 607-616.

Faubert, B., Boily, G., Izreig, S., Griss, T., Samborska, B., Dong, Z., Dupuy, F., Chambers, C., Fuerth, B.J., Viollet, B., *et al.* (2013). AMPK is a negative regulator of the Warburg effect and suppresses tumor growth in vivo. Cell metabolism *17*, 113-124.

Feijo Delgado, F., Cermak, N., Hecht, V.C., Son, S., Li, Y., Knudsen, S.M., Olcum, S., Higgins, J.M., Chen, J., Grover, W.H., *et al.* (2013). Intracellular water exchange for measuring the dry mass, water mass and changes in chemical composition of living cells. PloS one *8*, e67590.

Gatenby, R.A., and Gillies, R.J. (2004). Why do cancers have high aerobic glycolysis? Nature reviews Cancer *4*, 891-899.

Herron, P.M., Stark, J.M., Holt, C., Hooker, T., and Cardon, Z.G. (2009). Microbial growth efficiencies across a soil moisture gradient assessed using C-13-acetic acid vapor and N-15-ammonia gas. Soil Biology & Biochemistry *41*, 1262-1269.

Hsu, P.P., and Sabatini, D.M. (2008). Cancer cell metabolism: Warburg and beyond. Cell *134*, 703-707.

Hume, D.A., Radik, J.L., Ferber, E., and Weidemann, M.J. (1978). Aerobic glycolysis and lymphocyte transformation. The Biochemical journal *174*, 703-709.

Jain, M., Nilsson, R., Sharma, S., Madhusudhan, N., Kitami, T., Souza, A.L., Kafri, R., Kirschner, M.W., Clish, C.B., and Mootha, V.K. (2012). Metabolite profiling identifies a key role for glycine in rapid cancer cell proliferation. Science *336*, 1040-1044.

Jiang, L., and Deberardinis, R.J. (2012). Cancer metabolism: When more is less. Nature *489*, 511-512.

Jiang, P., Du, W., Wang, X., Mancuso, A., Gao, X., Wu, M., and Yang, X. (2011). p53 regulates biosynthesis through direct inactivation of glucose-6-phosphate dehydrogenase. Nature cell biology *13*, 310-316.

Kamphorst, J.J., Cross, J.R., Fan, J., de Stanchina, E., Mathew, R., White, E.P., Thompson, C.B., and Rabinowitz, J.D. (2013). Hypoxic and Ras-transformed cells support growth by scavenging unsaturated fatty acids from lysophospholipids. Proceedings of the National Academy of Sciences of the United States of America *110*, 8882-8887.

Kilsdonk, E.P., Dorsman, A.N., van Gent, T., and van Tol, A. (1992). Effect of phospholipid fatty acid composition of endothelial cells on cholesterol efflux rates. Journal of lipid research *33*, 1373-1382.

Kim, S.M., Lun, M., Wang, M., Senyo, S.E., Guillermier, C., Patwari, P., and Steinhauser, M.L. (2014). Loss of white adipose hyperplastic potential is associated with enhanced susceptibility to insulin resistance. Cell metabolism *20*, 1049-1058.

Koppenol, W.H., Bounds, P.L., and Dang, C.V. (2011). Otto Warburg's contributions to current concepts of cancer metabolism. Nature reviews Cancer *11*, 325-337.

Kučera, P., Raddatz, E., and Baroffio, A. (1984). Oxygen and glucose uptakes in the early chick embryo. In Respiration and metabolism of embryonic vertebrates, R. Seymour, ed. (Springer Netherlands), pp. 299-309.

Labuschagne, C.F., van den Broek, N.J., Mackay, G.M., Vousden, K.H., and Maddocks, O.D. (2014). Serine, but not glycine, supports one-carbon metabolism and proliferation of cancer cells. Cell reports *7*, 1248-1258.

Lao, L., Franklin, R.B., and Costello, L.C. (1993). High-affinity L-aspartate transporter in prostate epithelial cells that is regulated by testosterone. Prostate *22*, 53-63.

Lemons, J.M., Feng, X.J., Bennett, B.D., Legesse-Miller, A., Johnson, E.L., Raitman, I., Pollina, E.A., Rabitz, H.A., Rabinowitz, J.D., and Coller, H.A. (2010). Quiescent fibroblasts exhibit high metabolic activity. PLoS Biol *8*, e1000514.

Lewis, C.A., Parker, S.J., Fiske, B.P., McCloskey, D., Gui, D.Y., Green, C.R., Vokes, N.I., Feist, A.M., Vander Heiden, M.G., and Metallo, C.M. (2014). Tracing compartmentalized NADPH metabolism in the cytosol and mitochondria of mammalian cells. Molecular cell *55*, 253-263.

Lunt, S.Y., and Vander Heiden, M.G. (2011). Aerobic glycolysis: meeting the metabolic requirements of cell proliferation. Annual review of cell and developmental biology *27*, 441-464.

Maddocks, O.D., Berkers, C.R., Mason, S.M., Zheng, L., Blyth, K., Gottlieb, E., and Vousden, K.H. (2013). Serine starvation induces stress and p53-dependent metabolic remodelling in cancer cells. Nature *493*, 542-546.

Marin-Valencia, I., Yang, C., Mashimo, T., Cho, S., Baek, H., Yang, X.L., Rajagopalan, K.N., Maddie, M., Vemireddy, V., Zhao, Z., et al. (2012). Analysis of tumor metabolism reveals mitochondrial glucose oxidation in genetically diverse human glioblastomas in the mouse brain in vivo. Cell metabolism *15*, 827-837.

McKearn, J.P., McCubrey, J., and Fagg, B. (1985). Enrichment of hematopoietic precursor cells and cloning of multipotential B-lymphocyte precursors. Proceedings of the National Academy of Sciences of the United States of America *82*, 7414-7418.

McMenamy, R.H., Lund, C.C., and Oncley, J.L. (1957). Unbound amino acid concentrations in human blood plasmas. The Journal of clinical investigation *36*, 1672-1679.

Metallo, C.M., Gameiro, P.A., Bell, E.L., Mattaini, K.R., Yang, J., Hiller, K., Jewell, C.M., Johnson, Z.R., Irvine, D.J., Guarente, L., et al. (2012). Reductive glutamine metabolism by IDH1 mediates lipogenesis under hypoxia. Nature *481*, 380-384.

Moran, E.T. (2007). Nutrition of the Developing Embryo and Hatchling. Poultry Science *86*, 1043-1049.

Mourant, J.R., Short, K.W., Carpenter, S., Kunapareddy, N., Coburn, L., Powers, T.M., and Freyer, J.P. (2005). Biochemical differences in tumorigenic and nontumorigenic cells measured by Raman and infrared spectroscopy. Journal of biomedical optics *10*, 031106.

Mullen, A.R., Wheaton, W.W., Jin, E.S., Chen, P.H., Sullivan, L.B., Cheng, T., Yang, Y., Linehan, W.M., Chandel, N.S., and DeBerardinis, R.J. (2012). Reductive carboxylation supports growth in tumour cells with defective mitochondria. Nature *481*, 385-388.

Newsholme, E.A., Crabtree, B., and Ardawi, M.S. (1985). The role of high rates of glycolysis and glutamine utilization in rapidly dividing cells. Bioscience reports *5*, 393-400.

Paredes, C., Sanfeliu, A., Cardenas, F., Cairo, J.J., and Godia, F. (1998). Estimation of the intracellular fluxes for a hybridoma cell line by material balances. Enzyme Microb Tech *23*, 187-198.

Raatz, S.K., Bibus, D., Thomas, W., and Kris-Etherton, P. (2001). Total fat intake modifies plasma fatty acid composition in humans. The Journal of nutrition *131*, 231-234.

Richards, R.H., Dowling, J.A., Vreman, H.J., Feldman, C., and Weiner, M.W. (1976). Acetate levels in human plasma. Proceedings of the Clinical Dialysis and Transplant Forum *6*, 73-79.

Roberts, R.B., Cowie, D.B., Abelson, P.H., Bolton, E.T., and Britten, R.J. (1955). Composition of the cells: Fractionation and hydrolysis. In Studies of biosynthesis in Escherichia coli (Washington, D. C.: Carnegie Institution of Washington).

Schoors, S., Bruning, U., Missiaen, R., Queiroz, K.C., Borgers, G., Elia, I., Zecchin, A., Cantelmo, A.R., Christen, S., Goveia, J., et al. (2015). Fatty acid carbon is essential for dNTP synthesis in endothelial cells. Nature 520, 192-197.

Schug, Z.T., Peck, B., Jones, D.T., Zhang, Q., Grosskurth, S., Alam, I.S., Goodwin, L.M., Smethurst, E., Mason, S., Blyth, K., et al. (2015). Acetyl-CoA synthetase 2 promotes acetate utilization and maintains cancer cell growth under metabolic stress. Cancer cell 27, 57-71.

Shestov, A.A., Liu, X., Ser, Z., Cluntun, A.A., Hung, Y.P., Huang, L., Kim, D., Le, A., Yellen, G., Albeck, J.G., et al. (2014). Quantitative determinants of aerobic glycolysis identify flux through the enzyme GAPDH as a limiting step. eLife 3.

Shlomi, T., Benyamini, T., Gottlieb, E., Sharan, R., and Ruppin, E. (2011). Genome-scale metabolic modeling elucidates the role of proliferative adaptation in causing the Warburg effect. PLoS computational biology 7, e1002018.

Stampfer, M.R., Pan, C.H., Hosoda, J., Bartholomew, J., Mendelsohn, J., and Yaswen, P. (1993). Blockage of EGF receptor signal transduction causes reversible arrest of normal and immortal human mammary epithelial cells with synchronous reentry into the cell cycle. Exp Cell Res 208, 175-188.

Storck, T., Schulte, S., Hofmann, K., and Stoffel, W. (1992). Structure, expression, and functional analysis of a Na(+)-dependent glutamate/aspartate transporter from rat brain. Proceedings of the National Academy of Sciences of the United States of America 89, 10955-10959.

Tardito, S., Oudin, A., Ahmed, S.U., Fack, F., Keunen, O., Zheng, L., Miletic, H., Sakariassen, P.O., Weinstock, A., Wagner, A., et al. (2015). Glutamine synthetase activity fuels nucleotide biosynthesis and supports growth of glutamine-restricted glioblastoma. Nature cell biology 17, 1556-1568.

Thiele, I., Swainston, N., Fleming, R.M., Hoppe, A., Sahoo, S., Aurich, M.K., Haraldsdottir, H., Mo, M.L., Rolfsson, O., Stobbe, M.D., et al. (2013). A community-driven global reconstruction of human metabolism. Nature biotechnology 31, 419-425.

Tollinger, C.D., Vreman, H.J., and Weiner, M.W. (1979). Measurement of acetate in human blood by gas chromatography: effects of sample preparation, feeding, and various diseases. Clinical chemistry 25, 1787-1790.

Vajreswari, A., Narayanareddy, K., and Rao, P.S. (1990). Fatty acid composition of erythrocyte membrane lipid obtained from children suffering from kwashiorkor and marasmus. Metabolism: clinical and experimental 39, 779-782.

Vander Heiden, M.G., Cantley, L.C., and Thompson, C.B. (2009). Understanding the Warburg effect: the metabolic requirements of cell proliferation. Science 324, 1029-1033.

Vazquez, A., Liu, J., Zhou, Y., and Oltvai, Z.N. (2010). Catabolic efficiency of aerobic glycolysis: the Warburg effect revisited. BMC systems biology 4, 58.

Walther, T.C., and Farese, R.V., Jr. (2012). Lipid droplets and cellular lipid metabolism. Annual review of biochemistry *81*, 687-714.

Wang, R., and Green, D.R. (2012). Metabolic reprogramming and metabolic dependency in T cells. Immunological reviews *249*, 14-26.

Willems, E., Decuypere, E., Buyse, J., and Everaert, N. (2014). Importance of albumen during embryonic development in avian species, with emphasis on domestic chicken. Worlds Poultry Science Journal *70*, 503-517.

Yuneva, M.O., Fan, T.W., Allen, T.D., Higashi, R.M., Ferraris, D.V., Tsukamoto, T., Mates, J.M., Alonso, F.J., Wang, C., Seo, Y., *et al.* (2012). The metabolic profile of tumors depends on both the responsible genetic lesion and tissue type. Cell metabolism *15*, 157-170.

Chapter 3: Lack of evidence for PKM2 protein kinase activity

Authors: Aaron M. Hosios[1,2], Brian P. Fiske[1,2], Dan Y. Gui[1,2], Matthew G. Vander Heiden[1,2,3]

Affiliations:
[1] Koch Institute for Integrative Cancer Research, Massachusetts Institute of Technology, Cambridge, MA 02139, USA.
[2] Department of Biology, Massachusetts Institute of Technology, Cambridge, MA 02139, USA.
[3] Department of Medical Oncology, Dana-Farber Cancer Institute, Boston, MA 02115, USA

Abstract

The role of pyruvate kinase M2 (PKM2) in cell proliferation is controversial. A unique function of PKM2 proposed to be important for the proliferation of some cancer cells involves the direct activity of this enzyme as a protein kinase; however, a detailed biochemical characterization of this activity is lacking. Using $[^{32}P]$-phosphoenolpyruvate (PEP) we examine the direct substrates of PKM2 using recombinant enzyme and *in vitro* systems where PKM2 is genetically deleted. Labeling of some protein species from $[^{32}P]$-PEP can be observed, however most were dependent on the presence of ADP, and none were dependent on the presence of PKM2. In addition, we also failed to observe PKM2-dependent transfer of phosphate from ATP directly to protein. These findings argue against a role for PKM2 as a protein kinase.

Introduction

The M2 isoform of pyruvate kinase (PKM2) is expressed in cancer cells and many normal cells with proliferative capacity and/or anabolic functions. Several lines of evidence argue that PKM2 is important for cancer cell proliferation in some contexts. PKM2 is expressed in cancers and cell lines, and regulation of PKM2 enzymatic activity can influence cell proliferation (Anastasiou et al., 2012; Chaneton et al., 2012; Israelsen et al., 2013; Lunt et al.). Two models, which are not mutually exclusive, seek to explain the importance of PKM2 expression in cancer (McKnight, 2014). One proposes that PKM2 exerts its effects through its canonical activity, which is regulated to control cell metabolism and macromolecular synthesis. The other proposes that PKM2 is a protein kinase involved in signaling and regulating gene expression.

Pyruvate kinase catalyzes the final step in glycolysis, transferring a phosphate group from phosphoenolpyruvate (PEP) to ADP to produce pyruvate and ATP. There are four mammalian isoforms,

110

and alternative splicing of the *PKM* gene produces the isoforms PKM1 and PKM2. The exon unique to

PKM2 is reported to confer protein kinase activity as well as regulatory properties that are lacking in

PKM1. For example, PKM2 requires its allosteric activator fructose-1,6-bisphosphate (FBP) to be fully

active, while PKM1 activity is constitutively high (Dombrauckas et al., 2005; Morgan et al., 2013). In

support of a metabolic role for pyruvate kinase in proliferation the glycolytic enzyme activity of PKM2,

but not PKM1, can be inhibited by growth signaling in rapidly proliferating cells, and the resulting low

levels of enzyme activity facilitate tumor growth (Christofk et al., 2008; Hitosugi et al., 2009). PKM2 is

also allosterically activated by the metabolites serine and SAICAR, enabling regulation of this enzyme by

nutrient conditions and coordination with metabolic pathways outside of glycolysis (Chaneton et al.,

2012; Keller et al., 2012; Kung et al., 2012). Synthetic activators of PKM2 impair tumor growth by

raising PKM2 activity to PKM1 levels (Anastasiou et al., 2012), and high pyruvate kinase activity impairs

mouse embryonic fibroblast (MEF) proliferation by limiting precursors for DNA replication (Lunt et al.).

Deletion of PKM2 does not prevent tumor growth, and results in compensatory PKM1 expression in non-

proliferating cells in the tumor, arguing that the ability of PKM2 to be active or inactive allows this

isoform to support different metabolic cell states in tissues (Israelsen et al., 2013).

The protein kinase activity reported for PKM2 is distinct from its role in glycolysis. Transfer of a

phosphate from PEP to proteins, which also generates pyruvate, has been reported to occur as a result of a

kinase activity that is unique to PKM2 among pyruvate kinase isoforms. PEP-dependent phosphorylation

is uncommon in cells, but has been observed in both bacterial and mammalian systems (Deutscher et al.,

2006; Vander Heiden et al., 2010). In both cases, phosphate is transferred from PEP is to a histidine

residue on a protein, and the bacterial PEP-dependent histidine kinases have no homology to PKM2 or

other enzymes in glycolysis. PKM2 has been reported to function as a dual-specificity kinase, transferring

phosphate to serine/threonine and tyrosine residues on different proteins (Gao et al., 2012; Yang et al.,

2012a). When studied, PKM2 protein kinase activity is catalyzed by dimeric PKM2, a state with much

lower glycolytic enzyme activity when compared with fully active tetrameric PKM2. In particular,

dimeric PKM2 localizes to the nucleus where it acts as a Stat3 kinase with an R399E mutant reported to

be an obligate dimer with elevated protein kinase activity (Gao et al., 2012). Subsequent work suggested that PKM2 also phosphorylates histone H3. EGFR signaling to ERK1/2 can result in nuclear translocation of PKM2, where PKM2 protein kinase activity leads to c-Myc and cyclin D1 expression to drive cell cycle progression beyond the G1/S checkpoint (Yang et al., 2012a; Yang et al., 2012b). PKM2 is also reported to be a kinase of spindle assembly checkpoint protein Bub3, playing an important role in ensuring faithful chromosome segregation (Jiang et al., 2014). Finally, SAICAR, the allosteric activator of canonical PKM2 activity, was reported to synergize with ERK2 to stimulate protein kinase activity of PKM2, enabling it to phosphorylate a large number of proteins (Keller et al., 2014).

Although tumors express PKM2 this enzyme is not essential for growth of all tumors. PKM2 deletion does not prevent tumorigenesis in a mouse model of breast cancer and loss of PKM2 can promote tumor progression (Israelsen et al., 2013). PKM2 is also not required for hematopoietic stem cell or leukemia cell proliferation, but PKM2 expression enhances transplantation of hematopoietic stem cells (Wang et al., 2014). Finally, knockdown of PKM2 using RNA interference does not alter formation or maintenance of xenograft tumors, although it partially obstructs proliferation *in vitro* (Cortes-Cros et al., 2013). These data argue against any model where PKM2 is essential for regulating cell cycle mediators or other events that are important for eukaryotic cell proliferation.

To date, studies examining PKM2 functions in cancer have not resolved differential roles for PKM2 in signaling and regulation of metabolism. We investigated the protein kinase activity of PKM2; however, we were unable to demonstrate PKM2-dependent phosphorylation of any proteins *in vitro* using either PEP or ATP as a phosphate donor. Instead, all PKM2-dependent phosphotransfer events observed involved regeneration of ATP from ADP and PEP, the known function of PKM2 in glycolysis. This study also establishes methods to track PEP-dependent protein phosphorylation in cells.

Results

PEP-dependent phosphorylation events in cell lysates are independent of PKM2

PEP-dependent phosphorylation events are well described as part of two-component signaling in bacteria (Deutscher et al., 2006). Transfer of phosphate from [^{32}P]-PEP to phosphoglycerate mutase (PGAM) has been shown in eukaryotic cell lysates, but this activity is not dependent on PKM2 (Vander Heiden et al., 2010). To identify other PEP-dependent phosphorylation events in mammalian cells, we tracked [^{32}P]-phosphate transfer to proteins as a sensitive measure of protein phosphorylation. The phosphorylation reaction was performed in the presence of vanadate to inhibit phosphatase activity, and also to minimize PGAM1 labeling as vanadate promotes PGAM1-His11 dephosphorylation (Carreras et al., 1982). PGAM1 labeled from PEP is the dominant species generated in this reaction (Vander Heiden et al., 2010), and we sought to minimize this to avoid masking phosphorylation events involving less abundant proteins. Vanadate was included as a phosphatase inhibitor in past studies of PKM2 protein kinase activity and thus is not expected to inhibit this enzyme activity of PKM2 (Gao et al., 2012; Yang et al., 2012a). [^{32}P]-PEP was added to hypotonic cell lysates prepared to minimize disruption of endogenous protein complexes and protein phosphorylation was visualized by SDS-PAGE and autoradiography (**Figure 1**). PGAM1 labeling was observed when phosphatase inhibitors were not included (**Figure 2A**). To determine whether the phosphotransfer events were dependent on ATP or PEP as a phosphate donor, 1 mM unlabeled PEP or ATP was added as a competitor for the reaction, a control lacking from published demonstrations of PKM2 protein kinase activity that rely heavily on antibodies to detect phosphorylation events. Most protein labeling events observed are competed by non-radioactive ATP and not non-radioactive PEP regardless of whether vanadate is included in the reaction (**Figures 1, 2B**). This finding is consistent with ATP serving as the direct phosphate donor for most phosphorylation events and is consistent with previous reports (Vander Heiden et al., 2010). Interestingly, diffuse bands of variable intensity that migrated on SDS-PAGE with the 15-20 kDa and 100-120 kDa molecular weight markers were labeled from [^{32}P]-PEP that were sensitive to competition by non-radioactive PEP but not non-
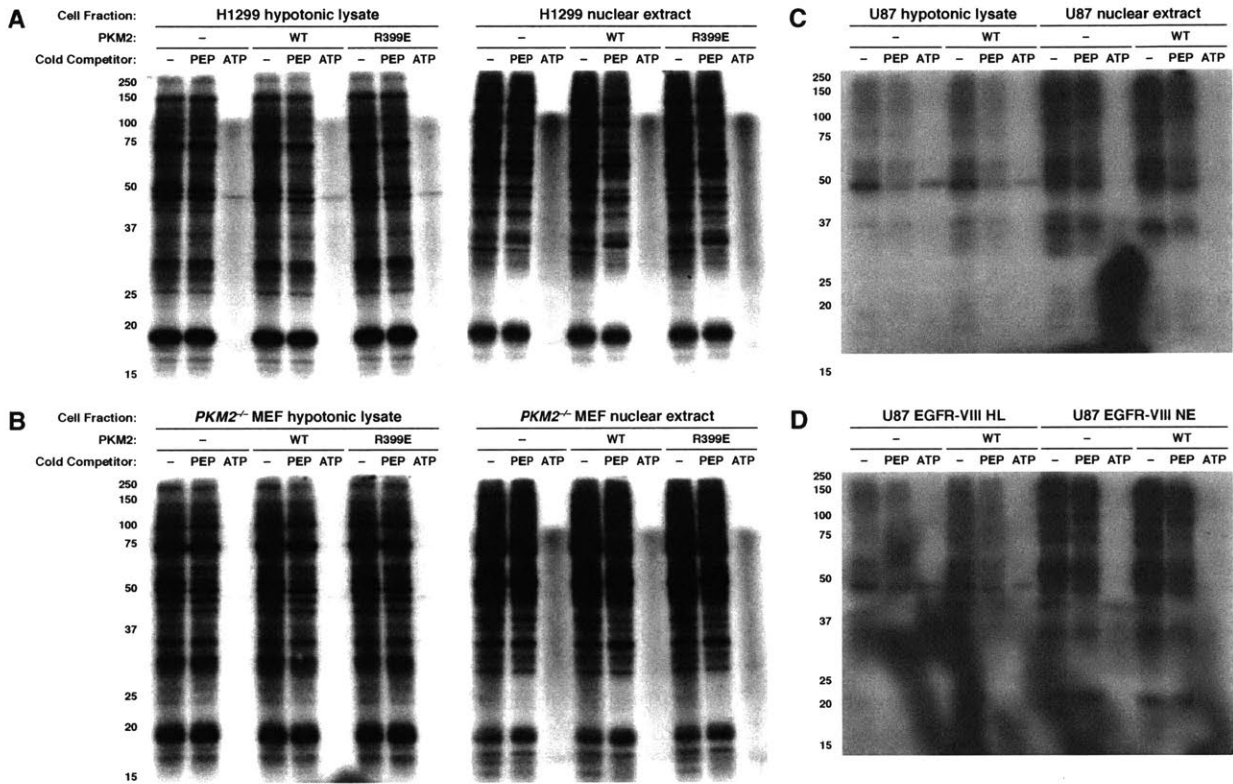
Figure 1: Assessment of phosphoenolpyruvate (PEP) as a phosphate donor for protein phosphorylation.

Hypotonic lysates and nuclear extracts from (*A*) H1299, (*B*) PKM2-null MEF, (*C*) U87, and (*D*) U87 EGFR-VIII cells were incubated for 1 h with impure [^{32}P]-PEP, and phosphorylated proteins analyzed by SDS-PAGE and autoradiography. Reactions were carried out with the addition of no enzyme, recombinant wild type (WT) or mutant (R399E) his-tagged PKM2 (each at 10 µg/mL) as indicated. In addition, no competitor or excess (1 mM) non-radioactive competitor PEP or ATP was also included where indicated.

radioactive ATP. A previous study had observed non-enzymatic labeling of proteins upon boiling

(Schieven and Martin, 1988), so to determine whether these bands were dependent on transfer to protein

in cell lysates, [^{32}P]-PEP or [γ-^{32}P]-ATP were added to loading buffer in the absence of added protein

(**Figure 2C**). The same bands were observed when [^{32}P]-PEP, but not [γ-^{32}P]-ATP, was subjected to

SDS-PAGE, and were sensitive to the addition of non-radioactive PEP to the loading dye. The same

bands are observed when [^{32}P]-PEP is loaded with glycerol alone, arguing that these events reflect an

artifact and are not protein phosphorylation events.

Consistent with PEP-dependent phosphorylation being uncommon, most other phosphorylation

events from [^{32}P]-PEP were competed by 1 mM ATP and not 1 mM PEP; however phosphorylation of a

species migrating at ~45 kDa that was not blocked by excess ATP was observed in both H1299 (human

non-small cell lung carcinoma) (**Figure 1A**) and mouse embryonic fibroblast (MEF) (**Figure 1B**) cell

lysates. No reported substrates of PKM2-dependent protein phosphorylation are consistent with this

molecular weight, suggesting that this event is a previously uncharacterized target of PEP-dependent

phosphorylation.

To determine whether addition of PKM2 would result in additional phosphorylation events, we

included recombinant PKM2 (rPKM2) in the reaction. rPKM2 has been used previously to show PKM2-

dependent phosphorylation (Gao et al., 2012; Keller et al., 2014; Yang et al., 2012a); however, we did not

observe any PEP-dependent phosphorylation events upon addition of either wild type (WT) rPKM2 or a

mutant PKM2 (R399E) that is reported to have higher protein kinase activity (Gao et al., 2012) (**Figure

1A**). Both WT- and R399E-rPKM2 enzymes exhibit pyruvate kinase activity as a glycolytic enzyme as

both can support synthesis of [γ-^{32}P]-ATP from [^{32}P]-PEP and cold ADP; although consistent with reports

that the R399E mutant favors a less active form of the enzyme, this protein is less efficient than WT

PKM2 in transferring [^{32}P]-phosphate from PEP to ADP (**Figure 2D**). Importantly, the WT PKM2

generated for these studies had a similar specific activity for conversion of PEP and ADP to pyruvate and

ATP as reported previously (**Figure 2E**) (Dombrauckas et al., 2005). Because most substrates of PKM2-

dependent phosphorylation are nuclear, we also tested the ability of PKM2 to phosphorylate proteins in a
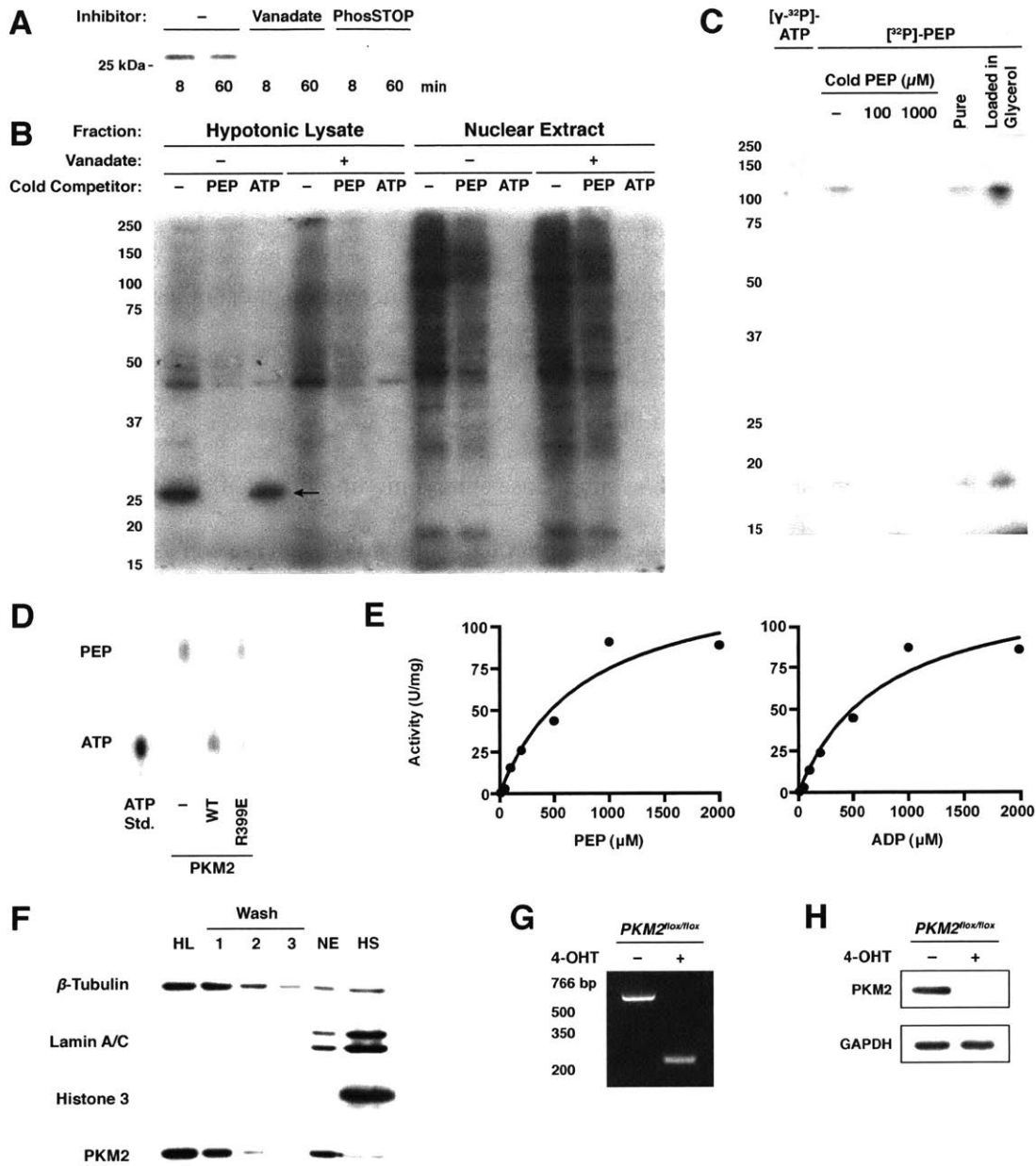
Figure 2: Validation of the assay for PEP- and PKM2-dependent protein phosphorylation.

(*A*) Phosphoglycerate mutase 1 (PGAM1) labeling from [^{32}P]-PEP is inhibited by orthovanadate. H1299 hypotonic lysates were incubated for 8 min or 1 h with [^{32}P]-PEP and 1 mM cold competitor ATP. The reaction was carried out without added phosphatase inhibitors or with the addition of 1 mM sodium orthovanadate (vanadate) or PhosSTOP (Roche), and proteins were resolved by SDS-PAGE and visualized by autoradiography. (*B*) Orthovanadate (vanadate, 1 mM) does not inhibit PEP-dependent phosphorylation. H1299 cell hypotonic lysate and nuclear extract were incubated with [^{32}P]-PEP and cold competitor PEP or ATP with or without the addition of 1 mM sodium orthovanadate. PGAM1 is indicated with an arrow. (*C*) [^{32}P]-PEP can label a polyacrylamide gel in the absence of added protein. [γ-^{32}P]-ATP (lane 1) and [^{32}P]-PEP (lanes 2-6) were analyzed by SDS-PAGE and autoradiography. These molecules migrate with the salt front of the gel as assessed by Geiger counting. This salt front is cut off before autoradiography, but [^{32}P]-PEP also labels what appears as two bands by autoradiography. Impure [^{32}P]-PEP was electrophoresed in the presence of no (lane 2), 100 μM (lane 3), or 1000 μM (lane 4) cold competitor PEP. HPLC-purified [^{32}P]-PEP (lane 5) and [^{32}P]-PEP loaded in ~7% (v/v) glycerol (as opposed to Lamelli sample buffer) (lane 6) produced a similar pattern. (*D*) Recombinant wild type and R399E mutant PKM2 display glycolytic pyruvate kinase activity. Lane 1: [γ-^{32}P]-ATP standard. Lanes 2-4: [^{32}P]-PEP and 0.5 mM ADP were incubated for 45 min with no enzyme or 10 μg/mL recombinant wild type or mutant (R399E) PKM2. PEP and ATP were resolved by TLC and visualized by autoradiography. (*E*) Specific activity of wild type rPKM2 with respect to substrate concentration determined by a linked assay to lactate dehydrogenase (Vander Heiden et al., 2010). In each case the substrate whose concentration was not varied was kept fixed at 5 mM. Data are the mean of N=3 ± S.D. (*F*) Protein levels of β-tubulin, lamin A/C, histone H3, and PKM2 were determined in cell extract fractions by western blotting. H1299 hypotonic lysate (HL) was prepared in buffer containing 10 mM KCl. The remaining material was washed three times with this buffer, and a nuclear extract (NE) was prepared from the resulting material using 500 mM NaCl. A high-salt (HS) extraction, containing histones, was then obtained by extraction with 2.5 M NaCl. (*G*) PKM2 can be deleted from MEFs. Cre-ER expressing MEFs homozygous for a *PKM* allele where exon 10 (specific to PKM2) is flanked by two loxP sites (*PKM2*$^{flox/flox}$) were treated with .1% (v/v) ethanol or 500 nM 4-hydroxytamoxifen (4-OHT) and .1% ethanol. Deletion of *PKM* exon 10 was confirmed by PCR using primers described previously (Israelsen et al., 2013). (*H*) PKM2 expression was analyzed by western blot analysis of cell lysates.

117

nuclear extract and again failed to observe any PEP-dependent phosphorylation events with or without

rPKM2 included in the reaction (**Figure 1**).

Because PKM2 is an abundant protein (Beck et al., 2011), we considered the possibility that

endogenous PKM2 present in the H1299 hypotonic and nuclear lysates (**Figure 2F**) could be sufficient to

catalyze PKM2-dependent phosphorylation, and that this might explain why addition of rPKM2 did not

produce any additional phosphorylated species. To definitively assess a requirement for PKM2 in any

PEP-dependent phosphotransfer events, we utilized PKM2-deleted MEFs (Lunt et al.) and confirmed that

PKM2-specific exon 10 was deleted from the genome and that PKM2 protein is absent from these cells

(**Figure 2G,H**). Upon deletion of this exon, PKM1 is expressed and the cells continue to possess pyruvate

kinase activity (Lunt et al., 2015). Phosphotransfer from PEP was similar to that in H1299 cells, and we

did not observe phosphorylation events dependent on the addition of rPKM2 to *PKM2$^{-/-}$* lysates (**Figure

1B**). PKM2 protein kinase activity is reported to be important specifically for glioblastoma development

downstream of EGFR activation (Gao et al., 2012; Keller et al., 2014; Yang et al., 2012a; Yang et al.,

2012b), however, we also failed to observe PEP-dependent phosphorylation events in hypotonic and

nuclear lysates of U87 glioblastoma multiforme cells and U87 cells expressing constitutively active

EGFR-VIII except for the species at 45 kDa, and this was not dependent on PKM2 addition (**Figure 1C,

D**).

PKM2-dependent regeneration of ATP can account for PEP-dependent phosphorylation

Most labeling from [^{32}P]-PEP was eliminated by addition of excess cold ATP, suggesting that [γ-

^{32}P]-ATP was either generated from [^{32}P]-PEP, or present as a contaminant in the reaction to serve as the

phosphate group donor for most of the observed phosphorylation events. Indeed, [^{32}P]-PEP is synthesized

from commercial [^{32}P]-ATP using pyruvate kinase (Mattoo and Waygood, 1983; Vander Heiden et al.,

2010), and despite a step to enrich for [^{32}P]-PEP, these preparations are contaminated by small quantities

of [γ-^{32}P]-ATP (**Figure 3A**). Preparative HPLC of [^{32}P]-PEP allowed for quantitative separation from the

contaminating [γ-^{32}P]-ATP. To test the contribution of each phosphate donor to protein phosphorylation

118

in a cell lystate, we incubated cells with crude [^{32}P]-PEP, HPLC purified [^{32}P]-PEP, and the HPLC

fraction containing [^{32}P]-ATP present as a contaminant in crude [^{32}P]-PEP. Most proteins phosphorylated

by the impure [^{32}P]-PEP were phosphorylated by the contaminating [γ-^{32}P]-ATP fraction but not the

purified [^{32}P]-PEP fraction (**Figure 3B**). Consistent with competition by cold ATP and PEP allowing

determination of direct phosphate donors, the ~45 kDa protein identified previously was labeled from

purified [^{32}P]-PEP. Addition of ADP to purified [^{32}P]-PEP restored phosphorylation of many proteins, and

the resulting phosphorylation events could be competed by both cold ATP and cold PEP. These data

argue that pyruvate kinase activity present in these reactions is sufficient to allow [γ-^{32}P]-ATP synthesis

from ADP and [^{32}P]-PEP (**Figure 3B, lanes 10-12**). Since [γ-^{32}P]-ATP is the phosphate donor for most

protein kinase activity in cells, these data suggest that the known role of PKM2 as a glycolytic enzyme

might explain PKM2-dependent phosphorylation whereby PKM2 transfers phosphate from [^{32}P]-PEP to

ADP present in cell lysate to synthesize [γ-^{32}P]-ATP and result in phosphorylation seemingly dependent

on PEP and the addition of PKM2. Consistent with this possibility, a hypotonic cell lysate contains

sufficient ADP to enable synthesis of [γ-^{32}P]-ATP from [^{32}P]-PEP when added to the lystate, and this

ability is diminished if size exclusion chromatography is used to deplete metabolites in the lysate (**Figure 4**).

We next considered the possibility that our failure to observe protein phosphorylation dependent

on both [^{32}P]-PEP and PKM2 in hypotonic or nuclear lysates may have been due to the absence of

relevant protein kinase substrates. For instance, histones, a putative target of PEP-dependent PKM2

protein kinase activity (Yang et al., 2012a), are not efficiently extracted by many protocols used to

prepare nuclear extracts (**Figure 2F**) (Shechter et al., 2007). To determine whether PKM2 can

phosphorylate histones in our assay, we incubated WT- or R399E-rPKM2 and commercially prepared

histones from calf thymus with impure [^{32}P]-PEP. Although we failed to observe any phosphorylation

upon addition of either rPKM2 or PKM2 (R399E), a nuclear extract of H1299 cells incubated with

impure [^{32}P]-PEP was able to phosphorylate proteins that run at the expected size of histones when

histones are added (**Figure 5A**), suggesting that the presence of PKM2 in a nuclear extract could enable
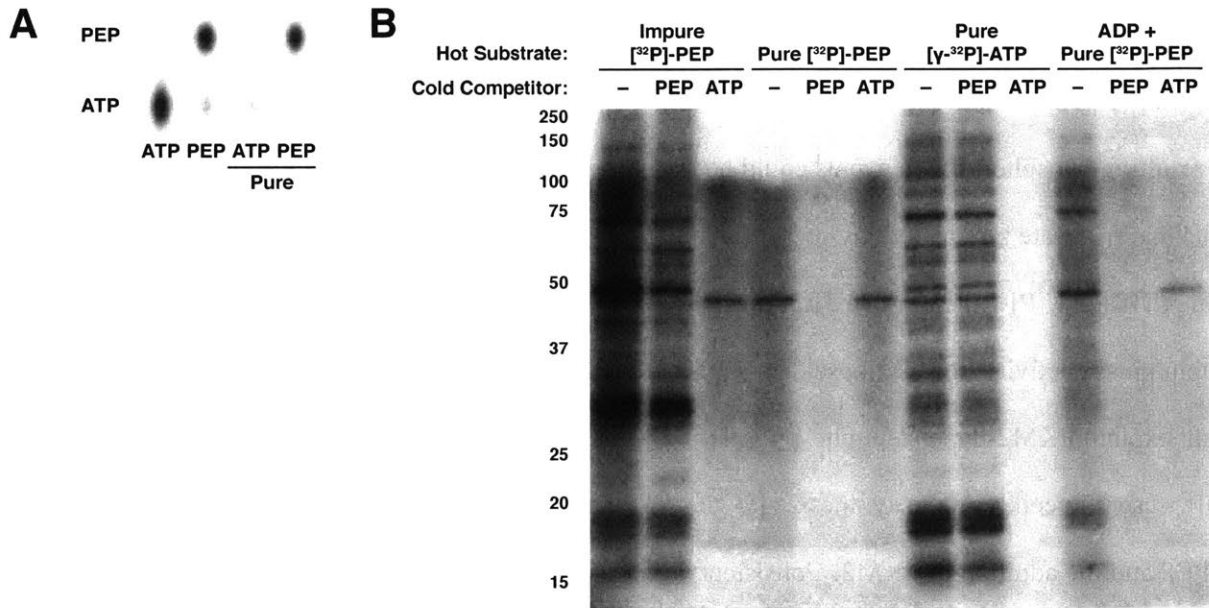
Figure 3: Contaminating [γ-^{32}P]-ATP is the predominant phosphoryl donor when using crude [^{32}P]-PEP.

(*A*) [^{32}P]-PEP synthesized from [γ-^{32}P]-ATP is contaminated by small amounts of [γ-^{32}P]-ATP, which can be separated by preparative HPLC. The purity of each fraction was analyzed by thin-layer chromatography and autoradiography. (*B*) The contaminating [γ-^{32}P]-ATP component of impure [^{32}P]-PEP is the phosphoryl donor for the majority of proteins phosphorylated by impure [^{32}P]-PEP. An H1299 hypotonic lysate was incubated for 1 h with recombinant PKM2 and different ^{32}P-containing metabolites as well as no competitor or excess (1 mM) non-radioactive competitor PEP or ATP as indicated. Phosphorylated proteins were analyzed by SDS-PAGE and autoradiography.
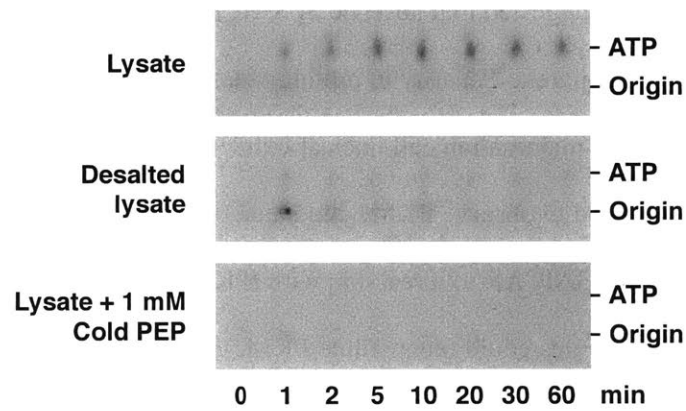
**Figure 4: A hypotonic lysate contains enough ADP to enable synthesis of [γ-^{32}P]-ATP.**

H1299 hypotonic lysates were incubated for the indicated times with rPKM2 and [^{32}P]-PEP. Labeled ATP produced by this reaction was measured by TLC and autoradiography.

indirect transfer of phosphate from PEP to histones. The inability of PKM2 to do this directly confirms

that any dependence on PKM2 is to transfer the phosphate to generate ATP rather than PKM2 acting

directly as a protein kinase. We also conducted the assay in a purely recombinant system using two

putative protein substrates of PKM2 using antibodies to detect protein phosphorylation and did not

observe direct PKM2 protein kinase activity (**Figure 6A,B**).

The purine precursor SAICAR may be an activator of PKM2 protein kinase activity (Keller et al.,

2014). In particular, it has been suggested that absence of SAICAR from *in vitro* phosphorylation

reactions could account for an apparent disparity in protein kinase activity between rPKM2 produced in

E. coli and PKM2 obtained from mammalian cell nuclear extracts. To determine if the absence of

SAICAR explained why we failed to observe PKM2-mediated protein kinase activity in cell and nuclear

extracts, we tested if addition of SAICAR to a reaction with rPKM2 and cell lysate, nuclear extract, or

purified histones and other substrates could reconstitute PKM2-depedent protein kinase activity (**Figures

5B, 6A-C**). In no case was SAICAR addition sufficient to cause protein phosphorylation that was

competed by PEP addition but not ATP addition, or that was dependent on the presence of PKM2. These

data suggest that any increase in PEP-dependent protein phosphorylation following SAICAR addition that

involves PKM2 is likely explained by the ability of SAICAR to activate the glycolytic enzyme function

of PKM2 (Keller et al., 2012), and promote generation of ATP as a phosphate donor for other protein

kinases.

Because ATP is present at millimolar concentrations in cells (Marcussen and Larsen, 1996), it is

unlikely that addition of 1 mM cold competitor ATP is sufficient to inhibit physiologically relevant

PKM2-dependent phosphorylation. However, we considered the possibility that addition of cold ATP

might inhibit apparent PKM2 protein kinase activity in vitro. To test this possibility, we incubated cell

lysates with 5'-(4-fluorosulfonobenzoyl)-adenosine (FSBA) to covalently inhibit endogenous ATP-

dependent kinases aid identification of PEP-dependent phosphorylation event without adding cold ATP.

FSBA was confirmed to be a partial inhibitor of ATP-dependent kinases in cell lysates and nuclear
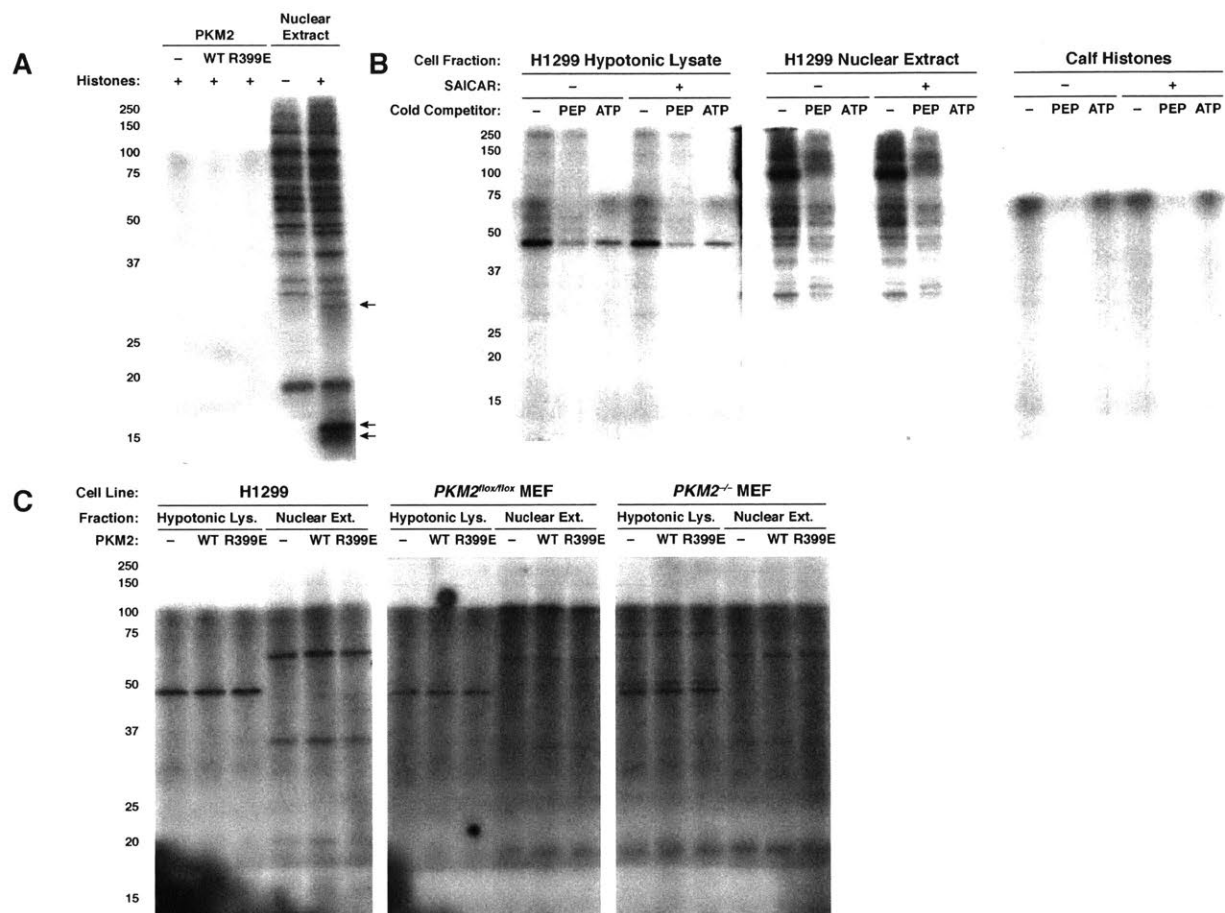
Figure 5: An improved assay for PEP-dependent phosphorylation.

(*A*) Calf thymus histones were incubated for 1 h with impure [^{32}P]-PEP and no enzyme, recombinant wild type (WT) or mutant (R399E) PKM2 (each at 10 μg/mL) as indicated. An H1299 nuclear extract was also incubated with impure [^{32}P]-PEP with and without calf thymus histones added. Phosphorylated proteins were analyzed by SDS-PAGE and autoradiography. Arrows indicate phosphorylated proteins with apparent molecular weights similar to histones (core histones, 11-17 kDa, many histone H1 isoforms 25-35 kDa) (Shechter et al., 2007). (*B*) H1299 cell hypotonic lysates and nuclear extracts and calf thymus histones were incubated for 1 h with [^{32}P]-PEP and 10 μg/mL rPKM2 with or without 0.5 mM SAICAR as well as no competitor or excess (1 mM) cold competitor PEP or ATP. (*C*) Hypotonic lysates and nuclear extracts from H1299 cells and PKM2-expressing (flox/flox) or PKM2-null (-/-) MEFs were desalted and incubated for 1 h with HPLC-purified [^{32}P]-PEP with no additional enzymes or with added recombinant wild type or mutant (R399E) rPKM2 (each at 10 μg/mL).
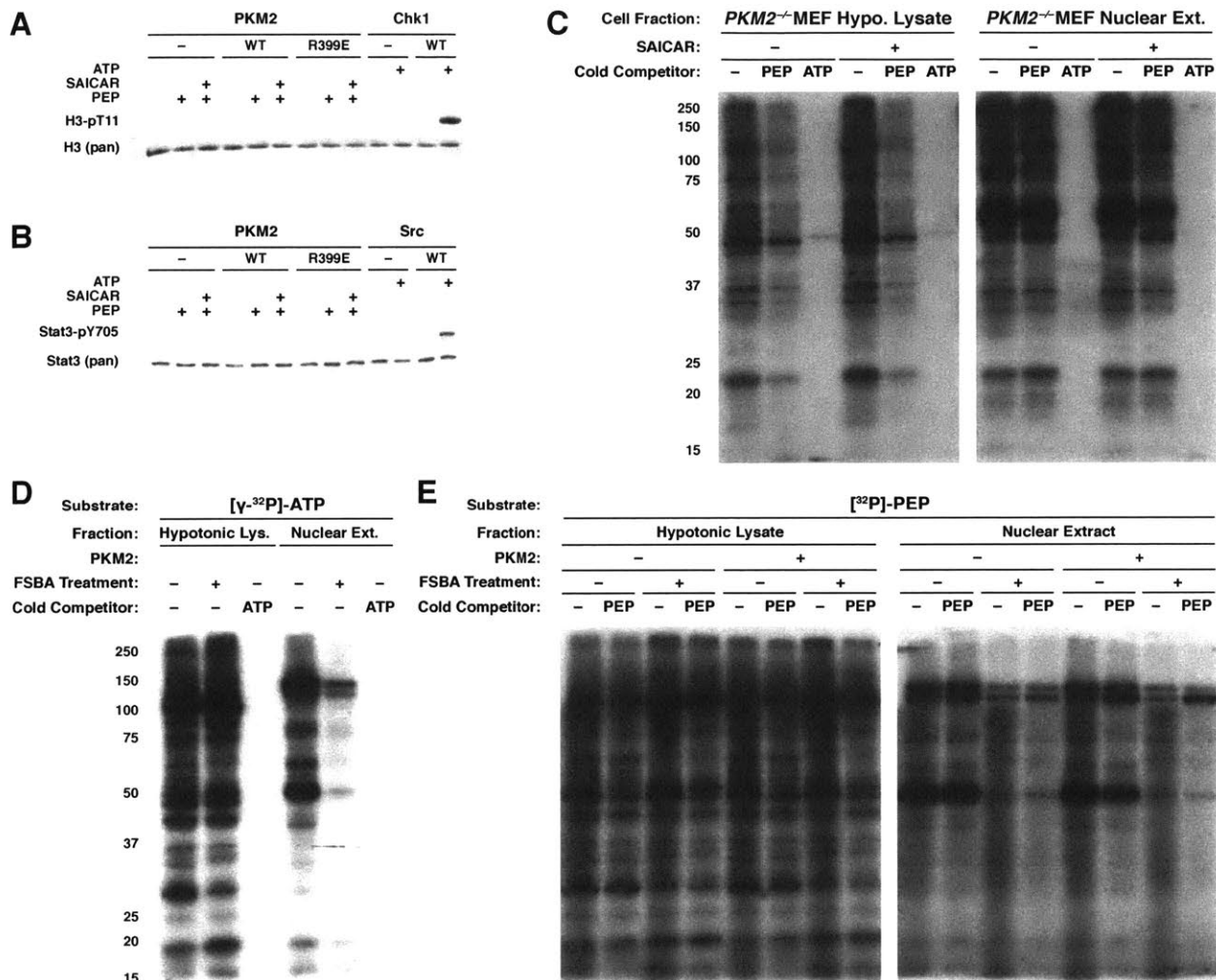
Figure 6: Lack of evidence for PKM2 PEP-dependent protein kinase activity.

Recombinant PKM2 and (*A*) Stat3 or (*B*) histone H3 were incubated for 1 hr at 30 °C with or without PEP and SAICAR as indicated. As a control, the same assay was repeated with recombinant protein kinases known to phosphorylate these proteins, (*A*) Chk1 and (*B*) Src, with the addition of cold ATP. (*C*) $PKM2^{-/-}$ MEF cell hypotonic lysate and nuclear extract were incubated for 1 h with [^{32}P]-PEP and rPKM2 with or without 0.5 mM SAICAR, and in the absence of competitor or in the presence of cold competitor PEP (1 mM) or ATP (1 mM) as indicated. (*D*) H1299 cell hypotonic lysate and nuclear extract were incubated with DMSO or 1 mM FSBA (5'-(4-fluorosulfonobenzoyl)adenosine) to inhibit ATP-dependent kinases. Protein phosphorylation events observed in lysates containing [γ-^{32}P]-ATP with or without FSBA are shown. (*E*) DMSO- or FSBA-treated cell extracts were incubated with [^{32}P]-PEP with or without the addition of PKM2 and cold competitor PEP to monitor PKM2 and PEP-dependent phosphorylation.

extracts (**Figure 6D**), however when the same lysates and nuclear extracts were assayed with only PEP as

a phosphate donor, we failed to observe any FSBA insensitive protein phosphorylation (**Figure 6E**).

To further search for PEP-dependent phosphorylation events that require PKM2 functions other

than its known action in generating ATP, we tested HPLC purified [^{32}P]-PEP in a reaction with protein

extracts that were first desalted to remove contaminating ADP, and with or without the addition of

rPKM2 or rPKM2-R399E. These reactions were performed with whole cell hypotonic lysates and nuclear

extracts prepared from PKM2-expressing H1299 cells and MEFs as well as PKM2-null MEFs (**Figure

5C**). Using this approach, we observed several phosphorylated species, including the ~45 kDa species

noted previously (**Figure 1A**); however no events were dependent on the addition of WT- or R399E-

rPKM2, including events in extracts prepared from PKM2-null MEFs. These data argue that a PKM2-

dependent protein phosphorylation activity is not present in these cells.

Lack of evidence for an ATP-dependent PKM2 protein kinase activity

Failure to observe PEP-dependent protein phosphorylation that is dependent on PKM2 does not

rule out the possibility that PKM2 possesses an ATP-dependent protein kinase activity. Both PEP and

ATP can act as phosphate donors for normal PKM2 enzymatic activity, so an alternative explanation for

reports of PKM2 protein kinase activity might involve PKM2 as an ATP-dependent protein kinase. The

ability to detect ATP-dependent phosphorylation events dependent on the addition of rPKM2 to a cell

lysate is complicated by the fact that many proteins undergo ATP-dependent phosphorylation. To mitigate

this complication, and to control for the presence or absence of PKM2 in the lysates, we fractionated

hypotonic and nuclear extracts from H1299 cells and from PKM2-expressing and PKM2-null MEFs by

anion exchange chromatography. We assayed each fraction for phosphorylation dependent on the addition

of rPKM2 (**Figure 7, 8A**). One phosphorylated species (**Figure 7A**, H1299 hypotonic lysate fractions 1-

2, MW ~60 kDa) showed dependence on the addition of rPKM2. rPKM2 also has a MW of ~60 kDa,

raising the possibility that phosphorylation of rPKM2 by kinases present in the lysate rather than

production of a PKM2-phosphorylated species explains this result. Prior work has suggested that PKM2
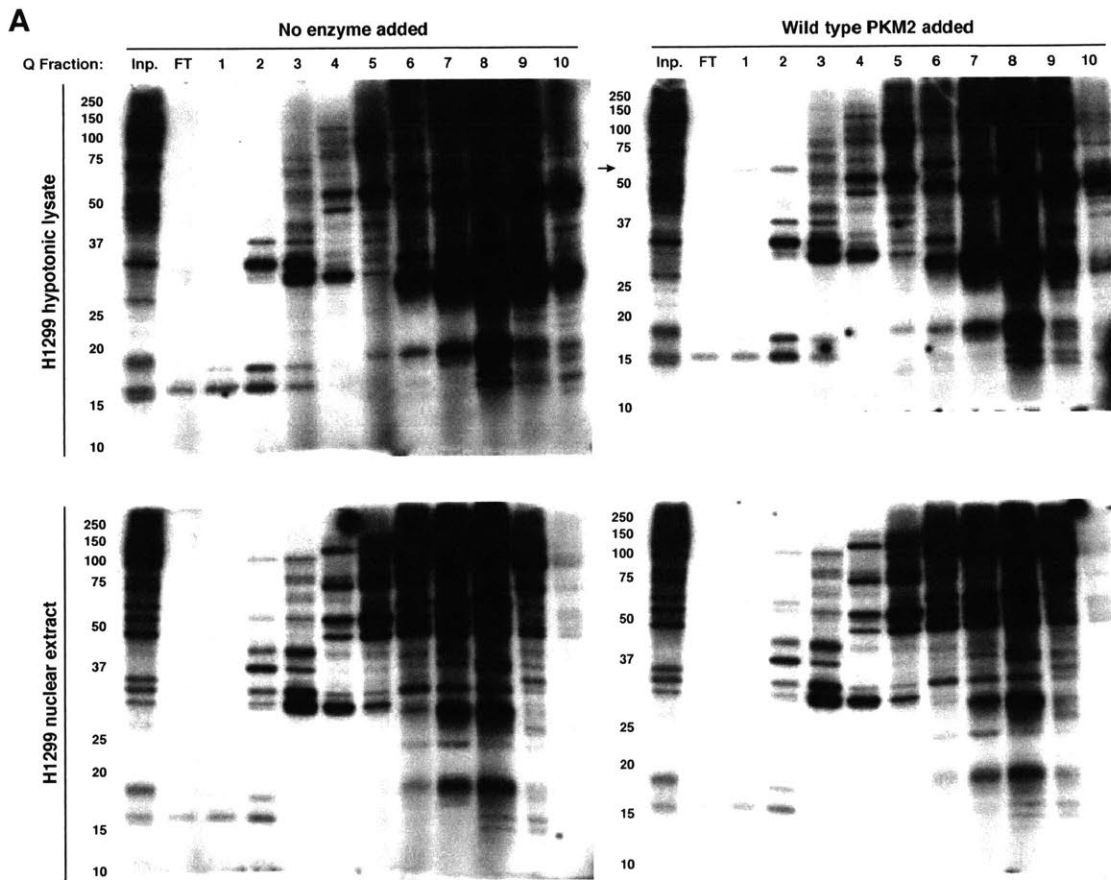
Figure 7: Lack of evidence for an ATP-dependent protein kinase activity for PKM2.

(*A*) H1299 and (*B*) PKM2-null MEF hypotonic lysates and nuclear extracts were used to identify substrates for PKM2 kinase activity. Lysates were fractionated on a 1mL Q Sepharose HP column (Inp., 1:10 dilution of column input; FT, flow through; 1-10, fractions 1-10), and incubated for 1 h with [γ-^{32}P]-ATP with or without the addition of 10 µg/mL rPKM2. Phosphorylated proteins were analyzed by SDS-PAGE and autoradiography.

B

Q Fraction:

PKM2⁻ᐟ⁻ MEF nuclear extract

PKM2⁻ᐟ⁻ MEF hypotonic lysate

No enzyme added

Wild type PKM2 added

Inp. FT 1 2 3 4 5 6 7 8 9 10

250 150 100 75 50 37 25 20 15 10
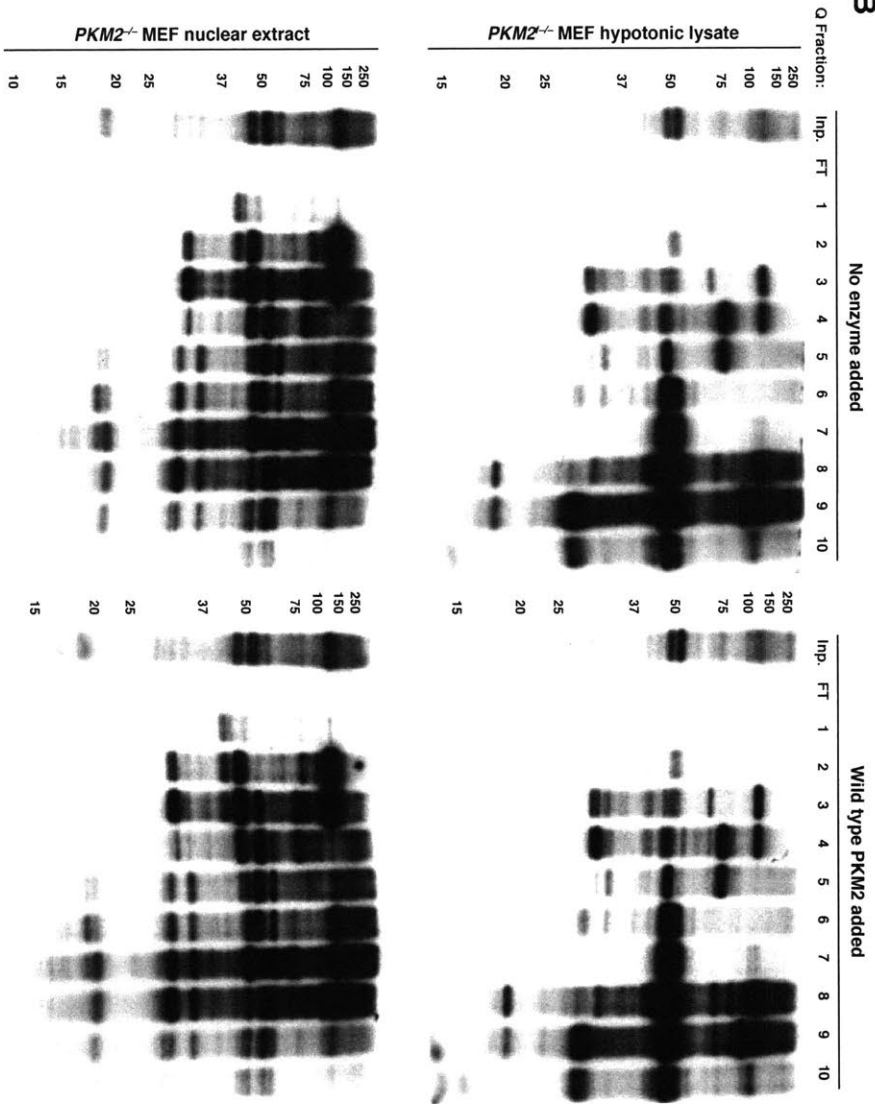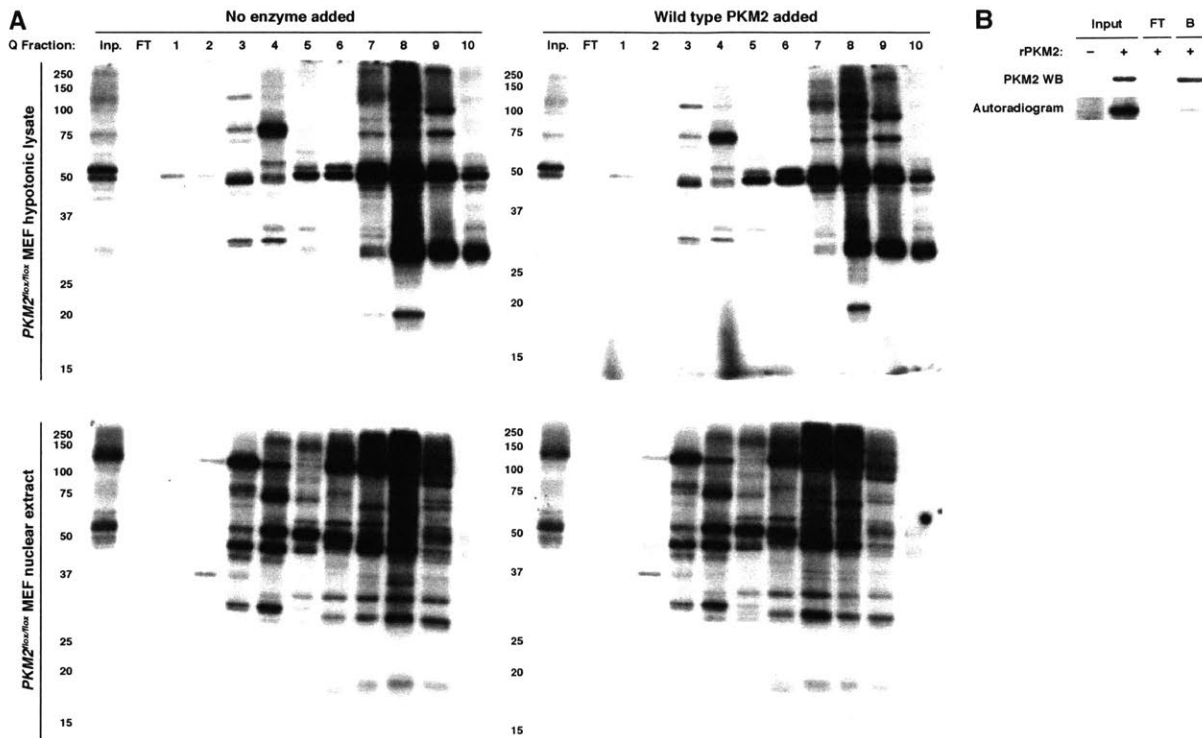
Figure 8: Lack of evidence for an ATP-dependent protein kinase activity for PKM2.

(*A*) rPKM2 was added to a fractionated hypotonic lysate and nuclear extract prepared from PKM2-expressing (PKM2$^{flox/flox}$) MEFs to identify potential PKM2 protein kinase activity using ATP as a substrate. (*B*) In Figure 4A, one protein (predominantly contained within H1299-hypotonic-lysate fractions 1 and 2) exhibited phosphorylation dependent on PKM2 addition. This phosphorylated protein co-purifies with PKM2 by nickel-affinity chromatography (Inp., Q column input; FT, nickel-affinity column flow through).

can be a substrate for phosphorylation (Hitosugi et al., 2009). In support of rPKM2 being phosphorylated by a kinase in the lysate, we were able to purify this species by Ni-NTA affinity chromatography (**Figure 8B**), indicating that this represents phosphorylated rPKM2 rather than a protein phosphorylated by PKM2. Taken together, these data argue against PKM2 having direct protein kinase activity.

Discussion

We were unable to find evidence for PKM2 activity as a protein kinase utilizing either [^{32}P]-PEP or [γ-^{32}P]-ATP as a substrate. While negative results cannot be definitive, sensitive ^{32}P-labeling failed to identify any proteins phosphorylated in a PKM2-dependent manner. Our findings demonstrate the importance of depleting contaminating adenine nucleotides from cell lystates and purification of enzymatically synthesized [^{32}P]-PEP to reduce [γ-^{32}P]-ATP generation *in situ*, which might otherwise lead to ATP-dependent phosphorylation events being misinterpreted as PEP-dependent. Omitting these steps can result in pyruvate kinase mediated regeneration of ATP and produce data that appear to be PEP-dependent phosphorylation events.

To have activity as a protein kinase, PKM2 would have to adopt a conformation in which both PEP and its protein substrate are simultaneously bound. To allow phosphotransfer reactions, water must be excluded from the enzyme active site or hydrolysis of high-energy phosphate anhydrides would be favored over the phosphate transfer reaction. To accommodate a large protein substrate in place of the much smaller ADP, the active site would need to be dramatically altered to exclude water and allow transfer of phosphate to a residue on the target protein. An alternative mechanism for phosphotransfer could involve a covalent phospho-enzyme intermediate; however, the known mechanism of the pyruvate kinase reaction involves direct phosphate transfer (Dombrauckas et al., 2005), and we did not observe labeling of PKM2 from [^{32}P]-PEP alone.

It has been suggested that protein substrates of PKM2 bind to the ADP binding site of this enzyme, supported by the apparent competitive inhibition of PKM2 protein kinase activity by ADP (Gao et al., 2012; Keller et al., 2014). This observation could also be explained by end-product inhibition of a contaminating ATP-dependent kinase by ADP. The ability of protein substrates to occupy the ADP-binding site of PKM2 is particularly surprising given that PKM2 has been reported to phosphorylate 149 protein substrates lacking a clear phosphorylation motif, suggesting degenerate specificity of the active site (Keller et al., 2014). By contrast, nucleotide binding is highly specific as PKM2 is unable to efficiently phosphorylate diverse nucleotide substrates, instead showing strong selectivity for ADP (Mazurek et al., 1998). In addition, PKM1 has the same binding site for ADP as PKM2, and shows similar selectivity for ADP (Morgan et al., 2013; Plowman and Krall, 1965). In fact, PKM2 and PKM1 have identical active sites. These isoforms differ by the alternative inclusion of one exon, which encodes only regulatory components of the protein further arguing against a specific kinase function for PKM2. A more plausible explanation is that PKM2 serves to regenerate ATP from PEP for other kinases as an explanation for reports of PKM2 protein kinase activity.

Although we did not detect protein kinase activity by PKM2, several protein species were labeled by [^{32}P]-PEP independent of the presence of PKM2: an unknown 45 kDa protein as well as PGAM, which has been previously identified as a target of PEP-dependent phosphorylation. While PGAM is labeled by the phosphate from PEP, it is important to note that PEP may be transferring more than just a phosphate to the unknown 45 kDa protein. Interestingly, another glycolytic intermediate, 1,3-bisphosphoglycerate, can post-translationally modify proteins on lysine to produce 3-phosphoglyceryl-lysine via a non-enzymatic mechanism (Moellering and Cravatt, 2013). Depletion of enolase from the reaction would distinguish between PEP-dependent and 2-PG-dependent phosphorylation, and will help clarify whether PEP-dependent labeling of the ~45 kDa protein is mediated by PEP or an enzymatic product of PEP other than ATP. Nevertheless, it appears that PEP-dependent phosphorylation is rare in mammalian cells and that PKM2 is not required for any of the events observed in this study. The methods to separate PEP-

dependent phosphorylation in mammalian cells from ATP-dependent events with high sensitivity will allow identification of both the targets and enzymes involved.

Materials and Methods

Cell Culture. H1299 cells, MEFs, U87 cells, and U87 EGFR-VIII cells were cultured in RPMI 1640 or DMEM, supplemented with 10% heat-inactivated fetal bovine serum, penicillin (100 U/mL), and streptomycin (100 μg/mL). MEFs expressing Cre-ER and homozygous for a PKM2 conditional allele were generated from mice as described previously (Lunt et al., 2015) and immortalized by knockdown of p53. To delete PKM2, the MEFs were treated with 1 μM 4-hydroxytamoxifen for at least 3 days.

Protein Extraction and Purification. To prepare hypotonic lysates and nuclear extracts, cells were washed with ice cold PBS, collected by centrifugation at 650 × g, and incubated in three volumes of hypotonic lysis buffer (10 mM HEPES/KOH pH 7.6, 10 mM KCl, 1.5 mM $MgCl_2$, 1 mM EDTA, 1 mM EGTA, .5 mM DTT, 1x cOmplete mini protease inhibitor (Roche)) for 10 min on ice. Lysis was accomplished by passing cells through a 22.5-gauge needle fifteen times. Nuclei were pelleted for 10 min at 855 × g, and washed five times with four volumes of hypotonic lysis buffer. They were next resuspended in one volume of nuclear extraction buffer (20 mM HEPES/KOH pH 7.6, 500 mM NaCl, 1.5 mM $MgCl_2$, 1 mM EDTA, 1 mM EGTA, .5 mM DTT, 25% (v/v) glycerol, 1x cOmplete mini protease inhibitor (Roche)) and incubated for 30 min on ice with occasional mixing. Lysates were clarified for 10 min at 20 000 × g, and a high-salt extraction was accomplished by incubating the resulting pellet in high-salt solubilization buffer (Shechter et al., 2007) for 30 min. Proteins were desalted into hypotonic lysis buffer by passing samples through a Sephadex G-25 Fine (GE Healthcare) gravity column. For Q-column fractionation, samples were first concentrated to 1 mL on Pierce Concentrators with a 9 kDa molecular weight cutoff (Thermo Scientific). Samples were then desalted into buffer A (20 mM bis-tris-propane-

HCl pH 8.7, 5 mM KCl, 1 mM MgCl₂) on a 5 mL HiTrap Desalting column (GE Healthcare) and then

loaded onto a 1 mL HiTrap Q HP column (GE Healthcare). Proteins were eluted in a linear gradient from

buffer A to buffer A with 1 M KCl, and 1 mL fractions were collected. Protein concentration was

determined by standard Bradford assay.

Expression and Purification of Recombinant PKM2. N-terminally 6xHis-tagged recombinant PKM2

and PKM2-R399E were expressed from the pET28a(+) vector in *E. coli* and batch purified using Ni-NTA

agarose beads (Qiagen) as described previously (Anastasiou et al., 2012).

Site-Directed Mutagenesis. The R399E mutation was introduced using the QuikChange II XL Site

Directed Mutagenesis Kit (Agilent Technologies) and the following primers: 5'-

CAATTATTTGAGGAACTCGAGCGCCTGGCGCCCATTACC-3' and 5'-

GGTAATGGGCGCCAGGCGCTCGAGTTCCTCAAATAATTG-3'.

[³²P]-PEP Synthesis and Purification. [³²P]-PEP was synthesized as described previously (Mattoo and

Waygood, 1983; Vander Heiden et al., 2010). Briefly, commercial rabbit muscle pyruvate kinase (Sigma)

catalyzed synthesis from pyruvate and [γ-³²P]-ATP (Perkin Elmer) at 37 °C for 45-60 min, followed by

crude separation of PEP from ATP using a Vivapure Q Mini H columns (Satorius) with sequential elution

in 0.3 and 0.6 M triethylammonium bicarbonate pH 8.5 (Sigma).

Further purification was accomplished by reverse-phase ion-pairing high performance liquid

chromatography. [³²P]-PEP (containing contaminating [γ-³²P]-ATP) was mixed with 100 μM of each of

cold PEP and ATP. This mixture was loaded on to a ZORBAX SB-C18 Analytical column (Agilent), and

eluted in a linear gradient from 5% (v/v) methanol, 15 mM acetic acid, and 10 mM tributylamine to 100%

methanol. 500 μL fractions were collected. Three fractions containing the highest amount of PEP or ATP

(as determined by TLC and autoradiography) were pooled and dried under nitrogen gas. Samples were resuspended in water for use in *in vitro* reactions.

***In Vitro* Phosphorylation Reactions.** Unless stated otherwise, reactions were carried out at 30 °C for 1 h in previously published buffer (50 mM Tris-HCl pH 7.5, 100 mM KCl, 50 mM $MgCl_2$, 1 mM DTT) with 1x PhosSTOP (Roche) (Gao et al., 2012; Yang et al., 2012a). Protein extracts prepared as described above or calf thymus histones (Worthington Biochemical) were included at 100 μg/mL. Recombinant PKM2 was included in the reaction at 10 μg/mL. Where indicated, 1 mM Na_3VO_4, 0.5 mM SAICAR, or 1 mM cold competitor ATP or PEP were included in the reaction. Radioactive phosphate group donor substrates were ~6 nM (~20 μCi/mL) [γ-^{32}P]-ATP (Perkin Elmer) or ~4.5 nM (~13 μCi/mL) impure [^{32}P]-PEP, or ~3.5 nM (~10 μCi/mL) pure [^{32}P]-PEP or ~.31 nM (~.9 μCi/mL) pure [γ-^{32}P]-ATP. Reactions were quenched with addition of Lamelli sample buffer, and phosphorylated proteins were analyzed by 10% SDS-PAGE followed by autoradiography. Nickel-affinity purification was accomplished by incubating phosphorylation reactions with Ni-NTA Beads (Qiagen) for 30 min. Beads were then washed with reaction buffer supplemented with 30 mM imidazole, and proteins were eluted by boiling in Lamelli sample buffer. Where indicated, lysates were incubated with 1% (v/v) DMSO or 1 mM (final) 5'-(4-fluorosulfonobenzoyl)-adenosine (FSBA, Sigma) with 1% (v/v) DMSO at 30 °C to inhibit endogenous ATP-dependent kinases. FSBA was removed by desalting in an Amicon Ultra centrifugal filter prior to phosphorylation assay and addition of PKM2. For *in vitro* phosphorylation detected by western blot, recombinant PKM2, Src, or Chk1 was present at 1 ng/μL and histone H3 or Stat3 was present at 3 ng/μL.

Thin-Layer Chromatography. 0.5 μL of each reaction or compound were spotted on to PEI-cellulose F (EMD Millipore), and metabolites were resolved with 0.25 M NH_4HCO_3. Plates were dried and then visualized by autoradiography.

SAICAR Synthesis and Purification. SAICAR was synthesized enzymatically using adenosuccinate lyase (ADSL) purified by a previously described approach (Lee and Colman, 2007). ADSL (50 μg/mL) catalyzed the reaction between 13.5 mg/mL AICAR (Toronto Research Chemicals) and 50 mM fumarate at 37°C overnight in a buffer containing 20 mM HEPES pH 7.4, 50 mM ammonium acetate, 50 mM KCl, 2 mM EDTA, and 1 mM DTT (Keller et al., 2012). The reaction was loaded on to a 5 mL HiTrap Q HP column and eluted in a linear gradient from water to 3 M ammonium acetate. Peak fractions were pooled and lyophilized. SAICAR was resuspended in 10 mM HEPES-KOH pH 7.5 prior to use in *in vitro* reactions.

Enzyme-Linked Pyruvate Kinase Assay. Pyruvate kinase activity was measured as previously described (Anastasiou et al., 2012). Briefly, rPKM2 (0.5 μg/mL) was mixed with various concentrations of PEP and ADP in a reaction buffer containing 50 mM HEPES-KOH (pH 7.5), 20 mM KCl, 2 mM $MgCl_2$, 1 mM DTT, 180 μM NADH, and 11 U lactate dehydrogenase (LDH, Sigma Aldrich). LDH activity was verified to be in excess of pyruvate kinase activity in these conditions, enabling disappearance of NADH (absorbance at 340 nm) to be used as a measure of pyruvate kinase activity.

Western Blotting. Total protein extracts were prepared by incubating cells for 15 min in ice-cold RIPA buffer followed by clarification for 10 min at 20 000 × g. To confirm absence of PKM2 in MEFs, 15 μg of protein were resolved by 8% SDS-PAGE. To determine contents of cell extracts, volumes proportionate to the extraction buffer volumes were resolved by 8 or 10% SDS-PAGE. Proteins were transferred to a PVDF membrane and, following immunoblotting, were visualized by ECL assay. Antibodies used: PKM2, histone 3, lamin A/C, histone H3, H3 phospho-T11, Stat3, Stat3 phospho-Y705 (Cell Signaling Technologies: 4053, 4499, 4777, 4499, 9764, 9132, 9145, respectively), *β*-tubulin (Abcam: 21058).

DNA Extraction and Genotyping. Genomic DNA was extracted using the PureLink Genomic DNA Mini Kit (Life Technologies). *PKM* exon 10 was amplified by polymerase chain reaction as described previously (Israelsen et al., 2013), and reaction products were resolved on a 2% agarose gel.

Acknowledgements

Author Contributions

A.M.H. and M.V.G.H conceived of and analyzed all experiments and wrote and edited this chapter. B.P.F. helped plan and devise some experiments, and D.Y.G. developed the method for SAICAR synthesis.

References

Anastasiou, D., Yu, Y., Israelsen, W.J., Jiang, J.K., Boxer, M.B., Hong, B.S., Tempel, W., Dimov, S., Shen, M., Jha, A., *et al.* (2012). Pyruvate kinase M2 activators promote tetramer formation and suppress tumorigenesis. Nat Chem Biol *8*, 839-847.

Beck, M., Schmidt, A., Malmstroem, J., Claassen, M., Ori, A., Szymborska, A., Herzog, F., Rinner, O., Ellenberg, J., and Aebersold, R. (2011). The quantitative proteome of a human cell line. Mol Syst Biol *7*, 549.

Carreras, J., Climent, F., Bartrons, R., and Pons, G. (1982). Effect of vanadate on the formation and stability of the phosphoenzyme forms of 2,3-bisphosphoglycerate-dependent phosphoglycerate mutase and of phosphoglucomutase. Biochim Biophys Acta *705*, 238-242.

Chaneton, B., Hillmann, P., Zheng, L., Martin, A.C., Maddocks, O.D., Chokkathukalam, A., Coyle, J.E., Jankevics, A., Holding, F.P., Vousden, K.H., *et al.* (2012). Serine is a natural ligand and allosteric activator of pyruvate kinase M2. Nature *491*, 458-462.

Christofk, H.R., Vander Heiden, M.G., Harris, M.H., Ramanathan, A., Gerszten, R.E., Wei, R., Fleming, M.D., Schreiber, S.L., and Cantley, L.C. (2008). The M2 splice isoform of pyruvate kinase is important for cancer metabolism and tumour growth. Nature *452*, 230-233.

Cortes-Cros, M., Hemmerlin, C., Ferretti, S., Zhang, J., Gounarides, J.S., Yin, H., Muller, A., Haberkorn, A., Chene, P., Sellers, W.R., *et al.* (2013). M2 isoform of pyruvate kinase is dispensable for tumor maintenance and growth. Proceedings of the National Academy of Sciences of the United States of America *110*, 489-494.

Deutscher, J., Francke, C., and Postma, P.W. (2006). How phosphotransferase system-related protein phosphorylation regulates carbohydrate metabolism in bacteria. Microbiol Mol Biol Rev *70*, 939-1031.

Dombrauckas, J.D., Santarsiero, B.D., and Mesecar, A.D. (2005). Structural basis for tumor pyruvate kinase M2 allosteric regulation and catalysis. Biochemistry *44*, 9417-9429.

Gao, X., Wang, H., Yang, J.J., Liu, X., and Liu, Z.R. (2012). Pyruvate kinase M2 regulates gene transcription by acting as a protein kinase. Molecular cell *45*, 598-609.

Hitosugi, T., Kang, S., Vander Heiden, M.G., Chung, T.W., Elf, S., Lythgoe, K., Dong, S., Lonial, S., Wang, X., Chen, G.Z., *et al.* (2009). Tyrosine phosphorylation inhibits PKM2 to promote the Warburg effect and tumor growth. Sci Signal *2*, ra73.

Israelsen, W.J., Dayton, T.L., Davidson, S.M., Fiske, B.P., Hosios, A.M., Bellinger, G., Li, J., Yu, Y., Sasaki, M., Horner, J.W., *et al.* (2013). PKM2 isoform-specific deletion reveals a differential requirement for pyruvate kinase in tumor cells. Cell *155*, 397-409.

Jiang, Y., Li, X., Yang, W., Hawke, D.H., Zheng, Y., Xia, Y., Aldape, K., Wei, C., Guo, F., Chen, Y., *et al.* (2014). PKM2 regulates chromosome segregation and mitosis progression of tumor cells. Molecular cell *53*, 75-87.

Keller, K.E., Doctor, Z.M., Dwyer, Z.W., and Lee, Y.S. (2014). SAICAR induces protein kinase activity of PKM2 that is necessary for sustained proliferative signaling of cancer cells. Molecular cell *53*, 700-709.

Keller, K.E., Tan, I.S., and Lee, Y.S. (2012). SAICAR stimulates pyruvate kinase isoform M2 and promotes cancer cell survival in glucose-limited conditions. Science *338*, 1069-1072.

Kung, C., Hixon, J., Choe, S., Marks, K., Gross, S., Murphy, E., DeLaBarre, B., Cianchetta, G., Sethumadhavan, S., Wang, X., *et al.* (2012). Small molecule activation of PKM2 in cancer cells induces serine auxotrophy. Chem Biol *19*, 1187-1198.

Lee, P., and Colman, R.F. (2007). Expression, purification, and characterization of stable, recombinant human adenylosuccinate lyase. Protein expression and purification *51*, 227-234.

Lunt, S.Y., Muralidhar, V., Hosios, A.M., Israelsen, W.J., Gui, D.Y., Newhouse, L., Ogrodzinski, M., Hecht, V., Xu, K., Acevedo, P.N., *et al.* (2015). Pyruvate kinase isoform expression alters nucleotide synthesis to impact cell proliferation. Molecular cell *57*, 95-107.

Marcussen, M., and Larsen, P.J. (1996). Cell cycle-dependent regulation of cellular ATP concentration, and depolymerization of the interphase microtubular network induced by elevated cellular ATP concentration in whole fibroblasts. Cell motility and the cytoskeleton *35*, 94-99.

Mattoo, R.L., and Waygood, E.B. (1983). An enzymatic method for [32P]phosphoenolpyruvate synthesis. Anal Biochem *128*, 245-249.

Mazurek, S., Grimm, H., Wilker, S., Leib, S., and Eigenbrodt, E. (1998). Metabolic characteristics of different malignant cancer cell lines. Anticancer research *18*, 3275-3282.

McKnight, S.L. (2014). Please keep me 2uned to PKM2. Molecular cell *53*, 683-684.

Moellering, R.E., and Cravatt, B.F. (2013). Functional lysine modification by an intrinsically reactive primary glycolytic metabolite. Science *341*, 549-553.

Morgan, H.P., O'Reilly, F.J., Wear, M.A., O'Neill, J.R., Fothergill-Gilmore, L.A., Hupp, T., and Walkinshaw, M.D. (2013). M2 pyruvate kinase provides a mechanism for nutrient sensing and regulation of cell proliferation. Proceedings of the National Academy of Sciences of the United States of America *110*, 5881-5886.

Plowman, K.M., and Krall, A.R. (1965). A kinetic study of nucleotide interactions with pyruvate kinase. Biochemistry *4*, 2809-2814.

Schieven, G., and Martin, G.S. (1988). Nonenzymatic phosphorylation of tyrosine and serine by ATP is catalyzed by manganese but not magnesium. J Biol Chem *263*, 15590-15593.

Shechter, D., Dormann, H.L., Allis, C.D., and Hake, S.B. (2007). Extraction, purification and analysis of histones. Nature protocols *2*, 1445-1457.

Vander Heiden, M.G., Locasale, J.W., Swanson, K.D., Sharfi, H., Heffron, G.J., Amador-Noguez, D., Christofk, H.R., Wagner, G., Rabinowitz, J.D., Asara, J.M., *et al.* (2010). Evidence for an alternative glycolytic pathway in rapidly proliferating cells. Science *329*, 1492-1499.

Wang, Y.H., Israelsen, W.J., Lee, D., Yu, V.W., Jeanson, N.T., Clish, C.B., Cantley, L.C., Vander Heiden, M.G., and Scadden, D.T. (2014). Cell-state-specific metabolic dependency in hematopoiesis and leukemogenesis. Cell *158*, 1309-1323.

Yang, W., Xia, Y., Hawke, D., Li, X., Liang, J., Xing, D., Aldape, K., Hunter, T., Alfred Yung, W.K., and Lu, Z. (2012a). PKM2 phosphorylates histone H3 and promotes gene transcription and tumorigenesis. Cell *150*, 685-696.

Yang, W., Zheng, Y., Xia, Y., Ji, H., Chen, X., Guo, F., Lyssiotis, C.A., Aldape, K., Cantley, L.C., and Lu, Z. (2012b). ERK1/2-dependent phosphorylation and nuclear translocation of PKM2 promotes the Warburg effect. Nature cell biology *14*, 1295-1304.

Chapter 4: Enolase is covalently inhibited by phosphoenolpyruvate

Authors: Aaron M. Hosios[1,2], Brian P. Fiske[1,2], Matthew G. Vander Heiden[1,2,3]

Affiliations:
[1] Koch Institute for Integrative Cancer Research, Massachusetts Institute of Technology, Cambridge, MA 02139, USA.
[2] Department of Biology, Massachusetts Institute of Technology, Cambridge, MA 02139, USA.
[3] Department of Medical Oncology, Dana-Farber Cancer Institute, Boston, MA 02115, USA

Abstract

Although most phosphorylation reactions involve transfer of phosphate from ATP, the ability of other metabolites to serve as phosphoryl-group donors has been described. Phosphoenolpyruvate (PEP), a high-energy glycolytic intermediate, has been speculated to serve as a substrate for protein kinases, and we sought to identify novel proteins modified by PEP. Past work suggests that such modifications are rare, suggesting that PEP likely does not modify proteins through a non-enzymatic mechanism. We identified a 47 kDa protein in mammalian cytosolic extracts that was labeled by a [^{32}P]-PEP tracer but not by [γ-^{32}P]-ATP. The modified protein was identified as mammalian enolase 1 (ENO1) following biochemical purification. Surprisingly, we observed covalent linkage of the entire PEP molecule to an active site lysine, which results in the inactivation of enzyme catalytic activity. Future work will clarify the extent to which enolase is modified in cells, how nutrient conditions affect this modification, and whether this serves as a mechanism to regulate enzyme activity.

Introduction

Phosphoenolpyruvate (PEP) sits at a critical node in glycolytic metabolism. It is the substrate for pyruvate kinase, an enzyme whose activity helps to define the metabolic program and proliferative capacity of mammalian cells. PEP is a high-energy compound, and the conversion of PEP to pyruvate is consequently energetically favourable (Mazurek et al., 2002). Pyruvate kinase harnesses this energy to transfer the phosphate from PEP to ADP to generate ATP, and there has been speculation that PEP might transfer this phosphate group to other molecules. There are numerous molecules other than ATP can serve as phosphoryl-group donors for phosphorylation reactions in eukaryotic cells. Cytosine triphosphate (CTP) and guanosine triphosphate (GTP) are respectively substrates for *S. cerevisiae* Dgk1 and mammalian PI5P4Kβ, kinases that phosphorylate lipid head groups (Han et al., 2008; Sumita et al., 2016). GTP also provides phosphate used to synthesize PEP during mammalian gluconeogenesis. Some proteins

140

may be phosphorylated using 1,3-bisphosphoglycerate (1,3-BPG) (Morino et al., 1991). Like PEP, this glycolytic intermediate contains a high-energy phosphate group that is canonically transferred to ADP to produce ATP but could potentially be transferred to another molecule. Reactive lysine residues in many proteins were recently demonstrated to undergo a non-enzymatic reaction with 1,3-BPG, resulting in displacement of the 1-phosphate and covalent linkage of a 3-phosphoglyceryl group to the proteins (Moellering and Cravatt, 2013). Inositol pyrophosphates are proposed to non-enzymatically phosphorylate serine residues in diverse eukaryotic proteins (Saiardi et al., 2004). Several other metabolites react non-enzymatically to modify proteins, raising the possibility that PEP, a high energy intermediate, could act similarly (Sullivan et al., 2016).

Pyruvate kinase isoform M2 (PKM2) was proposed to phosphorylate proteins using PEP as a phosphoryl-group donor, but we have been unable to recapitulate this activity (see Chapter 3) (Hosios et al., 2015). PEP phosphate may also label proteins independent of PKM2. A PEP-dependent protein kinase has been postulated to exist in mammalian muscle, for example (Khandelwal et al., 1983). Although the source of this activity was never identified, prior work did resolve the kinase and its substrate by chromatography, indicating that a PEP-dependent kinase and substrate pair may exist in mammals. The PEP phosphate group can also be traced to an active site histidine in phosphoglycerate mutase 1 (PGAM1) (Vander Heiden et al., 2010), although the mechanism by which this occurs remains unknown. Protein kinases that use PEP would be expected to produce pyruvate, allowing glycolysis to bypass pyruvate kinase. The best-described contexts in which this occurs are bacterial phosphotransferase systems (Deutscher et al., 2006). These systems comprise multiple proteins that ultimately transfer phosphate from PEP to a sugar, producing pyruvate and a phospho-sugar. The first enzyme in this cascade autophosphorylates using PEP and subsequently transfers this phosphoryl-group to another protein.

Previously, we identified a protein that was consistently labeled by [^{32}P]-PEP in cell lysates (see Chapter 3) (Hosios et al., 2015). In a stringent assay for PEP-dependent phosphorylation, where contaminating sources of ATP were eliminated, this protein was still labeled in a manner that was inconsistent with non-specific modification by PEP. To understand the functional significance of this

phosphorylation, we undertook a classical biochemical purification to identify the cytosolic protein

labeled by PEP.

Results

[^{32}P]-Phosphoenolpyruvate covalently labels a 47 kDa protein

Phosphoenolpyruvate (PEP) might serve as the phosphoryl-group donor in protein

phosphorylation reactions. In our previous study investigating whether PKM2 was able to catalyze these

reactions, we observed a 47 kDa protein that was consistently labeled with [^{32}P]-PEP *in vitro*. This

activity was localized to the cytosolic fraction of cell extracts (**Chapter 3, Figures 1 and 5B,C**). Labeling

of this protein did not depend on PKM2 and occurred in lysates prepared from mouse embryonic

fibroblasts (MEFs) where PKM2 was genetically deleted. Importantly, labeling of this protein by [^{32}P]-

PEP was undetectable when 1 mM non-radioactive competitor PEP was included in the reaction but was

not altered when 1 mM ATP was included. This indicates the protein is subject to a PEP-dependent

modification independent of ATP. PEP-dependent labeling of this 47 kDa protein was detected in

hypotonic lysates derived from a variety of human cell lines and from primary MEFs, but it was not

detected in human mammary epithelial cell (HMEC) lysates (**Figure 1A**).

Phosphoglycerate mutase 1 (PGAM1) is the species predominantly labeled by [^{32}P]-PEP in cell

extracts (Hosios et al., 2015; Vander Heiden et al., 2010), but this phosphorylation has been previously

shown to be inhibited by vanadate, a commonly used phosphatase inhibitor. Vanadate had no effect on

phosphorylation of the 47 kDa protein; however, when vanadate was not included, we observed strong

PEP-dependent labeling of PGAM1 in a tissue homogenate (**Figure 1B**, ~28 kDa protein). This lysate

was subject to successive rounds of precipitation with increasing ammonium sulphate concentrations.

PGAM1 labeling was detectable in each fraction; however, the 47 kDa protein was detected only in two

fractions. Interestingly, PGAM1 labeling was reduced in fractions where the 47 kDa protein was detected
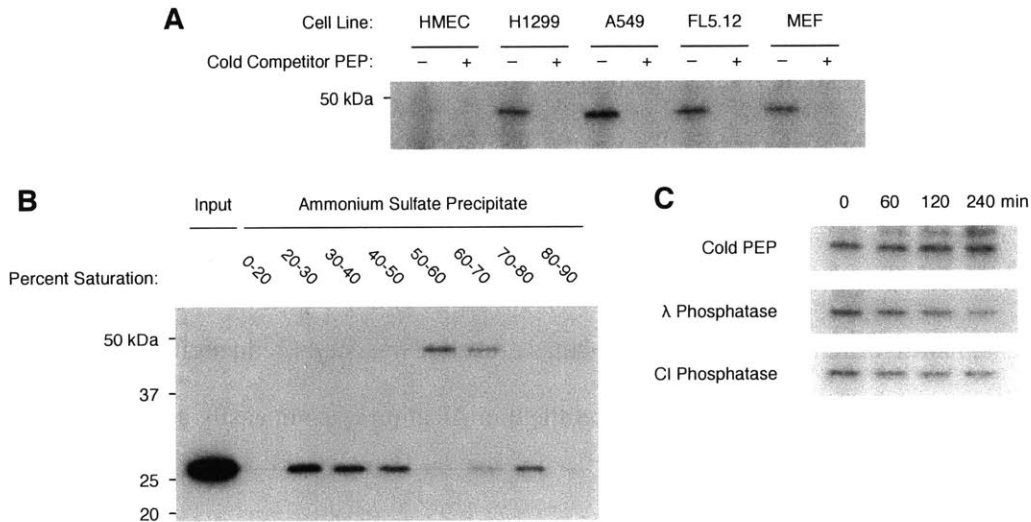
Figure 1: A 47 kDa protein is covalently modified by phosphoenolpyruvate.

Protein samples were labeled with [^{32}P]-PEP in the presence of 1 mM non-radioactive (cold) ATP to prevent visualization of ATP-dependent phosphorylation. Proteins were analyzed by SDS-PAGE and autoradiography. (A) Activity assay in cell line hypotonic lysates, with or without added 1 mM cold competitor PEP. (B) Assay of activity in calf thymus homogenate (input) or fractions following ammonium sulphate precipitation. The ranges specify the ammonium sulphate concentration as a percent of saturation. (C) Cell lysates pre-labeled with [^{32}P]-PEP were incubated with 1 mM cold PEP, λ protein phosphatase, or calf intestinal (CI) phosphatase for the indicated times.

relative to fractions precipitated with more or less ammonium sulphate. This might suggest that PGAM1 and the 47 kDa protein might compete for the available [^{32}P]-PEP, although we did not observe substantial depletion of PEP by thin layer chromatography (data not shown).

PEP was expected to covalently modify the 47 kDa protein, as the label was preserved when the phosphorylated protein was subject to denaturing conditions. To further characterize the modification, we labeled the protein in hypotonic lysates and monitored how the modification changed when excess non-radioactive PEP or phosphatases were added to the reaction after phosphorylation occurred (**Figure 1C**). No loss of label was observed when cold PEP was added, suggesting that the covalent modification is effectively irreversible as loss of the ^{32}P-label could not be driven by cold PEP. Treatment with either calf intestinal phosphatase or lambda protein phosphatase resulted in a slight reduction in the intensity of labeling of the 47 kDa protein. This implied that the modification was not easily accessed by either phosphatase enzyme.

Identification of enolase as the protein modified by PEP

To identify the 47 kDa protein, we undertook a conventional biochemical purification of the activity from calf thymus homogenates. The peak ammonium sulphate fractions (**Figure 1B**) were subject to successive rounds of fractionation by ion exchange chromatography (**Figure 2A-E**). This did not result in a loss of activity, which suggested that only one protein was required for this activity (rather than a kinase and substrate pair). Although labeling of this protein was dependent on PEP, it was possible that PEP was not directly used to label the protein. The activity was not competed by ATP (**Figure 1A**), but PEP can be converted to other high-energy glycolytic intermediates that can potentially serve as phosphate donors. We therefore investigated whether the 47 kDa protein could be chromatographically resolved from the activities of PGAM1 and enolase, two glycolytic enzymes upstream of PEP (**Figure 2C**). After two rounds of fractionation, minimal PGAM1 activity was retained (**Figure 2F**), but enolase activity co-purified with the 47 kDa protein (**Figure 2B,E**). Following size exclusion chromatography,
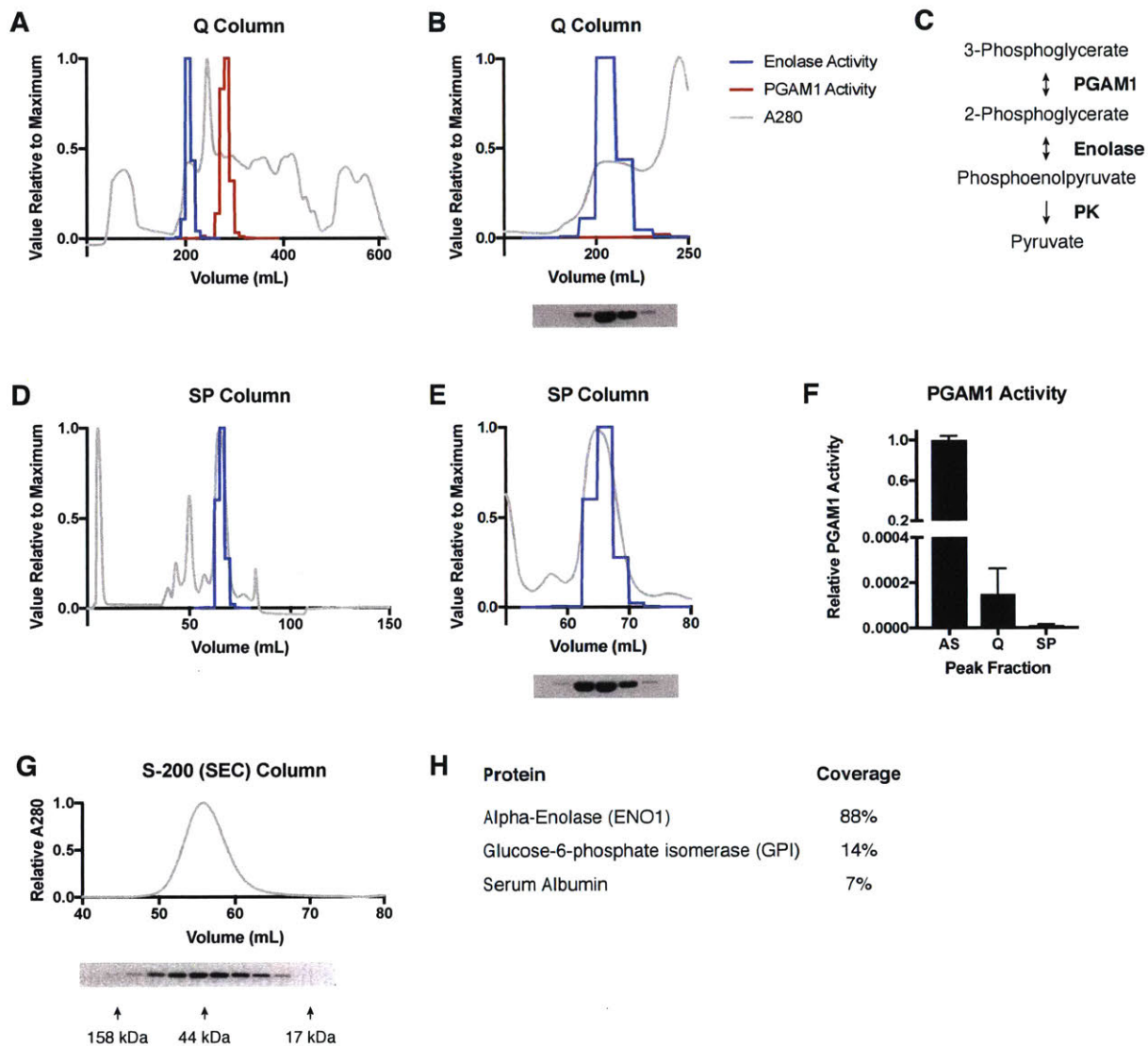
Figure 2: Purification of the activity that responsible for protein labeling by PEP.

Calf thymus lysate was fractionated by ion exchange chromatography. (A) Q column chromatogram displaying absorbance at 280 nm (A280) and enolase and PGAM1 activities in selected fractions. (B) Expanded Q column chromatogram. An assay of $[^{32}P]$-PEP-dependent labeling in the presence of 1 mM cold ATP is shown in the lower panel. (C) Enzymes and intermediates of lower glycolysis. (D) SP column chromatogram displaying A280 and enolase activity in selected fractions. (E) Expanded SP column chromatogram with $[^{32}P]$-PEP-dependent labeling assayed in the lower panel. (F) Relative PGAM1 activity in the peak fractions following fractionation by ammonium sulphate precipitation (AS), Q column (Q), and SP column (SP). (G) S-200 size exclusion (SEC) chromatogram displaying A280 and $[^{32}P]$-PEP-dependent labeling assayed in the lower panel. Elution times of protein standards are indicated. (G) Bovine proteins identified by mass spectrometry in the peak S-200 fraction.

the protein was digested and analyzed by proteomics mass spectrometry (**Figure 2G,H**). Of the bovine proteins identified, only α-enolase matched the molecular weight predicted by SDS-PAGE, indicating that it was likely the protein covalently modified by PEP.

Enolase is inhibited by PEP-ylation

Enolase is the glycolytic enzyme that produces PEP; however, this does not occur via a covalent mechanism (**Figure 3A**) (Lebioda and Stec, 1991). We therefore sought to confirm that PEP did, in fact, covalently modify enolase. Mammals express three isoforms of enolase, encoded by three distinct genes: *ENO1*, *ENO2*, and *ENO3*, which respectively encode α-, γ-, and β-enolase. Each isoform was expressed in 293-F cells and FLAG-immunopurified, and both hypotonic lysates and purified enolase isoforms were incubated with [^{32}P]-PEP (**Figure 3B**). Each enolase isoform was labeled by ^{32}P in this reaction. These proteins had a higher molecular weight than the endogenous enolase because they are linked to a FLAG-peptide. The PEP-dependent protein labeling activity was retained in the immunopurified material, confirming that enolase is the modified protein we had identified in our previous study (Chapter 3).

Although we were unable to observe turnover of the label in a crude lysate, we made an additional attempt to determine whether this modification was irreversible using the fractions with maximal activity following ion exchange chromatography (**Figure 2E**). This fraction was labeled with [^{32}P]-PEP as before, followed by addition of thymus lysate, HMEC lysate, or phosphatase (**Figure 3C**). In no instance was the modification lost, confirming our previous result. HMEC lysate was unable to remove the modification, indicating that our failure to detect this modification in HMEC lysates likely did not result from an additional activity that reversed the modification.

Modification by PEP is not confined to mammalian enolases: enolase from *Saccharomyces cerevisiae* yeast could also be labeled with [^{32}P]-PEP (**Figure 4A**). We labeled this protein with PEP and analyzed its tryptic peptides by mass spectrometry to identify the modified residue. Surprisingly, we did not observe transfer of phosphate from PEP to enolase. Rather, the entire PEP molecule had reacted with K346 (corresponding to K343 in human ENO1) (**Figure 4B**). Modification by PEP-ylation corresponds to

an increase in the mass of lysine by approximately 168 Da (**Figure 4C**). As noted above, enolase does not produce PEP by a covalent mechanism, and the detection of this modification was unexpected. K346 is located in the enzyme active site and is required to deprotonate 2-phospholgycerate during catalysis; mutating this residue greatly reduces the enzyme's k_{cat} (Reed et al., 1996). We therefore hypothesized that PEP-ylated enolase might have reduced catalytic activity. Enolase was incubated overnight with PEP to modify the protein, and unreacted PEP was removed by desalting. In a linked enzyme assay, we found that compared to enolase incubated in buffer, enolase pre-treated with PEP exhibited significantly reduced catalytic activity (**Figure 4D**). Enolase similarly pre-treated with pyruvate was not affected.

Based on these findings, we conclude that PEP can react with an active site lysine to inhibit enolase, the enzyme that produces it. This modification involves a covalent adduct that contains the entire PEP molecule, and may proceed via a Michael addition (**Figure 4C**) to PEP-ylate the active site.

Discussion

In our attempt to isolate proteins subject to PEP-dependent phosphorylation, we identified enolase as a target of PEP-ylation, a reaction that covalently links the entire PEP molecule to lysine. PEP-ylation appears to be irreversible, as we have been unable to identify an activity in cell extracts that reverses the modification. Because PEP modifies an active site lysine, it could inhibit enolase activity in two ways: its presence likely occludes the active site and prevents additional substrates from binding, and it reacts with a catalytic lysine residue, rendering this amino acid incapable of general acid-base catalysis required for enolase activity (Lebioda and Stec, 1991; Reed et al., 1996). We next aim to quantify the extent to which endogenous enolase is modified in whole cells and whether this reduces total cellular enolase activity. Although we have been unable to demonstrate turnover of PEP-ylated enolase in cell extracts, the cytosolic PEP concentration and the rates of enolase synthesis and degradation are at least
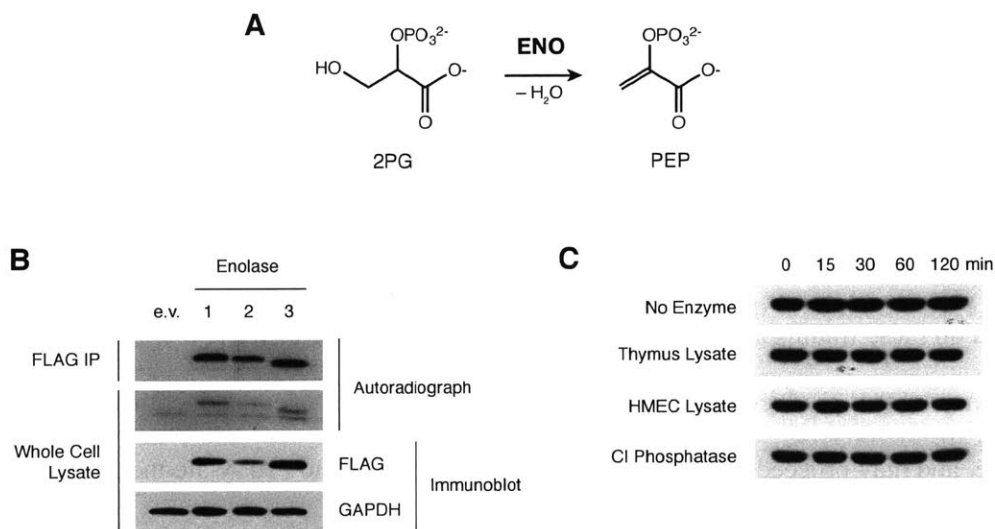
Figure 3: Enolase is the protein covalently modified by PEP.

(A) Enolase carries out the dehydration of 2-phosphoglycerate (2PG) to produce phosphoenolpyruvate (PEP). (B) [^{32}P]-PEP-dependent labeling was assayed in lysates or immunoprecipitates (FLAG-IP) of FreeStyle 293-F cells overexpressing human enolase 1, 2, or 3 or an empty vector (e.v.). Whole cell lysates were analyzed by immunoblot. (C) Purified calf thymus enolase was labeled with [^{32}P]-PEP and then incubated with no added enzyme or the addition of thymus lysate, human mammary epithelial cell (HMEC) lysate, or calf intestinal (CI) phosphatase for the indicated times.
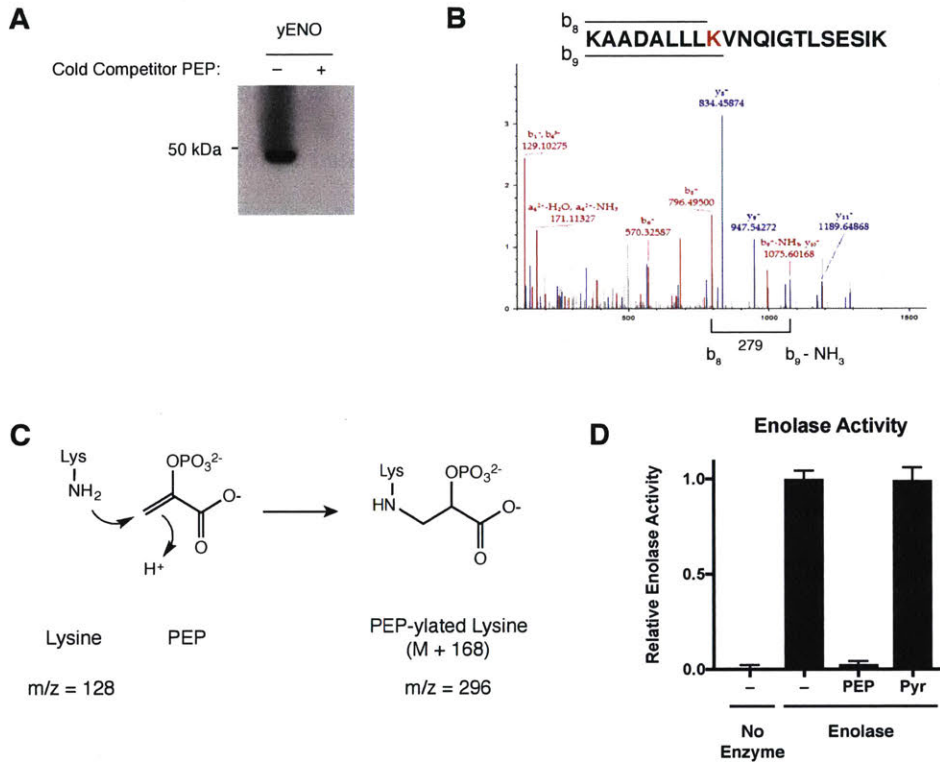
Figure 4: Enolase is irreversible inhibited by PEP-ylation of an active site lysine.

(A) Autoradiograph yeast enolase (yENO) labeled with [^{32}P]-PEP with or without 1 mM cold competitor PEP. (B) Fragmentation mass spectrum spectrum of a tryptic peptide from yeast enolase. The sequences of peptide and two fragments (b_8 and b_9) are shown. (C) Potential mechanism for the formation of covalent PEP-ylated lysine residue from PEP and enolase lysine-345. (D) Activity of yeast enolase following overnight incubation in the presence of PEP or pyruvate.

two factors that will determine the extent to which enolase is modified in cells and whether this affects glycolysis.

Our findings imply that PEP can selectively function as a reactive metabolite. Reactive metabolites can non-enzymatically modify proteins and exert either regulatory or deleterious effects on their targets (Sullivan et al., 2016). The paucity of PEP-ylated proteins (see Chapter 3) suggests that PEP is not a broadly reactive metabolite, but rather must be concentrated within the right environment, such as the active site of enolase. Despite being weakly reactive, PEP can be bound by enolase and will often be in proximity to the active site lysine; this would increase the number of opportunities for the PEP-ylation reaction to occur. Alternatively, the chemical environment of the enolase active site may enhance the reactivity of PEP, allowing it to participate in a reaction that would otherwise not occur. Whether this property was selected for to regulate enolase activity or is merely a side reaction tolerated by nature remains to be determined; however, our data argue that the property is conserved from yeast to mammals.

The data presented in this study clarify an earlier proposal by Moellering and Cravatt (2013) that mammalian ENO1 is non-enzymatically modified by 1,3-BPG. They initially observed that a lysine residue on glyceraldehyde-3-phosphate dehydrogenase (GAPDH) could react *in vitro* with this metabolite to form 3-phosphoglyceryl- (3PG) lysine. Using a proteomics approach, they sought additional lysine residues bearing this modification in cells and identified human ENO1-K343. 3PG-lysine and PEP-lysine have different structures, but they have identical mass values (M+168) and therefore cannot be readily distinguished by proteomic mass spectrometry. In our system, PEP-lysine was formed using enolase purified from upstream glycolytic enzymes, which precludes the formation of 1,3-BPG and allows us to rule out the possibility that we produced 3PG-lysine. Because K343 is located within the enolase active site, we propose that 1,3-BPG would not easily access this residue, implying that Moellering and Cravatt may have observed PEP-ylated enolase in their study. They detected more modified ENO1-K343 and reduced ENO1 catalytic activity in cells cultured in 25 mM glucose as opposed to 10 mM glucose, implying that growth conditions could influence enolase activity through this modification.

Although these glucose concentrations are both supraphysiological, glycolytic rate does differ between them, and it is possible that this influences the degree of ENO1-K343 PEP-ylation. In future work, we aim to characterize the fraction of enolase that is PEP-ylated in mammalian cells cultured in different conditions and to understand the extent to which enolase activity is reduced in these conditions. Intracellular PEP concentrations are expected to vary in other instances where glycolytic rate changes, particularly when PKM2 activity is reduced (Cortes-Cros et al., 2013; Vander Heiden et al., 2010) or when cells are acutely starved of glucose (Brauer et al., 2006; Xu et al., 2012). If PEP-ylation increases in these conditions, enolase activity would be lowered, perhaps augmenting glycolytic inhibition. In some contexts, this might favour proliferative metabolism that depends upon reduced pyruvate kinase activity (see Chapter 1). To support this hypothesis, additional experiments will clarify both the extent of PEP-ylation and the kinetics of formation in different contexts.

Future work should also seek to clarify how enolase PEP-ylation and PGAM1 phosphorylation are related. During ammonium sulphate precipitation, we observed the fractions containing enolase exhibit a reduction in the PEP-dependent phosphorylation of PGAM1 (**Figure 1B**). In this condition, we did not observe a significant depletion of $[^{32}P]$-PEP in the reaction mixture, indicating that these modifications are not simply competing for a limited amount of PEP. Alternatively, another protein present in the tissue homogenate but not in the assayed fractions could influence the relative labeling of these proteins.

PEP has been implicated as an inhibitor of other proteins as well. Recent work has suggested that PEP can inhibit the calcium transporter SERCA, coupling glycolysis to intracellular calcium signaling in T cells (Ho et al., 2015). Active glycolysis is expected to raise PEP levels, especially when PKM2 is less active, to exert this effect. PEP can also inhibit triose-phosphate isomerase, an upstream glycolytic enzyme, and this could provide an additional way for PEP to inhibit glycolysis (Gruning et al., 2014). Our findings add enolase to this list of enzymes inhibited by PEP. This modification may not be subject to regulation but nevertheless has the potential to reduce intracellular enolase activity to exert an effect on cellular metabolism.

Materials and Methods

Cell culture and preparation of cell extracts: Cell lines were cultured in DMEM supplemented with 10% heat-inactivated fetal bovine serum, penicillin (100 U/mL), and streptomycin (100 µg/mL) using standard tissue culture techniques. FL5.12 cell cultures were further supplemented with 0.35 ng/mL IL-3 (Chemicon International). Human mammary epithelial cells (HMECs) were cultured in MCDB 170 medium containing 5 µg/mL insulin, 0.5% (v/v) bovine pituitary extract, 5 µg/mL transferrin, 0.5 µg/mL hydrocortisone, 10 µM isoproterenol, and 5 ng/mL epidermal growth factor. FreeStyle 293-F cells were cultured in FreeStyle 293 Expression Medium (Life Technologies) in suspension, rotating at 125 rpm. Cytosolic extracts were prepared by resuspending cells in 3 volumes of hypotonic lysis buffer (10 mM HEPES-KOH pH 7.6, 10 mM KCl, 1.5 mM MgCl2, 1 mM EDTA, 1 mM EGTA, .5 mM DTT, 1x cOmplete mini protease inhibitor (Roche)) and incubating for 10 min on ice. Cells were mechanically lysed by passing them through a 22.5-gauge needle fifteen times. Lysates were clarified for 10 min at 20 000 × g, and protein concentration was determined by Bradford assay using a bovine serum albumin standard.

Enzymatic synthesis of [^{32}P]-PEP: [^{32}P]-phosphoenolpyruvate was synthesized and purified as described previously from pyruvate and [γ-^{32}P]-ATP using rabbit muscle pyruvate kinase (Sigma-Aldrich) (Hosios et al., 2015; Mattoo and Waygood, 1983; Vander Heiden et al., 2010). Synthesized PEP was resolved from residual ATP on a Vivapure Q Mini H column (Satorius) with sequential elution in 0.3 and 0.6 M triethylammonium bicarbonate pH 8.5 (Sigma).

Protein labeling with [^{32}P]-PEP: All reactions were carried out in a buffer containing 50 mM Tris-HCl pH 7.5, 100 mM KCl, 5 mM MgCl$_2$, 1 mM DTT, and 1x PhosSTOP phosphatase inhibitors (Roche). Unless otherwise stated, 1 mM ATP was included in the reaction as well. [^{32}P]-PEP synthesized as described above was included at a concentration of ~4.5 nM (~13 µCi/mL). Reactions were allowed to

proceed at 30 °C for 1 hour and were quenched by addition of Lamelli Sample Buffer, and phosphorylated proteins were resolved by SDS-PAGE and visualized by autoradiography.

Purification of enolase from tissue lysates: Calf thymus was homogenized in buffer A (20 mM HEPES-KOH pH 7.0, 5 mM KCl, 1 mM $MgCl_2$, 5 mM DTT, 1 mM benzamidine, and 1 mM PMSF). The lysate was centrifuged two times for 1 hour each at 4 °C for 13000 × g, and the supernatant was filtered through Whatman grade 4 filter paper to remove particulate matter. The lysate was clarified at 25000 × g for 20 hours at 4 °C. Ammonium sulphate was added to 55% saturation, and the lysate was stirred one ice for 1 hour and then centrifuged at 16 000 × g for 1 hour at 0 °C. Ammonium sulphate was added the supernatant to increase its concentration to 65% saturation, and this precipitation was repeated. The precipitated material was resuspended in buffer A and desalted into buffer B (20 mM Bis-Tris propane-HCl pH 8.7, 5 mM KCl, 1 mM $MgCl_2$) on a column packed with Sephadex G-25 Fine (GE Healthcare Life Sciences). Protein was then loaded on to a Q Sepharose HP column (GE Healthcare) pre-equilibrated with buffer B and eluted in a linear gradient from buffer B to buffer B with 1 M KCl. The fractions with maximal activity were pooled and desalted into buffer C (20 mM MES-KOH pH 5.5, 5 mM KCl, 1 mM $MgCl_2$). The sample was then loaded on to a HiTrap SP HP column (GE Healthcare) pre-equilibrated with buffer C and eluted in a linear gradient from buffer C to buffer C with 1 M KCl. Fractions with maximal activity were pooled, concentrated, and fractionated on a HiPrep 16/60 Sephacryl S-200 column (GE Healthcare) pre-equilibrated with either buffer C (for subsequent activity assays) or 150 mM ammonium acetate (for subsequent analysis by mass spectrometry).

Immunoprecipitation of FLAG-tagged enolase: FreeStyle 293-F cells were transiently transfected with p3xFLAG-CMV14 (Sigma-Aldrich), either empty vector or containing the coding sequence of enolase 1 (Eno1), Eno2, or Eno3 with a C-terminal FLAG-tag. Four days later, cells were lysed as described above, and lysates were incubated with Anti-FLAG M2 Affinity Gel (Sigma-Aldrich) for 30 min at 4 °C. Beads were washed extensively with lysis buffer and eluted in lysis buffer containing 150 µg/mL 3x FLAG

Peptide (Sigma-Aldrich). Eluates were used directly in activity assays. To confirm construct expression, samples were analyzed by SDS-PAGE, and proteins were detected by immunoblot and ECL assay. Antibodies used: DYKDDDDK and GAPDH (Cell Signalling Technologies: 2368 and 2118, respectively).

Glycolytic enzyme activity assays: Enolase and phosphoglycerate mutase 1 (PGAM1) activities were quantified by a linked enzymatic assay. Each reaction was carried out at room temperature in a 100 μL volume, containing buffer D (50 mM Tris-HCl pH 7.5, 100 mM KCl, 5 mM $MgCl_2$, .5 mM DTT), 180 μM NADH, 600 μM ADP, 16 U lactic dehydrogenase (Sigma-Aldrich), and 2 U rabbit muscle pyruvate kinase (Sigma-Aldrich). The enolase activity assay also contained 500 μM 2-phosphoglycerate, and the PGAM1 activity assay contained 500 μM 3-phosphoglycerate, 10 μM 2,3-bisphosphoglycerate, and .08 U enolase from baker's yeast (Sigma-Aldrich). Reactions were monitored by the loss of NADH fluorescence (excitation: 340 nm, emission: 460 nm). To understand the effect of PEP-ylation on enzyme activity, enolase from baker's yeast (Sigma-Aldrich) was incubated overnight in the presence of buffer D, PEP, or pyruvate and desalted using a HiTrap Desalting Column pre-equilibrated with buffer D. Enolase activity was assayed as above.

Mass spectrometry: The S-200 fraction with peak activity was prepared for mass spectrometry in solution, and yeast enolase pre-incubated with or without cold PEP were resolved by SDS-PAGE and prepared from Coomassie-stained gel fragments. Samples in solution were reduced with 5 mM DTT (20 mM for gel fragments) and then alkylated with 25 mM iodoacetimide (60 mM for gel fragments), followed by overnight digestion with Sequencing Grade Modified Trypsin (Promega). For samples digested in solution, the resulting peptides were desalted using C-18 pipette tips and eluted into a solution of 80% acetonitrile and 0.1% acetic acid. For samples digested in gel fragments, peptides were eluted with each of 100 mM ammonium bicarbonate, 50% acetonitrile with 5% formic acid, and 100% acetonitrile, and eluates were pooled. Samples were dried under vacuum and resuspended in 0.1% formic

154

acid prior to analysis with a Q Exactive Mass Spectrometer (Thermo). Data were analyzed with Proteome

Discoverer (Thermo) using the Mascot database.

Author Contributions

A.M.H. and M.V.G.H conceived of and analyzed all experiments and wrote and edited this chapter.

B.P.F. provided input regarding protein purification and assay development.

References

Brauer, M.J., Yuan, J., Bennett, B.D., Lu, W., Kimball, E., Botstein, D., and Rabinowitz, J.D. (2006). Conservation of the metabolomic response to starvation across two divergent microbes. Proceedings of the National Academy of Sciences of the United States of America *103*, 19302-19307.

Cortes-Cros, M., Hemmerlin, C., Ferretti, S., Zhang, J., Gounarides, J.S., Yin, H., Muller, A., Haberkorn, A., Chene, P., Sellers, W.R., *et al.* (2013). M2 isoform of pyruvate kinase is dispensable for tumor maintenance and growth. Proceedings of the National Academy of Sciences of the United States of America *110*, 489-494.

Deutscher, J., Francke, C., and Postma, P.W. (2006). How phosphotransferase system-related protein phosphorylation regulates carbohydrate metabolism in bacteria. Microbiol Mol Biol Rev *70*, 939-1031.

Gruning, N.M., Du, D., Keller, M.A., Luisi, B.F., and Ralser, M. (2014). Inhibition of triosephosphate isomerase by phosphoenolpyruvate in the feedback-regulation of glycolysis. Open Biol *4*, 130232.

Han, G.S., O'Hara, L., Siniossoglou, S., and Carman, G.M. (2008). Characterization of the yeast DGK1-encoded CTP-dependent diacylglycerol kinase. J Biol Chem *283*, 20443-20453.

Ho, P.C., Bihuniak, J.D., Macintyre, A.N., Staron, M., Liu, X., Amezquita, R., Tsui, Y.C., Cui, G., Micevic, G., Perales, J.C., *et al.* (2015). Phosphoenolpyruvate Is a Metabolic Checkpoint of Anti-tumor T Cell Responses. Cell *162*, 1217-1228.

Hosios, A.M., Fiske, B.P., Gui, D.Y., and Vander Heiden, M.G. (2015). Lack of Evidence for PKM2 Protein Kinase Activity. Molecular cell *59*, 850-857.

Khandelwal, R.L., Mattoo, R.L., and Waygood, E.B. (1983). Phosphoenolpyruvate-dependent protein kinase activity in rat skeletal muscle. FEBS Lett *162*, 127-132.

Lebioda, L., and Stec, B. (1991). Mechanism of enolase: the crystal structure of enolase-Mg2(+)-2-phosphoglycerate/phosphoenolpyruvate complex at 2.2-A resolution. Biochemistry *30*, 2817-2822.

Mattoo, R.L., and Waygood, E.B. (1983). An enzymatic method for [32P]phosphoenolpyruvate synthesis. Anal Biochem *128*, 245-249.

Mazurek, S., Grimm, H., Boschek, C.B., Vaupel, P., and Eigenbrodt, E. (2002). Pyruvate kinase type M2: a crossroad in the tumor metabolome. Br J Nutr *87 Suppl 1*, S23-29.

Moellering, R.E., and Cravatt, B.F. (2013). Functional lysine modification by an intrinsically reactive primary glycolytic metabolite. Science *341*, 549-553.

Morino, H., Fischer-Bovenkerk, C., Kish, P.E., and Ueda, T. (1991). Phosphoglycerates and protein phosphorylation: identification of a protein substrate as glucose-1,6-bisphosphate synthetase. J Neurochem *56*, 1049-1057.

Reed, G.H., Poyner, R.R., Larsen, T.M., Wedekind, J.E., and Rayment, I. (1996). Structural and mechanistic studies of enolase. Curr Opin Struct Biol *6*, 736-743.

Saiardi, A., Bhandari, R., Resnick, A.C., Snowman, A.M., and Snyder, S.H. (2004). Phosphorylation of proteins by inositol pyrophosphates. Science *306*, 2101-2105.

Sullivan, L.B., Gui, D.Y., and Vander Heiden, M.G. (2016). Altered metabolite levels in cancer: implications for tumour biology and cancer therapy. Nature reviews Cancer *16*, 680-693.

Sumita, K., Lo, Y.H., Takeuchi, K., Senda, M., Kofuji, S., Ikeda, Y., Terakawa, J., Sasaki, M., Yoshino, H., Majd, N., *et al.* (2016). The Lipid Kinase PI5P4Kbeta Is an Intracellular GTP Sensor for Metabolism and Tumorigenesis. Molecular cell *61*, 187-198.

Vander Heiden, M.G., Locasale, J.W., Swanson, K.D., Sharfi, H., Heffron, G.J., Amador-Noguez, D., Christofk, H.R., Wagner, G., Rabinowitz, J.D., Asara, J.M., *et al.* (2010). Evidence for an alternative glycolytic pathway in rapidly proliferating cells. Science *329*, 1492-1499.

Xu, Y.F., Zhao, X., Glass, D.S., Absalan, F., Perlman, D.H., Broach, J.R., and Rabinowitz, J.D. (2012). Regulation of yeast pyruvate kinase by ultrasensitive allostery independent of phosphorylation. Molecular cell *48*, 52-62.

Chapter 5: Discussion and future directions

Summary

Proliferation requires the synthesis of new cell mass, and proliferating cells rely on specific metabolic pathways to generate this cell mass. Cell composition is relatively invariant, and in a general sense, proliferating cells share a common set of biosynthetic demands despite employing different pathways to meet them. Previous studies investigated specific metabolic pathways cells use to generate macromolecule precursors but lacked a general framework to account for the sources of cell mass. To ascertain what nutrients contribute to new cell mass, I used labeled nutrients to quantify the incorporation of glucose, amino acid, and lipid carbon into cell mass. Although glucose and glutamine are consumed in vast excess to any other nutrient, they do not make a similarly large contribution to cell mass. These findings imply that high glycolytic and glutaminolytic fluxes observed in many proliferating cells do not directly drive biosynthesis. Nonetheless, these processes are important to enable biosynthesis, and their high flux may provide other advantages to cells. Although a cell's biosynthetic requirements may be rigid, there is great plasticity in how these requirements are met, and it is of interest to understand how a cell decides which pathways it uses to acquire new mass.

I have also explored the biochemistry of two glycolytic enzymes, pyruvate kinase and enolase. Expression of pyruvate kinase M2 (PKM2), as opposed to its other isoforms, enables cellular proliferation both in normal and disease states. While some have argued that this is because PKM2 can act as a phosphoenolpyruvate (PEP)-dependent protein kinase to drive growth and cell division, I have been unable to biochemically support this hypothesis. PKM2 expression is a contributing factor to aerobic glycolysis and enables enhanced biosynthesis, and PKM2 most likely supports proliferation through these effects. Although PKM2 does not use PEP to modify proteins, I have identified enolase as a protein that can be specifically labeled by PEP. This modification inactivates a catalytic lysine residue, but further

work will be required to understand whether this modification is present in sufficient quantities to affect glucose metabolism and whether it contributes to glycolytic regulation in different contexts.

These studies collectively explore how different nutrients are able to contribute to mammalian cell mass. I have directly assessed which nutrients are consumed and utilized by proliferating cells, and I have also examined specific biochemical steps that are important to proliferative metabolism. The findings presented provide a basis for future investigations of both nutrient acquisition and utilization by cells as well as the biochemical role of pyruvate kinase in enabling rapid proliferation.

Discussion

Many major questions remain unresolved in our understanding of cellular metabolism, and several are discussed below. There is great interest in therapeutically targeting the metabolism of proliferating cells, and a holistic understanding of how the metabolic network supports proliferation is required to do so. Future research should explore these questions to gain insight into the metabolic pathways essential to proliferating cells.

How does the *in vivo* environment influence cellular metabolism?

To date, most mechanistic and tracer studies of cellular metabolism have been conducted *in vitro*, using well-established cell culture systems; however, it is becoming increasingly clear that the extracellular environment is an integral factor contributing to a cell's metabolic phenotype and that the tissue culture environment is often a poor recapitulation of the *in vivo* extracellular environment. Lessons learned about metabolism of cells in culture have been invaluable to our understanding of proliferative metabolism but can be insufficient to completely explain metabolism of cells in tissues. Consequently, there has been great interest in tracing the fate of nutrients *in vivo* as well as in developing *in vitro* systems that more faithfully mimic conditions in the body.

Extracellular metabolite levels, the concentration of plasma (or serum) components, and oxygen tension are all known to be different in the body, and culture systems typically lack the matrix proteins and heterogeneous cell types that comprise the extracellular milieu for many cells in the body. As a result, several metabolic phenotypes are known to differ *in vivo*, and recent work has begun to identify factors in tissue culture media that can explain some of these differences (Gui et al., 2016; Tardito et al., 2015). Some drugs that target metabolic enzymes, such as metformin, are more potent *in vivo*, yet others, such as glutaminase inhibitors, are less effective than they are *in vitro* (Davidson et al., 2016; Gui et al., 2016). Nutrient environment is one variable that contributes to these differences because the same cells have differential sensitivity to inhibition of specific pathways when cultured in media compared to when they form tumors in mice.

Despite the importance of characterizing metabolism *in vivo*, cell culture systems will remain instrumental to the study of cellular metabolism. The power to study *in vivo* metabolism has increased greatly in recent years, but although they can better recapitulate what happens in humans, studies in whole animals lack the control and experimental power that cell culture systems offer. The very factors that make *in vivo* systems more powerful also weaken their utility for metabolic studies. Current approaches analyse tissue metabolites together, preventing an analysis of the different metabolic programs that exist in heterogeneous cell types within one tissue. Additionally, interpreting the fate of many metabolic tracers is difficult in animals when delivered for lengthy periods of time because metabolites are interconverted by whole body metabolism.

The study described in Chapter 2 could be extended to proliferating cells growing in mice, using multi-isotope imaging mass spectrometry (MIMS) to circumvent some of these issues (Steinhauser et al., 2012). To quantify the contribution of different nutrients to cell mass, I allowed cell lines to proliferate *in vitro* in the presence of tracers until the entire mass of the culture had turned over, but this is not feasible *in vivo* for the reasons described above. MIMS measures the isotopic enrichment of carbon (i.e. proportion of carbon-12 and carbon-13) and nitrogen in individual cells in tissue sections, and this technique can quantify the extent to which a single cell is labeled by a given nutrient without

contamination from neighbouring non-proliferating cells. By studying mass turnover in rapidly proliferating stem cells, a reliable assessment of cell mass labeling from glucose, glutamine, or other metabolites could be obtained *in vivo*.

A major obstacle to understanding a cell's metabolic phenotype *in vivo* is that this is, in large part, a function of what nutrients the cell consumes in this context. In culture, nutrient consumption rates can be reliably calculated, but this is difficult to directly measure *in vivo*. Metabolic tracers are increasingly employed to study *in vivo* metabolism, but tracers studies can fail to accurately capture *net* flux of reactions, both *in vivo* and *in vitro*, limiting the extent to which utilization of some nutrients can be carefully studied *in vivo* (discussed at length in Appendix E). Where the utility of tracers is diminished, studies have successfully assessed nutrient consumption *in vivo* by sampling blood entering and exiting a proliferating tissue. This has been done for both tumor and fetal tissues, providing case studies in the careful assessment of consumption rates in the body. Both of these tissues are highly proliferative, and can have few blood vessels connecting them to the circulatory system. By sampling blood entering and exiting tumors or fetuses, researchers have successfully quantified consumption and excretion of glucose, lactate, and amino acids.

Seminal studies by Otto Warburg and Carl and Gerty Cori demonstrated the net production of lactate by rat and chicken tumors, providing *in vivo* evidence for rapid glycolytic flux in tumors (Cori and Cori, 1925; Warburg et al., 1927). Warburg also demonstrated that normal tissue, in contrast, consumes both glucose and lactate. A later study by Gullino *et al.* (1964) quantified additional nutrients in blood entering and exiting rat tumors. Glucose was reproducibly consumed and lactate excreted by these tumors; however, total amino acid levels were not greatly changed between blood entering and exiting the tumor. This corroborates my observations that amino acid consumption rates are negligible relative to glycolytic flux *in vitro*. Substantial work has examined nutrient consumption by ovine fetuses because afferent and efferent umbilical cord blood can be easily sampled in sheep. In contrast to many other proliferating tissues, ovine fetuses appreciably consume both lactate and amino acids (Lemons et al., 1976; Sparks et al., 1982). Interestingly, lactate and amino acids are consumed in excess of the

160

biosynthetic demands of the developing fetus, indicating that both are oxidized for energy. This stands in contrast to tumor tissues, which are typically less oxidative, and this discrepancy may be in part be explained by metabolic specialization and heterogeneity between fetal tissues. The fetus also produces a substantial amount of lactate from glucose, confirming that some of its tissues are more glycolytic while others are more oxidative. Although the techniques used to study tumor and fetal nutrient consumption may not be easily applied in a typical *in vivo* study of proliferative metabolism, they do highlight how an understanding of net flux can be informative *in vivo*.

Evaluating consumption and excretion by proliferating tissues is often not feasible, and an understanding of *in vivo* metabolism can also benefit from a careful analysis of the metabolic components of the extracellular environment. The concentration of many metabolites in plasma and in tissue/tumor interstitial fluid differ greatly from those in standard culture media, and some metabolites present *in vivo* are not included in media. Tissue culture media were formulated to optimize cell grown *in vitro* and not to recapitulate conditions *in vivo* (Eagle, 1955), and efforts to produce culture media that more accurately reflect *in vivo* conditions will allow the experimental power of cell culture systems to explain metabolism of cells proliferating in the body.

Beyond the nutrient environment, other factors dictate which nutrients and metabolic pathways a cell uses, and recent work has explored the roles of genetics and lineage on cellular metabolism *in vivo*. In the case of cancer cells, genetic mutations in oncogenes and tumor suppressors can produce particular metabolic phenotypes (Cairns et al., 2011; Iurlaro et al., 2014; Pavlova and Thompson, 2016). Many normal proliferating cells rely upon growth factor signalling to activate the same signalling pathways, and the downstream metabolic effects are expected to be similar in many cases. The role of cell lineage, independent of intracellular signalling, has also been the subject of research interest. Several studies have investigated the differences in metabolic phenotypes that exist between tumors induced by the same driver mutations in different tissues of origin, focussing on both glucose and amino acid metabolism (Mayers et al., 2016; Yuneva et al., 2012). Other studies have demonstrated that vascular endothelial cells

and cells derived from them depend upon fatty acid oxidation to proliferate, indicating a lineage-specific metabolic phenotype (Schoors et al., 2015; Wong et al., 2016).

An understanding of how extracellular environment and cell-intrinsic factors converge on cellular metabolism *in vivo* may help to explain why cells consume some nutrients but synthesize others. Many nutrients are non-essential to proliferating cells and can be obtained both by *de novo* synthesis and by consumption from the extracellular environment. For example, serine is abundant in plasma (see Appendix A), but many cancers overexpress enzymes of the serine synthesis pathway (DeNicola et al., 2015; Locasale et al., 2011). Fatty acids are similarly abundant, but their *de novo* synthesis is commonly increased in cancers as well (Svensson and Shaw, 2017). This raises the question of what factors determine the relative importance of each mechanism for generating these and other macromolecule precursors, and ultimately a variety of factors are likely at play. Due to their lineages and activities of signal transduction pathways, cells may engage in specific growth programs. Extracellular environment and the local availability of different nutrients are important factors as well, as the relative abundances of different nutrient sources can influence how much they are used. Amino acid transporters, for example, can transport many substrates with differing affinities, and how these affinities compare to the concentrations of amino acids observed *in vivo* is currently not well-understood (Hyde et al., 2003).

What is limiting for proliferating cells?

A full understanding of the metabolic nodes crucial for proliferation raises the question of which metabolic process limits growth. The doubling of cell mass that occurs over the cell cycle can be thought of as an intricate, large-scale chemical reaction. This reaction would subsume nutrient consumption, production of macromolecule precursors, and synthesis of macromolecules themselves. In this framework, there might be nutrients or activities of metabolic enzymes that are rate limiting for the acquisition of new cell mass. By definition, increasing the amount of a rate-limiting metabolite or enzymatic activity should enhance proliferation rate, but the converse could apply to a wider set of metabolic components. ATP is often proposed to be the rate-limiting substrate for proliferation, and this

has in part been used to explain the high glycolytic flux observed in many proliferating cells. However, others have argued against ATP production limiting proliferation, and alternative rate-limiting metabolites, such as NADPH, have been proposed (Lunt et al., 2015b; Racker, 1976; Ward and Thompson, 2012). Metabolic perturbations are often pleiotropic, complicating studies that seek to identify rate-limiting metabolic processes.

In recent years, several groups have provided evidence that the regeneration of NAD^+ might be rate-limiting to proliferating cells (Birsoy et al., 2015; Sullivan et al., 2015; Titov et al., 2016). NAD^+ is converted to NADH by reactions that oxidize metabolic substrates, and several biosynthetic reactions essential for proliferation use this cofactor. NAD^+ is regenerated by the activity of lactate dehydrogenase (LDH) and by mitochondrial electron transport. LDH activity consumes pyruvate and other α-keto-acids, and supplying either of these exogenously to some cells can slightly accelerate their growth in culture, consistent with NAD^+ regeneration limiting proliferation in this context (Sullivan et al., 2015). *In vivo*, oxygen tension is expected to be much lower than it is in culture, limiting mitochondrial electron transport and implying that NAD^+ regeneration could limit proliferation in the body as well (Bertout et al., 2008). Several studies have proposed that NAD^+ regeneration is most immediately limiting for aspartate biosynthesis, and it is possible that production of this amino acid, which is necessarily acquired by *de novo* synthesis, limits proliferation *in vivo* (Birsoy et al., 2015; Sullivan et al., 2015).

Importantly, other metabolic processes and substrates may limit proliferation under different conditions. Theories of metabolic control analysis suggest that, in a metabolic pathways, no single enzyme limits pathway flux (Fell, 2005; Lane and Fan, 2015). Rather, several enzymes catalyze reactions that are partially rate limiting and enhancing the activity of each is sufficient to raise pathway flux. In this light, multiple reactions or substrates within the metabolic network might be limiting for macromolecule synthesis and proliferation. Inhibition of any essential metabolic pathway could make it limiting, but proliferation will be most sensitive to inhibition of pathways that are rate limiting in basal conditions. Accordingly, identifying these rate-limiting steps could inform development of inhibitors to effectively block proliferation.

Why do cells have high glycolytic flux?

This question is central to many studies of proliferative metabolism and has been an outstanding question since Warburg first observed aerobic glycolysis in tumor slices. Many explanations have been proposed to account for the abundant conversion of glucose to lactate by proliferating cells, but the multiple, complex effects of glycolytic inhibition have made a definitive answer hard to prove. One commonly invoked theory holds that rapid glycolytic flux promotes anabolic metabolism (Hsu and Sabatini, 2008; Hume and Weidemann, 1979; Pavlova and Thompson, 2016; Vander Heiden et al., 2009). Recent work demonstrating that expression of PKM1 is sufficient to reduce lactate production and anabolism *in vitro* support this association (Christofk et al., 2008a; Christofk et al., 2008b; Lunt et al., 2015a). Opinions differ, however, on how these two processes are connected. Some have proposed that rapid glycolytic flux ensures higher concentrations of glycolytic intermediates that can be used biosynthetically (Hume and Weidemann, 1979), but glycolytic intermediates are not consistently elevated in proliferating cells (Lunt et al., 2015a; Williamson et al., 1970). I have also observed that the vast majority of glucose carbon is not incorporated, arguing against glycolysis allowing mass action to drive biosynthesis (see Chapter 2). Newsholme and Crabtree proposed that high glycolytic flux ensures precise regulation of low flux biosynthetic pathways branching from glycolysis (Newsholme et al., 1985). However, only synthesis of nucleotides (partially), several amino acids, and glycerol-3-phosphate derive from glycolysis and it is unclear whether their synthesis limits proliferation. Finally, glycolysis has been proposed to be a primary source of ATP for proliferating cells, but there is no evidence that cells are limited for ATP production. In fact, neither glycolysis nor oxidative phosphorylation proceeds at its maximal possible rate, at least where measured in culture.

To better understand the link between glycolytic flux and proliferation, I have cultured cells in varying concentrations of glucose and calculated glucose uptake rate and proliferation rate in each condition (**Figure 1**). Surprisingly, at glucose concentrations above 1 mM, proliferation rate is insensitive to glucose concentration but glycolytic rate still increases. These results decouple glycolytic rate from proliferation rate, arguing against a strict link between the two. Both rates show a linear relationship when
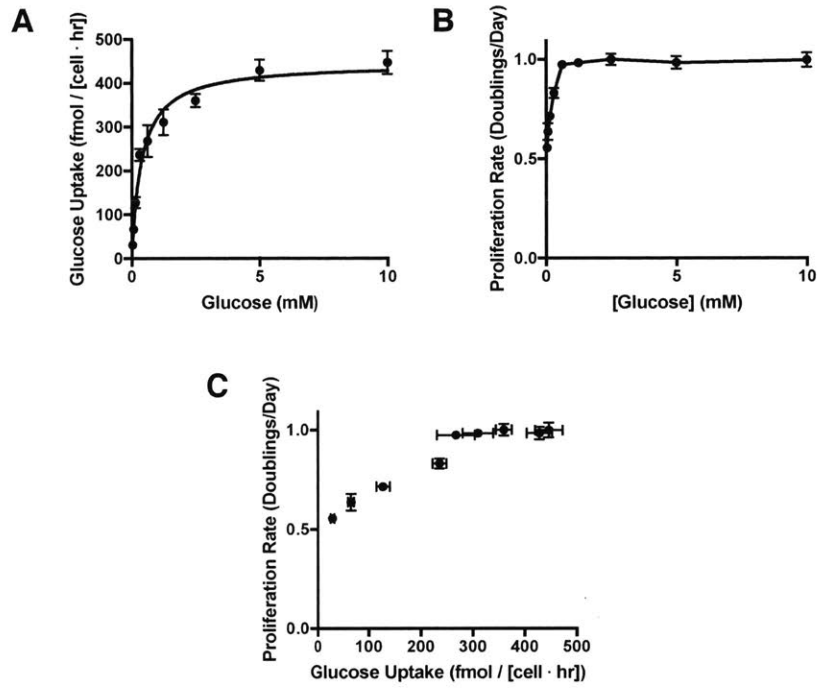
Figure 1: Glucose consumption rate and proliferation rate can be decoupled in mammalian cells.

(A) Glucose consumption and (B) proliferation rates of A549 cells cultured in medium containing varied concentrations of glucose. (C) Glucose consumption rates and their respective proliferation rates for each concentration of glucose assayed. Each point represents the average of N=3 replicates, ±S.D.

glucose is low, and glucose uptake rate is half maximal around 390 μM (**Figure 1A**), a concentration

below what is typical for human plasma. In this regime, glycolytic flux could directly limit biosynthesis

or energy production. Oncogenic and normal signals that stimulate proliferation also induce glucose

uptake, and upregulation of glucose transporters and glycolytic enzymes may allow cells to proliferate in

a manner insensitive to fluctuating glucose concentrations in the body. It follows then that rapid

glycolytic flux is a consequence of this proliferative signalling, and allows cells to efficiently and robustly

proliferate *in vivo*. Concomitant expression of PKM2 and LDH both enhance lactate production and

provide cells with a means to dispose of unneeded glycolytic material and to regenerate NAD^+. In support

of this hypothesis, transgenic expression of proteins that enhance NAD^+ regeneration can alter the

glycolytic outputs of both yeast and mammalian cells (Titov et al., 2016; Vemuri et al., 2007).

A definitive explanation for rapid glycolytic flux in proliferating cells will likely be hard to

demonstrate. Any perturbation to probe the pathway can alter many fluxes, macromolecule biosynthesis,

proliferation, and signalling pathway activity, and most results from such experiments are at best

correlative. Nevertheless, current research interest in cellular metabolism holds the potential to further

explore and understand glycolytic activity in proliferating cells, and each paradigm provides a different

framework through which metabolic pathways beyond glycolysis can be explored and understood.

Is pyruvate kinase an essential enzyme?

Work in recent years has enhanced our understanding of how pyruvate kinase isoform expression

contributes to aerobic glycolysis and proliferation of both normal and transformed mammalian cells

(reviewed in Israelsen and Vander Heiden, 2015). A common finding of these studies is that proliferation

relies upon low cellular pyruvate kinase activity, and increasing pyruvate kinase activity with chemical

activators or by overexpressing constitutively active PKM1 can impair proliferation both *in vitro* and *in*

vivo. Deletion of the PKM2-specific exon does not completely eliminate *PKM* gene expression and

results in variable PKM1 expression. In some contexts, this expression is growth-inhibitory, but in several

in vivo studies, PKM1 expression is not high enough to suppress proliferation (Dayton et al., 2016;

166

Israelsen et al., 2013; Lunt et al., 2015a). In a genetically engineered model of breast cancer, genetic loss of PKM2 resulted in spatially heterogeneous PKM1 expression, and interestingly, some proliferative tumor regions lacked PKM1 expression detectable by immunohistochemistry (Israelsen et al., 2013). This led us to question whether cells could, in fact, proliferate without any pyruvate kinase expression.

Using CRISPR-Cas9 technology, we generated a clone with pyruvate kinase expression undetectable by immunoblot (see Appendix D). Trace pyruvate kinase enzyme activity was detected in this clone, indicating incomplete loss of pyruvate kinase; however, this clone had a glycolytic rate that was only slightly partially reduced relative to the parental cell line. This discrepancy between pyruvate kinase activity and glycolytic rate in these cells suggests that an alternative activity could sustain glycolytic flux independent of pyruvate kinase. Importantly, pyruvate kinase is essential for *S. cerevisiae* yeast to proliferate on glucose, but stains deficient for both isoforms can grow on ethanol, suggesting that they are unable to bypass pyruvate kinase in glycolysis (Boles et al., 1998; Boles et al., 1997). Future work will generate mammalian cell lines where both pyruvate kinase genes, *PKM* and *PKLR*, are ablated to carefully understand whether this enzyme is essential for cell-autonomous proliferation. One intriguing possibility is that glycolysis independent of pyruvate kinase does not generate ATP, ensuring rapid pathway flux even when ATP consumption is limiting.

Conclusion

An understanding of the contributors to mammalian cell mass is far from complete. Although significant progress has been made in characterizing nutrients and metabolic pathways that contribute to rapid proliferation, most work to date has examined cancer cell metabolism. This has been, in part, motivated by interest in cancer therapy as well as the ease of culturing and manipulating transformed cells. Many lessons from cancer cell metabolism can be applied to normal proliferating cells, but differences exist as well, and understanding these differences will be critical to the careful development of

new therapies. Furthermore, the metabolic differences that exist between cells grown in culture and cells grown in the body are becoming increasingly clear, and future work should seek to understand the factors that contribute to these differences.

Subsequent studies of cancer cell metabolism should focus both on whole-cell metabolism as well as the regulation and functions of specific metabolic pathways and enzymes. In the studies described in this dissertation, I have characterized both the nutrient sources that contribute to proliferating cell mass and the biochemical properties of glycolytic enzymes. I have quantified the contributions of glucose, amino acids, and lipids to cell mass, and future studies will clarify how and why cells balance *de novo* synthesis and consumption of exogenous macromolecule precursors to support maximal proliferation. Considering the fate and utilization of glycolytic material, I have shown that phosphoenolpyruvate is not a PKM2 protein-kinase substrate but can modify enolase to inhibit its function. How PKM2 expression supports anabolism and proliferation is an outstanding question, but findings in recent years hold the potential to begin to provide an answer.

Perspectives gained in recent years have offered new insight into how cells produce the macromolecule precursors they need to synthesize new cell mass, and my graduate work has contributed to a framework of how metabolism supports proliferation. Our understanding of proliferating metabolism has grown considerably since Warburg's original findings, and the coming years hold the promise of major insights into how metabolism sustains proliferation and how this can be taken advantage of clinically.

References

Bertout, J.A., Patel, S.A., and Simon, M.C. (2008). The impact of O2 availability on human cancer. Nature reviews Cancer *8*, 967-975.

Birsoy, K., Wang, T., Chen, W.W., Freinkman, E., Abu-Remaileh, M., and Sabatini, D.M. (2015). An Essential Role of the Mitochondrial Electron Transport Chain in Cell Proliferation Is to Enable Aspartate Synthesis. Cell *162*, 540-551.

Boles, E., de Jong-Gubbels, P., and Pronk, J.T. (1998). Identification and characterization of MAE1, the Saccharomyces cerevisiae structural gene encoding mitochondrial malic enzyme. J Bacteriol *180*, 2875-2882.

Boles, E., Schulte, F., Miosga, T., Freidel, K., Schluter, E., Zimmermann, F.K., Hollenberg, C.P., and Heinisch, J.J. (1997). Characterization of a glucose-repressed pyruvate kinase (Pyk2p) in Saccharomyces cerevisiae that is catalytically insensitive to fructose-1,6-bisphosphate. J Bacteriol *179*, 2987-2993.

Cairns, R.A., Harris, I.S., and Mak, T.W. (2011). Regulation of cancer cell metabolism. Nature reviews Cancer *11*, 85-95.

Christofk, H.R., Vander Heiden, M.G., Harris, M.H., Ramanathan, A., Gerszten, R.E., Wei, R., Fleming, M.D., Schreiber, S.L., and Cantley, L.C. (2008a). The M2 splice isoform of pyruvate kinase is important for cancer metabolism and tumour growth. Nature *452*, 230-233.

Christofk, H.R., Vander Heiden, M.G., Wu, N., Asara, J.M., and Cantley, L.C. (2008b). Pyruvate kinase M2 is a phosphotyrosine-binding protein. Nature *452*, 181-186.

Cori, C.F., and Cori, G.T. (1925). The carbohydrate metabolism of tumors: II. Changes in the sugar, lactic acid, and CO_2-combining power of blood passing through a tumor. Journal of Biological Chemistry *65*, 397-405.

Davidson, S.M., Papagiannakopoulos, T., Olenchock, B.A., Heyman, J.E., Keibler, M.A., Luengo, A., Bauer, M.R., Jha, A.K., O'Brien, J.P., Pierce, K.A., *et al.* (2016). Environment impacts the metabolic dependencies of Ras-driven non-small cell lung cancer. Cell metabolism *In Press*.

Dayton, T.L., Gocheva, V., Miller, K.M., Israelsen, W.J., Bhutkar, A., Clish, C.B., Davidson, S.M., Luengo, A., Bronson, R.T., Jacks, T., *et al.* (2016). Germline loss of PKM2 promotes metabolic distress and hepatocellular carcinoma. Genes Dev *30*, 1020-1033.

DeNicola, G.M., Chen, P.H., Mullarky, E., Sudderth, J.A., Hu, Z., Wu, D., Tang, H., Xie, Y., Asara, J.M., Huffman, K.E., *et al.* (2015). NRF2 regulates serine biosynthesis in non-small cell lung cancer. Nat Genet *47*, 1475-1481.

Eagle, H. (1955). Nutrition needs of mammalian cells in tissue culture. Science *122*, 501-514.

Fell, D.A. (2005). Metabolic Control Analysis. In Systems Biology: Definitions and Perspectives, L. Alberghina, and H.V. Westerhoff, eds. (Berlin, Heidelberg: Springer Berlin Heidelberg), pp. 69-80.

Gui, D.Y., Sullivan, L.B., Luengo, A., Hosios, A.M., Bush, L.N., Gitego, N., Davidson, S.M., Freinkman, E., Thomas, C.J., and Vander Heiden, M.G. (2016). Environment Dictates Dependence on Mitochondrial Complex I for NAD+ and Aspartate Production and Determines Cancer Cell Sensitivity to Metformin. Cell metabolism *24*, 716-727.

Gullino, P.M., Clark, S.H., and Grantham, F.H. (1964). The Interstitial Fluid of Solid Tumors. Cancer Res *24*, 780-794.

Hsu, P.P., and Sabatini, D.M. (2008). Cancer cell metabolism: Warburg and beyond. Cell *134*, 703-707.

Hume, D.A., and Weidemann, M.J. (1979). Role and regulation of glucose metabolism in proliferating cells. J Natl Cancer Inst *62*, 3-8.

Hyde, R., Taylor, P.M., and Hundal, H.S. (2003). Amino acid transporters: roles in amino acid sensing and signalling in animal cells. The Biochemical journal *373*, 1-18.

Israelsen, W.J., Dayton, T.L., Davidson, S.M., Fiske, B.P., Hosios, A.M., Bellinger, G., Li, J., Yu, Y., Sasaki, M., Horner, J.W., *et al.* (2013). PKM2 isoform-specific deletion reveals a differential requirement for pyruvate kinase in tumor cells. Cell *155*, 397-409.

Israelsen, W.J., and Vander Heiden, M.G. (2015). Pyruvate kinase: Function, regulation and role in cancer. Seminars in cell & developmental biology *43*, 43-51.

Iurlaro, R., Leon-Annicchiarico, C.L., and Munoz-Pinedo, C. (2014). Regulation of cancer metabolism by oncogenes and tumor suppressors. Methods Enzymol *542*, 59-80.

Lane, A.N., and Fan, T.W. (2015). Regulation of mammalian nucleotide metabolism and biosynthesis. Nucleic Acids Res *43*, 2466-2485.

Lemons, J.A., Adcock, E.W., 3rd, Jones, M.D., Jr., Naughton, M.A., Meschia, G., and Battaglia, F.C. (1976). Umbilical uptake of amino acids in the unstressed fetal lamb. The Journal of clinical investigation *58*, 1428-1434.

Locasale, J.W., Grassian, A.R., Melman, T., Lyssiotis, C.A., Mattaini, K.R., Bass, A.J., Heffron, G., Metallo, C.M., Muranen, T., Sharfi, H., *et al.* (2011). Phosphoglycerate dehydrogenase diverts glycolytic flux and contributes to oncogenesis. Nat Genet *43*, 869-874.

Lunt, S.Y., Muralidhar, V., Hosios, A.M., Israelsen, W.J., Gui, D.Y., Newhouse, L., Ogrodzinski, M., Hecht, V., Xu, K., Acevedo, P.N., *et al.* (2015a). Pyruvate kinase isoform expression alters nucleotide synthesis to impact cell proliferation. Molecular cell *57*, 95-107.

Lunt, Sophia Y., Muralidhar, V., Hosios, Aaron M., Israelsen, William J., Gui, Dan Y., Newhouse, L., Ogrodzinski, M., Hecht, V., Xu, K., Acevedo, Paula N.M., *et al.* (2015b). Pyruvate Kinase Isoform Expression Alters Nucleotide Synthesis to Impact Cell Proliferation. Molecular cell.

Mayers, J.R., Torrence, M.E., Danai, L.V., Papagiannakopoulos, T., Davidson, S.M., Bauer, M.R., Lau, A.N., Ji, B.W., Dixit, P.D., Hosios, A.M., *et al.* (2016). Tissue of origin dictates branched-chain amino acid metabolism in mutant Kras-driven cancers. Science *353*, 1161-1165.

Newsholme, E.A., Crabtree, B., and Ardawi, M.S. (1985). The role of high rates of glycolysis and glutamine utilization in rapidly dividing cells. Bioscience reports *5*, 393-400.

Pavlova, N.N., and Thompson, C.B. (2016). The Emerging Hallmarks of Cancer Metabolism. Cell metabolism *23*, 27-47.

Racker, E. (1976). Why do tumor cells have a high aerobic glycolysis? J Cell Physiol *89*, 697-700.

Schoors, S., Bruning, U., Missiaen, R., Queiroz, K.C., Borgers, G., Elia, I., Zecchin, A., Cantelmo, A.R., Christen, S., Goveia, J., *et al.* (2015). Fatty acid carbon is essential for dNTP synthesis in endothelial cells. Nature *520*, 192-197.

Sparks, J.W., Hay, W.W., Jr., Bonds, D., Meschia, G., and Battaglia, F.C. (1982). Simultaneous measurements of lactate turnover rate and umbilical lactate uptake in the fetal lamb. The Journal of clinical investigation *70*, 179-192.

Steinhauser, M.L., Bailey, A.P., Senyo, S.E., Guillermier, C., Perlstein, T.S., Gould, A.P., Lee, R.T., and Lechene, C.P. (2012). Multi-isotope imaging mass spectrometry quantifies stem cell division and metabolism. Nature *481*, 516-519.

Sullivan, L.B., Gui, D.Y., Hosios, A.M., Bush, L.N., Freinkman, E., and Vander Heiden, M.G. (2015). Supporting Aspartate Biosynthesis Is an Essential Function of Respiration in Proliferating Cells. Cell *162*, 552-563.

Svensson, R.U., and Shaw, R.J. (2017). Lipid Synthesis Is a Metabolic Liability of Non-Small Cell Lung Cancer. Cold Spring Harb Symp Quant Biol.

Tardito, S., Oudin, A., Ahmed, S.U., Fack, F., Keunen, O., Zheng, L., Miletic, H., Sakariassen, P.O., Weinstock, A., Wagner, A., *et al.* (2015). Glutamine synthetase activity fuels nucleotide biosynthesis and supports growth of glutamine-restricted glioblastoma. Nature cell biology *17*, 1556-1568.

Titov, D.V., Cracan, V., Goodman, R.P., Peng, J., Grabarek, Z., and Mootha, V.K. (2016). Complementation of mitochondrial electron transport chain by manipulation of the NAD+/NADH ratio. Science *352*, 231-235.

Vander Heiden, M.G., Cantley, L.C., and Thompson, C.B. (2009). Understanding the Warburg effect: the metabolic requirements of cell proliferation. Science *324*, 1029-1033.

Vemuri, G.N., Eiteman, M.A., McEwen, J.E., Olsson, L., and Nielsen, J. (2007). Increasing NADH oxidation reduces overflow metabolism in Saccharomyces cerevisiae. Proceedings of the National Academy of Sciences of the United States of America *104*, 2402-2407.

Warburg, O., Wind, F., and Negelein, E. (1927). The Metabolism of Tumors in the Body. J Gen Physiol *8*, 519-530.

Ward, P.S., and Thompson, C.B. (2012). Metabolic reprogramming: a cancer hallmark even warburg did not anticipate. Cancer cell *21*, 297-308.

Williamson, D.H., Krebs, H.A., Stubbs, M., Page, M.A., Morris, H.P., and Weber, G. (1970). Metabolism of renal tumors in situ and during ischemia. Cancer Res *30*, 2049-2054.

Wong, B.W., Wang, X., Zecchin, A., Thienpont, B., Cornelissen, I., Kalucka, J., Garcia-Caballero, M., Missiaen, R., Huang, H., Bruning, U., *et al.* (2016). The role of fatty acid beta-oxidation in lymphangiogenesis. Nature.

Yuneva, M.O., Fan, T.W., Allen, T.D., Higashi, R.M., Ferraris, D.V., Tsukamoto, T., Mates, J.M., Alonso, F.J., Wang, C., Seo, Y., *et al.* (2012). The metabolic profile of tumors depends on both the responsible genetic lesion and tissue type. Cell metabolism *15*, 157-170.

Appendix A: Concentrations of key metabolites in the body

Table 1: Average concentrations of selected free metabolites in human plasma (in μM).

Source	Canepa et al. (2002)	Caballero et al. (1991)	McMenamy et al. (1957)	Stein and Moore (1954)	NIH Medline	Pitkanen et al. (2003)	Wuu et al. (1988)
Alanine			320	383	200-510	347-418	243.7
Arginine	45.1		68	87	13-120	99-131	25.5
Asparagine	32.9			43.9	15-130	53-68	77
Aspartate	1.8			2.25	<26	13-29	9.1
Citrulline	18.5			28.53	16-55	35-48	27.3
Cysteine				49.11		2-16	
Cystine					19-65		23.2
Glutamate	59.4		<20	48	18-140	41-67	19.5
Glutamine	411		450	567.95	390-730	515-611	261.8
Glycine	168		235	205	110-330	244-315	168.7
Histidine	67.8		88	74	26-120	81-112	65.5
Isoleucine	52.4	54-75	57	68	37-140	51-79	95.1
Leucine	103.4	109-142	79	129	66-170	103-166	121.8
Lysine	148.3		143	186	120-290	181-232	182.9
Methionine	35.7		28	25	13-30	21-33	17.1
Ornithine	34.3		58	55	27-90	64-80	72.5
Phenylalanine	38.2	54-61	56	51	26-86	58-76	55.5
Proline			142	205	110-360		131.1
Serine	97		85	107	56-150	127-167	117.9
Threonine	82.3		135	117	67-240	128-200	97.1
Tryptophan		52-63	21	54.35	54.35	46-65	126.4
Tyrosine	35.3	52-63	70	57	26-110	58-80	54.2
Valine	184.3	192-238	174	246	150-350	186-267	176.4

Source	Johnson and Edwards (1937)	Kelsay et al. (1972)	Tsuchiya et al. (2003)
Pyruvate	110-180	93	62-64
Lactate	800-2200	683.5	830-860

Table 2: Average concentrations of selected free metabolites in human bodily fluids (in μM).

Source	Gutierrez et al. (1999)		Maggs et al. (1995)			(McGale et al., 1977)	
Bodily Fluid	Plasma	Muscle IF	Plasma	Adipose IF	Muscle IF	Plasma	CSF
Alanine	284 ± 35	341 ± 36	244 ± 27	248 ± 22	233 ± 35		
Arginine	76 ± 9	88 ± 9				80.9	22.4
Asparagine	52 ± 5	58 ± 7	45 ± 3	52 ± 3	56 ± 4	111.7	13.5
Aspartate			9 ± 1	62 ± 6	43 ± 4		
Citrulline	33 ± 3	47 ± 6	28 ± 1	51 ± 5	48 ± 11		
Cysteine			49 ± 2	34 ± 4	34 ± 4		
Cystine						123.7	
Glutamate	40 ± 5	55 ± 6	42 ± 4	43 ± 8	66 ± 9	61.3	26.1
Glutamine	619 ± 45	729 ± 67	506 ± 30	529 ± 56	672 ± 80	641	552
Glycine	229 ± 25	256 ± 23	194 ± 15	565 ± 92	400 ± 48	282.7	5.9
Histidine	80 ± 10	103 ± 14				79.8	12.3
Isoleucine	59 ± 5	69 ± 8	53 ± 5	65 ± 7	70 ± 10	76.7	6.2
Leucine	132 ± 9	167 ± 29	128 ± 6	149 ± 12	165 ± 19	155.3	14.8
Lysine	168 ± 16	187 ± 17				170.7	20.8
Methionine	27 ± 3	36 ± 3	20 ± 2	18 ± 3	14 ± 2	27.7	2.5
Ornithine	55 ± 8	46 ± 4				73.5	3.8
Phenylalanine	53 ± 2	64 ± 5	50 ± 2	58 ± 3	72 ± 7	64	9.9
Proline						323.7	
Serine	106 ± 5	117 ± 15	98 ± 7	195 ± 19	125 ± 9	139.7	29.5
Threonine	130 ± 15	130 ± 21				165.5	35.5
Tryptophan	41 ± 2	16 ± 1	124 ± 9	163 ± 6	185 ± 17		
Tyrosine	50 ± 6	66 ± 5	53 ± 3	54 ± 4	62 ± 15	73	9.5
Valine	231 ± 22	240 ± 29	216 ± 10	222 ± 14	492 ± 53	308.6	19.9
Glucose						4200	3300

IF, interstitial fluid; CSF, cerebrospinal fluid

Table 3: Average concentrations of selected free amino acids in canine plasma and lymph (in μM).

Source	Braun et al. (1956)	
Bodily Fluid	Plasma	Lymph
Arginine	40-92	46-109
Aspartate	15-45	15-45
Cystine	25-88	21-67
Glutamine	259-599	218-544
Glycine	107-267	80-187
Histidine	45-77	26-97
Isoleucine	99-183	107-229
Leucine		
Lysine	48-110	27-130
Phenylalanine	36-73	36-127
Proline	148-191	104-174
Serine	57-114	48-133
Threonine	76-235	101-261
Tryptophan	29-64	54-83
Tyrosine	44-83	39-99
Valine	85-154	77-188

References:

Braun, P., Foldi, M., Kisfaludy, S., and Szabo, G. (1956). Free amino-acid content of the lymph. Nature *177*, 1133-1134.

Caballero, B., Gleason, R.E., and Wurtman, R.J. (1991). Plasma amino acid concentrations in healthy elderly men and women. Am J Clin Nutr *53*, 1249-1252.

Canepa, A., Filho, J.C., Gutierrez, A., Carrea, A., Forsberg, A.M., Nilsson, E., Verrina, E., Perfumo, F., and Bergstrom, J. (2002). Free amino acids in plasma, red blood cells, polymorphonuclear leukocytes, and muscle in normal and uraemic children. Nephrol Dial Transplant *17*, 413-421.

Gutierrez, A., Anderstam, B., and Alvestrand, A. (1999). Amino acid concentration in the interstitium of human skeletal muscle: a microdialysis study. Eur J Clin Invest *29*, 947-952.

Johnson, R.E., and Edwards, H.T. (1937). LACTATE AND PYRUVATE IN BLOOD AND URINE AFTER EXERCISE. Journal of Biological Chemistry *118*, 427-432.

Kelsay, J.L., Behall, K.M., Holden, J.M., and Crutchfield, H.C. (1972). Pyruvate and lactate in human blood and saliva in response to different carbohydrates. The Journal of nutrition *102*, 661-666.

Maggs, D.G., Jacob, R., Rife, F., Lange, R., Leone, P., During, M.J., Tamborlane, W.V., and Sherwin, R.S. (1995). Interstitial fluid concentrations of glycerol, glucose, and amino acids in human quadricep muscle and adipose tissue. Evidence for significant lipolysis in skeletal muscle. The Journal of clinical investigation *96*, 370-377.

McGale, E.H., Pye, I.F., Stonier, C., Hutchinson, E.C., and Aber, G.M. (1977). Studies of the inter-relationship between cerebrospinal fluid and plasma amino acid concentrations in normal individuals. J Neurochem *29*, 291-297.

McMenamy, R., Lund, C.C., and Oncley, J.L. (1957). Unbound amino acid concentrations in human blood plasmas. The Journal of clinical investigation *36*, 1672-1679.

Pitkanen, H.T., Oja, S.S., Kemppainen, K., Seppa, J.M., and Mero, A.A. (2003). Serum amino acid concentrations in aging men and women. Amino Acids *24*, 413-421.

Stein, W.H., and Moore, S. (1954). The free amino acids of human blood plasma. J Biol Chem *211*, 915-926.

Tsuchiya, Y., Shimizu, T., Tazawa, T., Shibuya, N., Nakamura, K., and Yamamoto, M. (2003). Changes in plasma lactate and pyruvate concentrations after taking a bath in hot deep seawater. Tohoku J Exp Med *201*, 201-211.

Wuu, J.A., Wen, L.Y., Chuang, T.Y., and Chang, G.G. (1988). Amino acid concentrations in serum and aqueous humor from subjects with extreme myopia or senile cataract. Clinical chemistry *34*, 1610-1613.

Appendix B: Proliferating cells are sensitive to cystine deprivation

Abstract

Cysteine is necessary both for protein synthesis and to combat oxidative stress. Many proliferating cells are unable to synthesize sufficient cysteine and die from oxidative damage when starved for this amino acid. We observed that cell viability in the absence of cysteine could be rescued when additional amino acids were removed. Without individual essential amino acids, cells cannot divide but cystine (cysteine dimer) deprivation is less toxic to cells, implicating proliferation as a factor in cell death following cystine starvation. Indeed, other inhibitors of proliferation can reduce toxicity of cystine depletion as well. Future work can expand upon these results to better understand the distinct roles that cysteine plays to support viability and proliferation.

Introduction

The amino acid cysteine plays several critical roles in proliferating cells. Like all amino acids, cysteine is used to synthesize protein, but it can also be incorporated into glutathione, an important cellular antioxidant. Cysteine contains a reactive sulfhydryl (–SH) group that allows glutathione to be oxidized to its disulfide form (–SS–) while toxic or oxidized intracellular components are eliminated or reduced. Cysteine itself can exist as a disulfide dimer, cystine, which predominates in plasma and is commonly supplied *in vitro* (Brigham et al., 1960). The system xc⁻ transporter (xCT, a heterodimer of SLC7A11 and SLC3A2) is an antiporter for cystine and glutamate, serving as the primary means by which cells consume cystine. This system plays a critical role in proliferation for some cell types, and genetic loss of the transporter causes intracellular cystine and glutathione levels to fall and is lethal to fibroblasts (Sato et al., 2005).

Recent work has characterized the mechanisms of cell death induced by cystine deprivation, resulting either from xCT inhibition or cystine starvation *in vitro*. Ferroptosis, an iron-dependent form of cell death, is induced in these conditions and can be rescued by antioxidants (Dixon et al., 2012; Xie et al., 2016; Yang and Stockwell, 2016). This mode of cell death is thought to be distinct from apoptosis, but there have been reports of cells undergoing apoptosis following xCT inhibition as well (Liu et al., 2011). Ferroptosis occurs when cells have an insufficient glutathione supply. In this context, cells are unable to reduce lipid peroxide species, and inhibitors of lipid peroxide reduction are sufficient to induce cell death. Interestingly, glutamine metabolism appears to be necessary for induction of ferroptosis, although the link between glutaminolysis and ferroptosis remains unknown (Gao et al., 2015). Other forms of cell death may also result from cystine starvation; both necrosis and apoptosis have been reported to occur in cells treated with oxidizing agents and sensitivity to these forms of oxidative death is glutathione dependent.

We had previously assayed proliferation of A549 and H1299 non-small cell lung cancer cell lines in media lacking non-essential amino acids (NEAA), including cystine (**Chapter 2, Figure 12B,C**). Each of these amino acids is not required for the growth and survival of adult humans but may be required by cell lines in culture. Unlike any other NEAA, deprivation of cystine alone was toxic to both cell lines. Surprisingly, cells cultured in the absence of all NEAA (including cystine) were viable, indicating that deprivation of one or more NEAA protected cells from the effects of cystine deprivation. The following study aims to understand the protective function of NEAA starvation to better understand cellular dependence on cystine.

Results

We first sought to characterize the cell death we observed in culture following cystine deprivation. Ferroptosis is a recently proposed cell death mechanism that is independent of classic apoptosis and occurs when cells are unable to consume cystine (Yang and Stockwell, 2016). This form of

cell death is characterized by iron dependence and the ability to be rescued by reducing agents (Dixon et al., 2012). We assessed viability of A549 cells and 143B osteosarcoma cells cultured in medium lacking cystine and observed that they died at different rates, with ~75% of cells being inviable after one and three days, respectively (**Figure 1A,B**). Viability was assayed by exclusion of the dye propidium iodide, which can only stain cells with compromised plasma membrane integrity and, therefore, does not stain early apoptotic cells (Darzynkiewicz et al., 1992). Viability was rescued by addition of deforoximine (DFO), an iron chelator, indicating that cell death in this condition was iron dependent. Cells were also rescued by addition of N-acetyl-cysteine (NAC) and β-mercaptoethanol (βME), which can both function as reducing agents. NAC can also be hydrolyzed in cells to yield cysteine and is therefore less informative as a cystine starvation, contrary to what has been previously described (Dixon et al., 2012). Consistent with this explanation, addition of NAC to cystine-free media not only restored cell viability but was also able to completely rescue proliferation (data not shown). These observations demonstrate that NAC can serve as a substitute for cystine. βME cannot be metabolized and only serves as a reducing agent; however, it was able to partially restore the proliferation of A549 cells (**Figure 1C**), suggesting that they might be able to synthesize some cysteine *de novo* under these conditions.

Cell death following cystine deprivation was rescued in a manner consistent with ferroptosis, which can be induced by high extracellular glutamate concentrations (typically $\geq$ 5 mM) that prevent cystine uptake by xCT. Since depletion of NEAA (including glutamate, present at 136 μM in our media) rescued death induced by cystine deprivation (**Chapter 2, Figure 12B,C**), we hypothesized that removal of glutamate might be sufficient to mediate this rescue. Removal of glutamate from the medium did not rescue viability in the absence of cystine (data not shown), indicating that removal of other NEAA contributed to our original observations. Some NEAA are non-essential for adult humans but are conditionally essential for cells in culture, such as arginine and tyrosine. Interestingly, when A549 and 143B cells were deprived of either of these amino acids in addition to cystine, viability was completely restored to levels observed in cystine-containing media (**Figure 2**). Removal of leucine, which is an
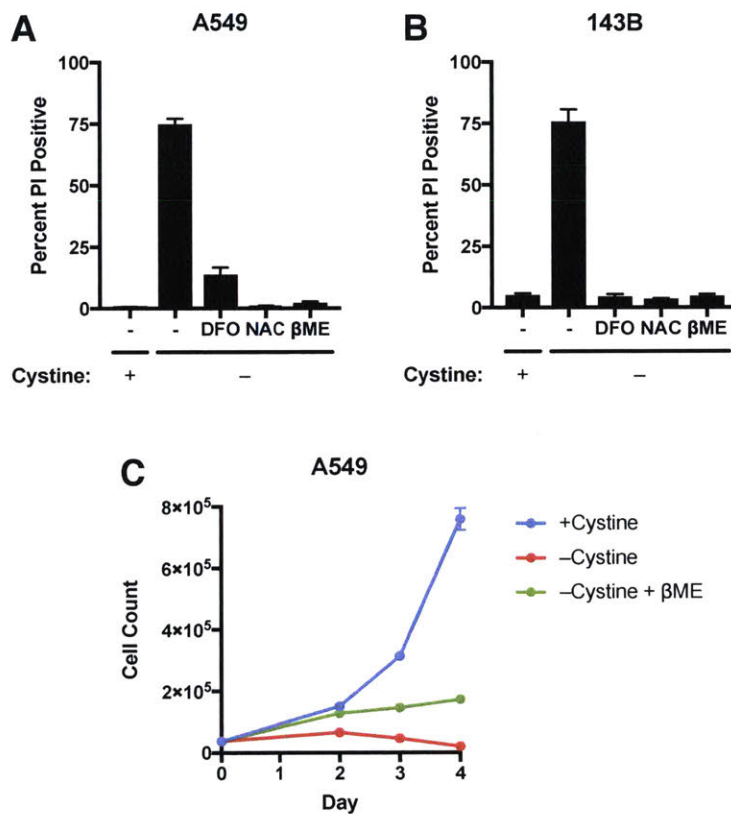
Figure 1: Cystine deprivation induces iron-dependent, oxidative cell death.

Fraction of cells staining positive for propidium iodide, a marker of inviable cells with compromised membrane integrity. (A) A549 cells were cultured for three days in the presence or absence of cystine, and (B) 143B cells were cultured for one day in this condition. Deferoxamine (DFO, 100 μM), N-acetyl-cysteine (NAC, 1 mM), or β-mercaptoethanol (βME, 50 μM) were added to cystine-free medium. (C) Proliferation of A549 cells in medium containing or lacking cystine with or without 50 μM βME supplemented. Each bar or point represents the average of N=3 replicates, ±S.D.
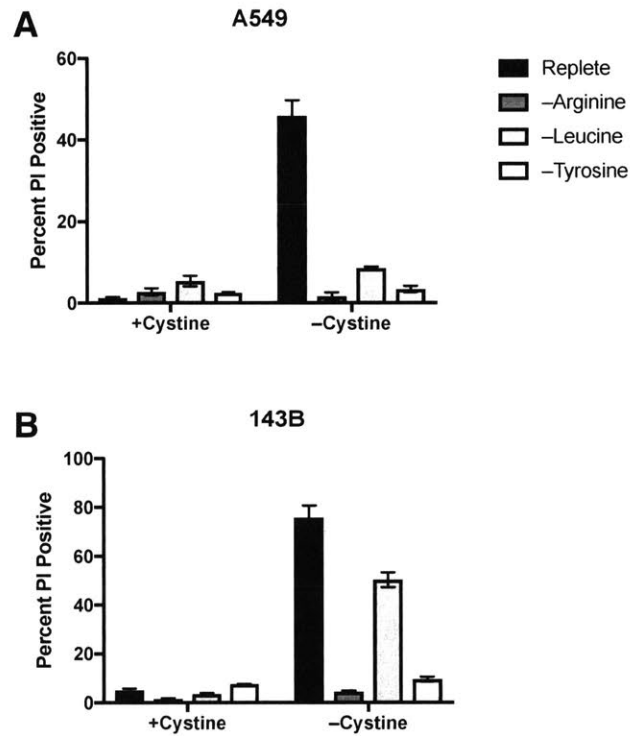
Figure 2: Depletion of essential amino acids rescues the viability of cells starved of cystine.

(A) A549 and (B) 143B cells were cultured for three or one day in medium containing or lacking cystine as well as arginine, leucine, or tyrosine. Viability was assessed by propidium iodide dye exclusion, and cells incorporating the dye are considered inviable. Each bar represents the average of N=3 replicates, ±S.D.

essential amino acid, produced the same effect in A549 cells but only partially rescued viability of 143B cells.

Each of these amino acids has distinct metabolic fates and effects on amino acid-sensing pathways, but they are all related in that starvation for each individually causes a proliferation arrest. To investigate whether proliferation itself might sensitize cells to cystine deprivation, we used orthogonal approaches to inhibit cell division. Thymidine induces cells to arrest at the G1/S transition, and addition of this nucleoside to A549 cells partially restored viability in the absence of cystine (**Figure 3A**). Viability of H1299 cells was completely rescued with thymidine supplementation (**Figure 3B**). 143B cells do not respond to thymidine block because they lack thymidylate kinase and are unable to salvage this nucleoside (Bacchetti and Graham, 1977).

Since thymidine block reduced the toxicity of cystine starvation, we examined whether other means of arresting proliferation affected viability of cystine-starved cells. A human mammary epithelial cell (HMEC) line that requires epidermal growth factor (EGF) to proliferate (see **Chapter 2, Figure 7A**) was cultured with or without EGF before being starved of cystine. Cells arrested by EGF depletion were completely viable when deprived of cystine, although HMECs were comparatively less sensitive to cystine starvation (**Figure 3C**). We finally attempted to block proliferation by using small molecule inhibitors of cell cycle progression. These can be toxic to cells, and we therefore chose to assay viability of 143B cells, which die rapidly following cystine starvation. Hydroxyurea is a nucleotide synthesis inhibitor and SU-9516 is a CDK2 inhibitor that both cause cell cycle arrest. Each was partially toxic to 143B cells in basal conditions but was able to slow the death of these cells when starved of cystine (**Figure 3D**). These results collectively imply that proliferating cells are particularly sensitive to cystine deprivation, as multiple means of inhibiting proliferation increase the viability of cystine-starved cells.

182
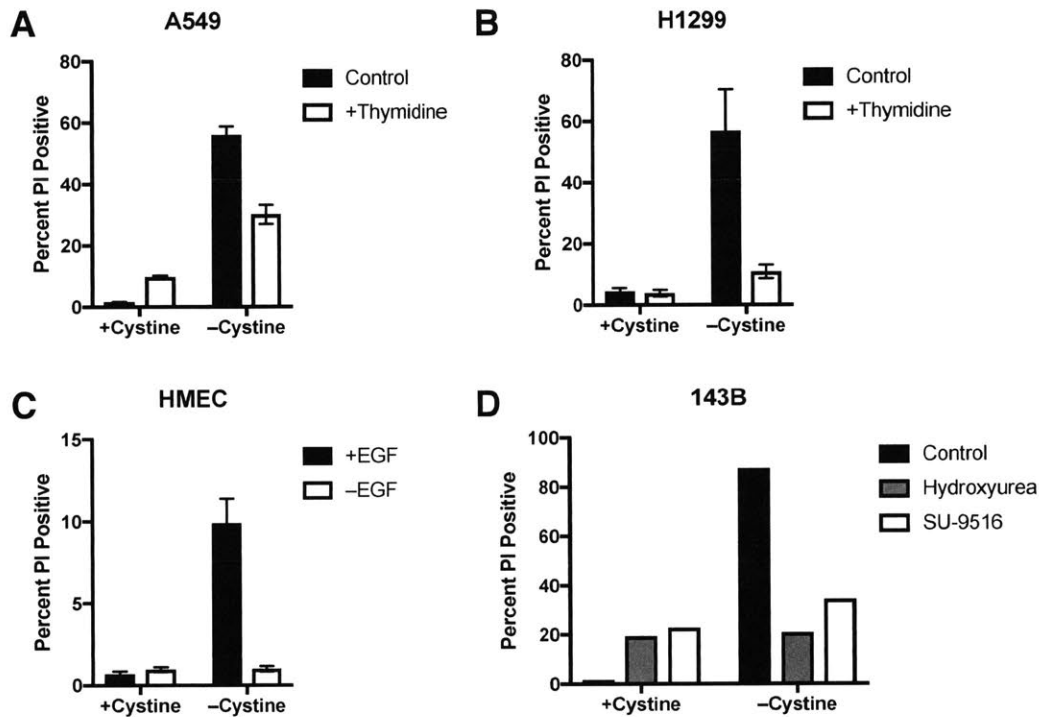
Figure 3: Proliferating cells are sensitive to cystine depletion.

The viability of (A) A549 and (B) H1299 cells cultured for three days in medium with or without cystine and thymidine (2 mM). (C) Human mammary epithelial cell (HMEC) viability when deprived of cystine in medium containing or lacking epidermal growth factor (EGF), which is essential for their proliferation. (D) Viability of 143B cells was assessed after one day in medium lacking cystine with hydroxyurea (2 mM) or SU-9516 (5 µM) added. Each bar in represents the average of N=3 replicates, ±S.D. in (A-C), and N=1 replicate in (D).

Discussion and Future Directions

For many cells in culture, cystine consumption is essential for both proliferation as well as viability. The data presented here implicate proliferation as a significant determinant of whether cells die in the absence of cystine. We confirmed that cell death following cystine starvation is dependent on both iron and oxidation, consistent with previous reports, but argue that NAC rescues this condition by functionally substituting for cystine. Treatments that prevent cell proliferation are protective during cystine starvation, preventing or reducing cell death. Essential amino acid starvation, thymidine block, growth factor withdrawal, and cell cycle inhibitors are all able to mediate this effect to varying degrees. These treatments have in common their ability to arrest cell proliferation, and together our data suggest that proliferating cells are more susceptible to cystine starvation. This result may, in part, explain why glutamine is required for ferroptosis. Gao *et al.* (2015) observed that ferroptosis following cystine deprivation is rescued when glutamine is omitted from culture media, and this is perhaps because glutamine is essential for proliferation of many cells in culture.

We were able to partially decouple the requirements of cysteine for cell viability and proliferation. Culturing A549 cells without cystine led to cell death, but addition of βME completely restored viability while only marginally rescuing proliferation. Cysteine is necessary for protein synthesis and to produce glutathione to combat reactive molecules, and βME can only fulfill the latter function. Therefore, cellular glutathione might determine viability while protein synthesis enables proliferation. It is also possible that βME provides reducing power to partially restore proliferation but that this cannot fully substitute for glutathione synthesis. Future work aimed at more directly inhibiting glutathione synthesis is needed to better decouple the functions of cysteine. That A549 cells can proliferate slowly in the absence of cystine and presence of βME suggests that they are capable of *de novo* cysteine biosynthesis albeit at rates insufficient to sustain full proliferation. Alternatively, slow proliferation might have been facilitated by accessing cellular cysteine stores. If autophagy were involved, , we would not expect cells to proliferate indefinitely in cystine-free media supplemented with βME. Alternatively

macropinocytosis of extracellular protein has been shown to compensate for starvation of individual amino acids and may be a source of cysteine in our study (Commisso et al., 2013). Additional work is required to determine whether *de novo* cysteine biosynthesis occurs in these cells.

The question still remains as to what sensitizes proliferating cells to cystine starvation. Withdrawal of individual essential amino acids reduces mTORC1 activity, ultimately resulting in arrested proliferation. mTORC1 is not equally sensitive to all amino acids, however, and cystine depletion does not significantly alter pathway activity (Hara et al., 1998). In that case, proliferating cells deprived of cystine may fail to arrest due to sustained mTORC1 signalling, and their continued growth and division could dilute the intracellular cysteine and glutathione pools, ultimately depleting them. Non-proliferating cells do not dilute their cytoplasms, potentially making them resistant to cystine starvation. To address this point, we plan to explore how the activity of signalling pathways (in particular those that sense amino acid levels) depends upon cysteine.

Unlike other amino acids, cysteine plays two essential roles: in protein biosynthesis to sustain proliferation and in glutathione to keep cells viable. Further work is required to better dissect the different fates of cysteine, especially from a quantitative perspective and how this amino acid interacts with signalling pathways that control both viability and proliferation.

Materials and Methods

Cell Culture: Cells were maintained in RPMI 1640 supplemented with 10% heat-inactivated fetal bovine serum (FBS), penicillin (100 U/mL), and streptomycin (100 µg/mL) using standard tissue culture techniques. Cells were washed three times with phosphate buffered saline (PBS) before changing to RPMI 1640 lacking specific amino acids, which contained 10% heat-inactivated dialyzed FBS. Other additives to the medium included: thymidine (2 mM), deferoxamine mesylate (100 µM), N-acetyl-cysteine (1 mM), β-mercaptoethanol (50 µM, refreshed daily), and hydroxyurea (2 mM) all from Sigma-

Aldrich; and SU-9516 (5 µM) from Tocris Bioscience. Human mammary epithelial cells (HMEC) were maintained in media described in Chapter 2 but were changed to RPMI 1640 containing the same growth factors for amino acid deprivation experiments.

Viability Assays: One day after plating, cells were washed twice with PBS and changed into the media to be assayed. HMEC were first cultured in medium lacking epidermal growth factor (EGF) for two days before being changed to the corresponding assay media. Cells were then incubated for either one day (for 143B) or three days (for A549, H1299, and HMEC). To assay viability, detached cells were collected and pooled with adherent cells harvested by trypsinization. These cells were washed once with PBS and resuspended in PBS containing 1% bovine serum albumin and 2 µg/mL propidium iodide (PI). A BD FACSCanto II and FACS Diva Software were used to determine the fraction of cells that stained PI-positive, and these cells were considered to be inviable.

Proliferation Assays: Cells seeded at low density (20 000 cells/well) one day prior to the experiment. The next day, cells were washed twice with PBS and changed to the assay media. On each day of the experiment, media were refreshed, and cells from each condition were trypsinized and counted.

References

Bacchetti, S., and Graham, F.L. (1977). Transfer of the gene for thymidine kinase to thymidine kinase-deficient human cells by purified herpes simplex viral DNA. Proceedings of the National Academy of Sciences of the United States of America *74*, 1590-1594.

Brigham, M.P., Stein, W.H., and Moore, S. (1960). The Concentrations of Cysteine and Cystine in Human Blood Plasma. The Journal of clinical investigation *39*, 1633-1638.

Commisso, C., Davidson, S.M., Soydaner-Azeloglu, R.G., Parker, S.J., Kamphorst, J.J., Hackett, S., Grabocka, E., Nofal, M., Drebin, J.A., Thompson, C.B., *et al.* (2013). Macropinocytosis of protein is an amino acid supply route in Ras-transformed cells. Nature *497*, 633-637.

Darzynkiewicz, Z., Bruno, S., Del Bino, G., Gorczyca, W., Hotz, M.A., Lassota, P., and Traganos, F. (1992). Features of apoptotic cells measured by flow cytometry. Cytometry *13*, 795-808.

Dixon, S.J., Lemberg, K.M., Lamprecht, M.R., Skouta, R., Zaitsev, E.M., Gleason, C.E., Patel, D.N., Bauer, A.J., Cantley, A.M., Yang, W.S., *et al.* (2012). Ferroptosis: an iron-dependent form of nonapoptotic cell death. Cell *149*, 1060-1072.

Gao, M., Monian, P., Quadri, N., Ramasamy, R., and Jiang, X. (2015). Glutaminolysis and Transferrin Regulate Ferroptosis. Molecular cell *59*, 298-308.

Hara, K., Yonezawa, K., Weng, Q.P., Kozlowski, M.T., Belham, C., and Avruch, J. (1998). Amino acid sufficiency and mTOR regulate p70 S6 kinase and eIF-4E BP1 through a common effector mechanism. J Biol Chem *273*, 14484-14494.

Liu, X.X., Li, X.J., Zhang, B., Liang, Y.J., Zhou, C.X., Cao, D.X., He, M., Chen, G.Q., He, J.R., and Zhao, Q. (2011). MicroRNA-26b is underexpressed in human breast cancer and induces cell apoptosis by targeting SLC7A11. FEBS Lett *585*, 1363-1367.

Sato, H., Shiiya, A., Kimata, M., Maebara, K., Tamba, M., Sakakura, Y., Makino, N., Sugiyama, F., Yagami, K., Moriguchi, T., *et al.* (2005). Redox imbalance in cystine/glutamate transporter-deficient mice. J Biol Chem *280*, 37423-37429.

Xie, Y., Hou, W., Song, X., Yu, Y., Huang, J., Sun, X., Kang, R., and Tang, D. (2016). Ferroptosis: process and function. Cell Death Differ *23*, 369-379.

Yang, W.S., and Stockwell, B.R. (2016). Ferroptosis: Death by Lipid Peroxidation. Trends Cell Biol *26*, 165-176.

# Appendix C: Biochemical properties of phosphoserine phosphatase

Introduction

Serine can be obtained from the environment or from *de novo* synthesis. The serine synthesis pathway produces serine from glucose via the oxidation, transamination, and dephosphorylation of 3-phosphoglycerate. The enzymes of this pathway are upregulated when cells are starved of serine, and the first enzyme in this pathway, phosphoglycerate dehydrogenase, is amplified in some cancers (Locasale et al., 2011). Elevated flux through this pathway is growth-promoting in some contexts, and there has been interest in studying this pathway and its regulation (Mattaini et al., 2016; Possemato et al., 2011). Phosphoserine phosphatase (PSPH) catalyzes the final step of serine biosynthesis and is reported to possess two activities (**Figure 1A**) (Borkenhagen and Kennedy, 1958; Neuhaus and Byrne, 1958):

1. When serine is scarce, PSPH acts as a phosphatase to generate serine from phosphoserine

2. When serine is abundant, PSPH acts as a phosphotransferase to move phosphate between phosphoserine and serine, without the net generation of a new serine molecule

We previously observed that phosphoserine becomes isotopically labeled in cells supplied with universally carbon-13 labeled ([U-^{13}C]) serine (**Figure 1B**). The mass isotopomer distributions of serine and phosphoserine were identical, indicating that the intracellular pools of these metabolites are in isotopic equilibrium. This observation could be explained by synthesis of phosphoserine from serine by PSPH. Alternatively, PSPH phosphotransferase activity could be sufficient to allow isotopically labeled serine supplied to cells to label phosphoserine without net synthesis of the latter, particularly if the phosphotransferase and phosphatase activities are comparable (see Appendix E). We therefore sought to investigate which of these hypotheses could better explain the generation of isotopically labeled phosphoserine from serine.

A **Phosphatase Activity**

Phosphoserine ⟶ Serine Phosphate

Phosphotransferase Activity

Phosphoserine Serine ⇌ Serine Phosphoserine

B

T.T MDA-MB-468
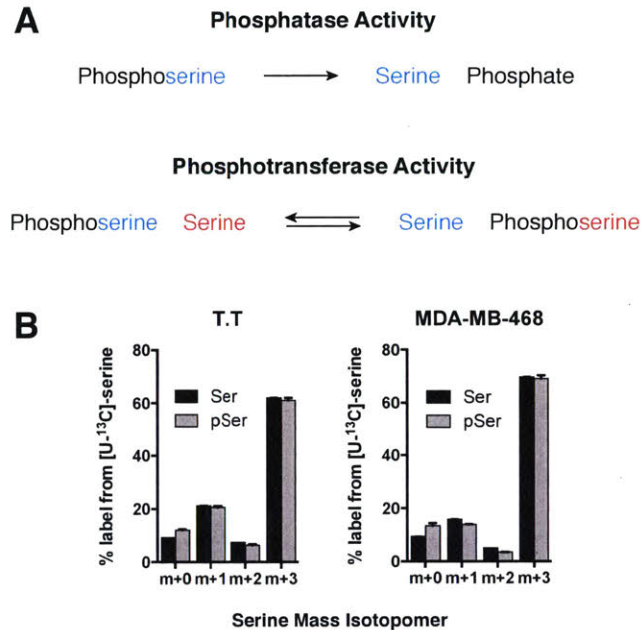
**Figure 1: Intracellular serine and phosphoserine are isotopically equilibrated.**

(A) The two catalytic functions of PSPH. When the intracellular serine concentration is low, PSPH acts as a phosphatase, cleaving 3-phosphoserine to generate serine. When serine is abundant, PSPH can act as a phosphotransferase to move a phosphate between 3-phosphoserine and serine. (B) T.T and MDA-MB-468 cells were labeled with [U-^{13}C]-serine for 24 hours. The mass isotopomer distribution of serine (Ser) and phosphoserine (pSer) are shown. Each bar is the average of N=3 ± S.E.M. M+0 represents the isotopomer of serine containing only carbon-12, and each higher value results from incorporation of an additional carbon-13 atom, increasing the mass by one. Although the labeled serine provided to cells is entirely M+3, intracellular serine hydroxymethyltransferase activity cleaves and re-generates serine, producing M+1 and M+2 species.

The data shown are courtesy of Caroline Lewis.

Results

To understand how serine alters the function of PSPH, we studied the activity of affinity-purified, recombinant human PSPH in a cell-free system. Phosphoserine alone is stable in solution, but is hydrolyzed by PSPH to produce serine (**Figure 2A**). When a higher concentration of PSPH was examined (**Figure 2B, left**), we observed near complete conversion of phosphoserine into serine, consistent with specific activity values reported elsewhere (Neuhaus and Byrne, 1958). When we added 5 mM serine to this reaction, phosphoserine hydrolysis was markedly slowed, even at this higher concentration of PSPH (**Figure 2B, right**). Serine may slow the net reaction through several mechanisms: serine could inhibit PSPH by binding to its active site, it could participate in the reverse reaction to produce phosphoserine, or it could cause the enzyme to favor phosphotransferase activity over hydrolysis.

Phosphoserine hydrolysis is energetically favourable, so we did not expect that the reverse reaction to occur at a substantial rate. When the reaction included 5 mM serine and 50 mM phosphate as substrates, PSPH was unable to synthesize phosphoserine (**Figure 2C**). It is possible that at higher concentrations, these substrates could drive the reaction. Intracellular free phosphate, however, is estimated to be close to 5 mM (Traut, 1994), and we therefore concluded that net synthesis of phosphoserine could not explain our initial observations that isotopically labeled phosphoserine was produced from [U-^{13}C]-serine in cells. To assay for phosphotransferase activity, we incubated PSPH with [U-^{14}C]-serine and varying concentrations of non-radioactive phosphoserine and monitored the production of [U-^{14}C]-phosphoserine. Radioactive phosphoserine was generated in proportion to the amount of non-radioactive phosphoserine included in the reaction (**Figure 2D**). This suggests that PSPH possesses sufficient phosphotransferase activity to enable high turnover of phosphoserine, explaining the labeling observed in cells.
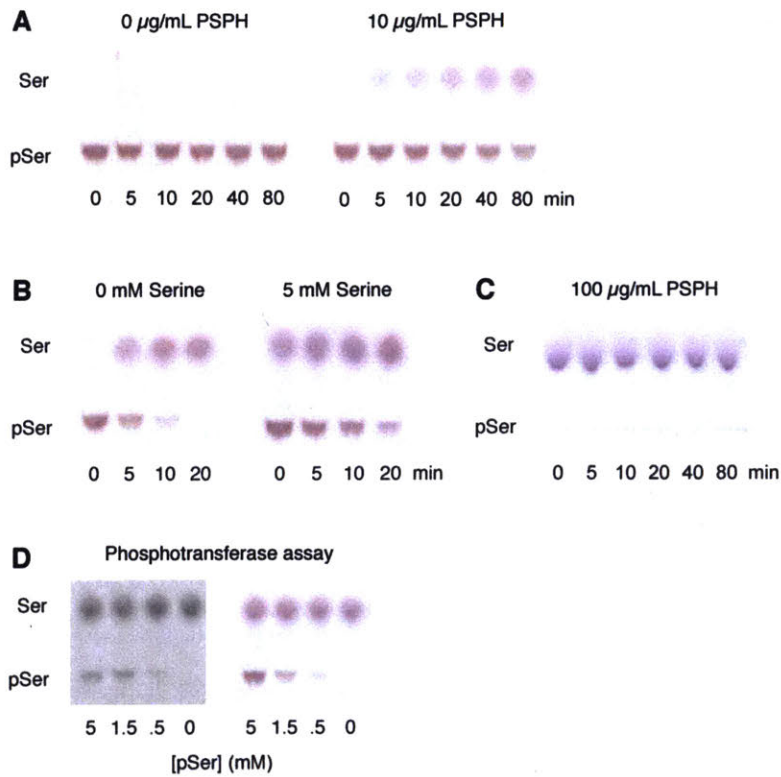
Figure 2: PSPH can isotopically equilibrate serine and phosphoserine without net synthesis of the latter.

Serine (Ser) and phosphoserine (pSer) can be resolved by thin layer chromatography (TLC), enabling PSPH activity to be monitored *in vitro*. (A) PSPH acts as a phosphatase, hydrolyzing phosphoserine to produce serine. Phosphoserine (5 mM) was incubated for the indicated times in the presence or absence of 10 µg/mL recombinant PSPH. (B) Phosphatase activity is inhibited by serine. Phosphoserine (5 mM) and PSPH (100 µg/mL) were incubated in the presence or absence of serine (5 mM) for the specified times. (C) PSPH cannot synthesize phosphoserine from serine (5 mM) and phosphate (50 mM). (D) PSPH enables phosphate exchange between serine and phosphoserine. PSPH was incubated for 40 min with serine (5 mM, including 1 µCi/mL [U-^{14}C]-serine) and the indicated concentrations of phosphoserine. The TLC plate was visualized by autoradiography (left) and ninhydrin stain (right). Radioactive phosphoserine is detected, demonstrating production of phosphoserine from serine.

Discussion

We propose that the phosphotransferase activity of PSPH is sufficient to account for the observation of carbon-13 labeled phosphoserine with the same mass isotopomer distribution as serine. Hydrolysis of phosphoserine is expected to be energetically favourable, and supraphysiological concentrations of serine and phosphate would be required to drive the reverse reaction (Guynn et al., 1986). The intracellular serine concentration is expected to be in the low millimolar range, sufficient to greatly reduce PSPH phosphatase activity. We show that this is not due to inactivation of the enzyme but rather because serine allows the enzyme to catalyze a phosphotransferase reaction. For the lower concentrations of phosphoserine assayed in the exchange reaction, we observed that the relative intensities of the radioactive phosphoserine and serine spots was qualitatively comparable to the relative intensities of ninhydrin stained material. This suggests near complete turnover of phosphoserine, resulting in a specific activity similar to serine. We conclude that PSPH has the ability to synthesize new (isotopically labeled) phosphoserine but that this does not represent *net* synthesis. In cell culture, phosphoserine is *de novo* synthesized from glucose, and this has the potential to reduce its labeling relative to [U-^{13}C]-serine. Because we observed identical phosphoserine and serine labeling, we expect the exchange catalyzed by PSPH to be fast relative to the rate of *de novo* synthesis. Our observations represent a specific case where an exchange reaction results in isotopic labeling *without* net synthesis. Where this is the case, production of an isotopically labeled metabolite from a labeled nutrient does not imply its net synthesis and metabolic tracers fail to identify the direction of a reaction's flux. These implications are discussed in further detail in Appendix E.

Together, these data argue that PSPH activity can equilibrate the intracellular phosphoserine and serine pools, even when both serine synthesized *de novo* and extracellular serine are available to cells., When serine is scarce, however, PSPH will rapidly hydrolyze phosphoserine to produce serine. Phosphoserine levels thus could provide cells with a readout of both serine synthesis flux and extracellular serine levels, but whether phosphoserine is sensed in cells remains a topic for further study.

Materials and Methods

Purification of N-terminally tagged 6xHis-tagged human PSPH: Recombinant PSPH was produced in BL21(DE3) pLysS bacteria transformed with pET28a-PSPH. During exponential growth, PSPH expression was induced with 0.5 mM IPTG for 6 hours at 37 °C. PSPH was purified by nickel affinity chromatography using Ni-NTA agarose beads (Qiagen) using the same approach we had previously used to purified recombinant PKM2 (Hosios et al., 2015). Protein concentration was determined by Bradford assay using bovine serum albumin as a standard.

PSPH activity assay: Enzyme activity was monitored using the specified concentrations of PSPH in a buffer containing 25 mM HEPES (pH 7.0), 50 mM KCl, 5 mM $MgCl_2$, and 1 mM DTT. Serine (5 mM), 3-phosphoserine (5 mM unless otherwise specified), and sodium phosphate (50 mM, pH 7.1) were added where specified. Reactions were allowed to proceed at room temperature for 40 min or the indicated times, and 1 µL was then spotted on to cellulose thin layer chromatography (TLC) plates and dried immediately to halt the reaction. Plates were developed with a solution of 80% isopropanol and 4% formic acid until the solvent front was 8 cm beyond the origin, and amino acids were visualized by ninhydrin staining. Where indicated, [U-^{14}C]-serine (1 µCi/mL final concentration) was included in the reaction, and the TLC plate was additionally visualized by autoradiography.

Acknowledgements

References

Borkenhagen, L.F., and Kennedy, E.P. (1958). The enzymic equilibration of L-serine with O-phospho-L-serine. Biochim Biophys Acta *28*, 222-223.

Guynn, R.W., Merrill, D.K., and Lund, K. (1986). The reactions of the phosphorylated pathway of L-serine biosynthesis: thermodynamic relationships in rat liver in vivo. Arch Biochem Biophys *245*, 204-211.

Hosios, A.M., Fiske, B.P., Gui, D.Y., and Vander Heiden, M.G. (2015). Lack of Evidence for PKM2 Protein Kinase Activity. Molecular cell *59*, 850-857.

Locasale, J.W., Grassian, A.R., Melman, T., Lyssiotis, C.A., Mattaini, K.R., Bass, A.J., Heffron, G., Metallo, C.M., Muranen, T., Sharfi, H., *et al.* (2011). Phosphoglycerate dehydrogenase diverts glycolytic flux and contributes to oncogenesis. Nat Genet *43*, 869-874.

Mattaini, K.R., Sullivan, M.R., and Vander Heiden, M.G. (2016). The importance of serine metabolism in cancer. J Cell Biol *214*, 249-257.

Neuhaus, F.C., and Byrne, W.L. (1958). O-Phosphoserine phosphatase. Biochim Biophys Acta *28*, 223-224.

Possemato, R., Marks, K.M., Shaul, Y.D., Pacold, M.E., Kim, D., Birsoy, K., Sethumadhavan, S., Woo, H.K., Jang, H.G., Jha, A.K., *et al.* (2011). Functional genomics reveal that the serine synthesis pathway is essential in breast cancer. Nature *476*, 346-350.

Traut, T.W. (1994). Physiological concentrations of purines and pyrimidines. Mol Cell Biochem *140*, 1-22.

Appendix D: Evidence for pyruvate kinase-independent glycolysis

Introduction

Pyruvate kinase catalyzes the final reaction in glycolysis, the production of pyruvate and ATP from phosphoenolpyruvate (PEP) and ADP. Mammals express four isoforms of pyruvate kinase that differ in their tissue localization. PKR and PKL are expressed from the *PKLR* gene, and they are expressed respectively in erythrocytes and the liver. The *PKM* gene encodes two isoforms that are expressed in all other adult tissues, PKM1 and PKM2 (Dayton et al., 2016). PKM2 is also ubiquitously expressed in embryonic tissues and is the predominant isoform expressed in cancerous tissue (Mazurek et al., 2002). Expression of PKM2 rather than PKM1 allows cells to engage in a unique metabolic program that favors aerobic glycolysis and anabolic metabolism, allowing cells to proliferate (Israelsen and Vander Heiden, 2015).

In spite of extensive evidence for preferential PKM2 expression in proliferating cells, PKM2 is not essential for these cells, and in some cases loss of PKM2 can promote proliferation. A previously generated mouse model allows for conditional deletion of PKM2 (Dayton et al., 2016; Israelsen et al., 2013). Which PKM isoform is expressed is determined by a mutually exclusive splicing event, and deletion of the PKM2-specific exon (*PKM* exon 10) uniquely prevents expression of this isoform. Upon PKM2 deletion, low levels of PKM1 expression are observed both in tissue culture and in mice; however, glycolytic rate is not changed. Since production of lactate from glucose is minimally altered in this context, we wondered if cells express an enzyme that allows them to bypass pyruvate kinase. This enzyme could sustain glycolytic rate when pyruvate kinase activity is dramatically reduced. PKM2 activity is also lowered in a variety of biological contexts without a corresponding decrease in glycolytic rate, further implying that cells might be able to circumvent this reaction (Christofk et al., 2008; Israelsen

and Vander Heiden, 2015). Previous work had postulated that glycolysis can bypass pyruvate kinase, but no enzyme with this function has been identified to date (Vander Heiden et al., 2010).

If this activity exists, we reasoned that cells should be able to proliferate without pyruvate kinase expression, and genetic approaches that reduce but do not eliminate pyruvate kinase activity are not sufficient to address this question. We therefore employed CRISPR-Cas9-mediated deletion to completely eliminate pyruvate kinase expression to understand whether pyruvate kinase activity is essential for proliferating cells.

Results and Future Directions

We introduced Cas9 and a small guide RNA targeting *PKM* exon 2 (sgPKM), an exon common to both PKM1 and PKM2, into 3553-T3 cells (cells previously derived from a mouse lung tumor deleted for p53 and expressing Kras^{G12D}). After single-cell cloning, one clone was obtained in which PKM2 was undetectable by protein immunoblot (**Figure 1A**). We confirmed that PKM1 was also not expressed and that there was no compensatory expression of PKL or PKR. Similar results were obtained by analyzing messenger RNA from parental cells and the clone by quantitative PCR (data not shown). The sgPKM clone displayed reduced proliferation compared to the parental cells (**Figure 1B**). This might be due to impaired glycolysis but may also be a consequence of the phenotypic variability necessarily resulting from single cell cloning. To assay glycolytic rate in these cells, we measured glucose consumption and lactate production (**Figure 1C**). Both of these rates were partially reduced in the sgPKM cells compared to the parental line; however, loss of pyruvate kinase expression did not eliminate glycolytic flux. Cells might therefore be capable of glycolysis even without pyruvate kinase expression, providing evidence for an alternative activity. We assayed pyruvate kinase activity in hypotonic lysates using a linked enzyme assay (**Figure 1D**) in which each reaction contained either PEP alone or PEP and ADP. When PEP alone was added, no activity was observed. The parental cell lysate demonstrated robust activity when PEP and
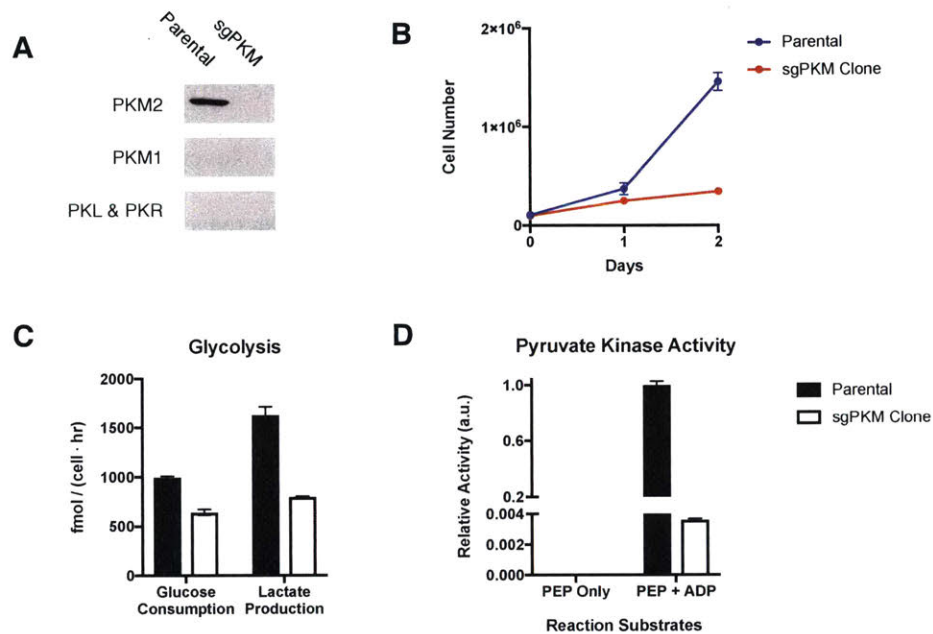
Figure 1: CRISPR-Cas9-mediated deletion of *PKM* partially impairs growth and glycolytic rate.

(A) Immunoblot for pyruvate kinase isoform M2 (PKM2), isoform M1 (PKM1), and isoforms L and R (PKL & PKR) in cell extracts from 3553-T3 cells (parental) or a clone generated following expression of Cas9 and a small guide RNA targeting *PKM* exon 2 (sgPKM). Analysis of (B) proliferation rate and (C) glucose consumption and lactate production rates of the parental cells and the sgPKM clone. (D) Pyruvate kinase activity was assayed in hypotonic lysates by a linked assay to lactate dehydrogenase to monitor pyruvate production. Reactions contained either PEP alone or PEP and ADP. Each bar or point represents the average of N=3 replicates, ±S.D.

The data presented in figures (A) and (C) were generously provided by Alba Luengo.

ADP were included, and we were also able to detect residual pyruvate kinase activity in the sgPKM clone lysate. Of note, the activity assay monitors consumption of NADH by lactic dehydrogenase downstream of pyruvate kinase, so we directly confirmed pyruvate production from PEP and ADP by mass spectrometry as well (data not shown). These results suggested that although no pyruvate kinase protein was detected in the sgPKM clone, residual low levels of pyruvate kinase activity remained, perhaps due to expression of PKL or PKR below the limit of detection by immunoblot. Nevertheless, these cells displayed a roughly 2-fold reduction in glycolytic rate but a 200-fold decrease in pyruvate kinase activity, suggesting that they may not depend exclusively on pyruvate kinase to enable glycolytic flux.

We next sought to generate a system where both pyruvate kinase isoforms could be efficiently deleted. Recently, complex CRISPR-Cas9 systems that express multiple guide RNAs have been developed, allowing allow multiple genes to be targeted simultaneously (Kabadi et al., 2014). We designed guides that target intronic regions flanking *PKM* exons 9 and 10 and *PKLR* exons 7 and 8 (**Figure 2A,B**). These *PKM* exons are specific to PKM1 and PKM2, respectively, and no PKM product can be produced when they are both excluded (Israelsen et al., 2013). Because two guides target each gene, Cas9 activity can excise a small portion of DNA. Non-homologous end joining to repair this lesion may result in three possible effects: (1) re-insertion of the excised region to regenerate the wild type allele, (2) loss of the excised region resulting in a deletion, or (3) re-insertion of the excised region resulting in its inversion. Each of these results can be monitored by PCR of genomic DNA. When the vectors expressing the guide RNAs were transiently transfected into HEK293T cells, we observed substantial formation of both deletion and inversion alleles not detectable when the sgRNAs were not present. This suggests that we can efficiently target *PKM* and *PKLR* for simultaneous deletion (**Figure 2C,D**). Future work includes deriving single-cell clones from cells targeted with these sgRNAs to discern whether cells can proliferate when all pyruvate kinase isoforms are genetically lost. If clones are obtained, we will seek to characterize them and identify the source of their glycolytic activity.

200
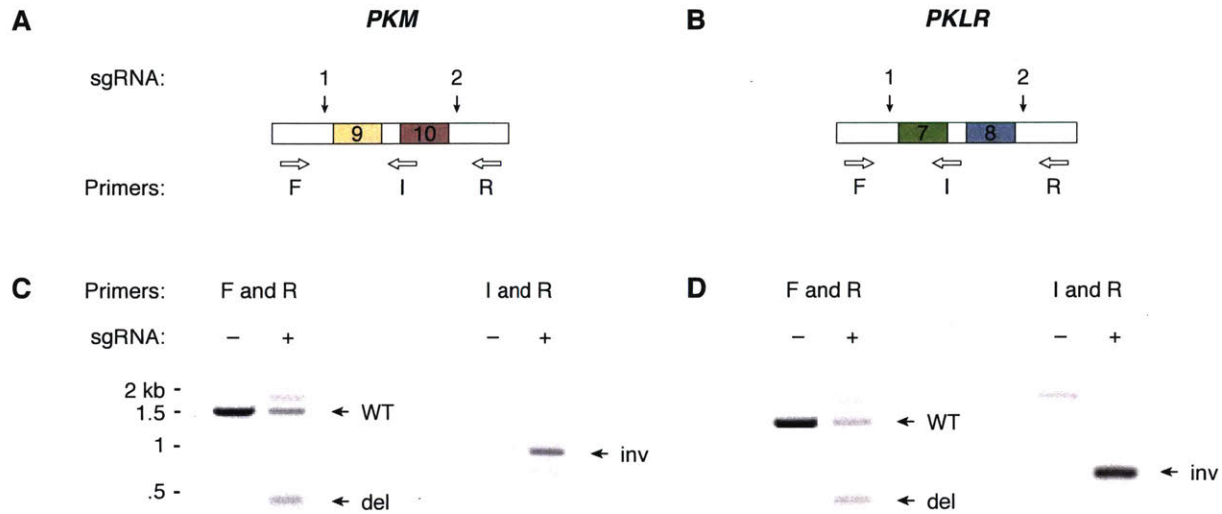
Figure 2: Deletion of *PKM* and *PKLR* using a multiplexed CRISPR-Cas9 approach.

PKM exons 9 and 10 encode regions specific to PKM1 and PKM2, respectively, and *PKLR* exons 7 and 8 encode a region common to PKL and PKR. We designed two small guide RNAs (sgRNAs) that target sites flanking these regions in (A) *PKM* and (B) *PKLR*. If both sites are cut by Cas9, the region could be excised, allowing *PKM* or *PKLR* to be deleted. Primers F, I, and R can be used to genotype the resulting loci. HEK293T cells were transiently transfected with Cas9 alone or in addition to vectors expressing the sgRNAs targeting (C) *PKM* or (D) *PKLR*. After 24 hours, genomic DNA was isolated and amplified with primers F and R to detect the wild type (WT) allele or a deletion (del) resulting from excision the targeted exons. Primers I and R amplify an inversion (inv) that can form when exons excised and re-ligated.

Acknowledgements

Materials and Methods

Cell culture: All cells were cultured in DMEM supplemented with 10% heat-inactivated fetal bovine serum (FBS), penicillin (100 U/mL), and streptomycin (100 μg/mL) using standard tissue culture techniques.

Immunoblot: Cells were lysed in cold RIPA buffer containing 1x cOmplete Mini Protease Inhbitors (Roche), and lysates were clarified for 10 min at 4 °C. Protein concentration was determined by Bradford assay, and samples were analyzed by SDS-PAGE followed by immunoblotting using the following antibodies: PKM2 and PKM1 (4053 and 7067, respectively, from Cell Signaling Technologies); and PKLR (D-10 from Santa Cruz Biotechnology).

Proliferation assay: Cells were sparsely seeded, and allowed to adhere overnight. The next day, cells were washed extensively with PBS and changed into fresh medium. Cells were trypsinized and counted at the indicated time points.

Measurement of nutrient consumption and excretion: One day prior to the experiment, cells were seeded in 6-well plates at a sufficiently low density to ensure their exponential proliferation over the duration of the experiment. The following day, the cells were washed with PBS and changed into fresh medium. Over the following 48-hour period, medium was collected and cell counts were determined from

the corresponding wells. Media were centrifuged at 3000 × g for 5 minutes to remove any cell debris and then stored at -20 °C. Glucose and lactate concentrations were later measured by enzymatic assay using a YSI-7100 MBS (Yellow Springs Instruments). To calculate consumption rates, we performed a linear regression of a nutrient's concentration relative to the integrated area under the curve (units: cells · time) of an exponential function fit to the growth curve.

Pyruvate kinase assay: To prepare hypotonic lysates, cells were washed twice with cold PBS, detached, and pelleted. The cell pellet was resuspended in a hypotonic buffer containing 20 mM HEPES-KOH pH 7.0, 5 mM KCl, 1 mM $MgCl_2$, 0.5 mM DTT, and 1x cOmplete mini protease inhibitor (Roche). Cells were incubated for 10 min on ice and lysed by passing them through a 22.5-gauge needle fifteen times. The resulting lysates were clarified for 10 min at 20 000 × g, and protein concentration was determined by Bradford assay using a bovine serum albumin standard. Pyruvate kinase activity was determined by an assay linked to lactic dehydrogenase (LDH). Reactions were carried out at room temperature in a 100 µL volume containing lysate, buffer (50 mM Tris-HCl pH 7.5, 100 mM KCl, 5 mM $MgCl_2$, .5 mM DTT), 180 µM NADH, 500 µM PEP, and 16 U LDH (Sigma-Aldrich). Where indicated, 600 µM ADP was also included. Activity was monitored by loss of NADH fluorescence (excitation at 340 nm; emission at 460 nm). The measured initial reaction rates were adjusted to account for the amount of lysate included in each reaction. To assay for the production of pyruvate by mass spectrometry, we excluded LDH and NADH from the reactions and quenched them after 15 minutes with excess cold acetone containing a norvaline standard (1 µg/reaction). The reactions were clarified for 10 min at 4 °C, and the soluble material was dried under nitrogen gas and analyzed by gas chromatography-mass spectrometry as described previously (Lewis et al., 2014).

Design and validation of sgRNAs: Guide RNA sequences (**Table 1**) were selected using crispr.mit.edu, and cloned into the vector system described previously by Kabadi *et al.* (2014). We followed the the authors' protocols using enzymes purchased from New England Biolabs and validated the resulting

vectors by Sanger sequencing. HEK293T cells were transiently transfected with pLV-hUbC-Cas9-T2A-GFP alone or in addition to the vectors encoding each sgRNA using Lipofectamine 3000 (Life Technologies). After 24 hours, genomic DNA was extracted from cells using the PureLink Genomic DNA Mini Kit (Life Technologies). DNA was amplified with Phusion polymerase (New England Biolabs) according to the manufacturer's instructions, using the primers listed below (**Table 2**). The reactions were analyzed by gel electrophoresis. Multiple guide RNAs were tested, and the pairs that resulted in the best genomic deletion are listed (**Table 1**).

Table 1: Sequences targeted by guide RNAs used in this study (see Figure 2A,B).

sgRNA	Recognition Sequence	Vector *
PKM Guide 1	GCCAATTTCCCCTGTATTGG	pmU6-gRNA
PKM Guide 2	GAGTGCTACCTAGAGTCCTT	phU6-gRNA
PKLR Guide 1	TGAGCGCAGAGTCTACACGC	ph7SK-gRNA
PKLR Guide 2	CTTGAGGTTCGGCACTCTGT	phH1-gRNA

* Kabadi *et al.* (2014)

Table 2: Primers used in this study (see Figure 2A,B).

Primer Name	Sequence
PKM_F	GCCTAATCAACCAGCCATGT
PKM_R	TGGAGGCACAGTAAACAGCA
PKM_I	ACGAGAGGGGGACAGAGC
PKLR_F	GTGGGTGGACTACCCCAATA
PKLR_R	GGTCACCTGTAATCCCCACTA
PKLR_I	CAAGCCTCACCTCTTCACG

References

Christofk, H.R., Vander Heiden, M.G., Wu, N., Asara, J.M., and Cantley, L.C. (2008). Pyruvate kinase M2 is a phosphotyrosine-binding protein. Nature *452*, 181-186.

Dayton, T.L., Gocheva, V., Miller, K.M., Israelsen, W.J., Bhutkar, A., Clish, C.B., Davidson, S.M., Luengo, A., Bronson, R.T., Jacks, T., *et al.* (2016). Germline loss of PKM2 promotes metabolic distress and hepatocellular carcinoma. Genes Dev *30*, 1020-1033.

Israelsen, W.J., Dayton, T.L., Davidson, S.M., Fiske, B.P., Hosios, A.M., Bellinger, G., Li, J., Yu, Y., Sasaki, M., Horner, J.W., *et al.* (2013). PKM2 isoform-specific deletion reveals a differential requirement for pyruvate kinase in tumor cells. Cell *155*, 397-409.

Israelsen, W.J., and Vander Heiden, M.G. (2015). Pyruvate kinase: Function, regulation and role in cancer. Seminars in cell & developmental biology *43*, 43-51.

Kabadi, A.M., Ousterout, D.G., Hilton, I.B., and Gersbach, C.A. (2014). Multiplex CRISPR/Cas9-based genome engineering from a single lentiviral vector. Nucleic Acids Res *42*, e147.

Lewis, C.A., Parker, S.J., Fiske, B.P., McCloskey, D., Gui, D.Y., Green, C.R., Vokes, N.I., Feist, A.M., Vander Heiden, M.G., and Metallo, C.M. (2014). Tracing compartmentalized NADPH metabolism in the cytosol and mitochondria of mammalian cells. Molecular cell *55*, 253-263.

Mazurek, S., Grimm, H., Boschek, C.B., Vaupel, P., and Eigenbrodt, E. (2002). Pyruvate kinase type M2: a crossroad in the tumor metabolome. Br J Nutr *87 Suppl 1*, S23-29.

Vander Heiden, M.G., Locasale, J.W., Swanson, K.D., Sharfi, H., Heffron, G.J., Amador-Noguez, D., Christofk, H.R., Wagner, G., Rabinowitz, J.D., Asara, J.M., *et al.* (2010). Evidence for an alternative glycolytic pathway in rapidly proliferating cells. Science *329*, 1492-1499.

Appendix E: Metabolic exchange and its implications

The recent resurgence of work in the field of molecular metabolism has lead to increased interest in understanding the rate, or flux, of metabolic pathways that catabolize nutrients and synthesize molecules crucial for proliferation and other cellular functions. Flux analysis commonly relies on the use of isotopically labeled (tracer) nutrients (Buescher et al., 2015). These tracers are chemically identical to their corresponding nutrients but contain a heavy isotope atom in place of one or more light atoms. In a typical experiment, a tracer is administered to cells or delivered into a whole organism. Metabolites are subsequently extracted and analyzed to determine if they contain heavy atoms as well. The abundance of a heavy metabolite relative to the total abundance of that metabolite (enrichment) is then used to infer the contribution of the tracer nutrient to that molecule. For example, if 95% of lactate has a mass M+3 (three daltons greater than its unlabeled mass) when a glucose tracer is used, we conclude that glycolysis produces the vast majority of cellular lactate. While this approach is powerful in its ability to quantify the metabolic fates of different nutrients, this analysis can fail to accurately determine flux when reversible reactions are being studied. These reactions have the potential to confound tracer studies by introducing metabolic exchange, which is described in detail below.

Consider a typical enzymatic reaction in which substrates A and B are interconverted (**Figure 1A**). In the example shown, the reaction has a forward flux f_1 and a reverse flux f_2. Where an understanding of metabolic pathway flux is concerned, the net flux ($f_{net} = f_1 - f_2$) is the relevant parameter. This value is a measure of the net production of B from A. This value is more biologically relevant than each of the forward and reverse fluxes as it is the rate at which anabolic and catabolic processes occur. An enzyme's substrates can be interconverted rapidly or slowly and still have the same net flux. In cases where the forward and reverse fluxes are large relative to the net flux ($f_{net} << f_1$ and f_2), A and B might exchange much more rapidly than they are produced and degraded. If tracers were administered in this case, the relative enrichments of A and B might be equal, and enrichments provide minimal information
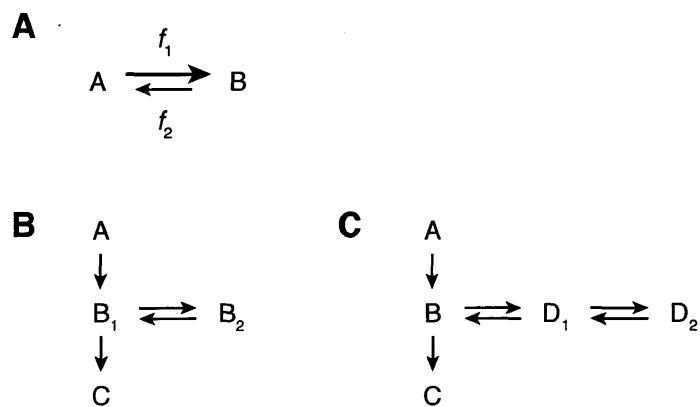
Figure 1: Reversible reactions can dilute isotopic labeling of metabolite pools

(A) A reversible enzymatic reaction interconverting metabolites A and B that has forward flux f_1 and reverse flux f_2. (B) Biosynthesis of product C from precursor A through intermediate B is subject to metabolic exchange if there are two pools of B that are differentially used by biosynthetic pathways. For example B_1 could be intracellular and B_2 could be extracellular. (C) Alternatively, B may interconvert readily with metabolite D, and D could exist as one or multiple pools.

concerning the *net* flux through this reaction. The activity of phosphoserine phosphatase (PSPH) provides

an example of such a reaction (see Appendix C). This enzyme can either net produce serine or exchange

phosphate between serine and phosphoserine, but it can never net synthesize phosphoserine (Mattaini et

al., 2016). Nevertheless, PSPH catalyzes exchange flux that is high relative to the rates of adjacent

reactions. When a carbon-13 serine tracer is administered to cells, its isotopic enrichment perfectly

matches that of phosphoserine, despite no *net* synthesis of phosphoserine. Therefore, exchange reactions

can isotopically label metabolites without net synthesis. In these cases, the application of tracers is

uninformative (or less informative) for discerning net fluxes that synthesize or degrade a given

metabolite, and these tracers instead reveal the existence of reactions with high exchange.

Where a metabolite can derive from multiple sources or can exist in distinct pools (for example,

in separate cellular compartments), metabolic exchange is an important consideration in tracer studies.

Consider the linear metabolic pathway containing unidirectional reactions from metabolite A to B to C

where B exists in two distinct but exchanging pools, B_1 and B_2 (**Figure 1B**). If tracer A is administered,

the enrichment of B and C might be significantly lower than that of A until all pools have been turned

over. This is seen when glucose is traced to serine (**Figure 2A**). Serine exists in intracellular and

extracellular pools that are in rapid exchange due to bidirectional amino acid transport (see Chapter 1).

When the fate of glucose is traced, the intracellular serine pool will have low enrichment relative to

glucose even if there is no net consumption of serine. In culture and *in vivo*, the extracellular pool of

serine is large and cannot be completely exchanged during a typical tracing experiment, and it therefore

acts as a 'sink' for serine synthesized *de novo*. Examining the enrichment of intracellular serine could,

therefore, underestimate the contribution of glucose to this pool (discussed at length in DeNicola et al.,

2015).

In addition to transport, many metabolic reactions are readily reversible and therefore introduce

the possibility of exchange flux. Isomerase, transaminase, and some dehydrogenase reactions are often

highly reversible. In the metabolic pathway from A to B to C, if B is rapidly interconverted with

metabolite D (which could also exist in multiple pools), D may appear to make a larger contribution to the

synthesis of B than is actually the case (**Figure 1C**). There is substantial interest, for example, in understanding whether lactate can be used in biosynthesis by proliferating cells. Proliferating mammalian cells in culture net produce lactate; however, if isotopically labeled lactate were administered to cells, facile transport of this metabolite would enable it to label the intracellular lactate pool (**Figure 2B**). Extremely rapid exchange through lactate dehydrogenase would then label the pyruvate pool, which could be used in downstream biosynthesis. Therefore, in cells that empirically produce lactate, a tracer study could seemingly show that lactate is used for biosynthesis. This could also be the case if lactate tracers were used *in vivo*, and caution should be used in such studies. Misinterpretation of exchange flux as net flux can be avoided by assessment of net excretion or consumption of a nutrient.

Some cases where metabolic exchange could be a confounding factor are subtler. As discussed in Chapter 1, rapid glutaminolysis is observed in culture, and as a result glutamine makes a large contribution to anaplerosis reactions in the TCA cycle. For some cell lines, up to ~50% of glutamine consumed is excreted as glutamate and therefore the net contribution of glutamine to the TCA cycle is lower. Glutamine and glutamate (and proline derived from them) are also used in protein biosynthesis, and any glutamine carbon that does not enter the TCA cycle cannot be anaplerotic. Oxaloacetate can be derived from glucose via pyruvate carboxylase (PC), but tracer studies might underestimate this contribution (**Figure 2C**). This is because there is high exchange between glutamate and α-ketoglutarate catalyzed by aminotransferases, which could dilute the enrichment of TCA cycle metabolites. Recent tracer studies have indicated that *in vivo* glucose makes a larger contribution to TCA cycle anaplerosis compared to *in vitro*. One explanation is that PC activity is higher in animals, but an alternative explanation is that reduced glutamine metabolism also observed *in vivo* unmasks PC flux that could not be appropriately traced *in vitro*. Further work is required to better understand whether PC flux is truly altered between these conditions.

A final example where metabolic exchange is confounding concerns utilization of acetyl-CoA in the TCA cycle (**Figure 2D**). With each turn of the TCA cycle, two carbon atoms enter in the form of acetyl-CoA, and two are lost as carbon dioxide. Therefore, acetyl-CoA cannot make a net contribution to
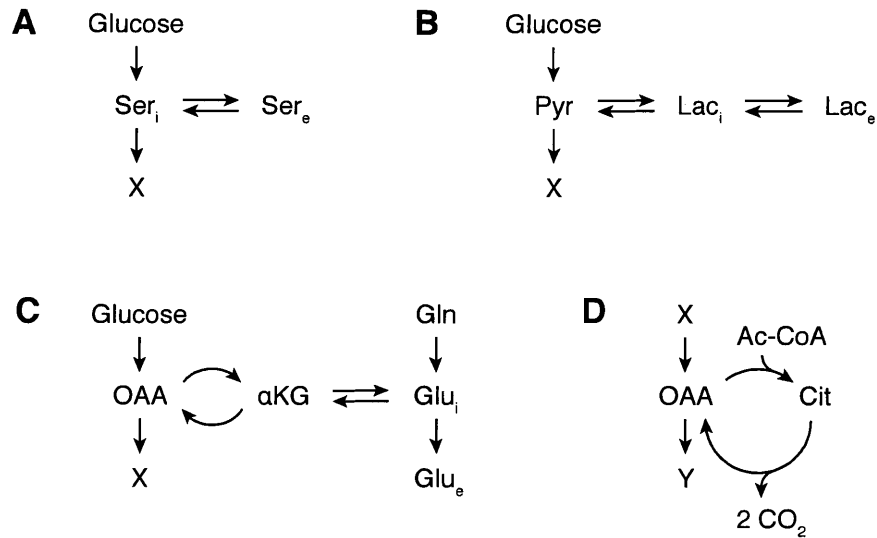
Figure 2: Examples of biosynthetic pathways potentially subject to exchange reactions

Isotopic tracing can be confounded by metabolic exchange reactions that dilute one pool of a metabolite against another pool or a parallel metabolic pathway. (A) Intracellular serine (Ser_i) is derived from *de novo* synthesis from glucose or extracellular sources (Ser_e) and is used to make downstream products X. The intracellular and extracellular serine pools are rapidly exchanged in many cell types. (B) Pyruvate generated by glycolysis is rapidly interconverted with lactate (Lac_i), and this pool may exchange with extracellular lactate (Lac_e) when it is present. (C) High flux from glutamine to glutamate creates an intracellular pool of material that can exchange with TCA-cycle intermediates derived from glucose. (D) TCA-cycle turning adds and removes two-carbon units from oxaloacetate, altering its labeling from precursor X.

αKG, α-ketoglutarate; Ac-CoA, acetyl-CoA; Cit, citrate; Gln, glutamine; Glu, glutamate; e, extracellular; i, intracellular; Lac, lactate; OAA, oxaloacetate; Pyr, pyruvate; Ser, serine.

211

the TCA cycle pool (i.e. it cannot serve as an anaplerotic source). The particular chemistry of the TCA cycle ensures that carbon from a specific acetyl-CoA molecule is not released in its first turn but only upon subsequent cycling, and therefore isotopically labeled acetyl-CoA can be traced around the cycle to oxaloacetate. Importantly, the transfer of carbon atoms from acetyl-CoA to oxaloacetate (or its downstream biosynthetic products, Y) does not imply that acetyl-CoA makes a net contribution to their synthesis. Here, TCA cycle carbon atoms are exchanged due to rapid flux from acetyl-CoA to carbon dioxide, which is at least comparable to the net flux of anaplerotic and cataplerotic reactions that generate and consume TCA cycle intermediates.

Not all reactions are subject to confounding metabolic exchange. Where a reaction is highly energetically favourable, it is effectively irreversible, and exchange cannot occur. Additionally, linear pathways cannot be influenced by exchange against other nutrients, and only where a branch point exists can this occur. Finally, many enzymes or transporters catalyze exchange at rates much slower than the net flux of the reactions they catalyze. Nevertheless, the possibility of metabolic exchange should always be considered when isotopic tracers are employed (reviewed in Buescher et al., 2015). The ability to trace the fates of metabolic reactions holds the potential to precisely discern the contribution of different nutrients to biosynthesis, and this promise will be best fulfilled when these considerations are incorporated into the analysis of metabolic flux and interpretation of tracer studies.

References

Buescher, J.M., Antoniewicz, M.R., Boros, L.G., Burgess, S.C., Brunengraber, H., Clish, C.B., DeBerardinis, R.J., Feron, O., Frezza, C., Ghesquiere, B., *et al.* (2015). A roadmap for interpreting (13)C metabolite labeling patterns from cells. Curr Opin Biotechnol *34*, 189-201.

DeNicola, G.M., Chen, P.H., Mullarky, E., Sudderth, J.A., Hu, Z., Wu, D., Tang, H., Xie, Y., Asara, J.M., Huffman, K.E., *et al.* (2015). NRF2 regulates serine biosynthesis in non-small cell lung cancer. Nat Genet *47*, 1475-1481.

Mattaini, K.R., Sullivan, M.R., and Vander Heiden, M.G. (2016). The importance of serine metabolism in cancer. J Cell Biol *214*, 249-257.